MEASUREMENT OF NONMETHANE ORGANIC CARBON

QUALITY ASSURANCE, INSTRUMENT DESIGN, AND ENCLOSURE STUDIES

Dissertation
zur Erlangung des Grades
Doktor der Naturwissenschaften

am Fachbereich Biologie
der Johannes Gutenberg-Universität in Mainz

vorgelegt von

Tamara Dindorf
geboren am 17. März 1974 in Mainz

Mainz, 2006

ZUSAMMENFASSUNG

Die vorliegende Dissertation behandelt die Messung flüchtiger organischer Kohlenstoffverbindungen unter Ausschluss von Methan (NMOC = nonmethane organic carbon), sowie deren Austausch durch Interaktionen zwischen Biosphäre und Atmosphäre. Bis heute bildet die Bestimmung dieser Verbindungen in Luftproben eine der größten Herausforderungen der qualitativen und quantitativen Analytik und führte dementsprechend zur Entwicklung einer Vielzahl unterschiedlicher Nachweismethoden. Im Rahmen verschiedener Qualitätssicherungsmaßnahmen erfolgte die Evaluierung zweier Messmethoden im Hinblick auf deren Genauigkeit, Präzision und Reproduzierbarkeit. Die Untersuchungen erfolgten im Verlauf zweier Vergleichsexperimente und umfassten:

(1) die Sammlung flüchtiger organischer Komponenten auf graphitisierten Kohlenstoffadsorbentien, deren nachfolgende thermische Desorption, sowie deren Analyse durch Gas-Chromatographie mit Flammen-Ionisations-Detektion (GC-FID) und

(2) die Sammlung kurzkettiger Carbonyle durch zwei verschiedene, mit 2,4-Dinitrophenylhydrazin (DNPH) belegte, Extraktionskartuschensysteme sowie deren nachfolgende Analyse durch Hochdruck-Flüssigkeits-Chromatographie (HPLC).

Die Evaluierung der Vergleichsexperimente zeigte, dass die vormals zur Kalibration der GC-FID Analyse verwendeten Flüssigstandards in starken Abweichungen zur spezifizierten Referenzkonzentration resultierten. Dementsprechend erfolgte die Applikation eines gasförmigen Kalibrationsstandards, unter dessen Verwendung die besten Resultate für die untersuchten Monoterpene α-Pinen und 3-Caren erbracht wurden. Die Genauigkeit der Analyse bewegte sich hier zwischen einer Unterschätzung des Sollwertes von bis zu 12% für α-Pinen, bzw. zwischen einer Unterschätzung des Sollwertes von 3 bis 20% für 3-Caren. Die Genauigkeit der Isoprenbestimmung bewegte sich zwischen einer Unterschätzung der Referenzkonzentration von 35% bis hin zu einer Überschätzung der Referenzkonzentration von 32%. Allerdings zeigte die Isoprenbestimmung, mit Ausnahme von α-Pinen, eine bessere Reproduzierbarkeit als die Analyse der untersuchten Monoterpenverbindungen. Im Rahmen der untersuchten Konzentrationsbereiche (0.2 bis 31 ppb) ließ sich kein Zusammenhang

zwischen der Höhe des untersuchten Mischungsverhältnisses und der Genauigkeit der Analyse feststellen. Untersuchungen zur Evaluierung des verwendeten Ozon-Filters zeigten keine Adsorptions- und Desorptionseffekte für die beiden untersuchten Verbindungen Isopren und β-Pinen. Die Untersuchung kurzkettiger Carbonylverbindungen erfolgte mittels zweier verschiedener Festphasen-Extraktionskartuschen-Systeme. Während das erste System auf einem Octadecyl-Trägermaterial basierte, basierte das zweite System auf einem Silica-Träger. Beide Systeme wurden mit DNPH beschichtet, wobei die Beschichtung entweder durch das MPI Labor (Octadecyl-Träger), oder vom Hersteller (Silica-Träger) vorgenommen wurde. Die beste Übereinstimmung zum spezifizierten Sollwert wurde dabei durch Verwendung der Silica-Festphasen-Extraktionskartuschen erreicht. Die Verwendung dieser Proben führte zu einer Überschätzung der Referenzkonzentration von 7% für Acetaldehyd und einer Unterschätzung von 3% für Aceton.

Die Auswertung solcher Qualitätssicherungsdaten ist u.a. auch für die Untersuchung von Austauschprozessen zwischen Biosphäre und Atmosphäre von Bedeutung. Bis heute berücksichtigen viele konventionelle Abschätzungen der Emission flüchtiger organischer Kohlenstoffverbindungen (VOC = volatile organic compound), Emissionsdaten nur auf Ökosystemebene. In diesem Zusammenhang wurden im Rahmen der vorliegenden Studie Küvettenexperimente an zwei dominierenden europäischen Laubbaumarten durchgeführt. Die Messungen erfolgten in den Sommermonaten der Jahre 2002 und 2003 and Sonnen- und Schattenblättern der Rotbuche (*Fagus sylvatica* L.), sowie and Sonnenblättern der Stieleiche (*Quercus robur* L.). Dabei konnte die Stieleiche als starker Isoprenemitter klassifiziert werden, wobei die Isoprenabgabe durch Licht und Temperatur reguliert wurde. Standardemissionsfaktoren, welche unter Verwendung der G97 Funktion berechnet wurden, betrugen 75 $\mu g\ g^{-1}\ h^{-1}$. Im Gegensatz hierzu wurde die Rotbuche eindeutig als Monoterpenemitter charakterisiert, wobei Sabinen den Hauptbestandteil der Emission bildete. Des Weiteren zeigte sich, dass auch die Monoterpenemission eine Funktion von Licht und Temperatur war. Standardemissionsfaktoren der untersuchten Sonnenblätter erreichten bis zu 13 $\mu g\ g^{-1}\ h^{-1}$, Emissionsfaktoren der Schattenblätter erreichten 20 $\mu g\ g^{-1}\ h^{-1}$. Ferner konnte bei hohen Außentemperaturen eine Mittagsdepression der Monoterpenemission festgestellt werden. Entsprechend ihrer breiten geographischen Verteilung sowie ihres hohen Standardemissionsfaktors, zeigte die Berücksichtigung der Rotbuche in Modellberechnungen, einen substantiellen Einfluss auf das europäische Monoterpenbudget, wobei in Bezug zu konventionellen Abschätzungen Anstiege von 16 bis 54% berechnet wurden. Auf lokaler Ebene konnten sogar Anstiege von > 100% verzeichnet werden.

Solche Studien des Spurengasaustauschs zwischen Biosphäre und Atmosphäre beziehen sich im Allgemeinen auf eine gut definierte, aber nur sehr limitierte Anzahl von Substanzen. Untersuchungen zum Austausch des Gesamtkohlenstoffes zwischen Vegetation und Atmosphäre liegen nicht vor und nur sehr wenige Studien berichten über Gesamtkohlenstoff-Konzentrationen in verschiedenen Luftproben. Obwohl die Integration verschiedener Einzelmessungen in Kohlenstoffkonzentrationen von mehreren hundert ppb resultiert, können nicht identifizierte Verbindungen einen großen Anteil an der Gesamtkohlenstoffmenge tragen. Im Rahmen der vorliegenden Arbeit erfolgte die Entwicklung eines Analysators zur Untersuchung des Gesamtkohlenstoffaustauschs zwischen Biosphäre und Atmosphäre. Das Gerät wurde unter Laborbedingungen getestet und im Rahmen der durchgeführten Küvettenexperimente an Rotbuche (*Fagus sylvatica* L.) im Freiland mit einer unabhängigen Methode verglichen. Das Gerät basierte auf den grundlegenden Prinzipien der Elementaranalyse und umfasste folgende Hauptbestandteile:

(1) eine Adsorptionseinheit zur Sammlung flüchtiger organischer Verbindungen, sowie deren Trennung von CO, CO_2 und CH_4,

(2) ein Oxidationsrohr zur Umwandlung der adsorbierten flüchtigen organischen Verbindungen zu CO_2 und schließlich

(3) eine Sammeleinheit zur Fokussierung des gebildeten CO_2, sowie dessen nachfolgende Bestimmung durch einen CO_2 Detektor.

Das Detektionslimit der Analyse lag bei 0.5 ng Kohlenstoff, die Reproduzierbarkeit bei einem Wert von ± 0.5%. Oxidationseffizienzen der Analyse von Kohlenmonoxid und Methan bewegten sich zwischen 91 und 101%. Widerfindungsraten verschiedener Kohlenstoffverbindungen lagen bei 48% und stellen somit die größte Unsicherheit der Messungen dar. Dennoch zeigte der Vergleich von Tagesgängen des Kohlenstoffaustauschs eine exzellente Übereinstimmung zwischen den Ergebnissen der Gesamtkohlenstoff-Analyse und den durchgeführten GC-FID Messungen. Gemäß dieser viel versprechenden Ergebnissen sollte die Weiterentwicklung der Gesamtkohlenstoffanalyse einen entscheidenden Beitrag zur Untersuchung des Gesamt-kohlenstoff Austauschs zwischen Biosphäre und Atmosphäre leisten.

CONTENTS

CHAPTER 1

BIOSPHERE-ATMOSPHERE EXCHANGE OF NONMETHANE ORGANIC CARBON-GENERAL INTRODUCTION

THE BIOGEOCHEMICAL CYCLE OF CARBON

The biogeochemical cycle of carbon refers to the short term exchange of carbon within and between four major reservoirs: the atmosphere, oceans, reserves of fossil fuels, and terrestrial ecosystems. According to Schlesinger (2003), carbon is known as the most widely distributed element on planet Earth, representing about 50% of the dry weight of living organisms. In form of various trace gases it influences the chemical and/or radiative properties of the atmosphere and therefore contributes to a natural greenhouse effect that keeps the planet warm enough to evolve and support life (Seinfeld and Pandis 1997; Finlayson-Pitts and Pitts 2000; Schlesinger 2003). With respect to the various anthropogenic influences on the earth's fragile carbon balance, a detailed knowledge of all processes involved in the global cycling of carbon is crucial for the prediction of future climate scenarios. A detailed description of the contemporary biogeochemical cycle of carbon can be obtained from biogeochemistry handbooks written by Park (2001) and Schlesinger (2003) or from atmospheric chemistry handbooks published by Seinfeld and Pandis (1997) and Finlayson-Pitts and Pitts (2000).

As shown by Figure 1.1., sedimentary carbonates represent by far the planet's largest carbon pool with persistent carbon stocks that account to > 60000000 Pg (Falkowski *et al.* 2000). Also fossil fuel reserves and the world's oceans represent huge carbon reservoirs that account up to 10000 and 39000 Pg of carbon (Schlesinger 2003). Under undisturbed conditions the fossil fuel reserves do not contribute to the active short term cycling of carbon that covers time frames ranging from seconds to centuries. Since fossil fuels are part of a carbon cycle that operates over millions of years, solely their anthropogenic induced oxidation to carbon dioxide (CO_2) leads to a mixing of short and long term carbon cycles, yielding a yearly net increase of 6.3 Pg of carbon that now takes part in the active short term cycling (IPCC 2001; Schlesinger 2003). Oceans on the other hand contribute an important carbon reservoir that may balance the increasing atmospheric CO_2 concentrations to some extent (Richter 1998). Due to the particular chemistry of the seawater, the apportionment of the liquid-vapour-equilibrium is shifted towards the oceanic compartment, where CO_2 is dissolved in form of bicarbonate or bicarbonate ions. Due to its enormous storage capacity, ocean-atmosphere exchange processes involve large carbon fluxes, accounting up to 90 and 92 Pg a^{-1} for oceanic emission and uptake, respectively (Schlesinger 2003). In contrast to the huge carbon reservoirs of fossil fuels and oceans, atmosphere and terrestrial ecosystems constitute a much smaller pool of carbon, representing carbon stocks of 780 and 2850 Pg, respectively. However, regardless of their small size, these reservoirs take a major part in the

planet's short term circulation of carbon. According to Park (2001) and Schlesinger (2003), atmospheric carbon is primarily present in form of the inorganic compound CO_2. The amount of carbon represented by methane (CH_4), carbon monoxide (CO), and nonmethane organic carbon (NMOCs) is less than 1% of the total atmospheric carbon (IPCC 1996; Seinfeld and Pandis 1997; Finlayson-Pitts and Pitts 2000). Also particulate organic carbon is found to be at most 5% of the carbon amount present in the atmosphere (Roberts *et al.* 1998). Even though CO_2 and CH_4 are denoted as trace gases, they particularly influence the planet's climate by absorption of infrared radiation. Since CO and NMOCs are known to contribute dominantly to the methane and ozone budget (both known as greenhouse gases) they may influence the planet's radiative balance as well (Seinfeld and Pandis 1997; Atkinson 2000; Finlayson-Pitts and Pitts 2000).

The organic carbon of terrestrial ecosystems exists in various forms including plant leaves and roots, animals, microbes, wood, decaying leaves, and soil humus. However, the world's

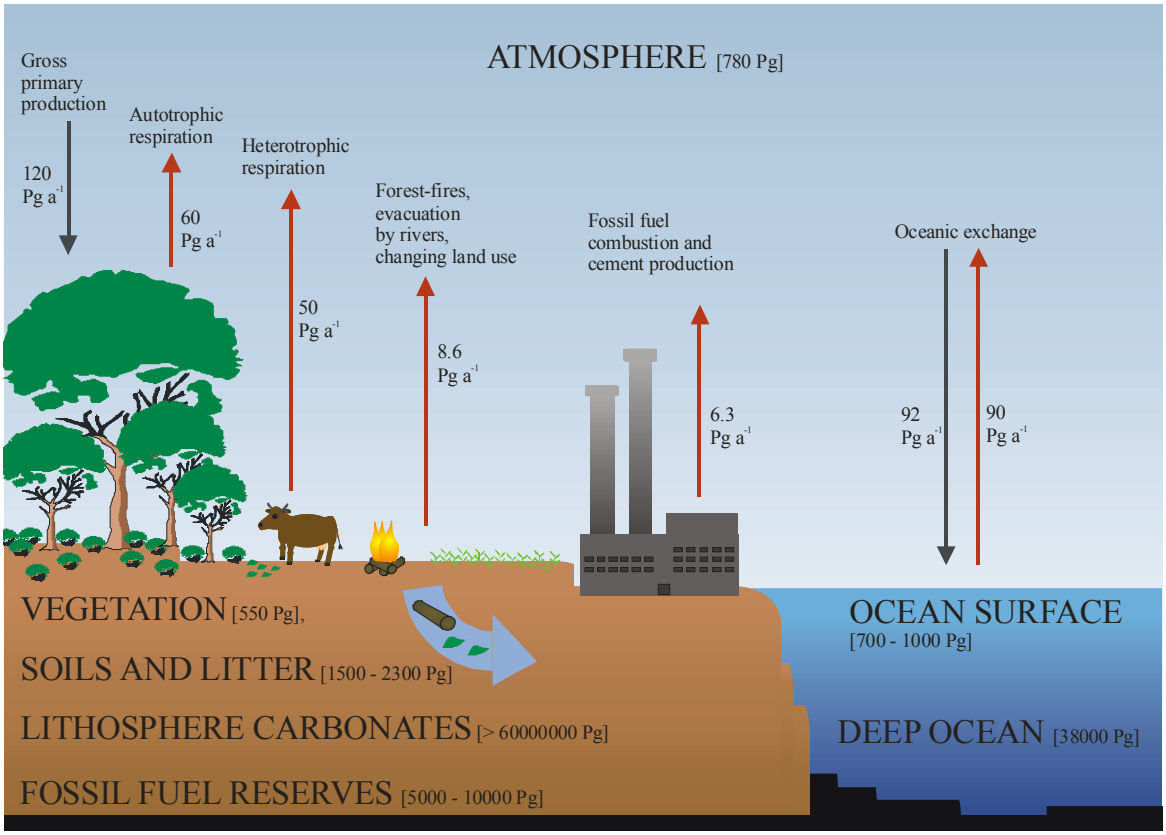

Figure 1.1. Biogeochemical cycling of carbon between and within the four major reservoirs: atmosphere, oceans, reserves of fossil fuels, and terrestrial ecosystems. Carbon reservoirs are shown in parentheses in units of Pg (= 10^{15}g). Emission is indicated by red arrows, deposition by black arrows, both in units of Pg a^{-1}. Adapted from IPCC (1996; 2001), Falkowski *et al.* (2000), Finlayson-Pitts and Pitts (2000), Kesselmeier *et al.* (2002b), and Schlesinger (2003).

carbon in terrestrial biota is nearly exclusively represented by vegetation. Animals (including humans) account for less than 0.1% of the carbon that is present in living organisms (Schlesinger 2003).

Atmospheric carbon is taken up by these terrestrial ecosystems through the process of photosynthesis that converts inorganic CO_2 to organic carbohydrates, yielding a global gross primary production (GPP) of 120 Pg a^{-1} (Ciais *et al.* 1997). However, at least half of this production is respired by the plants themselves (autotrophic respiration, R_a, about 60 Pg a^{-1} (Lloyd and Farquhar 1996; Waring *et al.* 1998)), leaving 60 Pg a^{-1} as the net primary production (NPP) of the world's ecosystems. Since all heterotrophic organisms finally depend on the net primary productivity of these ecosystems that serve as a reservoir of carbon and energy, carbon amounts of about 50 Pg a^{-1} will be consumed (respired) by animals or decomposing microorganisms and will be released to the atmosphere (heterotrophic respiration, R_h). The residual carbon amount of about 10 Pg a^{-1} that is left within the ecosystem is referred to as the net ecosystem production (NEP, IPCC 2001). However, additional carbon is lost through combustion processes in fires, by evacuation of carbon that is dissolved in the rivers of an ecosystem, and by harvesting or forest clearing. The ultimate residual of carbon emitted or deposited by an ecosystem is referred to as the net biome production (NBP). Figure 1.2. gives an overview of the various ecophysiological levels associated with the cycling of carbon between terrestrial ecosystems and other carbon reservoirs. As shown by this figure, the terrestrial biosphere is specified as a net carbon sink.

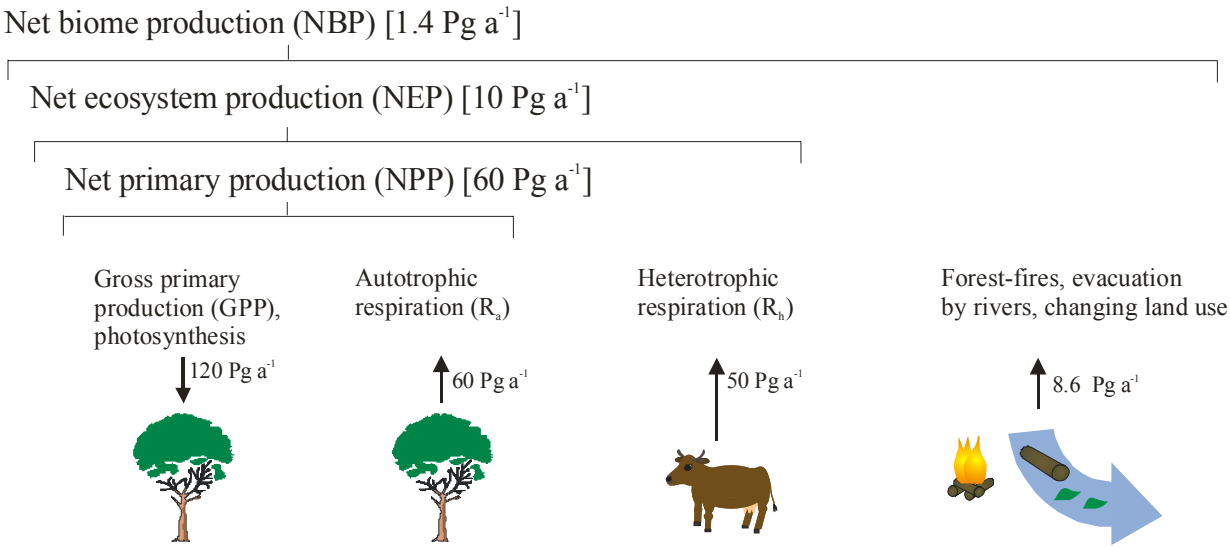

Figure 1.2. Ecophysiological levels associated with the cycling of carbon between terrestrial ecosystems and other carbon reservoirs.

Considering the time period of 1980 – 1989 this terrestrial sink was estimated to range at 0.2 ± 0.7 Pg a^{-1}. In the time period of 1989 – 1998 the terrestrial sink increased to 1.4 ± 0.7 Pg a^{-1} (IPCC 2001). According to Schimel *et al.* (2001) this increase can be attributed to the northern extra tropical areas, implying that the evolution of the carbon sink is largely the result of changes in land use over time, such as regrowth on abandoned agricultural land and fire prevention, in addition to responses to environmental changes, such as longer growing seasons, and fertilization by CO_2 and nitrogen. However, there are still large uncertainties surrounding the quantity of carbon that is stored and flowing through some parts of the carbon cycle (Park 2001).

This may be especially true considering the amount of carbon that is lost or gained by an ecosystem in form of nonmethane organic compounds. According to Kesselmeier *et al.* (2002b), the emission of these compounds from an ecosystem can be highly significant in relation to the net ecosystem productivity and is in the same order of magnitude than the net biome productivity (note, that the amount of carbon loss in form of NMOC compounds is already included in the carbon exchange of these ecophysiological levels). As outlined by the latter authors, these emitted volatiles may have different kinds of fate, implying also different consequences for the global carbon cycle:

(i) they can be transformed to atmospheric CO_2 by (photo)chemical reactions, yielding a net transfer of carbon from the terrestrial biosphere to the atmosphere,

(ii) they can be returned to the terrestrial biosphere with or without intermediate chemical transformation, which represents only an internal cycling of carbon compounds within the terrestrial biosphere itself, and

(iii) they can be deposited to the oceans which represents a net transfer of carbon to the marine biosphere and the oceanic carbon reservoir.

According to their major impact on the chemistry of the atmosphere, the following paragraph will give a short overview on the implications of these volatile organics in the formation of several secondary air pollutants. Moreover, the processes leading to their emission or deposition by the terrestrial biosphere will be presented, as well as the metabolic pathways leading to the production of several volatiles. Finally the following paragraph will give a short overview of regulation processes and ecophysiological functions of the VOC emission.

NONMETHANE ORGANIC CARBON COMPOUNDS AND ATMOSPHERIC CHEMISTRY

Historically, the organic molecules that are present in the atmosphere have been measured as "NonMethane HydroCarbon" (NMHC) compounds but with the recognition, that a variety of other organic molecules might impact the chemistry of the atmosphere as well, other terminologies have evolved. The probably most frequently used term for the description of organic volatiles is "Volatile Organic Compound" (VOC, e.g. Fehsenfeld 1992; Guenther *et al.* 1995; Kesselmeier and Staudt 1999). The notation includes all organic compounds that have a vapour pressure of > 0.27 kPa (at 25°C, National Pollutant Inventory, Australia). Methane and other compounds may be excluded from this terminology by particular definition, but some authors distinguish also between VOCs and "Non Methane VOC" (NMVOC, e.g. Monson 2002). Other frequently used terminologies refer moreover to the atmospheric lifetime of these organic compounds, such as "other VOC" (OVOC, lifetimes of > 1 day under typical tropospheric conditions) and "other reactive VOC" (ORVOC, lifetimes of < 1 day under typical tropospheric conditions, Guenther *et al.* 1995; 2002). To distinguish VOCs that are emitted from the biosphere the terms "Biogenic VOC" (BVOC) and "Biogenic Oxygenated VOC" (BOVOC) have been defined. The term "Reactive Carbon Compound" (RCC) has been used as well (Guenther *et al.* 2002). Another terminology that distinguishes the reactive volatile organics clearly from the stable volatile compound methane is the term "Non Methane Organic Carbon" (NMOC) that has evolved recently (Roberts *et al.* 1998; Maris *et al.* 2003).

To date, several thousands of different NMOC species have been identified by analytical techniques (e.g. Isidorov *et al.* 1985; Fehsenfeld 1992; Singh and Zimmermann 1992; Helas *et al.* 1997; Fall 1999; Atkinson and Arey 2003). In combination with the emission of nitrogen oxides (NO_x, i.e. NO + NO_2) derived from fossil fuel combustion, they may have severe health and environmental impacts either directly, or as a result of their photochemical oxidation (i.e. the oxidation in the presence of sunlight) leading to the formation of several secondary photochemical pollutants.

The degradation of emitted NMOC species can be initiated in a number of ways, including reactions with OH and NO_3 radicals, ozone and direct photolysis (e .g Atkinson 2000). Due to their complex molecular structure, that often includes multiple double bonds, NMOCs are generally very reactive organic compounds. A detailed description including several reaction mechanisms for the degradation of volatile organics can be obtained from atmospheric chemistry handbooks like Seinfeld and Pandis (1997) and Finlayson-Pitts and Pitts (2000) or

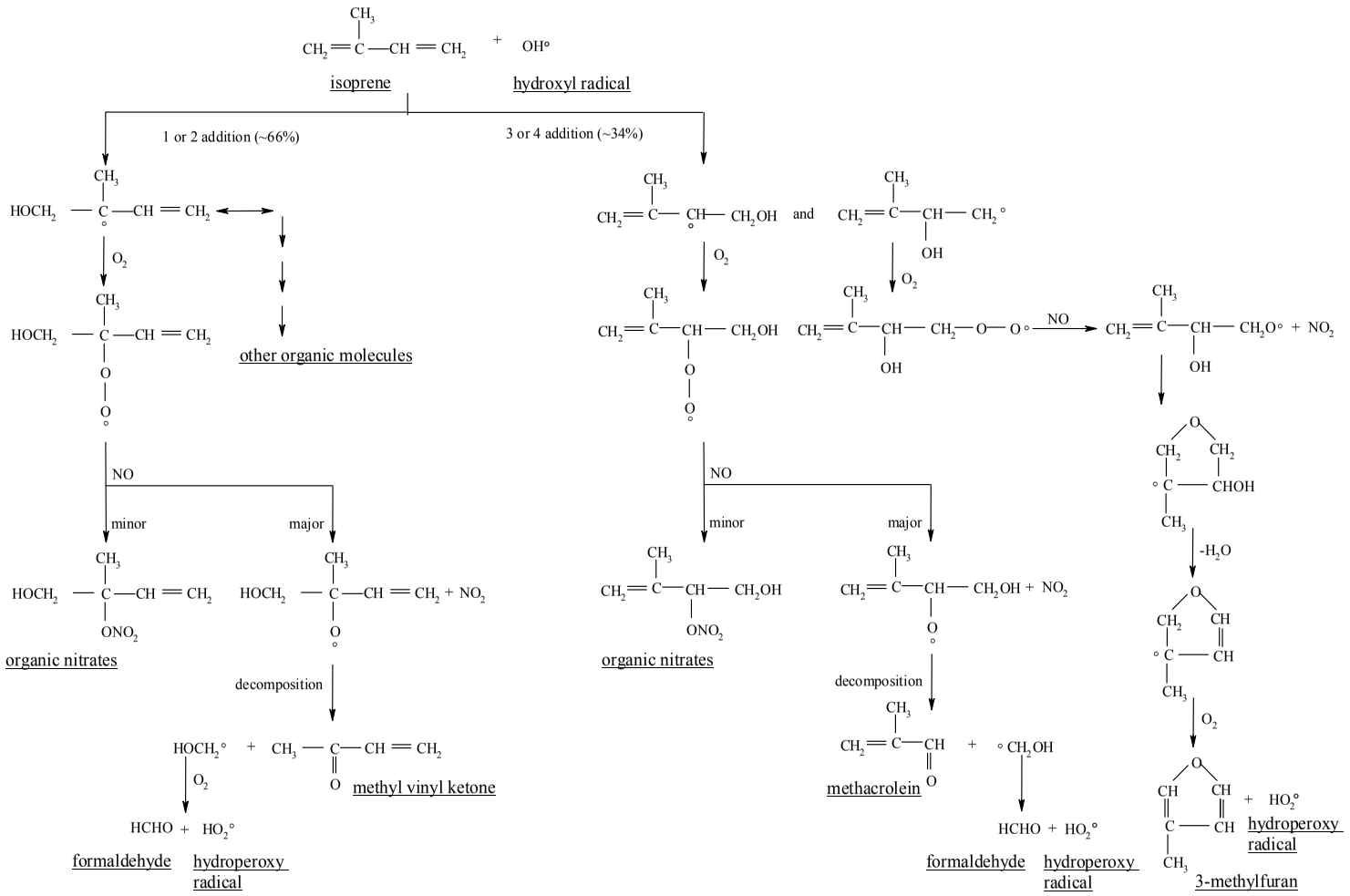

Figure 1.3. Atmopheric degradation of isoprene by OH radicals. Reaction pathways given on the left side of the figure show the addition of OH radicals to the 1 or 2 position of the isoprene molecule, leading to the formation of methyl vinyl ketone. Reaction pathways of the right side of the figure show the addition of the OH radical to the 3 or 4 position of the isoprene molecule leading to the formation of methacrolein. Adapted from Carter and Atkinson (1996) and Finlayson-Pitts and Pitts (2000).

from Atkinson (2000) and Atkinson and Arey (2003). In general the reaction with OH radicals represents the major decomposition process of all NMOC present in the atmosphere, whereas reactions with O_3 and NO_3 are mainly limited to alkene compounds. Photolysis on the other hand represents an important sink for atmospheric carbonyls and halocarbons.

Considering the reaction of (biogenic) alkenes with OH radicals, NO_3 radicals, or O_3 molecules, the primary reaction pathway proceeds always via addition of the reactant to a double bond of the alkene molecule (Finlayson-Pitts and Pitts 2000). Figure 1.3. gives an overview of the reactions involved in the atmospheric degradation of isoprene molecules (i.e. 2-methyl-1,3-butadiene, C_5H_8) by OH radicals ($OH^{\bullet}$). As shown by the figure, several reaction products can be formed from the isoprene-OH reaction. While the addition of $OH^{\bullet}$ to the 1 (or 2)-position of the isoprene molecule yields methyl vinyl ketone (MVK), the addition of $OH^{\bullet}$ to the 3 (or 4)-position of the molecule yields methacrolein (MACR). Additionally small yields of 3-methyl-furan have been reported (e.g. Carter and Atkinson 1996) and the reaction with NO_2 will lead to the formation of organic nitrates (e.g. Chen *et al.* 1998). Moreover formaldehyde and hydroperoxy radicals ($HO_2^{\bullet}$) are formed during the degradation of isoprene. The multitude of different products that can be derived from the isoprene-OH reaction represents a typical attribute of atmospheric degradation processes. Considering e.g. the reaction of the monoterpene compound α–pinene ($C_{10}H_{16}$) with O_3, more than 30 reaction products can be formed. Since several of these reaction products are less volatile than their precursors, the atmospheric degradation of monoterpenes is known to promote the formation

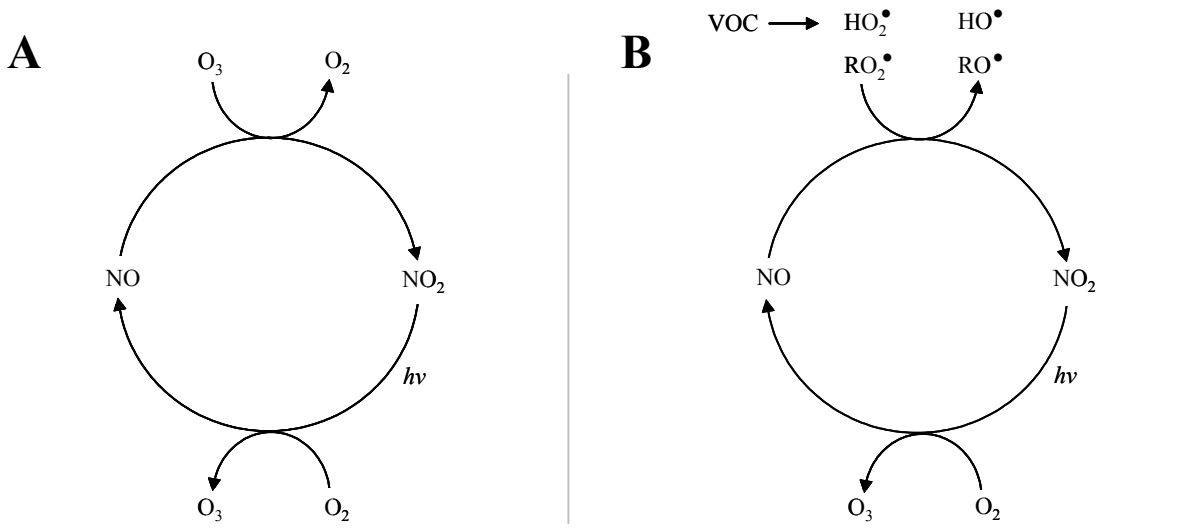

Figure 1.4. Photochemical production of tropospheric O_3. (A) Photoequilibrium of the NO-NO_2-O_3 system. (B) Net formation of tropospheric O_3 by intruduction of volatile organics into the stable NO-NO_2-O_3 system. Adapted from Atkinson (2000).

of secondary organic aerosol (SOA) particles in the atmosphere. Moreover, the degradation of isoprene by OH radicals has been discussed recently to contribute significantly to the SOA formation in tropical environments (Claeys *et al.* 2004).

In combination with anthropogenic NO_x emissions, volatile organics have a major influence on the formation of photochemical air pollution which can be found in many urban areas around the world. In these regions the primary pollutants (NO_x and VOCs) undergo several photochemical reactions leading to the formation of several secondary pollutants, the most prominent of which is O_3. In general, the net photochemical formation of O_3 depends on the actual NO mixing ratio of the atmosphere and occurs at concentrations of > 10-30 ppt. Lower NO concentrations will lead to a net destruction of the tropospheric O_3. As shown by Figure 1.4. A, the sole $NO\text{-}NO_2\text{-}O_3$ system results in a photoequilibrium state that does not promote the net formation of tropospheric O_3 molecules. If volatile organics are introduced into the system (see Figure 1.4. B) their photochemical degradation will lead to the formation of hydroperoxide radicals ($HO_2^{\bullet}$) and alkyl peroxy radicals ($RO_2^{\bullet}$, see also Figure 1.3.).

Since these radicals will react with NO to form NO_2 as well as hydroxyl radicals ($OH^{\bullet}$) and alkoxy radicals ($RO^{\bullet}$), the common sink of O_3 molecules is missing from the photoequilibrium state, leading to a net formation of tropospheric O_3. However, at low NO concentrations HO_2 radicals will react either with themselves or with O_3 molecules, leading to a net destruction of tropospheric O_3.

As outlined by Atkinson and Arey (2003), the volatile organics that are derived from biogenic sources are much more reactive than volatile organics that are emitted by anthropogenic activities. Moreover, on a global scale, the emission of BVOCs exceeds the emission of volatiles derived from anthropogenic sources by a factor of 10 (World meteorological organisation 1995). Therefore biogenic volatiles play a dominant role in the chemistry of the lower troposphere (Fuentes *et al.* 2000).

EXCHANGE OF NONMETHANE ORGANIC CARBON COMPOUNDS BY TERRESTRIAL PLANTS

Terrestrial vegetation was shown to be the dominant source of atmospheric volatile organic compounds. On a global scale about 1150 Tg of carbon are emitted in form of volatile organics (Guenther *et al.* 1995; 1999). In general these biogenic VOCs include a variety of different compounds like alkanes, alkenes, carbonyls, alcohols, esters, ethers, acids, and isoprenoids. Table 1.1. gives an overview of some different NMOC species that are released from natural and anthropogenic sources. As shown by the table, NMOC emissions that are

derived from the canopy foliage of the terrestrial vegetation represent the predominant contribution to the total amount of emitted NMOC compounds. Isoprene and monoterpenes, both belonging to the class of isoprenoids, were specified as prevalent compounds that are released by these biogenic sources. Moreover, besides their emission, volatile organics can also be deposited on the terrestrial vegetation as reported by several authors (e.g. Giese *et al.* 1994; Kondo *et al.* 1995; 1996a; 1996b; 1998; Staudt *et al.* 2000; Kesselmeier 2001, Kuhn *et al.* 2002; Rottenberger *et al.* 2004, 2005). A detailed overview on the emission and deposition processes of volatile organics can be obtained from the reviews of Kesselmeier and Staudt 1999, Fall 2003, Lerdau and Grey 2003, and Sharkey and Yeh 2001. The following paragraphs will give only a short overview of the present state of knowledge considering the emission and deposition of volatile organics by terrestrial plants, with special emphasis on isoprenoid compounds.

Table 1.1. Estimates of global VOC emission rates in terms of carbon [Tg a^{-1}]. Adapted from Guenther *et al.* (1999) and Finlayson-Pitts and Pitts (2000).

Source	Isoprene	Monoterpenes	Other VOCs
Canopy foliage	460	115	500
Terrestrial ground cover and soils	40	13	50
Flowers	0	2	2
Ocean and freshwater	1	< 0.001	10
Animals, humans, insects	0.003	< 0.001	0.003
Anthropogenic emissions	0.01	1	93
Total	~500	~130	~650

EMISSION OF ISOPRENOIDS FROM TERRESTRIAL PLANTS

As formulated by the “biogenetic isoprene rule”, all isoprenoid compounds are derived by repetitive fusion of single five carbon units (Leopold Ruzicka 1945). According to the number of these C_5 units, the isoprenoids are subdivided into hemiterpenes, monoterpenes, sesquiterpenes, diterpenes, triterpenes, tetraterpenes, and polyterpenes. Table 1.2. gives a small overview of the different isoprenoid classes that can be found in the metabolism of higher plants. A detailed description of the isoprenoid metabolism and biosynthesis is given by Croteau *et al.* (2000). As shown by Table 1.2., the smallest isoprenoid compounds – the hemiterpenes- comprise only one of these five carbon units. Isoprene is probably the best

known compound of the latter isoprenoid class. On a global scale, the estimated annual foliar isoprene emission that is released from the world's forest canopies accounts up to 460 Tg carbon per year (Guenther *et al.* 1999). Monoterpenes on the other hand, consist of two five carbon units and are best known as components of the volatile essences of flowers and essential oils. Monoterpenes can be found in cyclic (e.g. α pinene, β-pinene) and acyclic (e.g. myrcene, ocimene) forms. On a global scale, the emission of monoterpenes that are released by the canopy foliage of terrestrial plants are estimated up to 115 Tg carbon per year and therefore lags behind the global emissions of isoprene (Guenther *et al.* 1999). As shown by Table 1.2., sesquiterpenes consist from a total of three five carbon units. Like monoterpenes, sesquiterpenes can be found in essential oils of various plant species. Although they are emitted only in small amounts to the atmospheric system, several authors reported their release from the terrestrial biosphere (Winer *et al.* 1992; König *et al.* 1995; Schuh *et al.* 1997; Ciccioli *et al.* 1999; Hakola *et al.* 2001, Tholl *et al.* 2005). Finally diterpenes, triterpenes, tetraterpenes, and polyterpenes are important products of plant's metabolism (e.g. they act as phytoalexins, preformed chemical defence compounds, gibberellin hormones, accessory pigments, or electron carrier molecules). However, since these isoprenoids are non volatile, they have no impact on the chemistry of the atmosphere.

Table 1.2. Isoprenoid compounds of plant's metabolism.

Isoprenoid class	Compound	Number of carbon atoms
Hemiterpenes	Isoprene, 2-Methy-3-butene-2-ol	C_5
Monoterpenes	e.g. α-pinene, β-pinene	C_{10}
Sesquiterpenes	e.g. β-caryophyllene	C_{15}
Diterpenes	e.g. Phytol	C_{20}
Triterpenes	e.g. Phytosterole	C_{30}
Tetraterpenes	e.g. β-carotene	C_{40}
Polyterpenes	Rubber, plastoquinone	$> C_{40}$

Biosynthesis of isopentenyldiphosphate

As reviewed in detail by Croteau *et al.* (2000), an important characteristic of the isoprenoid biosynthesis is its location at different sub cellular compartments. While sesquiterpenes, triterpenes, and polyterpenes are produced in the cytosol and endoplasmatic reticulum, isoprene, monoterpenes, diterpenes, and tetraterpenes are produced within plant's chloroplasts. Mitochondria on the other hand may generate the prenyl group of ubiquinone.

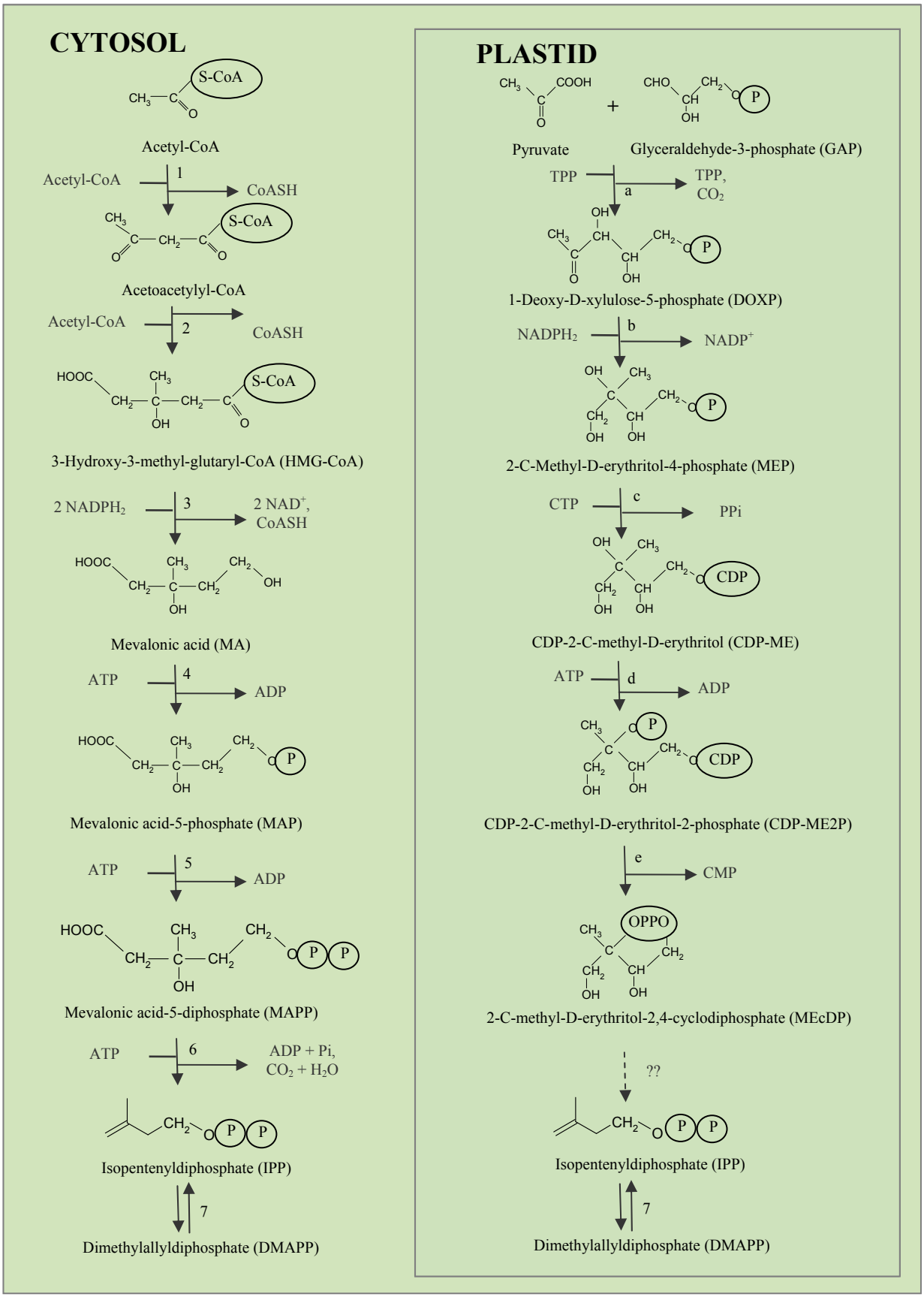

Figure 1.5. Biosynthesis of isopentenylpyrophosphate (IPP) and Dimethylallyldiphosphate (DMAPP) via the classical acetate/mevalonate pathway (left panel) and by the MEP pathway (right panel). Adapted from Lichtenthaler (1999), Croteau *et al.* (2000), and Sharkey and Yeh (2001).

Abbreviations to Figure 1.5.: [ADP] adenosine-diphosphate, [ATP] adenosine-triphosphate, [CDP] cytidine-diphosphate, [CTP] cytidine-triphosphate, [CoA] coenzyme A, [$NADPH_2$/NADP] redox pair of nicotinamid-adenin-dinucleotide-phosphate, [P] phosphate moiety, [TTP] thiamine-pyrophosphate, [1] thiolase, [2] HMG-CoA synthase, [3] HMG-CoA reductase, [4] MA kinase, [5] MAP kinase, [6] MAPP decarboxylase, [7] IPP isomerase, [a] DOXP synthase, [b] DOXP reductoisomerase, [c] MEP cytidyltransferase, [d] CDP-ME kinase, [e] MEcDP synthase.

Likewise its organisation at these different sub cellular compartments, the biosynthesis of the universal precursor compound isopentenyldiphosphate (IPP) proceeds by different metabolic pathways, i.e. by the classical acetate/mevalonate pathway in the cytosol and by the 2-deoxy-xylulose-5-phosphate/2-methylerythritol-4-phosphate (MEP) pathway in plant's plastids (see e.g. Rohmer 1993; 1996; Lichtenthaler 1999; Eisenreich *et al.* 2004). As shown by Figure 1.5., IPP biosynthesis performed by the acetate/mevalonate pathway involves the two step condensation of three molecules acetyl-coenzyme A (acetyl-CoA) and proceeds via 3-hydroxy-3-methyl-glutaryl-CoA (HMG-CoA) and mevalonic acid (MA). Regulation of the latter biosynthesis may be controlled by the enzyme HMG-CoA reductase which is located in the membrane of the endoplasmatic reticulum (Bach *et al.* 1999). Specific HMG-CoA reductase genes can be induced by wounding or pathogen infection. Moreover, the enzymatic activity may be controlled by posttranslational regulation (e.g. phosphorylation) and allosteric modulation. IPP synthesis in plant's plastids involves the condensation of pyruvate with glyceraldehyde-3-phosphate (GAP) to form 1-deoxy-D-xylulose-5-phosphate (DOXP) which is then rearranged and reduced to 2-C-methyl-erythritol-4-phosphate (MEP). After addition of cytidine-triphosphate (CTP), phosphorylation, and cyclisation, IPP is finally formed. Although several intermediate steps of the MEP pathway have not been fully elucidated yet, it seems much more efficient than the classical acetate/mevalonate pathway. According to Sharkey and Yeh (2001) isoprene production via the MEP pathway involves 6 carbon atoms, 20 ATP and 14 $NADPH_2$. Isoprene production via the classical acetate/mevalonate pathway would involve 9 carbon atoms, 24 ATP, and 14 $NADPH_2$. However, even though there are distinct pathways to produce IPP in different compartments, Bartram *et al.* (2006), demonstrated that IPP may be exchanged between the plastidic and cytosolic compartment.

As shown by Figure 1.6., the formation of the various terpene compounds proceeds from condensation of IPP and its reactive isomer dimethylallyl-diphosphate (DMAPP). Electrophilic elongation reactions that yield the respective C_{10}, C_{15}, and C_{20} prenyldiphos-

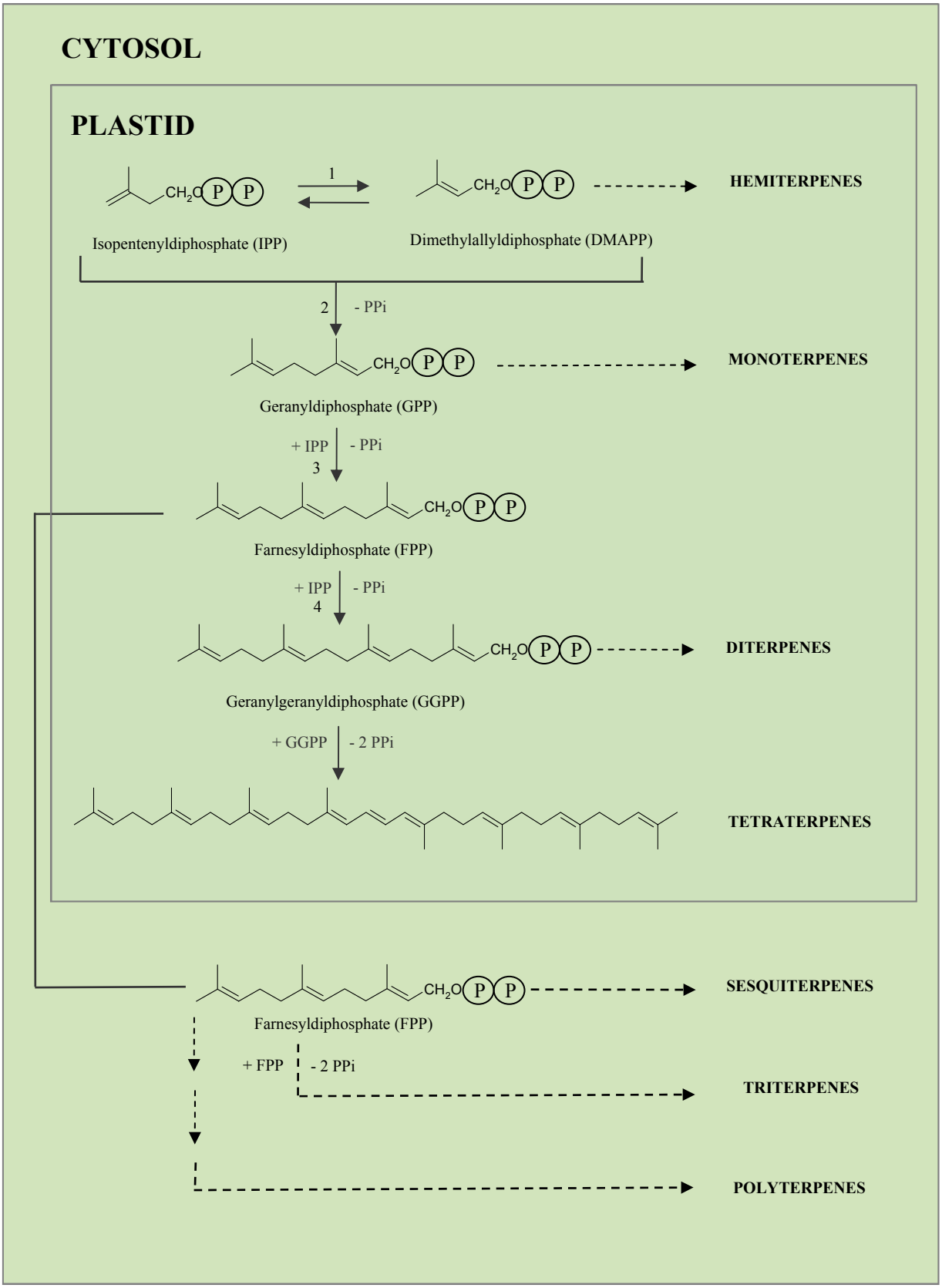

Figure 1.6. Compartmentation of isoprenoid synthesis in higher plants. Adapted from Lichtenthaler (1999) and Croteau *et al.* (2000). Abbreviation: [P] phosphate moiety, [1] IPP isomerase, [2] GPP synthase, [3] FPP synthase, [4] GGPP synthase.

phates are catalysed by specific prenyltransferases named for their products (e.g. farnesyldiphosphate synthase). Enzymes that are responsible for the formation of the respective isoprenoids from geranyldiphosphate (GPP), farnesyldiphosphate (FPP), and geranylgeranyldiphosphate (GGPP) are known as monoterpene-, sesquiterpene, and diterpene synthases.

Biosynthesis of isoprene

The biosynthesis of isoprene proceeds in plants plastids in a light dependent way. A detailed overview of isoprene biosynthesis and emission is given by Sharkey and Yeh (2001). In general isoprene synthesis proceeds from the reactive DMAPP by isoprene synthase (Silver and Fall 1994). The latter enzyme has a pH optimum at ~8 and a requirement for Mg^{2+} (Silver and Fall 1995; Schnitzler *et al.* 1996). Its molecular weight varies between 95 kDa for *Quercus robur* (Schnitzler *et al.* 1996) and 58 + 62 kDa for a doublet enzyme that has been found in aspen and kudzu (Silver and Fall 1995; Sharkey and Yeh 2001). Regulation of the enzyme may be achieved by guaninetriphosphate (GTP) or palmitoyl-CoA (Sharkey and Yeh 2001). As discussed in detail by Wolfertz *et al.* (2003), the basal isoprene emission seems to

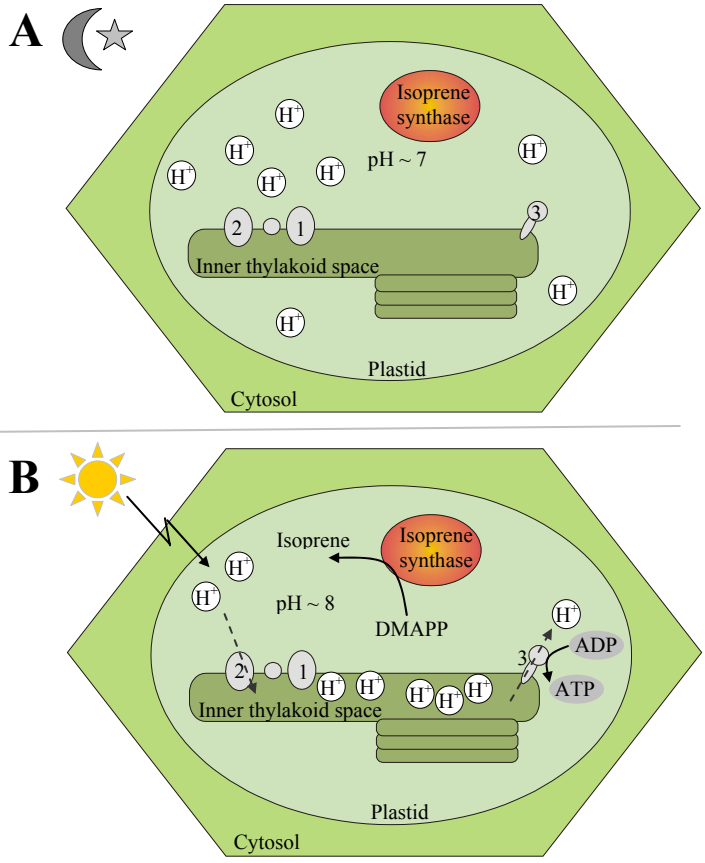

Figure 1.7. Model of isoprene production and its dependency on the plastidic proton concentration. (A) Proton concentrations of the outer thylakoid space (stroma) during darkness. (B) Proton concentrations decrease in the outer thylakoid space caused by a light induced proton transport to the inner thylakoid space (lumen). Abbreviation: [ADP] adenosinediphosphate, [ATP] adenosinetriphosphate, [H^+] proton. [1] photosystem complex I, [2] photosystem complex II, and [3] ATPase. According to the experiments performed by Fall and Wildermuth 1998.

be directly controlled by the activity of isoprene synthase. An interesting characteristic of the isoprene synthesis is its linkage to ambient light conditions and plants photosynthesis. Both effects may partly be a product of the general features of isoprene synthase. As shown by Figure 1.7., under non-light conditions, the proton concentration of the outer thylakoid space that is present in plant's plastids ranges around neutrality (pH ~7). Solely under the influence of light, an increase of protons in the thylakoid lumen is induced by the cleavage of water and the photosynthetic electron transport chain located in the thylakoid membrane. Due to these activities the proton concentration in the stroma decreases to a pH of ~8, which coincides with the pH optimum of isoprene synthase. Therefore adequate ambient light conditions and plants photosynthesis may promote the biosynthesis of isoprene. However, isoprene cessation under non-light conditions can not be explained only by the latter model, since enzymatic activity is also measurable at pH ~7 (non-light conditions).

Biosynthesis of monoterpenes

The biosynthesis of monoterpene compounds proceeds by catalysis of monoterpene synthase from the C_{10} precursor molecule GPP (see e.g. Croteau *et al.* 2000). Up to now, a diversity of different monoterpene synthases has been isolated from a variety of angio- and gymnosperm species. In general these enzymes exhibit a molecular mass of 50 to 100 kDa (either monomers or homodimers) and have a requirement for divalent metal ions (Mn^{2+} or Mg^{2+}). As described in detail by the review of Bohlmann *et al.* (1998), all monoterpene synthases are operationally soluble proteins with a pH optimum within the range of neutrality. In general, the synthases of gymnosperms are distinguishable from their angiosperm counterparts by the requirement for a monovalent cation and a preference for Mn^{2+} over Mg^{2+} as a cofactor. Moreover gymnosperm synthases exhibit a higher pH optimum than angiosperm synthases

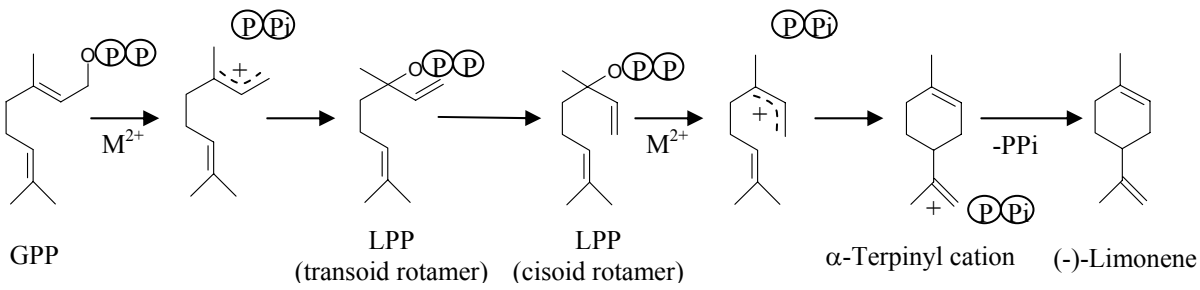

Figure 1.8. Limonene biosynthesis by limonene synthase. Abbreviation: [GPP] geranyldiphosphate, [LPP] linalyldiphosphate, [PP] phosphate moiety, [M^{2+}] divalent metal ion. Adapted from Croteau *et al*. (2000).

(Bohlmann *et al.* 1998; Phillips *et al.* 1999; Croteau *et al.* 2000; Fischbach *et al.* 2000; Lucker *et al.* 2002). As described in detail by Croteau *et al.* (2000), an interesting characteristic of monoterpene synthases is their ability to produce more than only one enzymatic product (e.g. pinene synthase may produce either α- or β-pinene). However, all monoterpene synthases use a similar reaction mechanism. As shown by Figure 1.8., the simplest monoterpene synthase reaction is catalysed by limonene synthase, were limonene biosynthesis proceeds via the initial ionisation of GPP by divalent metal ions. The latter ionisation leads to the formation of several rotameric forms of linalyldiphosphate which are then transformed via an α-terpinyl-cation to limonene.

EXCHANGE OF OTHER VOLATILE ORGANICS BY TERRESTRIAL PLANTS

Besides the predominant group of isoprenoid compounds, a variety of other volatile organics can be emitted or deposited by plants, including alkanes, alkenes, organic acids, carbonyls, as well as alcohols and esters. According to several studies, the emission of alkanes by terrestrial vegetation is only low, but biogenic alkene emissions were specified to be significant (Owen *et al.* 1997; Hakola *et al.* 1998; Kirstine *et al.* 1998). Within this context ethene is probably the most important biogenic alkene compound, since it is produced (and emitted) by terrestrial plants e.g. in response to several stress effects like injury or in response to the impact of extreme temperatures (see Kimmerer and Kozlowski 1982; Yang and Hoffman 1984). Moreover several organic acids were shown to be exchanged in a bidirectional fashion (emission and/or deposition) demonstrating the plant's potential to produce and metabolize these compounds (e.g. Talbot *et al.* 1990; Kesselmeier *et al.* 1997; 1998b; Gabriel *et al.* 1999; Kesselmeier 2001; Kuhn *et al.* 2002a). Likewise short chain carbonyl compounds were shown to be exchanged in a bidirectional way, and several authors discussed this inconsistency as a function of the ambient carbonyl mixing ratios (e.g. Jork 1996; Dindorf 2000; Kesselmeier 2001; Rottenberger 2004; 2005). Moreover, acetaldehyde was discussed to be released in response to stress effects like flooding of the root system (Kimmerer and Kozlowski 1982; Kreuzwieser *et al.* 1999; Holzinger *et al.* 2000; Rottenberger 2003). C_6 aldehydes like hexanal, cis-3-hexenal, and trans-2-hexenal are responsible for the characteristic flavour of fresh leaves (e.g. Hatanaka and Harada 1973; Hatanaka *et al.* 1987; Hatanaka 1996). Likewise a high number of alcohol and ester compounds are assigned to be an essential part of flower odour. According to Arey *et al.* (1991) and Winer *et al.* (1992), leaf alcohol and leaf ester (i.e. (Z)-3-hexene-1-ol and (Z)-3-hexenylacetate) accounted up to 50-100% of the VOC emission

of several plant species. Moreover methanol was reported to be emitted from various plant species at emission rates similar to those of isoprene and monoterpenes (MacDonald and Fall 1993). A first estimate of the global methanol emission has been reported by Galbally and Kirstine (2002), who calculated an annual methanol release of about 100 Tg a^{-1}.

REGULATION OF NMOC EMISSION

According to Kesselmeier and Staudt (1999), one can distinguish two different groups of trace gases: while the first group is stored in specialised cells or organs (e.g. the resign ducts of conifers) after its production, the second group comprises trace gases that are directly emitted after their synthesis. As a result, the emission of volatiles that belong to the second group of trace gases will be much more sensitive with regard to changes of physiological control mechanisms. For a long time period isoprene has been regarded as a prime example of a non-storing volatile organic, while monoterpenes were regarded to be always emitted from storage pools. This concept has been improved only recently, since several authors reported a direct (and light dependent, see below) emission of monoterpenes without significant intermediate storage (Kesselmeier *et al.* 1996; 1997; 1998a; Bertin *et al.* 1997; Ciccioli *et al.* 1997; Schuh *et al.* 1997; Staudt and Seufert 1997; Kuhn *et al*. 2002b; Rinne *et al.* 2002; Pio *et al.* 2005). Considering abiotic factors that may influence the emission of volatile organics from plants, ambient light and temperature conditions seem to be the most important environmental parameters. On a short term basis, ambient temperature (and as a consequence leaf temperature) seem to influence the emission of both isoprene and monoterpenes. For non-stored volatile organics the dependency of VOC emission on leaf temperature was shown to follow an optimum curve (generated by the temperature dependence of the participating enzymes, Guenther *et al.* 1993). VOC emission from storage pools followed instead a clear exponential temperature function which is described by Tingey (1981) and Guenther *et al.* (1993). Moreover, long term temperature effects may influence the emission strength of a plant individual, and may therefore lead to seasonality effects as observed by several authors (Peñuelas and Llusia 1999a; Llusia and Peñuelas 2000; Sabillon and Cremades 2001; Staudt *et al.* 2003; Kuhn *et al.* 2004a). In addition, several non-stored volatile organics like isoprene are regulated by ambient light conditions, reflecting the close link between emission and their production from photosynthetic products. Consistently their emission is regarded as a function of light and followed a saturation curve (Guenther *et al.* 1993). Moreover, other environmental parameters (e.g. drought, flooding of the root system) may influence the emission strength of volatile organics as well. The probably most important physiological

mechanism controlling the short term release of volatile organics is the regulation of the stomatal aperture, since several trace gases were reported to be emitted as a function of the latter (e.g. Fall and Benson 1996; Kesselmeier *et al.* 1997). However, isoprene and monoterpene compounds seem to be emitted indeed by the way of the stomata, but were not controlled by the stomatal aperture due to their high production rates (Loreto *et al.* 1996; Niinemets and Reichstein 2003). Other control mechanisms may involve different physiological controls leading e.g. to a clear dependency of VOC emission on the present developmental stage of the respective plant organism (e.g. Hakola *et al.* 2001; Kuhn *et al.* 2004b).

A detailed investigation of these environmental and physiological regulation mechanisms provides the opportunity to simulate the emission of volatile organics from various plant species and ecosystems. Therefore, several algorithms have been developed that describe the emission of volatile organics as a function of a basic emission strength (i.e. a standard emission factor or basal emission rate) combined with environmental parameters like ambient light and temperature conditions (Tingey *et al.* 1981; Guenther *et al.* 1993; 1995; 1997; Schuh *et al.* 1997). To incorporate moreover physiological regulation mechanisms, several complex model approaches have been developed recently (Zimmer *et al.* 2003; Simon *et al.* 2005).

ECOPHYSIOLOGICAL AND METABOLIC FUNCTION OF NMOC EMISSION

Considering the plant organism, the emission of volatile organics represents a loss of carbon and energy that were previously gained in photosynthetic processes. According to Fehsenfeld *et al.* (1992) the loss of assimilated carbon in form of VOC emissions ranges between a few thousandths and some percent, but can reach losses of up to 50% in extreme cases (Sharkey and Loreto 1993; Staudt *et al.* 1997; Staudt and Bertin 1998). Therefore, it is still a matter of debate whether these losses should be discussed as leakage and waste products of the plant's metabolism, or if they serve as physiological and ecophysiological reactions that yield advances for the respective organism. Considering the enormous amounts of terpenes that are emitted every year from the terrestrial vegetation, their physiological and metabolic functions have still not been fully elucidated yet.

According to Fischer (1991), several monoterpenes are known to have allelopathic functions, i.e. they limit the growth of other plant species and some authors discussed monoterpenes as defence compounds against pathogens and herbivores (Cheniclet 1987; Lewinsohn *et al.* 1991a; 1991b; Gershenzon and Croteau 1991; Funk *et al.* 1994). Isoprene on

the other hand may protect the photosynthetic apparatus of leaves by dissipating excessive energy and serving as a reactant to regenerate $NADP^+$. Moreover, membrane protection against heat stress has been discussed as a potential function of isoprene (Sharkey and Singsaas 1995; Singsaas *et al.* 1997) and monoterpene production (Loreto *et al.* 1998).

Recent studies that focussed on plant-plant and plant-insect interactions revealed that a variety of volatile organics may be used also as communication signals- a fact that led to a concept known as "talking and listening trees" (for an overview see e.g. Baldwin and Preston 1999; Baldwin *et al.* 2001; 2002; Farmer 2001; Pickett and Poppy 2001; Arimura *et al.* 2005). As outlined by Baldwin *et al.* 2002, plants are able to release a complex mixture of volatile organics after being attacked by herbivores. Although some emissions seem to be only a passive consequence resulting from the damage of some compartments in which these VOCs are stored, other compounds have been demonstrated to result from the *de novo* synthesis of these molecules. According to Bleecker and Kende (2000) ethylene, a compound implicated in development and defence, was the first gaseous hormone discovered in nature. Recently a variety of other phytopherhormones has been characterised as well.

Within this context the volatile methyl esters of jasmonate and salicylate seem to play an important role. According to Preston *et al.* (2001), methyl jasmonate was shown to be synthesised and released in response to mechanical damage from *Artemisia tridentata*. Also Karban *et al.* 2000 reported the production of volatile methyl-jasmonate in damaged sagebrush plants that caused neighbouring tobacco plants to be more resistant to herbivores. Methyl salicylate was shown to deter aphids from colonising plants (Pettersson *et al.* 1994) and many insects seem to be effected by the latter compound on a neurophysiological level (see Pickett and Poppy 2001 and references therein). Ozawa *et al.* 2000 demonstrated that also exogenous jasmonic acid treatments were able to trigger a VOC release. Conjugates of fatty-acids and amino-acids like volicitin (i.e. N-17-hydroxylinolenoyl-L-glutamine), a compound that can be found in the saliva of herbivores, have been shown to elicit endogenous jasmonic acid as well as a herbivore-induced VOC release in native tobacco plants (Halitschke *et al*. 2001). Application of gaseous cis-jasmone was shown to induce (E)-β-ocimene and also the expression of α-tubulin genes (Birkett *et al.* 2000). However, the molecular and physiological control over the herbivore-induced release of volatiles is still only poor understood. Within this context an interesting question is, whether these volatile signals act directly as phytopherhormones which are detected by a particular receptor or whether these compounds are simply adsorbed and then circulated within the plant organism. To date, receptors have only been detected for the low molecular weight compound ethylene.

OBJECTIVES AND THESIS STRUCTURE

One of the major limitations in advancing the understanding of tropospheric ozone formation, aerosol generation, and biosphere-atmosphere exchange processes of volatile organics, is the technical ability to accurately measure these compounds. Therefore, a great variety of analytical techniques has been developed in the past but the analysis of biogenic volatiles is still a challenging task in terms of qualitative and quantitative aspects.

Highly accurate concentration measurements are particular crucial for the evaluation of biosphere-atmosphere exchange processes. To access the accuracy, precision, and reproducebility of conventional VOC analysis that was performed in here by two different techniques, a series of two intensive intercomparison experiments were carried out during the present study. Chapter 2 will give an overview of the respective experiments and will discuss the results obtained for various VOC species to evaluate the performance of the applied analytical methods.

As outlined previously, vegetation represents the dominant source of volatile organic carbon in the atmosphere. Conventional estimates of the global VOC budget consider carbon emission factors based only on an ecosystem level and thus high uncertainties may be associated with these calculations. Application of species specific emission factors may lead to an improvement, in particular in environments with high biodiversity. Moreover, disregarding physiological and environmental regulation processes of VOC emissions may lead to incorrect results. Within this context, Chapter 3 will present the results obtained from plant enclosure studies performed on two predominant European deciduous tree species under natural conditions. The measurements were conducted during two consecutive field experiments in the summers of 2002 and 2003. The obtained basal emission rates of these tree species will be discussed with respect to environmental and physiological regulation processes and will present a model estimate considering their impact on the European VOC budget.

In general, the emission of organic volatiles represents a substantial loss of organic carbon for the biosphere but previous studies focussed only on the detection of a limited number of NMOC compounds. Measurements of the total NMOC exchange between vegetation and the atmosphere are not reported hitherto and only very few studies reported on total NMOC concentration measurements in ambient air. Even though summation of reported single-VOC measurements results in carbon concentrations of up to hundreds of ppb, additional unidentified organic compounds may represent a substantial share of total NMOC concentrations. Chapter 4 will describe the setup of a total NMOC analyser designed to investigate the bio-

sphere-atmosphere exchange of total organic carbon. The instruments performance was characterised during laboratory tests and evaluated versus an independent conventional method performing branch enclosure studies in the field. The results will be discussed in terms of qualitative and quantitative aspects and may help to quantify the exchange of total carbon between terrestrial plants and the atmosphere.

CHAPTER 2

MEASUREMENT OF VOLATILE ORGANIC CARBON BY CONVENTIONAL TECHNIQUES-INTERCOMPARISON EXPERIMENTS

ABSTRACT

Within the framework of the ECHO project (Emission and CHemical transformation of biogenic volatile Organic compounds, AFO 2000) two intercomparison experiments were carried out for quality inspection of VOC analysis. The following chapter will present the results of the GC-FID and HPLC analysis that was performed by the Max Planck Institute for Chemistry during both intercomparison experiments. All experiments were conducted in a "non-blind" fashion, with each participant using his own calibration methodology. VOC mixing ratios were set by utilisation of a permeation device and ranged between 0.2 and 31 ppb during both experiments. The data quality was assessed by its accuracy, precision, and reproducibility.

Regarding the analysis of short chain carbonyl compounds by HPLC analysis, best agreement with the reference concentration was obtained for acetaldehyde and acetone by utilisation of commercially available solid phase extraction silica cartridges. Utilisation of these cartridges resulted in an overestimation of the reference mixing ratio by 7% for acetaldehyde and in an underestimation of the reference mixing ratio by 3% for acetone.

The application of syringe injections of liquid VOC standards for GC-FID measurements was shown to cause major problems for an accurate VOC quantification and improved accuracy was obtained by utilisation of a gaseous calibration standard containing several n-alkanes. With the latter standard best agreement with the reference concentration was obtained for α-pinene, resulting in an underestimation of 0 to 12% and for 3-carene, resulting in an underestimation of 3 to 20%. In comparison to these monoterpene measurements, the accuracy of isoprene measurements showed a higher variability ranging between an underestimation of the reference by 35% and an overestimation of the reference by 32%. However, the reproducibility of the isoprene measurements was ± 2 to ± 6% and with exception of α-pinene (reproducibility of ± 1 to ± 4%), better than for monoterpenes. The accuracy of the aromatic compound benzene ranged between an underestimation of the reference concentration by 15% and an overestimation of 37%. Toluene measurements ranged between an underestimation of the reference mixing ratio by 13% and an overestimation of the reference mixing ratio 13%.

No dependency between the specified mixing ratio and the measured accuracy was observed within the range of evaluated VOC concentrations. Highest blank values were observed for the aromatic compounds benzene and toluene. Moreover, for benzene, 3-carene, and α-pinene blank values of intercomparison I exceeded the blanks of intercomparison II

significantly. Tests, evaluating the performance of a particular ozone scrubber assembly consisting of MnO_2 covered copper nets showed, that neither adsorption nor desorption effects were detectable for isoprene and β-pinene using dry air conditions.

INTRODUCTION

Various intercomparison experiments have been performed in the past. However, most of them addressed primarily the analysis of non-oxygenated and anthropogenic volatile organic compounds (VOC, De Saeger and Tsani-Bazaca 1992; Hahn 1994; Apel *et al.* 1999; 2003a; 2003b; Slemr *et al.* 2002; Volz-Thomas *et al.* 2002; Kuster *et al.* 2004) and only few experiments were focussed on the intercomparison of biogenic VOCs so far (e.g. Larsen *et al.* 1997; Komenda *et al.* 2003; Ammann *et al.* 2004). In general, intercomparison experiments can be performed in two different ways:

(i) a "blind" fashion (i.e. compounds and/or concentration ranges of the test gas mixture are unknown by the participants) and

(ii) a "non-blind" fashion (i.e. compounds and/or concentration ranges are published to the participants).

Since prediction of coelution from chromatographic columns and breakthrough of compounds during the preconcentration step is much more difficult if the composition of volatiles and the concentration ranges are unknown, most of the previous intercomparison experiments were carried out in a "blind" fashion. Moreover, some of these previous intercomparison experiments comprised several tasks of increasing complexity for the participating laboratories.

Within this context two large intercomparison experiments including several of these tasks were carried out in Europe (AMOHA, Accurate Measurements Of Hydrocarbons in the Atmosphere, Slemr *et al.* 2002) and in the USA (NOMHICE, NOnMethane Hydrocarbon InterComparison Experiment, Apel *et al.* 1994; 1999; 2003a; 2003b). Both experiments started with the analysis of a synthetic mixture of few hydrocarbon compounds and nitrogen. In a second and/or third task the participating laboratories were asked to analyse a more complex synthetic test gas mixture comprising up to 60 different compounds. The final, most challenging task is, however, the analysis of ambient air samples that was carried out during

the latest published experiments of AMOHA (Slemr *et al.* 2002) and NOMHICE (Apel *et al.* 2003a; 2003b). Here, major problems were caused by interference of CO_2, water vapour, and also by the coelution of various other volatile organic compounds.

Another problem that especially occurs by utilisation of ambient air samples for intercomparison experiments is furthermore the specification of the accurate reference concentration. However, also for synthetic test gas mixtures different references were set by various authors, and so some authors rely on the pure calculation of mixing ratios by gravimetric approaches (Komenda *et al.* 2003), others refer to different reference laboratories (Apel *et al.* 1994; 1999; 2003a; 2003b) and some refer to the average that was measured by all participating groups (ambient air measurements, Slemr *et al.* 2002). Moreover, another difficult question is which calibration standards should be used for the intercomparison experiments. While during NOMHICE each participating laboratory utilized its own calibration standard, general synthetic standard mixtures were used during AMOHA for all participants. As was shown by several experiments, the use of the appropriate calibration standard is a critical issue that might generate major discrepancies to the specified reference. As outlined by Larsen *et al.* (1997), the preparation of calibration standards is the most common error source in the analysis of organic trace gases. Utilisation of a general standard mixture will prevent errors derived from the use of individual calibration standards and will lead to better agreement with the reference value. On the other hand, individual calibrations are used during the routine laboratory work of the participating laboratories, and neglecting the uncertainty of different calibrations, will lead to artificially improved results.

Another issue in performing intercomparison studies is also the evaluation of the discrepancies discovered during the experiments. While some authors identified measurements with more than 30% deviation from the reference as outliers from the overall performance of the participating laboratories (Slemr *et al.* 2002), other authors defined specific data quality objectives (DQO) to prove the quality of their measurements (Volz-Thomas *et al.* 2002).

Since most of the previous intercomparison experiments were focused on the analysis of stable anthropogenic compounds, test gas mixtures were sent in special canisters to the participating laboratories. Mixing ratios of these canisters were usually tested by the reference laboratories before shipment and after return from the participating groups (Apel *et al.* 1994; 1999; 2003a; 2003b; Slemr *et al.* 2002; Volz-Thomas *et al.* 2002). However, for the less stable biogenic or oxygenated compounds this procedure is not recommended. While the distribution of isoprene canister samples during AMOHA and NOMHICE provided good

results, the distribution of α-pinene samples generated major discrepancies to the reference value due to compound losses in the parent cylinder and the canister samples (Apel *et al.* 1999). Since storage of biogenic volatiles is a critical issue, better results have been obtained by non-storing techniques as performed by permeation and diffusion systems for the generation of VOC mixing ratios (Larsen *et al.* 1997; Komenda *et al.* 2003). However, if the reference values are derived only by gravimetric calculations, major discrepancies to the reference concentrations might be obtained due to adsorption effects on the walls of the permeation/diffusion system.

Within the framework of the ECHO project (Emission and CHemical transformation of biogenic volatile Organic compounds, AFO 2000, see http://www.fz-juelich.de/icg/icg-ii/echo) two intercomparison experiments were carried out for quality inspection of VOC analysis. During both experiments 21 different chemical compounds were analysed by 11 analytical systems that were applied by 7 participating institutes. The following chapter will present the results and respective intercomparison of the GC-FID measurements (i.e. Gas Chromatography coupled to a Flame Ionisation Detector) and HPLC analysis (i.e. High Pressure Liquid Chromatography) that was performed by the Max Planck Institute (MPI) for Chemistry.

METHODS

SAMPLING AND ANALYSIS OF VOLATILE ORGANIC COMPOUNDS

Construction of the permeation system

For the intercomparison experiments I and II sampling of volatile organics was performed on permeation devices that were built up by the Research Centre Jülich. As outlined by Volz-Thomas *et al.* (2002) the latter technique provided more reliable results for compounds with higher boiling points than synthetic canister samples. The configuration of the permeation source was similar to the system described by Schuh *et al.* (1997) and is specified in detail by Komenda *et al.* (2003) and Ammann *et al.* (2004). In principle, the volatile organics were stored as liquid substances in small glass vials in a temperature controlled permeation chamber (temperature 25°C). Each vial contained a small punctured Teflon membrane through that the relevant compound was permeating/diffusing. The respective component was mixed with high purity nitrogen to mixing rations at a level of parts per million (ppm). By use of a capillary restrictor flow split, part of the calibration gas was diluted with humidified

synthetic air to mixing ratios at the level of parts per billion (ppb) or parts per trillion (ppt). Mixing ratios were calculated gravimetrically by the mass loss of the relevant permeation vial and from the flow of dilution gas. For the sampling and measurement of volatile organics all gas flows were mixed and conducted to a distribution device. To enable the differentiation of isobaric compounds (i.e. compounds owing the same molecular mass) for some measurement techniques, utilisation of different permeation chambers was crucial and was applied during intercomparison II. Overall 21 different volatile organic compounds were investigated during the experiments of intercomparison I to II by 7 different institutes, including online and offline analysis. The following chapter will focus on the measurement of non-oxygenated compounds and short chain carbonyls.

Sampling of VOCs on solid adsorbents as performed by the MPI for Chemistry

The sampling of volatile organics was conducted offline by utilisation of an automatic cartridge sampling device that was built by the MPI for Chemistry and is described in detail by Kuhn *et al.* (2005). As shown by Figure 2.1. A and B, the system consisted of a cartridge magazine as well as a control unit that could easily be mounted on a scaffold tower. The cartridge magazine comprised two independent sampling loops with 10 cartridge positions and one bypass each. Thus the setup allowed either the sampling from two different sources in parallel or simultaneous sampling of two different cartridge types. Moreover, if both loops were connected to a single source, sequential sampling of up to 20 cartridges was possible. To prevent contamination and/or the loss of volatiles, most surfaces prior to the adsorbent cartridges were made from perflouroalkoxy (PFA) Teflon. Each cartridge was guarded by two miniaturized sampling valves (at the inlet and outlet) that were operated by a microprocessor. The processor was part of the control unit and operated also the sampling flow, sampling time and the sampling volume. In the standard mode, the control unit contained two flow controller [size 500 sccm, MKS Instruments, USA] and a conventional membrane pump [KNF Neuberger, Germany] that generated the required air flow for sampling. Typical sampling flows were adapted to the actual cartridge type used and ranged between 80 and 300 ml min^{-1}. The cartridge magazine was connected via a heated PFA Teflon tubing [Metron Technology N.V., USA] to the distribution device of the permeation system. As outlined by Larsen *et al.* (1997) the retention of volatiles by condensing humidity in sampling systems might be a seroius problem for some volatile compounds. Therefore, the application of a heated inlet tubing was essential for the measurements, to prevent a condensation of water vapour. Thus, the tubing was heated slightly above ambient temperatures by the use of an anti-condensation

heating tape [RS-Components GmbH, Germany] that was fixed together with the inlet tubing in a conventional isolation hose.

Sampling of isoprene, monoterpenes, benzene, and toluene was performed by the use of graphitised carbon blacks (GCB). As reported in detail by Bruner *et al.* (1990) and Matisová and Škrabaková (1995), these materials are characterised by their excellent chemical inertness as well as their high thermal stability. In general, the retention of volatile organics is performed by London dispersion forces on the external homogenous surface of these adsorbent materials and is a function of temperature, the molecular size, and the shape of the adsorbed molecule. Since surface-to-surface interactions increase with an increasing adsorbent surface and an increasing length of the adsorbed molecules, higher specific retention volumes can be obtained for larger compounds. Furthermore most adsorption sites are nonpolar and the materials can be characterised as hydrophobic. Thus interferences from the co-trapping of water vapour are prevented. The adsorption cartridges that were used for VOC measurements during the present study were prepared in the late 1990s by the MPI for Chemistry and were utilised for various experiments in advance of intercomparison I and II (e.g. see Kesselmeier *et al.* 2002a; Kuhn *et al.* 2004a). As shown by Figure 2.2. A and B the cartridges consisted from two adsorbent types: 130 mg Carbograph 1 (90 m^2 g^{-1}, 20-40 mesh) and 130 mg Carbograph 5 (560 m^2 g^{-1}, 20-40 mesh) [LARA, Italy] that were packed into tubes made from Silicosteel® [¼" OD, 89 mm length, RESTEK, USA] and were separated

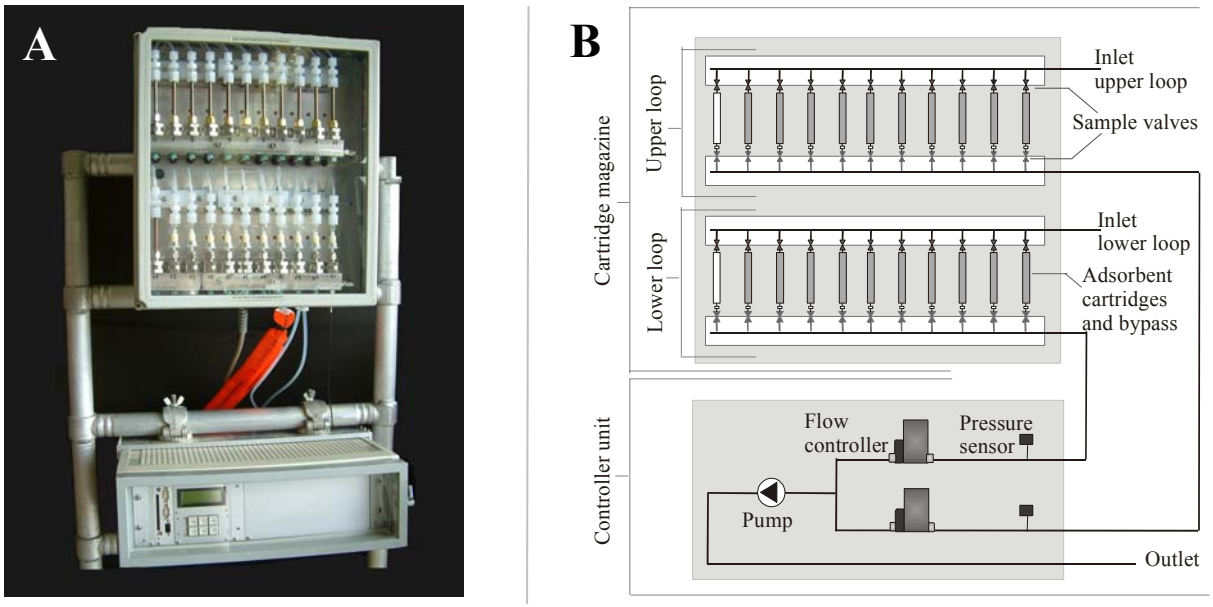

Figure 2.1. Automated cartridge sampling device. (A) Cartridge magazine and control unit mounted on a scaffold. (B) Schematic drawing of basic components of the cartridge magazine and control unit (electrical connection and microprocessor control not shown).

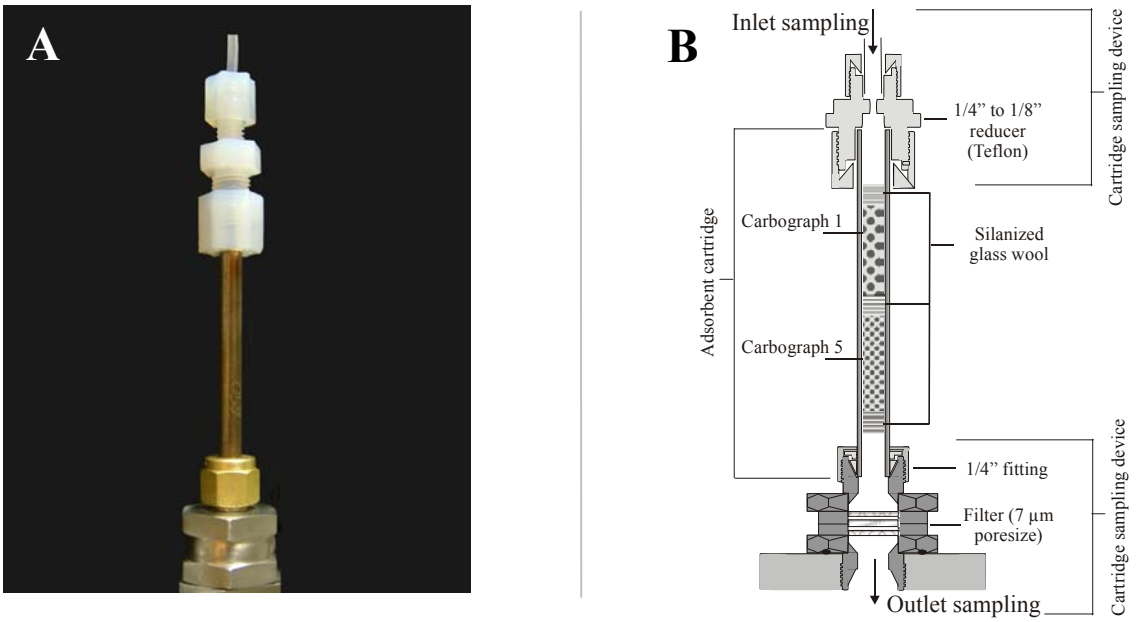

Figure 2.2.: Adsorbent cartridge for sampling of volatile organic compounds. (A) Assembly of adsorbent cartridge, inlet tubing and filter as used in the automatic sampling device. (B) Schematic drawing of the adsorbent cartridge mounted in the cartridge magazine of the automatic sampling device. When sampling volatile organic compounds the airflow sequentially passes Carbograph 1 and Carbograph 5.

from each other by silanized glass wool. As reported by Brancaleoni *et al*. (1999), both adsorbents are classified as class I adsorbent materials (i.e. they interact non-specifically with all groups of adsorbates). Moreover, they demonstrated that Carbograph 5 was much more effective in retaining small volatile organics than other GCB materials (see also Sampaolo *et al.* 1999; Mastrogiacomo and Pierini 2000). As reported by Mastrogiacomo *et al.* (2002) this effect was caused by the contribution of micropores (pore size < 6 nm) that increased the adsorbent surface to even more than 560 m^{-2} g^{-1} (the manufacturers specification refers to the non-graphitised material). Moreover these authors reported that the standard free energy of adsorption is extraordinary low for Carbograph 5 and decreases constantly with the number of carbon atoms in the adsorbate. The latter effect is indicative of the adsorption of volatiles in a plane position in parallel to the adsorbent surface (Troube's effect), and explains the higher retention volumes that are obtained for larger adsorbates. To protect the high surface area of Carbograph 5 from irreversibly adsorbed molecules during the sampling of volatile organics, the adsorbent tube was arranged in the automatic sampling device in a way that the air flow first passed the weakest adsorbent (i.e. Carbograph 1). According to the results of various laboratory tests that were performed by the Max Planck Institute for Chemistry and in agreement with the safe sampling volumes reported by Brancaleoni *et al.* (1999), the

sampling of volatile organics was performed at room temperature at a flow rate adjusted to 80 and 150 ml min^{-1}. With sampling times of 60 and 30 min, typical sampling volumes ranged at 4800 and 4500 ml.

Sampling of VOCs on solid phase extraction cartridges as performed by the MPI for Chemistry

Sampling of short chain carbonyl compounds (i.e. formaldehyde, acetaldehyde or acetone) was performed by the use of solid adsorbents that were coated with 2,4-dinitrophenylhydrazine ($C_6H_6N_4O_4$, DNPH). As shown by Figure 2.3 and reported in detail by Vairavamurthy *et al.* (1992), the short chain carbonyl compounds were trapped by nucleophilic addition of DNPH to the carbonyl C-atom resulting in the formation of the relevant hydrazone and water. In general, the reaction for carbonyl compounds is preferred if the organic residuals R1 and/or R2 are small. Moreover, the reaction times for ketones are slower than for aldehydes (Staudinger *et al.* 1968). In liquid solutions protonation of the carbonyl group promotes the nucleophilic addition and a maximum yield of the hydrazone-derivative is obtained at a characteristic pH level. Also ambient temperature and DNPH concentration play a crucial role for the reaction yields. By utilisation of DNPH impregnated solid sorbents, the formation of hydrazones can take place in the remaining liquid-phase film as well as by gas-solid phase reaction. Due to higher loadings of DNPH on the solid sorbent, the derivatisation may proceed faster than in liquid solution. Furthermore, the low water availability on solid sorbents facilitates the equilibrium reaction towards the hydrazone for-

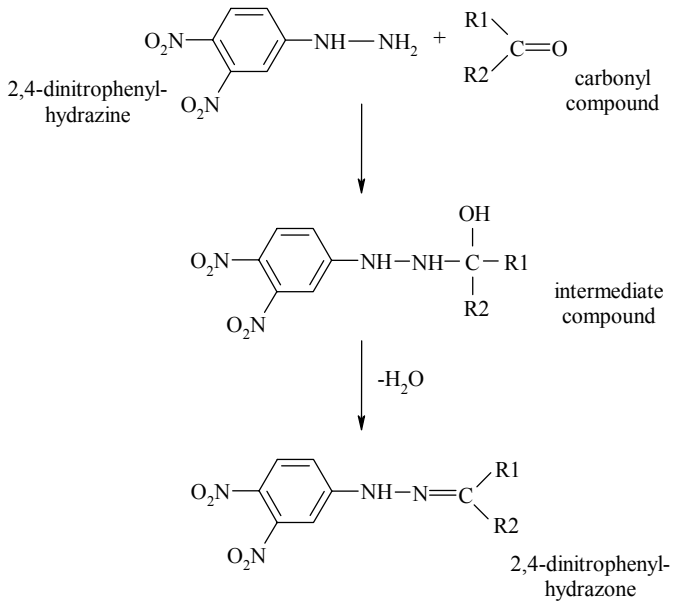

Figure 2.3. Reaction of carbonyls with 2,4-dinitrophenylhydrazine (DNPH). In a first step, aldehydes and ketones react with DNPH by nucleophilic addition of the hydrazine to the carbonyl C-atom to form an intermediate product. In a second step, the intermediate decomposes by 1,2-elimination of water to form the 2,4 dinitrophenylhydrazone-derivative (Schwetlik 2004).

mation, yielding lower derivatisation times. For sampling of short chain carbonyl compounds during the experiments of intercomparison I and II, two different solid phase materials were investigated. During intercomparison I the sampling of carbonyls was achieved by the use of solid phase extraction (SPE) cartridges that were filled with 500 mg (~3 ml) octadecylsilane (ODS, C_{18}) bonded silica [Bakerbond spe^{TM} columns, borosilicatglass with PTFE filter, packed with ODS, endcapped, see Figure 2.5. C and D, J.T. Baker, USA]. In contrast to the pure silica matrix that contains a multitude of hydroxyl groups, C_{18} cartridges are characterised by their hydrophobic, nonpolar, and inert surface. For sampling of volatiles the cartridges were coated with 60 µg DNPH. Sample preparation was accomplished in analogy to the method described by Zhou and Mopper (1990) and Kesselmeier *et al.* (1997).

As shown by Figure 2.4., sample preparation comprised several steps starting with the purification of commercially available DNPH [MERCK, Germany] by recrystallisation in acetonitrile [ACN, Rathburn, Great Britain] and the preparation of an acidified DNPH stock-solution. This stock solution, mixed with ACN and Milli-Q water, was utilised for the preparation of the final coating solution that was prepared on a day to day basis. To eliminate potential contaminations only clean and inert materials (e.g. glassware, Teflon) were used. Moreover, all solutions were analysed for impurities before their use. New C_{18} cartridges bought from the manufacturer had to be purged from contaminations prior to their utilisation for VOC sampling. Therefore, new cartridges were flushed with ACN and were coated with DNPH. Preconditioning was achieved by storage for at least 24 h. For the sampling of short chain carbonyls, the preconditioned C_{18} cartridges were flushed again with ACN and were covered with DNPH coating solution. After drying with high purity nitrogen, the cartridges were closed by Teflon caps and were wrapped with aluminium foil to grant a sufficient protection from sunlight. The cartridges were stable for at least 2 weeks when stored at 4°C (Schäfer 1997). According to Kesselmeier *et al.* (2002a) the sampling efficiency for form- and acetaldehyde was better than 95%. In contrast, the commercially available cartridge type used for the intercomparison II experiment was packed with 349 mg pure silica adsorbent material that was coated by the manufacturer with ~1 mg DNPH (particle size 500-1000 µm, 18/35 mesh) [XPoSure^{TM} Aldehyde Sampler, see Figure 2.5. A and B, WATERS, USA]. According to the manual that was supplied by the manufacturer, no protection of the silica cartridges from sunlight was necessary.

As shown by Figure 2.5. A and B, silica cartridges were inserted in the automatic sampling device by use of inert glass adapters. C_{18} cartridges were inserted by the use of PTFE Teflon adapters (Figure 2.5. C and D). According to the results of various laboratory measurements

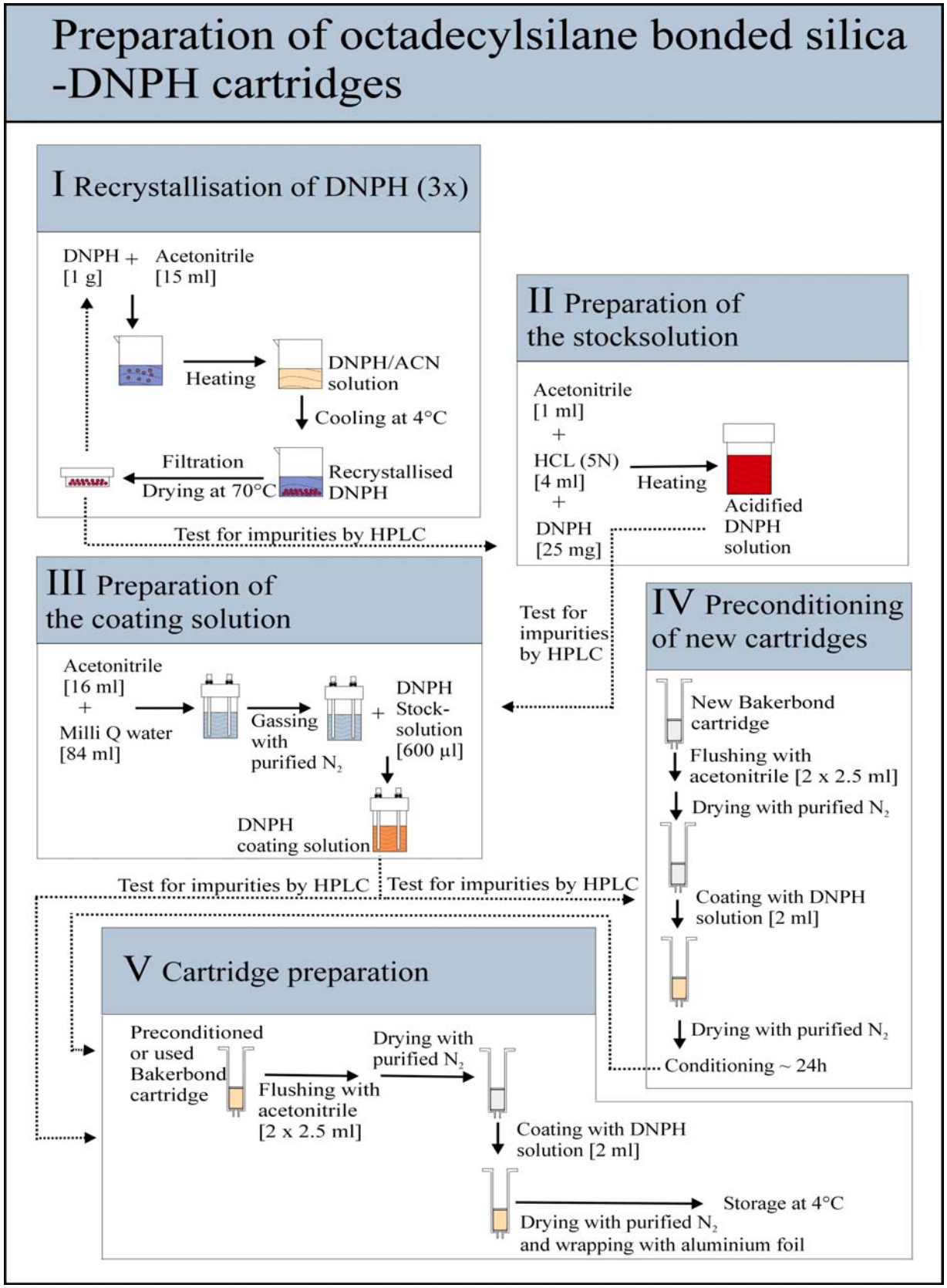

Figure 2.4. Preparation of octadecylsilane bonded silica-DNPH cartridges. Production includes DNPH purification by recrystallisation, preparation of a stock- and coating solution, preconditioning of new cartridges, and coating of preconditioned or used cartridges.

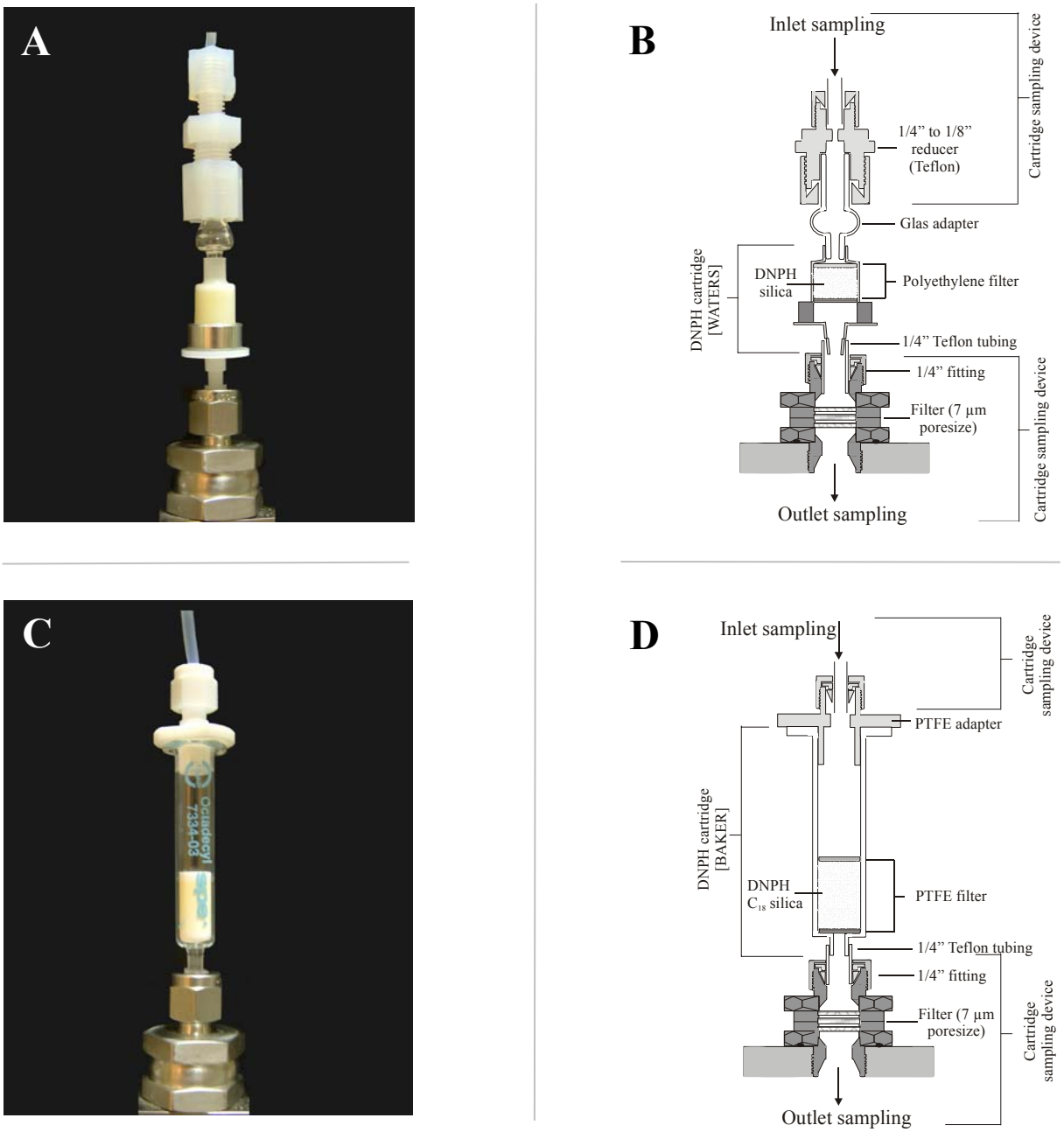

Figure 2.5. Solid phase extraction (SPE) cartridges for sampling short chain carbonyl compounds. (A) and (B) assembly and components of SPE silica cartridges [XPoSure, Waters, USA] as mounted in the automatic sampling device. (C) and (D) assembly and components of SPE C_{18} cartridges [Bakerbond, Baker, USA] mounted in the sampling device.

and field campaigns (e.g. Schäfer 1997; Kesselmeier *et al.* 2002a; Rottenberger *et al.* 2004), sampling of short chain carbonyl compounds was performed at flow rates of 300 ml min^{-1} for sampling times ranging between 30 min and 3 hours, depending of the carbonyl mixing ratio of the test gas (corresponding sample volumes ranged between 18 to 54 l).

Oxidant interference and ozone scrubber

For the measurement of volatile organics in ambient air it is necessary to remove oxidants prior to the concentration step. Especially interference from the co-trapping of ozone on adsorbent materials may lead to the formation of artefacts from reactions with the trapping material as well as losses and/or artefact formation from reactions with trapped volatile organics (e.g. Pellizzari *et al.* 1984; Roberts *et al.* 1984; Jüttner 1988; Hoffmann *et al.* 1993; Peters *et al.* 1994; Hoffmann 1995; Calogirou *et al.* 1996; Larsen *et al.* 1997). According to Pellizzari and Krost (1984) and Calogirou *et al.* (1996), the degree of decomposition of adsorbed volatile organics is a function of their molecular structure. However, the sensibility towards an interference of ozone to trapped volatile organics also depends on the type of adsorbent material that is used (carbon type adsorbent materials seem to be less prone to ozone interferences, see Cao and Hewitt 1994; Larsen *et al.* 1997).

But ozone removal prior to the preconcentration step is also crucial for the application of derivatisation techniques (Arnts and Tejada 1989; Sirju and Shepson 1995; Kleindienst *et al.* 1998; Ferrari *et al.* 1999). Ozone interference to DNPH coated carrier materials lead to a depletion of DNPH, radical formation, and/or to the depletion of the carbonyl derivatives that were formed. Moreover various carbonyl-hydrazones and other DNPH-products were formed when the samples were exposed to ozone. Comparison of different carrier materials revealed that surface passivated carrier materials (e.g. ODS bonded silica) were less prone to interferences than the pure silica carrier materials, because their C_{18} phase can scavenge produced radicals (Arnts and Tejada 1989).

To prevent ozone interferences various ozone scrubbing techniques have been used. A detailed overview on these different scrubber techniques is given by Helmig (1997). A technique that has been applied in particular for the analysis of biogenic compounds is the utilisation of manganese dioxide (MnO_2). Although, the recovery of many volatile organic compounds depends on the design and the production of the MnO_2 coated carrier material (Helmig 1997), good results were achieved by use of MnO_2 coated copper screens taken from commercially available ozone analysers (Hoffmann 1995). As reported by Calogirou *et al.* (1996) good results were obtained by utilisation of a miniaturized scrubber that consisted of 8 plies of MnO_2 covered copper nets with a total surface of about 4 cm^2 (flow rates adjusted to 50-200 ml min^{-1}). In general the utilisation of these MnO_2 covered copper screens prevented an underestimation of various terpenes in ambient air (Hoffmann *et al.* 1993; Hoffmann 1995; Calogirou *et al.* 1996). However, as reported by Fick *et al.* 2000, the recovery for some organics, in particular oxygenated compounds decreased by use of this scrubber material.

The ozone scrubber used during the experiments of intercomparison I to II was installed directly prior to the inlet of the cartridge magazine. As shown by Figure 2.6. it consisted of 10 MnO_2 covered copper nets that were cut from commercially available scrubbers [Ansyco, Germany] and placed in a ½" PFA Teflon tubing, yielding a total scrubber surface of 6 cm^2. To protect the sample valves inside the cartridge magazine from MnO_2 dust particles, the ozone scrubber assembly was guarded by Teflon filters of 2 µm poresize that were mounted up- and downstream of the MnO_2 covered copper screens [Pall, USA].

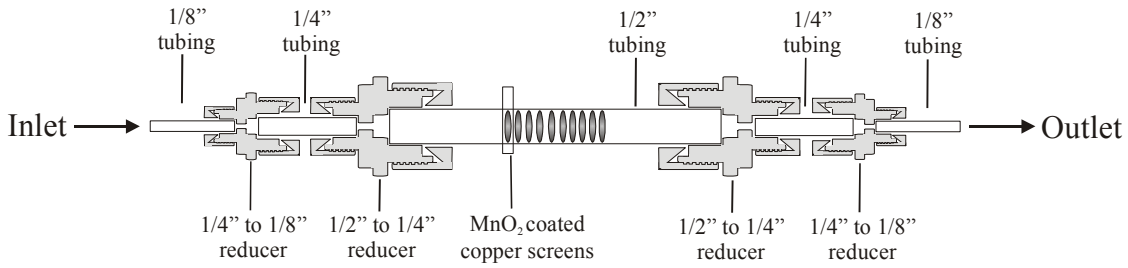

Figure 2.6. Ozone scrubber assembly. In combination with a Teflon filter the scrubber assembly can be connected to the automatic sampling device.

Potential effects of this scrubber assembly on the recovery of two volatile organic compounds (isoprene and β-pinene) were tested by laboratory experiments conducted at the Max Planck Institute for Chemistry with a proton transfer reaction mass spectrometer [PTR-MS, Ionicon Analytik GmbH, Austria]. The latter technique is based on chemical ionisation of volatiles by a primary reactant ion (here H_3O^+) and allows measurements at very high time resolutions. Since most volatile organics have a proton affinity exceeding that of water molecules they can be gently protonated by H_3O^+ reaction and can be detected by conventional mass spectrometry. A detailed overview of the measurement technique can be obtained from literature (e.g. see Hansel *et al.* 1995; Lindinger *et al.* 1998; Kleiss 2004). For evaluation of potential scrubber effects, the instrument was connected to a gas mixing device that consisted of a glass vial containing the respective volatile, kept under a constant flow of nitrogen at 0°C. After passing through the volatile solution, the nitrogen was diluted to mixing ratios at the level of several parts per billion (ppb) prior passing through the scrubber assembly at flow rates of about 125 ml min^{-1}. Since adsorption effects are expected to be more pronounced at dry air conditions when the scrubber surface areas are not covered by water molecules, no humidification was applied during the latter experiment. By regulation of the dilution gas flow various mixing ratios were set.

Analysis of VOCs sampled on solid adsorbents

Analysis of collected volatile organics was achieved at the Max Planck Institute for Chemistry by use of chromatographic techniques. Volatile organics, that were sampled on graphitised carbon black adsorbents by utilisation of the automated cartridge sampling device were analysed by gas chromatography coupled to flame ionization detection (GC-FID). Analysis and reintegration of the GC-FID samples was performed by the GC-laboratory group of the MPI for Chemistry in Mainz.

As reported in detail by Ciccioli *et al.* (2002) the net retention volume for a specific volatile organic on graphitised carbon black adsorbents decreases exponentially with increasing temperatures. Thus, heating of the adsorbent material induces a rapid release of sampled compounds. As described previously by Kesselmeier *et al.* (2002a) cartridges filled with Carbograph 1 and 5 were desorbed thermally by utilisation of a two step desorption system [Model ATD400, Perkin Elmer, Germany] that was connected to a GC-FID [Model AutoSystem XL, Perkin Elmer, Germany]. Thermal desorption was achieved at 260°C with flow rates of 63 ml min^{-1} (helium 6.0) in a backflush mode (i.e. inverse to the sampling direction) for a time period of 10 min. In order to enhance the chromatographic resolution resulting in less peak broadening, the second stage focus consisted of a small quartz tube that was packed with 20 mg Carbograph 1 kept at -30°C. For a rapid injection of sampled volatiles, the latter VOC-trap was heated to 280°C within a few seconds at flow rates adjusted to 7.3 ml min^{-1}. The volatile organics were transferred via a heated inlet line to the GC-FID at flow rates of 1.1 ml min^{-1} (resulting from a split ratio of 6.2/1.1 ml min^{-1}). Peak separation was achieved by partition chromatography on a capillary column containing a liquid film of a non polar stationary phase [model HP-1, 100 m length, 0.25 mm ID, 100% dimethylpolysiloxane ($(CH_3)_3$-Si-[O-Si-$(CH_3)_2$-]$_n$-O-Si-$(CH_3)_3$), film thickness 0.5 µm, Agilend Technologies, USA]. The temperature program used for analysis ranged between -10 and 220°C (-10 to 40°C at 20°C min^{-1}, 40 to 145°C at 1.5°C min^{-1}, and 145 to 220°C at 30°C min^{-1}). Chromatographic separation of one sample was performed within 90 min. Peak detection was accomplished by utilisation of a build in flame ionisation detector (FID).

As described by Gottwald (1995), the current produced in the detector is proportional to the mass of volatiles that are detected. In general, the detector consists from a burner that burns a mixture of high purity hydrogen (H_2) and synthetic air and an ion collector electrode kept at about -200 V (manufacturer specifications, Perkin Elmer, 1997). For detection of volatiles the H_2 gas flow is mixed with carrier gas derived from the chromatographic column. According to Holm 1999, formylium ions (CHO^+) and electrons (e^-) are formed by chemi-

ionisation at a yield of approximately one ion per 10^6 carbon atoms if volatiles are present. In general, the formylium ions are formed by reaction of hydrocarbon-radicals with oxygen-radicals (originating from synthetic air). The hydrocarbon-radicals are derived from methane that is produced from the hydrogenolysis of VOCs inside the flame. Since every 10^{6th} carbon atom finally produces a formylium ion, the FID signal derived from hydrocarbons is proportional to the number of carbons present in the original molecule (rule of equal response per carbon).

However, some chemical structures are less prone to hydrogenolysis. As reported by Holm (1999), a carbon atom bonded to a heteroatom may or may not be converted to methane, resulting in a lower signal response from the detector. The latter effect was the basis for the development of the empirical "effective carbon number concept" that defines the relative contribution of different functional groups to the signal response. According to Sternberg *et al.* (1962), the contribution of different functional groups to the number of "effective carbon atoms" in a molecule varies between zero and 1.0 (see also the studies of Ackmann 1964 and Blades 1976). As shown by Table 2.1. for aliphatic, aromatic, an approximately also for olefinic molecules the "effective carbon number" is equal to the real carbon number of the molecule. Carbonyl groups on the other hand have no contribution to the effective carbon number.

Table 2.1. Contribution of different functional groups to the effective carbon number (modified according to Sternberg *et al.* 1962).

Type of functional group	Contribution to effective carbon number
Aliphatic	1.0
Aromatic	1.0
Olefinic	0.95
Carbonyl	0

Based on the latter concept and the experiments performed by Komenda (2001), calibration for volatile organics containing no heteroatoms was achieved by utilisation of a gaseous standard mixture containing isoprene and several n-alkanes (n-pentane, n-hexane, n-heptane, n-octane, n-nonane, and n-decane), yielding a signal response that is proportional to the real carbon number (which in this case is equivalent to the effective carbon number). Volatile organics that were evaluated by these analysis were summarised in Table 2.2.. The

peak identification and integration was performed by use of the software Turbochrom 4 [Perkin Elmer, Germany]. All compounds were identified by their respective retention times.

Table 2.2.: Volatile organics evaluated by GC-FID analysis. Annotation: [a] compound of calibration gas standard, [b] compound evaluated during intercomparison I and II.

Volatile organic compound		Chemical structure	Retention time [min]
Alkanes	n-pentane [a]		~14.5
	n-hexane [a]		~18.8
	n-heptane [a]	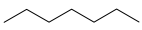	~26.1
	n-octane [a]		~36.2
	n-nonane [a]		~47.9
	n-decane [a]	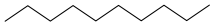	~59.9
Hemiterpenes	Isoprene [a, b]		~14.8
Monoterpenes	Camphene		~54.3
	Δ-3-carene [b]	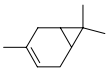	~61.4
	p-cymene	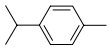	~62.1
	Limonene	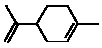	~63.3
	myrcene	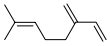	~58.2
	α-pinene [b]		~52.5
	ß-pinene [b]		~57.5
	Sabinene	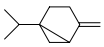	~56.6
	α-terpinene	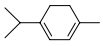	~61.8
	γ-terpinene	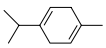	~66.4
Aromatic	Benzene [b]		~22.4
compounds	Toluene [b]		~31.8
	o-xylene		~46.1

Analysis of VOCs sampled on solid phase extraction cartridges

Analysis of carbonyl-DNPH derivatives was performed by use of high pressure liquid chromatography (HPLC) coupled with an UV-VIS detection system. Carbonyl-hydrazones that were trapped on SPE C_{18}-cartridges were eluted with ~2 ml ACN (measured by a gravimetric approach on a laboratory balance [L 610D, Sartorius, Germany]). Carbonyl-derivatives that were trapped on pure silica cartridges had to be eluted with ~10 ml of ACN according to the higher loading of DNPH on the latter cartridges.

Independent of the system used, 2 ml of the latter eluate were transferred to small glass vials. For analysis 20 µl of the eluate were injected to the HPLC system by use of a temperature controlled automatic injector [model SIL- 10AD vp, tempered to 4°C, Shimadzu, Japan]. Chromatographic separation of carbonyl-derivatives was obtained by use of reversed phase chromatography as described previously by Dindorf (2000), consisting of a hydrophobic stationary phase and a hydrophilic mobile phase. For best results the stationary phase consisted of a Hypersil ODS column [model HSOD 10512 S1202, 125 mm length, 2 mm ID, particle size 5 µm, Grom, Germany]. The mobile phase comprised a gradient of acetonitrile and ultra pure water [Millipore, USA] that was specified as follows: 0.1 to 3 min 38% ACN, 6 min 43% ACN, 12 min 70% ACN, 20 min 90% ACN, and 35 min 38% ACN. To prevent embolism, both solvents were purified from dissolved gases by use of a degasser unit [model DGU-14A, Shimadzu, Japan]. The degaser unit was mounted at the system inlet prior to the high pressure pumping and mixing chamber system [model LC-10AD vp, Shimadzu, Japan] that was installed in front of the chromatographic column. Detection of carbonyl-hydrazones was achieved by a UV-VIS detector [model SPD 10AV vp, deuterium lamp, Shimadzu, Japan].

As reported in detail by Vairavamurthy *et al.* (1992), absorption maxima of specific carbonyl-hydrazones vary significantly from each other (e.g. formaldehyde-DNPH (353, 350, 345 nm), acetaldehyde-DNPH (363, 360 nm), acetone-DNPH (367 nm), DNPH-reagent (357 nm)). Thus, detection is usually performed at wavelength ranging between 360-375 nm. Consequently we applied a wavelength of 365 nm for the present study.

Calibration of the system was performed by utilisation of several carbonyl-hydrazone standard mixtures [Supelco, USA] that were diluted with ACN. Peak identification and integration was performed by the software Class vp 5.0 [Shimadzu, Japan]. All elements of the HPLC-UV-VIS system were regulated by a controller unit [model SCL 10AV vp, Shimadzu, Japan]. Carbonyl-hydrazones that were evaluated from these analysis were summarised in Table 2.3.. All analysed compounds were identified by their retention times.

Table 2.3. Volatile organics evaluated by HPLC-UV-VIS analysis. Annotation: [a] compound in standard mixture, [b] compound evaluated during intercomparison I and II.

Volatile organic compound		Chemical structure	Retention time [min]
Aldehydes	Formaldehyde [a]	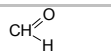	~5.5
	Acetaldehyde [a,b]		~7.5
Ketones	Acetone [a,b]	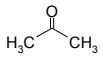	~9.3

CALCULATION OF VOC MIXING RATIOS

Calculation of calibration factors for GC-FID analysis

The calibration of the GC-FID system was performed by the GC-laboratory group of the MPI for Chemistry in Mainz. According to Larsen *et al.* (1997), the preparation of calibration standards is the most common error source in the analysis of organic trace compounds. On a first approach, mixing ratios derived from GC-FID analysis during intercomparison I were calculated by use of liquid standards. These standards comprised a mixture of the relevant organic compound in methanol and were injected to the adsorption tubes by use of a syringe. Thereafter the adsorption tubes were desorbed thermally according to the procedure described above. However, preliminary tests revealed that mixing ratios derived from utilisation of these liquid standards generated major discrepancies to the VOC concentrations specified during intercomparison I.

In agreement with the concept of "effective carbon numbers "and based on the experiments performed by Apel *et al.* (1994; 2003a; 2003b) and Komenda (2001), mixing ratios for volatile organics that contain solely carbon in their molecular structure were therefore calculated using a gaseous standard of stable n-alkanes (n-pentane, n-hexane, n- heptane, n-octane, n-nonane, n-decane) and isoprene mixed with high purity nitrogen [calibration gas standard, Apel-Riemer, USA]. Mixing ratios of the standard used for GC-FID calibration ranged between 9 and 16 ppb for the relevant standard compound. The standard mixture was sampled under laboratory conditions on adsorbent cartridges resulting in normalised standard amounts ranging between 1 and 473 ng per cartridge (standard conditions 0°C, 56 standard injections). After analysis by GC-FID, calibration factors were calculated from the slope of linear regression according to Formula 2.1..

$$\text{Cal Factor} = \frac{\text{Area}_{\text{Standard}}}{\text{Amount}_{\text{Standard}}} \qquad 2.1.$$

Formula 2.1.: $\text{Amount}_{\text{Standard}}$ = amount of the standard [ng], $\text{Area}_{\text{Standard}}$ = area of the standard [µV s], Cal Factor = calibration factor [µV s ng^{-1}]

The calibration of n-pentane and n-decane is shown in Figure 2.7. for all standards analysed by GC-FID in the years of 2002 and 2003. As summarised by Table 2.4. and in consensus to the "concept of effective carbon numbers" (Sternberg *et al.* 1962), the calibration factors for n-alkanes were in reasonable agreement with each other. Calibration factors calculated for isoprene varied by 22% between both years. Calibration factors calculated for n-alkanes varied between ± 6% between both years but were generally lower in 2002. Correlation coefficients (r^2) ranged between values of 1.00 for all data obtained in the year 2002 and values of 0.82 for n-pentane obtained in the year 2003. In general, the correlation coefficients for the year 2002 were better than in 2003. This is likely a result of higher amounts of standard gas that were used in the year 2002.

As shown in Table 2.4., calibration factors calculated for isoprene increased in 2003. As reported by Apel *et al.* (1994) a decrease of isoprene concentrations in electro polished stain-

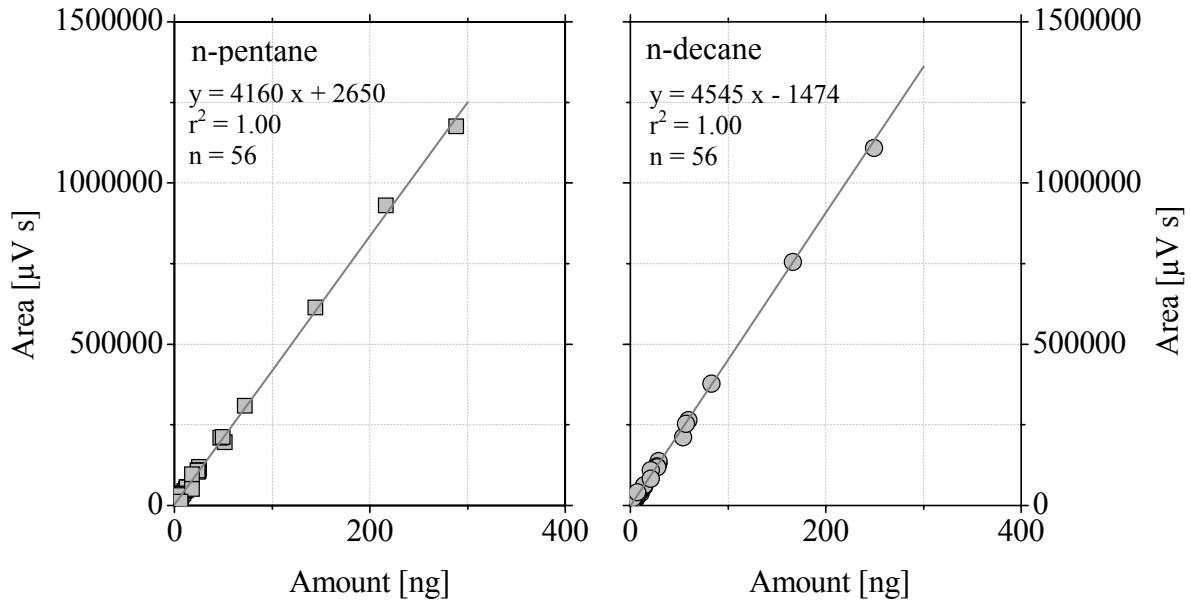

Figure 2.7. Calibration of hydrocarbons by utilisation of a gaseous standard mixture [Apel-Riemer, USA] in the years of 2002 and 2003. Standards of n-pentane (square) and n-decane (circles) were collected on adsorbent traps that were analysed by GC-FID. The slope and intercept of linear regression analysis (grey line) are indicated in the relevant graph for the respective compounds.

less steel canisters was observed over a period of 14 month. However, during the present study an increase of isoprene response was observed. Since the calibration factors of other hydrocarbons are in good agreement between both years, analytical problems regarding the performance of the chromatographic column or the FID response are unlikely and an explanation for the increase in isoprene response remains unclear. Due to the reported increase in the FID response of isoprene, a common calibration factor was used, integrating only all n-alkane-standards measured by GC-FID in the years of 2002 and 2003. The latter factor was calculated to 4468 µV s ng^{-1} (at standard conditions of 0°C) and was used for the calculation of all sample-compounds that excluded hetero-atoms in their molecular structure. Differences of the individual n-alkane calibration factors to this summarised factor ranged below ± 10%. Differences between isoprene calibration factors obtained in 2002 and the summarised factor accounted only to -2%. The differences between isoprene calibration factors obtained in 2003 to the summarised factor accounted to + 25%.

Table 2.4. Calibration factors of hydrocarbons for the years of 2002 and 2003 (GC-FID analysis).

	Calibration factor in µV s ng^{-1} and [r^2]		
Volatile organic compound	year 2002	year 2003	year 2002 and 2003
n-pentane	4158 [1.00]	4010 [0.82]	4160 [1.00]
Isoprene	4561 [1.00]	5570 [0.98]	4558 [1.00]
n-hexane	4503 [1.00]	4756 [0.97]	4503 [1.00]
n-heptane	4465 [1.00]	4443 [0.95]	4463 [1.00]
n-octane	4488 [1.00]	4259 [0.90]	4487 [1.00]
n-nonane	4517 [1.00]	4235 [0.89]	4516 [1.00]
n-decane	4555 [1.00]	4515 [0.96]	4545 [1.00]

Calculation of calibration factors for HPLC analysis

For DNPH-derivatives calibration was achieved by use of liquid standards ranging between 100 and 10000 nmol l^{-1} that were injected directly to the HPLC system. Calibration factors were calculated in analogy to Formula 2.1. and ranged at 27 µV s $nmol^{-1}$ l^{-1} for acetaldehyde and acetone.

Calculation of mixing ratios

For GC-FID analysis the calculation of VOC mixing ratios in units of parts per billion (ppb) followed Formula 2.2.. The calibration factor was given in units of µV s ng^{-1}. For HPLC

analysis VOC mixing ratios were calculated accordingly by Formula 2.3. Here, the calibration factor was given in units of μV s $nmol^{-1}$ l^{-1}.

$$\text{Mixing Ratio} = \frac{\text{MV}}{\text{Cal Factor} \cdot \text{MW}} \cdot \frac{(\text{Area}_{\text{Sample}} - \text{Area}_{\text{Blank}})}{\text{SV}} \qquad 2.2.$$

$$\text{Mixing Ratio} = \frac{\text{MV}}{\text{Cal Factor} \cdot \text{EV}} \cdot \frac{(\text{Area}_{\text{Sample}} - \text{Area}_{\text{Blank}})}{\text{SV}} \qquad 2.3.$$

Formula 2.2. and 2.3.: $Area_{Sample}$ = area of the sample [μV s], $Area_{Blank}$ = area of the blank [μV s], Cal Factor = calibration factor [μV s ng^{-1}] or [μV s $nmol^{-1}$ l^{-1}], EV = volume eluted from DNPH-cartridge [l], MV = mole volume of an ideal gas [22.4 l mol^{-1}, 0°C, 1 bar], MW = molecular weight of the respective compound [g mol^{-1}], SV = air volume sampled on the respective cartridge [l], Mixing ratio = mixing ratio of the respective compound [ppb]

APPLIED STATISTICS

The measured data were evaluated using several statistical procedures. The following paragraph will focus of the statistical techniques that were applied. A detailed overview of these statistical methods can be obtained from statistical handbooks like Doerffel (1996) and Lozan and Kausch (1998).

Average, standard deviation and empirical variance

The arithmetic average and the standard deviation of a group of symmetrical distributed data points were calculated by application of the Formulas 2.4. and 2.5.. Considering the calculation of the standard deviation, Formula 2.5. calculates the deviation of random samples from their arithmetic mean. The empirical variance is given as the square of the standard deviation.

$$\bar{x} = \frac{\sum x_i}{n} \qquad 2.4.$$

$$s = \sqrt{\frac{n \cdot \sum x_i^{\,2} - \left(\sum x_i\right)^2}{n \cdot (n-1)}} \qquad 2.5.$$

Formula 2.4. and 2.5.: n = number of data points, s = standard deviation, x = arithmetic mean, x_i = single value

Slope, intercept and Pearson product moment correlation coefficient

The slope of linear regression from a group of data pairs (x_i, y_i) was calculated by application of Formula 2.6.. The y-axis intercept was calculated by use of the linear slope b according to Formula 2.7. with $\bar{x}$ and $\bar{y}$ representing the respective average of all x and y values.

$$b = \frac{n\sum x_i y_i - \left(\sum x_i\right)\cdot\left(\sum y_i\right)}{n\sum {x_i}^2 - \left(\sum x_i\right)^2} \qquad 2.6.$$

$$a = \bar{y} - b\cdot\bar{x} \qquad 2.7.$$

To give a measure of the linear correlation between two datasets (x_i, y_i), the Pearson product moment correlation coefficient was calculated according to Formula 2.8., yielding a coefficient ranging between +1 and -1, with +1 and -1 giving the best correlation between two datasets.

$$r = \frac{n\left(\sum x_i \cdot y_i\right) - \left(\sum x_i\right)\cdot\left(\sum y_i\right)}{\sqrt{\left(n\sum {x_i}^2 - \left(\sum x_i\right)^2\right)\cdot\left(n\sum {y_i}^2 - \left(\sum y_i\right)^2\right)}} \qquad 2.8.$$

Formula 2.6. to 2.8.: a = y-axis intercept, b = slope of linear regression, n = number of data points or data pairs, r = Pearson product moment correlation coefficient, x = arithmetic average of all x values, x_i = single value, x-axis, y = arithmetic average of all y values, y_i = single value, y-axis

Nalimov-outlier test

By assuming a normally distributed group of data points, outliers from the Gaussian function can be identified by using an outlier test. Here, we applied the outlier test according to Nalimov (see e.g. Lozan and Kausch 1998) that calculates a test statistic r* that is compared to a tabular value of r. r* is calculated by application of Formula 2.9., were x* is the value suspected to be an outlier. If r* > r, x* is identified as an outlier with a respective likelihood (95 to 99.9%).

$$r^* = \frac{\left|x^* - \bar{x}\right|}{s}\cdot\sqrt{\frac{n}{n-1}} \qquad 2.9.$$

Formula 2.9.: n = number of data points, r* = test statistic, s = standard deviation, x = arithmetic average, x* = value suspected to be an outlier

F-test

The F-test serves as an evaluation of two variances that were calculated from two homogeneous normally distributed data groups (x_{i1} and x_{i2}). For application of the F-test, a test statistic f* is calculated according to Formula 2.10., with s_1 and s_2 giving the respective standard deviation of a data group with the indices 1 and 2. Note, that in the formula stated below index 1 is always used for the highest standard deviation. After calculation of the test statistic, f* is compared to a tabular value of f (with $f_1 = n_1-1$ and $f_2 = n_2-1$) yielding the respective likelihood that s_1 and s_2 are different from each other (95 to 99.9%).

$$f^* = \frac{{s_1}^2}{{s_2}^2} \qquad 2.10.$$

Formula 2.10.: f* = test statistic, s_1 = standard deviation data group 1, s_2 = standard deviation data group 2

T-test

The T-test is an objective measure whether two averages may be combined to one common, i.e. both single averages are equal to each other. The T-test is applied by calculation of a test statistic t* that is compared to a tabular value of t. The test statistic t* is calculated according to the Formulas 2.11. and 2.12.. If t* < t, both average values are equal to each other with the respective likelihood (95 to 99.9%).

$$t^* = \left| \frac{\bar{x}_1 - \bar{x}_2}{s_d} \right| \cdot \sqrt{\frac{n_1 \cdot n_2}{n_1 + n_2}} \qquad 2.11.$$

$$s_d = \sqrt{\frac{(n_1 - 1) \cdot {s_1}^2 + (n_2 - 1) \cdot {s_2}^2}{n_1 + n_2 - 2}} \qquad 2.12.$$

Formula 2.11. and 2.12.: n_1 = number of data points data group 1, n_2 = number of data points data group 2, s_1 = standard deviation data group 1, s_2 = standard deviation data group 2, x_1 = arithmetic average data group 1, x_2 = arithmetic average data group 2

UNCERTAINTY OF CALCULATED VOC CONCENTRATIONS

Accuracy, precision, and reproducibility are measures for the uncertainty of calculated mixing ratios of volatile organic compounds. Under the assumption that errors were not correlated with each other and are distributed normally, precision can be calculated by error propagation

for a single measurement. Reproducibility can be calculated from the average and standard deviation of a series of samples of the same quantity. Since precision and reproducibility are a measure of the repeatability for individual measurements, they will be influenced by random errors. Accuracy on the other hand is a measure of agreement of the calculated-, and the "true" concentration and will therefore be influenced only by systematic errors.

Accuracy of VOC concentrations

Accuracy is influenced only by systematic errors and is a measure of the deviation between the real and the measured value. An example of systematic errors that will lead to a decreased accuracy of VOC determination is e.g. the application of wrong calibration standard concentrations that may lead to a systematic under- or overestimation of present VOC mixing ratios. In the following paragraphs, accuracy will be specified by the percentage difference between the measured VOC concentration and the reference VOC concentrations that were set by the permeation device.

Precision of VOC concentrations

The precision of all mixing ratios was calculated by Gaussian error propagation and gives the sum of uncertainty of all components used for the calculation of these mixing ratios (calibration factor, sample flow, blank values, see Formula 2.13.).

$$\text{Precision}_{MR} = MR \cdot \left(\frac{\sqrt{\left(\text{Area}_{\text{Sample-Blank}} \cdot \sqrt{\left(\frac{\left(P_{Analyt} \cdot \text{CalFactor} \right)}{\text{Area}_{\text{Sample-Blank}}} \right)^2 + P_{Flow}{}^2} \right)^2 + s_{AreaBlank}{}^2}}{\text{Area}_{\text{Sample-Blank}}} \right) \qquad 2.13.$$

Formula 2.13.: $\text{Area}_{\text{Sample-Blank}}$ = difference of sample and average blank area [e.g. µV s], CalFactor = calibration factor [e.g. µV s ng^{-1}], MR = mixing ratio [e.g. ppb], P_{Flow} = relative uncertainty of flow and volume measurement [%], P_{Analyt} = precision of analysis [e.g. ng], Precision_{MR} = precision of VOC mixing ratio [e.g. ppb], $s_{AreaBlank}$ = standard deviation of blank values on an area basis [e.g. µV s]

For terms that were linked by multiplication or division during the calculation of the mixing ratios, relative uncertainties were used for error propagation. For terms that were linked by addition or subtraction, absolute uncertainties were used. Formula 2.13. gives an

example for the calculation of the precision of mixing ratios for the GC-FID analysis. It combines the calculated precision of analysis, flow, and the standard deviation of blank values with the factor of calibration and the difference of sample and blank area. Due to the above mentioned context the precision of analysis and flow were inserted in Formula 2.13. on the basis of relative uncertainties (the relative precision of analysis is given by the term: P_{analyt} CalFactor/$Area_{Sample-Blank}$). On the other hand the precision of blank values (standard deviation) was added as absolute uncertainty on an area basis.

The precision for HPLC-analysis was calculated in analogy to Formula 2.13., additionally including the relative precision of the gravimetric volume determination (see below for details).

Precision of analysis

The analytical precision, which is a measure of the uncertainty of the calibration factor, was calculated from the linear regression of standard concentrations (x-axis) and the associated standard areas (y-axis) by Formulas 2.14. to 2.16. (Doerffel 1996).

The terms S_0 and S_b that are included in Formula 2.14., were calculated according to Formulas 2.15. and 2.16. with x_i representing the standard amounts and y_i representing the standard areas. The factor Y_i represents the calculated standard amount from regression analysis following $Y_i = a + bx$.

$$P_{Analyt.} = \frac{S_0}{b} \cdot \sqrt{\left(\frac{1}{n}\right) + \left(\frac{1}{1}\right) + \left(\frac{S_b}{b}\right)^2 \cdot \left(\frac{Area_{Sample-Blank} - \left(\sum Area_{Standard}/n\right)}{S_0}\right)^2} \qquad 2.14.$$

$$S_0 = \sqrt{\frac{\sum (y_i - Y_i)^2}{n-2}} \qquad 2.15.$$

$$S_b = \sqrt{\frac{\left(n \cdot {S_0}^2\right)}{\left(n \cdot \sum {x_i}^2 - \left(\sum x_i\right)^2\right)}} \qquad 2.16.$$

Formula 2.14. to 2.16.: a = intercept of the linear regression (calibration curve) [µV s], $Area_{Sample-Blank}$ = difference of sample and average blank area [µV s], $Area_{Standard}$ = area of the standard used for calibration [µV s], b = slope of the linear regression (calibration curve) [e.g. µV s ng^{-1}], n = number of paired values (i.e. number of standards and associated areas) , x_i = standard amount or concentration (x-axis) [e.g. ng], y_i = standard area (y-axis) [µV s], Y_i = calculated standard amount or concentration from regression analysis ($Y_i = a + bx$) [e.g. ng]

Following the latter formulas will calculate the analytical precision in units of the respective standard amount or concentration used (e.g. ng or nmol l^{-1}). Consequently an analytical precision of 2.31 ng was calculated for all GC-FID analysis performed. For HPLC analysis an analytical precision of 93 nmol l^{-1} acetaldehyde and 64 nmol l^{-1} acetone (precision intercomparison I) was calculated. Table 2.5. will give an overview of the calculated analytical precision at VOC mixing ratios of 1 and 10 ppb considering the typical sampling and eluate volumes applied.

Table 2.5. Analytical precision of VOC mixing ratios at concentrations of 1 and 10 ppb. Sampling volume = 4500 ml for samples analysed by GC-FID and 18000 ml for samples analysed by HPLC. Eluate volume of HPLC samples = 2 ml.

	Precision at mixing ratios of	
Compound	1 ppb	10 ppb
Isoprene	17%	2%
Acetaldehyde	23%	2%
Acetone	16%	2%

Precision of volume and flow

The sampling of specific air volumes was performed by the use of flow controller units [size 500 sccm, MKS Instruments, USA]. As the relative precision for these flow controller units was specified by the manufacturer to 1% of the maximum flow rate, the absolute precision of sampling volume and flow was calculated to 5 ml min^{-1}.

Precision of blank values

After the performance of a Nalimov-outlier test (for details see above) the average blank values of volatile organics were subtracted from the respective samples on an area basis. Therefore the standard deviation of these average blank values was used for the calculation of the precision of sample analysis.

Precision of gravimetric volume determination

Measurement of carbonyl derivatives comprised the determination of the eluate volume that was utilised for HPLC analysis. This volume was measured gravimetrically with a laboratory balance [model L610D, Sartorius, Germany] at a precision of 0.001 g.

Reproducibility of VOC concentrations

Reproducibility is influenced only by random errors and can be calculated from the average and standard deviation of a series of measurements of the same quantity. Application of Formula 2.17. will calculate the reproducibility for a series of samples in percent.

$$E = \left(\frac{s}{\bar{x}} \right) \cdot 100 \qquad 2.17.$$

Formula 2.17.: E = reproducibility [%], s = standard deviation , x = arithmetic average

SAMPLING PROCEDURES AND PROTOCOL

During the experiments that were performed within the framework of the ECHO project, 21 different chemical compounds were analysed by different analytical systems that were applied by 7 participating institutes. Table 2.6. gives an overview of participants as well as the applied analytical techniques that were evaluated during both intercomparison experiments. All instruments were connected individually to a common gas distribution device with exception of the offline GC-MS system (applied by the Italian Research Council, CNR). The latter samples were collected by utilisation of the automatic sampling device in analogy to the samples collected by the MPI (including application of the ozone scrubber assembly). Analysis was performed later on at the laboratory in Rome. All experiments were carried out in a non-blind fashion, i.e. compounds and specified concentrations were published to the participants in advance. No common standards were supplied and so each group used its own calibration standard for the calculation of VOC concentrations. The data quality was assessed by its accuracy, precision and reproducibility. An accuracy resulting in an under- or overestimation of ± 25% was considered as good, ± 50% as reasonable and < ± 50% as poor.

As outlined previously, the application of specified VOC mixing ratios for the comparison of measured and set VOC concentrations might lead to serious misinterpretations and comparison to other analytical procedures is required. In addition to the calculated VOC concentrations derived from the distribution device (in the following referred to as source), the online GC-MS system operated by the Research Centre Jülich (ICGIIIoxy) was chosen as a further reference. A detailed description of the system can be obtained from Heiden *et al.* (1999). The system was calibrated against a custom made permeation source (see Schuh *et al.* 1997), similar to the permeation source applied during the intercomparison experiments. Moreover, field experiments (see chapter 3) were conducted in strong cooperation with the

Table 2.6. Institutions and instruments evaluated during the experiments of intercomparison I and II. MPI data and analytical methodologies used for comparison with the MPI data are labelled [a], analytical methodologies that are not shown in the graphs are labelled [b]. MPIgc: offline analysis of isoprene, monoterpenes, benzene, and toluene. MPIhplc: offline analysis of acetaldehyde and acetone. MPIcims: online analysis by chemical ionisation mass spectrometry (data not shown).

Institution	Abbreviation	Participation intercomparison I or II	Analysis offline or online	Specification of analysis
Max Planck Institute for Chemistry [a]	MPIgc	Intercomparison I + II	Offline	Carbon adsorbents, GC-FID
Max Planck Institute for Chemistry [a]	MPIhplc	Intercomparison I + II	Offline	DNPH cartridges, HPLC
Max Planck Institute for Chemistry [b]	MPIcims	Intercomparison I + II	Online	Chemical ionisation mass spectrometry
Italian Research Council [a]	CNR	Intercomparison II	Offline	Carbon adsorbents, GC-MS
Swiss Federal Research Station for Agroecology and Agriculture [a]	FAL	Intercomparison I + II	Online	PTR-MS
Research Centre Jülich [a]	ICGIIIoxy	Intercomparison I + II	Online	Tenax/Carbotrap adsorbents, GC-MS
Research Centre Jülich [b]	ICGIIIterp	Intercomparison I + II	Online	Tenax/Carbotrap adsorbents, GC-MS
Research Centre Jülich [b]	ICGIIiso	Intercomparison I + II	Online	Tenax/CarbopackX adsorbents, GC-FID
Research Centre Jülich [b]	ICGIIterp	Intercomparison II	Offline	Tenax/Carbotrap, GC-FID/MS
Institute of Spectrochemistry and applied spectroscopy [b]	ISAS	Intercomparison I + II	Offline	Tenax/Carbotrap adsorbents, GC-MS
University of Innsbruck [b]	UI	Intercomparison II	Online	PTR-MS

Italian Research Council (CNR) and the Swiss Federal Research Station for Agroecology and Agriculture (FAL) and comparison of the MPI data was also focussed on the data obtained by these institutes. A detailed description of the PTR-MS system applied by the FAL group, including the results obtained during intercomparison II (phase 4, see below) is given by Ammann *et al.* (2004). A detailed description of the GC-MS analysis applied by CNR is given by Ciccioli *et al.* (1992) and Brancaleoni *et al.* (1999).

RESULTS

ISOPRENE AND MONOTERPENES

Ozone scrubber test with isoprene and β-pinene

Ozone induced decomposition of volatile organics is a serious problem in measuring ambient VOC concentrations (e.g. see Pellizzari *et al.* 1984; Jüttner 1988; Arnts and Tejada 1989; Hoffmann *et al.* 1993; Cao and Hewitt 1994; Peters *et al.* 1994; Hoffmann 1995; Calogirou *et al.* 1996; Larsen *et al.* 1997; Kleindienst *et al.* 1998; Ferrari *et al.* 1999; Fick *et al.* 2001). To overcome the decomposition of volatiles by ozone, several scrubber techniques have been utilised in the past. However, adsorption- and desorption effects on the ozone scrubber surface might also lead to incorrect results. For the sampling of volatile organics with the automatic sampling device, a specific ozone scrubber assembly (see Figure 2.6.) was utilised during all laboratory and field experiments (ambient air measurements). To evaluate the effects of this assembly on two volatile organic compounds- isoprene and β-pinene- we conducted a laboratory test with online VOC analysis by PTR-MS.

As shown by Figure 2.8. VOC concentrations were adjusted to mixing ratios of 13 and 3 ppb for isoprene and β-pinene, respectively. To exclude potential adsorption effects by the scrubber assembly, it was connected directly in front of the PTR-MS inlet (measuring cycle 261 in Figure 2.8.). As shown by the figure, the inclusion of the scrubber assembly did not introduce any bias to the previous VOC concentrations. Also the adjustment to higher VOC concentrations of 256 ppb isoprene and 49 ppb β-pinene resulted in no increase in VOC concentrations after removal of the scrubber from the instrument inlet (measuring cycle 391 in Figure 2.8.). The latter results were also confirmed by a T-test that proved no difference between the calculated averages with and without utilisation of the scrubber assembly. To test on potential desorption effects from the scrubber surface it was connected to the PTR-MS inlet again after adjustment to lower VOC concentrations (measurement cycle 441). As shown

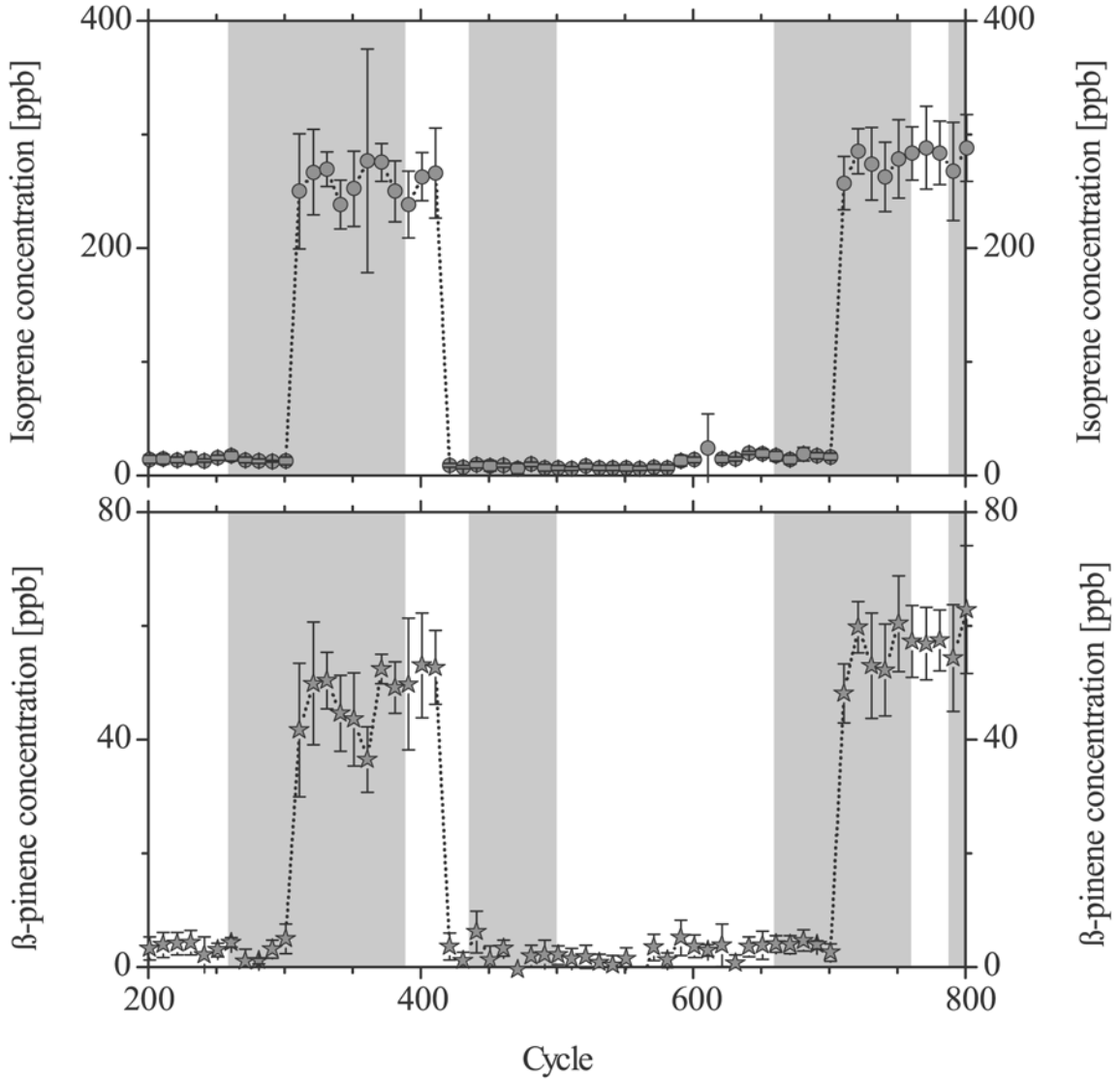

Figure 2.8. Ozone scrubber experiment. Mixing ratios for isoprene (top graph) and β-pinene (bottom graph) were measured online by PTR-MS over a period of 600 measurement cycles (1 cycle = 11 to 45 s). Data points show the appropriate average and standard deviation of 5 measurement-cycles each. Utilized (< cycle 500) and new ozone scrubber assemblies (> cycle 661) were inserted to the inlet directly prior the PTR-MS instrument and were removed from the inlet again. Cycles measured with an ozone scrubber assembly are indicated by grey areas.

by Figure 2.8., no desorption effects were observed from the scrubber surface. Since both experiments were conducted with a scrubber assembly that was already utilised for a previous field campaign in the year 2001 (LBA-Claire 2001, Cooperative Lba Airborne Regional Experiment 2001, as part of the Large scale Biosphere-atmosphere experiment in Amazonia), a new scrubber assembly, that was connected to the PTR-MS at cycle 661 was tested as well. Likewise, no adsorption effects were observed with the new scrubber assembly, neither at low, nor at high VOC concentrations.

Recovery of isoprene during intercomparison I and II

Various VOC concentrations were set by the permeation source during the experiments of intercomparison I and II. Dew point temperatures were adjusted to 10°C for all experiments, resulting in a relative humidity of 53% at 20°C ambient temperatures. Since several problems occurred during both laboratory experiments (e.g. condensation of water in the distribution device during the experiments of intercomparison I), only two mixing ratios were evaluated for each intercomparison experiment (referred to as phase 1 to 4). Figure 2.9. gives an overview of the experiments applied.

Isoprene mixing ratios were adjusted by the permeation source to concentrations of 3.4 and 12.4 ppb for intercomparison I. For intercomparison II concentrations of 3.6 and 5.4 ppb isoprene were set. The calculated uncertainty of these gas mixing ratios was specified by the Research Centre Jülich and accounted to ± 13% of the respective isoprene concentration. As shown by Figure 2.9., isoprene mixing ratios measured by GC-FID analysis by the MPI laboratory underestimated the source concentrations for intercomparison I, but overestimated the source concentrations for intercomparison II. Average isoprene blanks for the GC-FID analysis were small and accounted to < 5% of the respective samples. Following the Gaussian

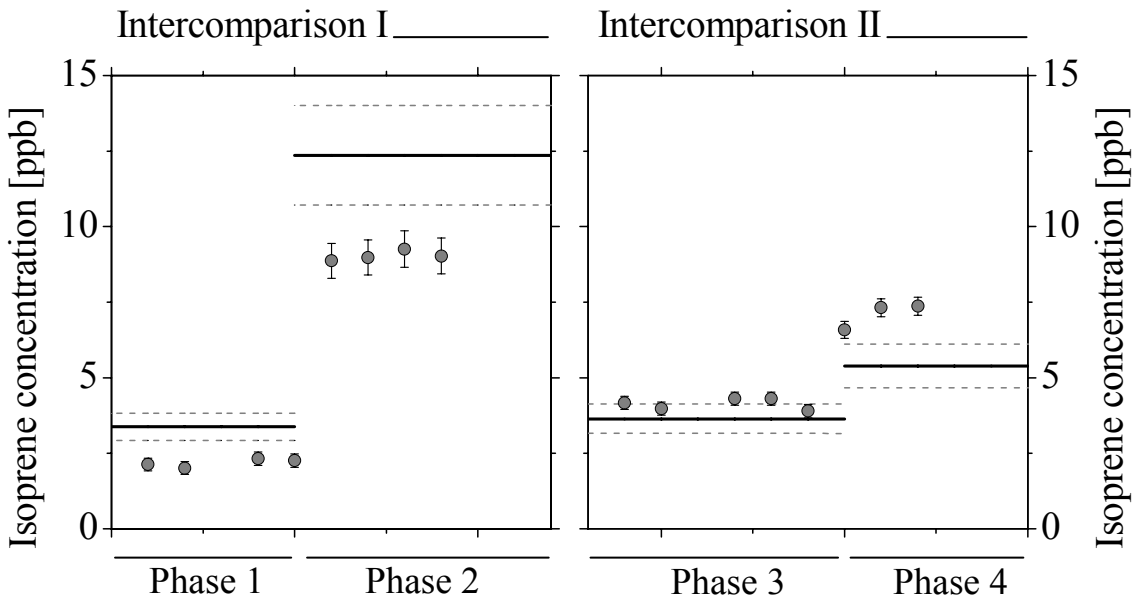

Figure 2.9. Isoprene concentration during intercomparison I (left panel) and intercomparison II (right panel). Comparison of isoprene mixing ratios measured by GC-FID analysis (grey circles) and specified isoprene mixing ratios derived from the distribution device (solid line). The specified isoprene concentrations were calculated by a gravimetric approach. The estimated error of these specified mixing ratios is given by the dashed grey line. The calculated error of the measured VOC mixing ratios is given by the error bars. If no error bars are visible, they reside within the diameter of the plotted symbol.

error propagation, the precision of the measured mixing ratios ranged between ± 4 and ± 10%. After removal of 4 outliers from the latter dataset, the reproducibility of the GC-FID analysis ranged between ± 2 and ± 6%. The average and the standard deviation that were calculated from the measured isoprene concentrations (GC-FID analysis) ranged at 2.2 ± 0.1 ppb (phase 1) and 9.0 ± 0.2 ppb (phase 2) for intercomparison I. For intercomparison II average concentrations of 4.1 ± 0.2 ppb (phase 3) and 7.1 ± 0.4 ppb (phase 4) isoprene were calculated. In general, the accuracy ranged between an underestimation of the reference concentration of up to 35% and an overestimation of the reference of up to 32% (see Figure 2.10.) and therefore demonstrated the high variability of isoprene analysis. Best agreement to the reference was obtained for the lower concentration applied during intercomparison II (phase 3, overestimation of 13%). Here, 3 of 5 measured samples agreed within the range of the source concentration. However, in general the accuracy was not found to be a function of the specified source concentration.

As shown by Figure 2.10., the results obtained by ICGIIIoxy overestimated the source concentrations during both intercomparison experiments by 20 to 45%. Regarding intercomparison I, data for CNR and FAL were not available. The agreement with the set con-

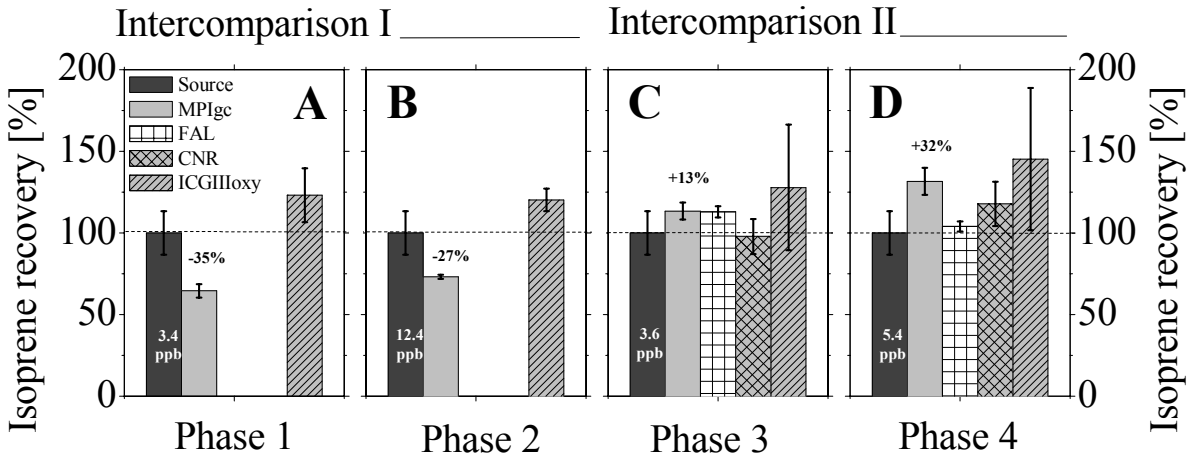

Figure 2.10. Isoprene accuracy during intercomparison I (A and B) and intercomparison II (C and D) by several groups. Isoprene mixing ratios derived from the distribution device were set to 100 ± 13%. The average accuracy and standard deviation is shown by the bar graphs for different participants (colour codes see caption in graph: source (distribution device), MPIgc (Max Planck Institute for Chemistry, GC-FID analysis), FAL (Agroscope, FAL), CNR (Italian Research Council), ICGIIIoxy (Research Centre Jülich). Isoprene mixing ratios specified during the respective experiment were indicated in the graph (column: source). The respective uncertainty of the source concentration is given by the error bars. Isoprene accuracy is indicated for the MPI data (column: MPIgc). The amount of samples (n) used for the calculation of the average and standard deviation of the MPI data ranged at 4 samples (phase 1 and 2), 5 samples (phase 3), and 3 samples (phase 4).

centrations (and the data obtained by CNR and FAL) was much better for intercomparison II, although the general setup was not changed. Both institutes, FAL and CNR, agreed with the source concentrations within the range of the specified uncertainty. For phase 3 the agreement between the MPI and the FAL group was excellent and good agreement was obtained between the MPI and CNR data. However, during phase 4 the agreement of the MPI data to the data obtained by FAL and CNR was much poorer.

Recovery of monoterpenes during intercomparison I and II

In analogy to the experiments described above, four monoterpene mixing ratios were set by the permeation source (phase 1 to 4). Monoterpenes evaluated from both intercomparison experiments were α-pinene, β-pinene and 3-carene. Specified mixing ratios for these three different monoterpene compounds ranged between 0.2 and 1.6 ppb. Relative uncertainties were indicated by the Research Centre Jülich and ranged between ± 2 to ± 18% for all monoterpene compounds.

As shown by Figure 2.11., good agreement with the reference VOC concentration was obtained for α-pinene (top graph), yielding an underestimation of 0 to 12%. After removal of 3 outliers from the dataset, the reproducibility of the measurements was good and ranged between ± 1 to ± 4%. However, the calculated precision ranged only between ± 8 to ± 46%. In general, the average blank values accounted to < 3% of the measured α-pinene concentration, but average blank values were 4 times higher during the experiments of intercomparison I than during intercomparison II.

Good results were also obtained for the measurement of 3-carene, with an accuracy ranging between an underestimation of the reference by 3 and 20%. Although 3 outliers were removed from the dataset, the reproducibility was poorer than for α-pinene and accounted to ± 1 to ± 23%. The calculated precision of single samples ranged between ± 9 and ± 40%. Average blank values were a factor of 9 higher during the experiments of intercomparison I and accounted to < 11% of the measured 3-carene concentration.

Poorest accuracy was obtained for the measurements of β-pinene, resulting in an underestimation of the reference by 8 to 39%. 4 outliers were removed from the dataset, but the reproducibility was still poor (± 2 to ± 23%). Blank values accounted to < 5% of the measured β-pinene samples and showed only minor discrepancies between both intercomparison experiments. The calculated precision of single samples ranged between ± 7 to ± 58%. Although the specified source concentrations were underestimated by the MPI measurements, monoterpene concentrations measured by the other participants were rather overestimated. In

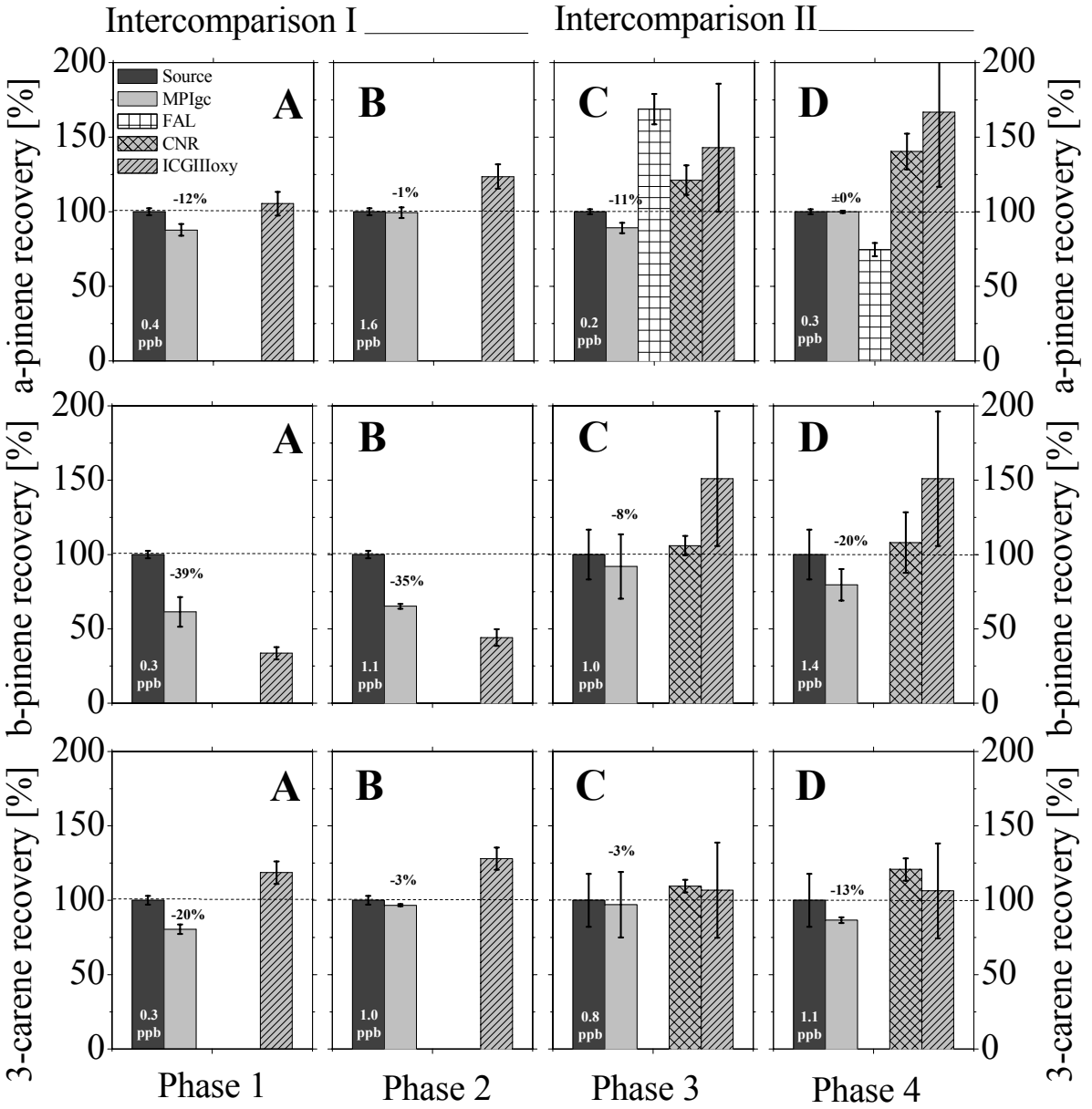

Figure 2.11. Accuracy of monoterpenes during intercomparison I (A and B) and intercomparison II (C and D) by several groups. Mixing ratios derived from the distribution device were set to 100%. The average accuracy and standard deviation is shown by the bar graphs for different participants (colour codes see caption in graph: source (distribution device), MPIgc (Max Planck Institute for Chemistry, GC-FID analysis), FAL (Agroscope, FAL), CNR (Italian Research Council), ICGIIIoxy (Research Centre Jülich). Accuracy of α-pinene (top graph), β-pinene (mid graph), and 3-carene (bottom graph). Monoterpene mixing ratios specified during the respective experiment were indicated in the graph (column: source). The respective uncertainty of the source concentration is given by the error bars. Monoterpene accuracy is indicated for the MPI data (column: MPIgc). The amount of α-pinene samples (n) for the MPI data ranged at 4 samples (phase 1), 5 samples (phase 2 and 3), and 3 samples (phase 4). For β-pinene n ranged at 4 samples (phase 1 to 4, MPI data). For 3-carene n ranged at 5 samples (phase 1) and 4 samples (phase 2 to 4) for the MPI data. Note, that the standard deviation of ICGIIIoxy (α-pinene) during phase 4 is out of scale.

general, no dependency between the specified monoterpene concentrations and the measured accuracy was obtained for the MPI data. Monoterpene measurements from FAL and CNR were not available for intercomparison I. Moreover, for intercomparison II no data were available for β-pinene and 3-carene from the FAL group, since discrimination of both compounds was not possible for the applied PTR-MS instrument. However, best agreement with the other participants was obtained for 3-carene during intercomparison II, since all participants agreed within the specified range of uncertainty. Also β-pinene measurements by CNR and ICGIIIoxy agreed within the range of the specified uncertainty for intercomparison II. However, for ICGIIIoxy this was mainly a result of the high standard deviation obtained for these measurements. In agreement with the MPI data, β-pinene concentrations during intercomparison I were underestimated by ICGIIoxy by far. This may be indicative of a loss of β-pinene within the source during intercomparison I. Even though the agreement of the MPI data to the source concentration was best for α-pinene, for intercomparison II only minor agreement with the other participants was obtained.

BENZENE AND TOLUENE

The VOC concentrations that were specified by the permeation source during both intercomparison experiments ranged from 0.8 to 11.3 ppb and from 0.2 to 3.1 ppb for benzene and toluene, respectively. The uncertainty for these mixing ratios was specified by the Research Centre Jülich to account to ± 1 and ± 2% for both compounds. Considering all experiments, the measured benzene concentrations were in reasonable or good agreement with the source concentrations, yielding an accuracy ranging between an underestimation of the reference by 15% and an overestimation of the reference by 37% (see Figure 2.12.). After removal of 3 outliers from the dataset the reproducibility was good and ranged between ± 2 to ± 12%. The precision of individual samples ranged at ± 11 to ± 41%. Benzene blanks were very high and accounted to < 42% of the measured samples. Moreover, these blanks were higher by a factor of 2 during intercomparison I.

Toluene concentrations were in good agreement with the source concentrations, yielding an accuracy that ranged between an underestimation of the reference by 13% and an over-estimation of 13%. In total 4 outliers were removed from the dataset and the reproducibility accountted to ± 1 to ± 12%. In contrast, the precision of single samples was highly variable and ranged between values of ± 7 and ± 72%. Toluene blanks were only slightly higher for the intercomparison I experiment, but accounted also to high values of < 43% of the

respective samples. Measurements of FAL and CNR were not available for intercomparison I. During phase 2 no benzene data were available for the ICGIIIoxy measurements. Benzene concentrations measured by ICGIIIoxy during phase I were in good agreement with the MPI data. Also good agreement between the other participants was obtained for phase 3. Benzene concentrations of phase 4 were overestimated by CNR and ICGIIIoxy. The same effect was observable for the toluene concentrations measured by CNR and ICGIIIoxy during phase 4.

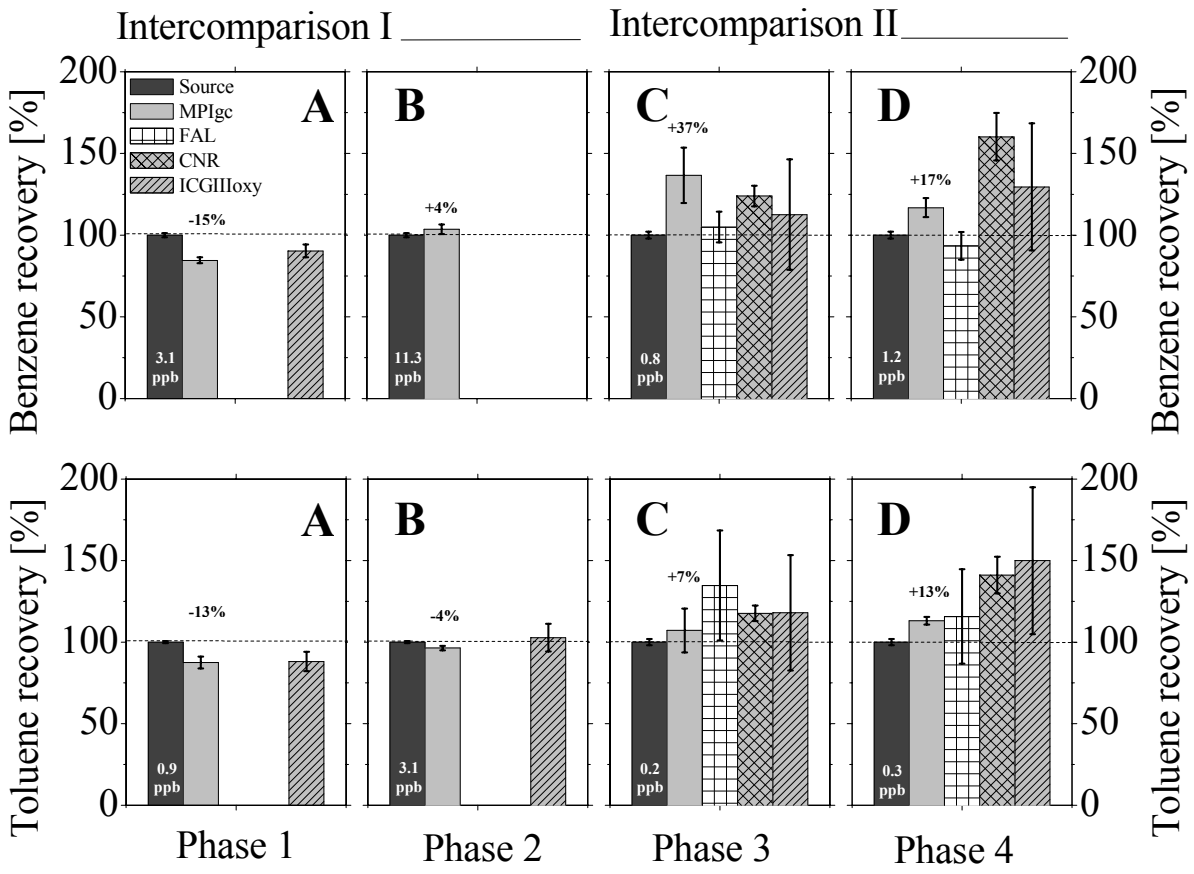

Figure 2.12. Accuracy of benzene and toluene during intercomparison I (A and B) and intercomparison II (C and D) by several groups. Mixing ratios derived from the distribution device were set to 100%. The average accuracy and standard deviation is shown by the bar graphs for different participants (colour codes see caption in graph: source (distribution device), MPIgc (Max Planck Institute for Chemistry, GC-FID analysis), FAL (Agroscope, FAL), CNR (Italian Research Council), ICGIIIoxy (Research Centre Jülich). Accuracy of benzene (top graph) and toluene (bottom graph). Mixing ratios specified during the respective experiment were indicated in the graph (column: source). The respective uncertainty of the source concentration is given by the error bars. Accuracy is indicated for the MPI data (column: MPIgc). The amount of samples (n) used for the calculation of the average and standard deviation of benzene from the MPI data ranged at 4 samples (phase 1), 5 samples (phase 2 and 3), and 3 samples (phase 4). The amount of samples (n) used for the calculation of the average and standard deviation of toluene from the MPI data ranged at 4 samples (phase 1 and 2), 5 samples (phase 3), and 3 samples (phase 4).

The MPI and FAL data of toluene concentrations were in better agreement with the source concentrations during phase 4. With exception of the FAL measurements during phase 3 good agreement with the source concentrations was observed for toluene during phase 1 to 3.

ACETALDEHYDE AND ACETONE

In analogy to the other VOC species described above, acetaldehyde and acetone concentrations were set by the permeation source. In general, the specified mixing ratios were smaller during intercomparison I for both compounds. The mixing ratios that were set at the permeation device ranged between 0.3 and 19.0 ppb for acetaldehyde and 2.2 and 31.4 ppb for acetone. The specified uncertainty of these gas mixing ratios was specified by the Research Centre Jülich and ranged between values of ± 9 and ± 30% for acetaldehyde and between ± 3 and ± 18% for acetone.

Sampling of both carbonyl compounds was performed by utilisation of two different adsorption systems. For intercomparison I, DNPH coated C_{18}-cartridges were used, while during intercomparison II pure silica-DNPH cartridges were applied. Considering phase 1 and 3 of both experiments, the measured and set acetaldehyde mixing ratios were in good agreement with each other (see Figure 2.13.). During phase 2 both datasets agreed within the range of the specified uncertainties (specified by the Research Centre Jülich and calculated precision by the MPI). During phase 4 (intercomparison II) measurements were not performed.

As shown by Figure 2.13., the precision for these gas mixing ratios ranged between ± 11 and ± 54% of the measured acetaldehyde concentration. The latter uncertainty was either a result of high blank values derived from the C_{18} cartridge system or was dominated by the increased eluate volume applied for the DNPH-silica cartridges. Considering the blank aspect, the performance of the silica cartridge system was better than the performance of the C_{18} cartridge system. Average acetaldehyde blanks of silica cartridges were 55% lower than blanks of the C_{18} cartridges (acetaldehyde blanks accounted to < 31% (C_{18} cartridges, intercomparison I) and < 10% (silica cartridges, intercomparison II) of the respective samples). In addition the standard deviation of these average blank values was much better for the silica cartridges.

In total two outliers were removed from the dataset (C_{18} cartridges and silica cartridges one outlier each), yielding a reproducibility for the silica cartridges of ± 2%. With exception of phase 2, the acetaldehyde concentrations were in good agreement with the source concentrations and the data obtained by the FAL group during intercomparison II (see Figure

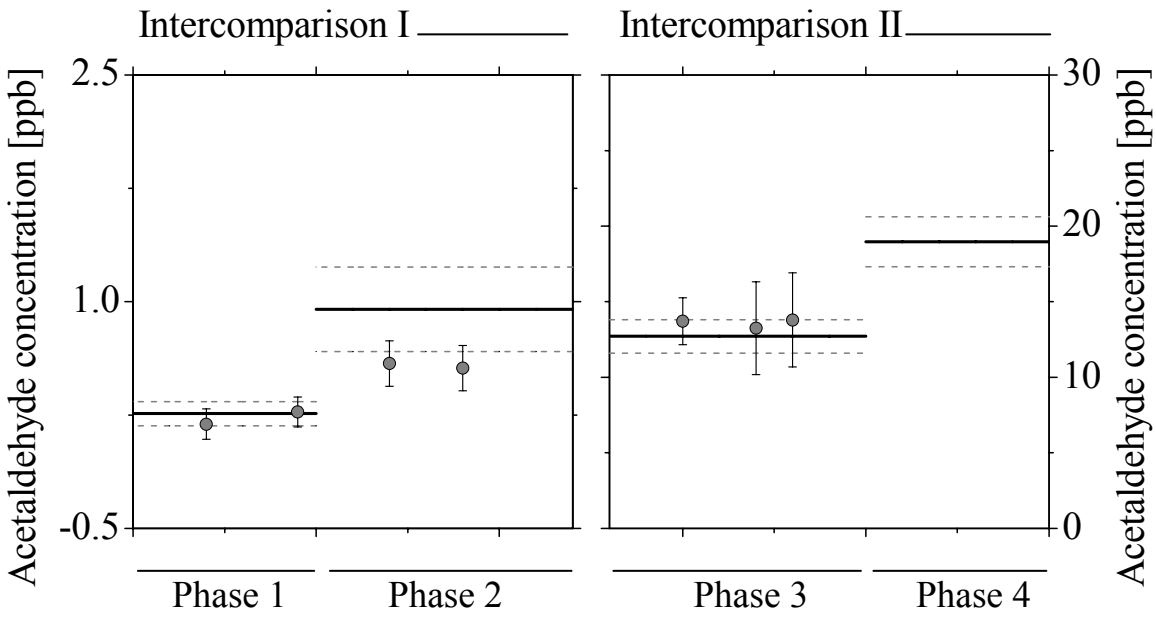

Figure 2.13. Acetaldehyde concentration during intercomparison I (left panel) and intercomparison II (right panel). Comparison of carbonyl mixing ratios measured by HPLC analysis (grey circles) and specified acetaldehyde mixing ratios derived from the distribution device (solid line). The specified acetaldehyde concentrations were calculated by a gravimetric approach. The estimated error of these specified mixing ratios is given by the dashed grey lines. Sampling of carbonyls was performed by utilisation of SPE C_{18} silica cartridges (intercomparison I) or by utilisation of SPE silica cartridges (intercomparison II). Note the different scales for intercomparison I and II.

2.14., top graph). The accuracy obtained for acetaldehyde ranged between an underestimation of the reference concentration of up to 41% and an overestimation of the reference of up to 7%. The accuracy obtained by utilisation of the silica cartridges was better than the accuracy obtained by the C_{18} cartridges. With exception of ICGIIIoxy, the data of other participants were not available for intercomparison I and the specified source concentrations were overestimated by the ICGIIIoxy group by far. Also for intercomparison II (phase 3) acetaldehyde data measured by CNR were not available. The MPI measurements obtained during phase 3 were in good agreement with the measurements performed by the FAL group.

Considering the specified acetone concentration the accuracy obtained by the C_{18} cartridges resulted in an underestimation of the reference mixing ratio of up to 69%. The accuracy obtained with the DNPH-silica system was much better resulting in an underestimation of the reference by only 3%. Moreover these measurements were in good agreement with the majority of data derived by the other participating groups (with exception of the ICGIIIoxy group). A drift of the acetone concentrations during phase 2 of intercompari-

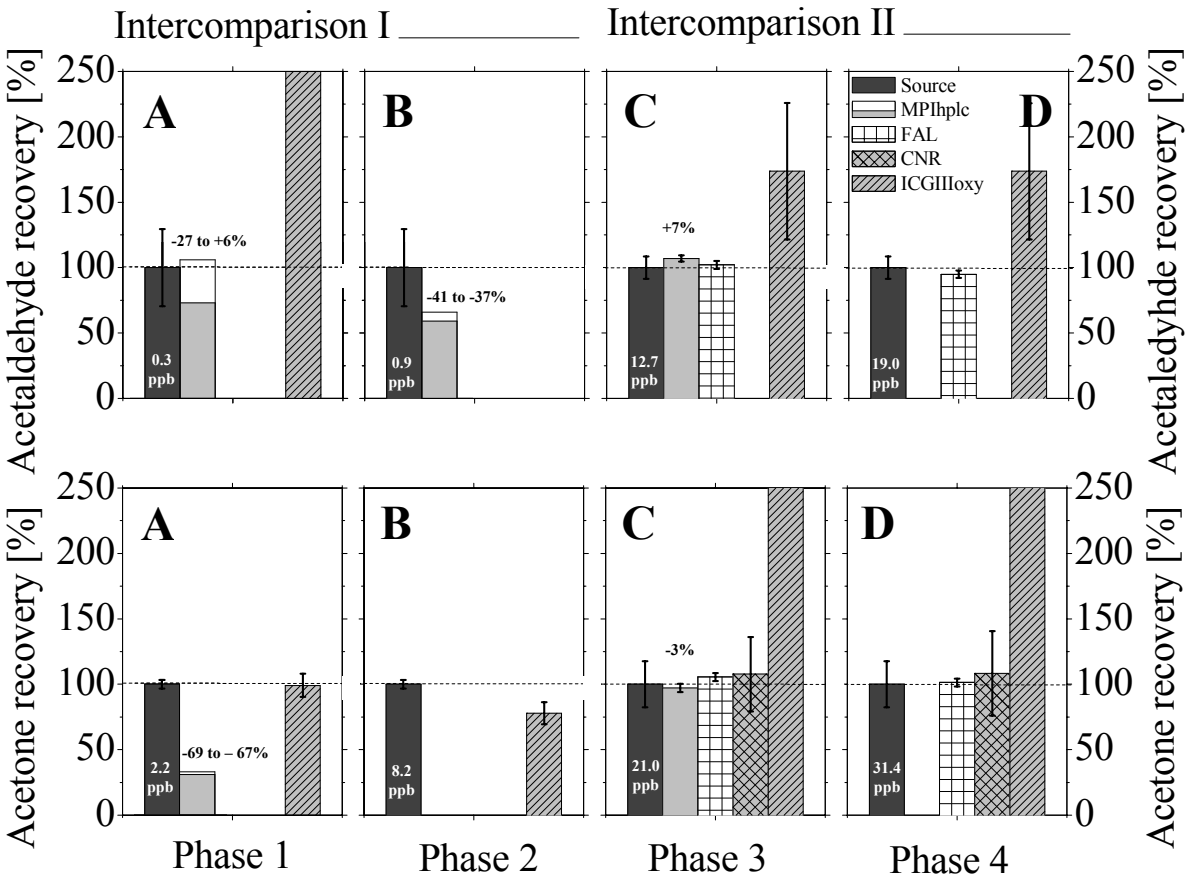

Figure 2.14. Accuracy of acetaldehyde and acetone during intercomparison I (A and B) and intercomparison II (C and D) by several groups. Mixing ratios derived from the distribution device were set to 100%. The recovery or average recovery and standard deviation is shown by the bar graphs for different participants (colour codes see caption in graph: source (distribution device), MPIhplc (Max Planck Institute for Chemistry, HPLC analysis), FAL (Agroscope, FAL), CNR (Italian Research Council), ICGIIIoxy (Research Centre Jülich). Recovery of acetaldehyde (top graph) and acetone (bottom graph). Sampling of carbonyls was performed by utilisation of SPE C_{18} silica cartridges (phase 1 and 2) or by utilisation of SPE silica cartridges (phase3). Mixing ratios specified during the respective experiment were indicated in the graph (column: source). The respective uncertainty of the source concentration is given by the error bars. Accuracy is indicated for the MPI data (column: MPIhplc). The amount of samples (n) used for the calculation of the average and standard deviation of acetaldehyde and acetone from the MPI data ranged at 3 samples for phase 3. Acetaldehyde and acetone data for phase 1 and 2 comprised only 2 samples each. Therefore, the average and standard deviation was not calculated for these experiments and the graph represents only the measured range of accuracy of each single analysis. Note, that the data measured for ICGIIIoxy for acetaldehyde (phase1, ICGIIIoxy = 2311%) and acetone (phase 3 and 4, ICGIIIoxy = 263%) were out of scale.

son I prevented the calculation of an average acetone concentration for the MPI data. Moreover for phase 4 no acetone data were available from the MPI group. For acetone a precision of ± 11 to ± 31% was calculated. After removal of one outlier from the dataset, the

reproducibility was ± 3% for the silica cartridges. Moreover, average acetone blanks were 19% lower in the silica- than in the C_{18} system (acetone blanks accounted to < 15% (C_{18} cartridges) and < 16% (silica cartridges) of the respective samples).

DISCUSSION

ADSORPTION AND DESORPTION OF VOLATILE ORGANICS ON THE OZONE SCRUBBER SURFACE

The results obtained from the ozone scrubber test clearly proved that neither adsorption nor desorption effects were detectable for isoprene and β-pinene under dry air conditions using a scrubber surface of 6 cm^2 and a flow rate of about 125 ml min^{-1}. Isoprene concentrations measured by the MPI and CNR during intercomparison II with humidified air were also in good agreement with the reference concentration and therefore indicated no adsorptive losses on the applied ozone scrubber surface. The recoveries obtained for α-pinene, 3-carene, benzene, and toluene during the intercomparison experiments were also good, but the variations between permeation source, CNR and MPI were too high, to exclude potential scrubber effects.

The results obtained from the present study are in agreement with previous experiments performed by other authors. Hoffmann (1995) investigated a similar scrubber assembly (MnO_2 covered copper screen, surface area 2.5 cm^2) and observed no adsorption effects for α-pinene, β-pinene and limonene applying laboratory conditions at zero ppb ozone. However, the scrubber surface used during the latter study was smaller than during the present study. Extensive laboratory experiments performed by Calogirou *et al.* (1996) indicated that the retention of volatiles by MnO_2 covered copper nets is a function of the scrubber's surface. Best results were obtained by these authors using a total surface area of 4 cm^2. With this setup most of the test compounds (e.g. α-pinene, β-pinene, camphene, sabinene, limonene, and camphor) could be quantitatively recovered at mixing ratios of 22 to 314 ng mol^{-1}. However, linalool, α-terpinene, and β-caryophyllene were retained (recovery of α-terpinene and β-caryophyllene at 30-40%). And using higher surface areas, also limonene, ocimene, and terpinolene were adsorbed on the scrubber surface. The results of the present study are also in agreement with observations conducted by Fick *et al.* (2001), who observed recovery rates of > 95% for 3-carene, α-pinene, β-pinene, limonene, and isoprene applying a MnO_2 scrubber with a total surface area of 38 cm^2. However, with exception of MACR (recovery at 90%),

oxygenated compounds were retained by the latter scrubber (e.g. nonpinone, α-pinene oxide, methylglyoxal). Moreover, the experiments performed by Kleindienst *et al.* (1998) indicated that MnO_2 covered ozone scrubbers removed formaldehyde quantitatively from ambient air samples. These adsorption effects of oxygenated compounds were not confirmed by the present study. Here, good recoveries were obtained for the two oxygenated compounds acetaldehyde and acetone measured by the MPI and CNR group during intercomparison II. The latter data are indicative of no or only minor scrubber effects on both compounds. However, these experiments were performed with humidified air (dew point temperature 10°C) and active sites on the ozone scrubber surface may be covered by water molecules that prevented adsorptive effects. Therefore, further tests are needed to prove these results.

CALIBRATION OF GC-FID ANALYSIS

In agreement with Apel *et al.* (2003a; 2003b) syringe injections of liquid calibration standards resulted in major discrepancies to the reference VOC concentrations when applying GC-FID measurements during the present study. Better accuracy was obtained by utilisation of a gaseous standard mixture of stable n-alkanes and assumption of a linear proportionality between carbon number and detector response (effective carbon number concept, Sternberg *et al.* (1962)). The latter concept is valid for aliphatic and aromatic compounds and by approximation also for olefinic molecules. However, as shown by Table 2.3., olefins have a slightly reduced detector response. Therefore, application of a general calibration factor that was obtained from the calibration of n-alkanes will result in a small underestimation of the real olefin concentration (e.g. monoterpenes and isoprene). Although monoterpene concentrations were slightly underestimated during the intercomparison experiment, the recovery of isoprene varied between under- and overestimation. Since these results are not consistent with each other, it remains unclear if the small underestimation of monoterpene concentrations was a result of the decreased detector response for olefins or if other effects have contributed to the decreased recovery. As reported by Apel *et al.* (2003a; 2003b) for the experiments performed during NOMHICE, best results were obtained by utilisation of FID detection- rather than MS detection systems and the latter effect was attributed to the different calibration procedures applied (assumption of a linear detector response per carbon for FID calibration or individual compound calibration for MS measurements).

As reported in detail by Slemr *et al.* (2002) the utilisation of multicomponent standards generated an improved performance of VOC analysis and eliminated errors that would have

been introduced by assumption of a proportional FID response. With the latter standard, errors introduced by the different behaviour of hydrocarbons within the analytical system can be eliminated (e.g. coelution or adsorptive losses). Therefore, the use of the above mentioned multicomponent standard reduced the differences between the participating groups during the AMOHA experiments, which would otherwise have been substantially higher than 10% (Slemr *et al.* 2002). As reported by De Saeger and Tsani-Bazaca (1992) the standardisation of sampling and calibration methods was also a prerequisite for the harmonisation of VOC measurements during the Tropospheric Ozone Research project (TOR).

Utilisation of a gaseous standard mixture contained in aluminium canisters is not recommended for the less stable biogenic compounds, since degradation effects are likely to occur and were observed e.g. for α-pinene (Apel *et al.* 1999). Better results for the calibration of biogenic VOC have been obtained by utilisation of non storing techniques like permeation or diffusion devices. However, use of these systems may introduce other uncertainties. As described in detail by Larsen *et al.* (1997), the negligence of adsorptive losses within the diffusion/permeation system may lead to an overestimation of VOC mixing ratios. Furthermore, even small impurities in the supplied liquid standards may change the diffusion rate through influences on the surface tension of the compound (change of Raoult's law constant) and may therefore lead to an under- or overestimation of VOC concentrations.

ACCURACY AND UNCERTAINTY OF VOC ANALYSIS

The data quality of VOC analysis was assessed by its accuracy, reproducibility and precision. Accuracies resulting in an under- or overestimation of the reference concentration by ± 25% were considered as good, accuracies of ± 50% as reasonable and > ± 50% as poor. Table 2.6. gives an overview of the results obtained for the different evaluated compounds. All outliers were removed from this data set by application of a Nalimov outlier test.

In general, the accuracy of VOC analysis was in reasonable or good agreement with the reference (permeation source) concentration. The measured reproducibility of a series of samples was always better than the precision that was calculated on the basis of the Gaussian error propagation. This indicates that the real uncertainty of VOC measurements was much smaller than the sum of all specified uncertainties.

The blank values of GC-FID analysis were highest for the two aromatic compounds benzene and toluene and accounted up to 42 and 43% of the respective samples. Moreover, blanks of α-pinene, 3-carene and benzene were highly variable, showing much higher values

Table 2.7. Observed range of accuracy, reproducibility and precision by the MPI for Chemistry for 8 evaluated VOCs during intercomparison I and II. Abbreviation: [1] intercomparison II only, [2] DNPH silica cartridges

Volatile organic compound	Range of uncertainty [%]		
	accuracy under/overestimation	measured reproducibility	calculated precision
isoprene	-35 to +32	± 2-6	± 4-10
α-pinene	-12 to ± 0	± 1-4	± 8-46
β-pinene [1]	-20 to -8	± 2-23	± 7-58
3-carene	-20 to -3	± 1-23	± 10-40
benzene	-15 to +37	± 2-12	± 11-41
toluene	-13 to +13	± 1-12	± 7-72
acetaldehyde [1,2]	+7	± 2	± 11-23
acetone [1,2]	-3	± 3	± 16-31

during intercomparison I. The latter results suggest that these compounds were not completely removed from the adsorption tube or GC-system during the previous analysis. The high blank values of benzene and toluene may also result from contaminations on the adsorption tube or within the GC-system. Within the range of evaluated VOC mixing ratios, the measured accuracy was not a function of the specified reference VOC concentrations. This effect is not in agreement to the experiments performed during AMOHA (Slemr *et al.* 2002). During the latter study a decrease of accuracy was observed with decreasing hydrocarbon concentrations, although a similar concentration range than during the present study was covered.

Best accuracy was obtained during the present study for the analysis of monoterpenes (α-pinene, β-pinene and 3-carene), but the reproducibility of these measurements accounted up to ± 23% for β-pinene and 3-carene. Although the reproducibility and precision were much better for isoprene than for the monoterpene measurements, the accuracy of the isoprene analysis was highly variable ranging between an underestimation of the reference mixing ratio by 35% and an overestimation of the reference by 32%. Moreover, the accuracy obtained for the benzene measurements was also highly variable. Benzene accuracies resulted in good to reasonable agreement with the reference concentrations, but an overestimation of up to 37% was also observed.

Accuracies obtained for acetaldehyde and acetone by the silica DNPH cartridge were good. With respect to the comparison of SPE C_{18}-silica DNPH cartridges and pure silica DNPH cartridges, the performance of the silica DNPH cartridges was much better than of the C_{18} DNPH system. The results are in agreement with previous experiments performed by

Kleindienst *et al.* (1998) who obtained a lower accuracy for formaldehyde with C_{18} DNPH cartridges than with silica DNPH cartridges. Also acetone mixing ratios were underestimated during the present study by the C_{18} DNPH system by far. These results are also in good agreement with previous measurements performed by Dindorf (2000) who reported acetone recovery rates of only 20%.

The results obtained from the present study are in agreement with the result reported by Volz-Thomas *et al.* (2002) for the German Tropospheric Research Focus (TFS). Here, deviations of ± 20% from the reference value were obtained for most hydrocarbon compounds during the comparison of synthetic test gas mixtures. However, the results obtained by the latter authors for ambient air measurements were much poorer. This was mainly a result of coelution effects, the lower mixing ratios, higher humidity, problems with peak identification, and blank- or memory effects. Solely the utilisation of a common harmonisation standard improved the results obtained for these ambient air measurements. However, for evaluation of their results, the latter authors defined specific data quality objectives (DQOs). These DQOs demanded an accuracy resulting in an under- or overestimation of the reference by ± 20% for alkenes and by ± 15% for aromatic compounds (at mixing ratios of > 100 ppt). The precision was demanded to range at ± 20% for alkenes and ± 10% for aromatics. Under the assumption that the reference concentrations were specified correctly in the present study, these DQOs are matched for most compounds (except isoprene and benzene) regarding the measured accuracy. Regarding reproducibility, β-pinene, 3-carene, benzene and toluene measurements showed slightly higher deviations than demanded.

Moreover, the results obtained from the present study are even better than the results obtained during the intercomparison experiment performed within the TOR project for several C_2-C_7 nonmethane hydrocarbons. Like for the ambient air measurements performed during TFS, a common primary calibration standard (n-butane and benzene) was used by the different participants within the framework of TOR. However, the deviation of volatile organics from the reference value accounted typically up to ± 35% during the latter project (Hahn 1994). In agreement with this approach, also during AMOHA a common calibration gas standard was used by the different participating groups. The utilisation of this primary standard resulted in an improved recovery ranging between deviations of ± 2-10% for a complex synthetic test gas mixture of 30 different VOCs.

However, comparatively good results were also obtained during the task 1 and 2 experiments performed during NOMHICE, even though no harmonisation standard was used by the different participants. During the latter study only few laboratories showed poorer recoveries

than ± 20% and more than half of the participating laboratories showed better recoveries than ± 10%. As reported by Volz Thomas *et al.* (2002), coelution of volatile organics was the most important error source for the analysis of ambient air samples during the TFS project. During the present study the utilisation of purified air minimizes the probability of coelution effects. However, coelution may still be possible, resulting in an overestimation of isoprene (possible coelution with propanal) and benzene (possible coelution with 2-butanone) during the experiments of intercomparison I and II. Therefore, further laboratory tests are needed to investigate these effects.

Underestimation of volatile organics on the other hand, may be caused by adsorptive losses during the preconcentration step or due to losses within the analytical system. Within this context, Slemr *et al.* (2002) reported of adsorptive losses that occurred for volatile organics with high boiling points (especially aromatic compounds like benzene). Therefore, the underestimation of the monoterpene compounds as observed during the present study may be also a result of adsorptive losses since the boiling points for monoterpenes exceed the boiling points for benzene and toluene.

Consistently, the measurements performed by Komenda *et al.* (2003) who applied a permeation device for the generation of a synthetic test gas mixture, showed also an underestimation of most evaluated monoterpene compounds. The accuracy obtained during these measurements for α-pinene ranged between an underestimation of 1 and 13%. The accuracy obtained for 3-carene ranged between an overestimation of 2 and 8% during the latter study. These results are indicative for the importance of adsorptive losses within a permeation and/or analytical system.

As reported in detail by Apel *et al.* (2003a; 2003b) for the NOMHICE experiments, the best results for VOC analysis were obtained by utilisation of glass beads used for the preconcentration step. During the latter study solid sorbents like Tenax or multibed carbon adsorbents generated the poorest results. However, for the measurement of ambient air the interference of water vapour, that was trapped during the preconcentration step on the glass beads may have a major impact on the recovery of several volatile organics (particularly for the sampling from humid environments like from enclosure measurements). As reported by Slemr *et al.* (2002) and Volz-Thomas *et al.* (2002), the interference of water vapour was also a major error source for the ambient air measurements performed during TFS and AMOHA. However, during the AMOHA study no outstanding measurement system could be identified.

CONCLUSION

The results obtained during the present study clearly indicated the importance of an accurate calibration for the measurement of volatile organic compounds. Although good results were obtained by assumption of a linear carbon response for GC-FID analysis, the utilisation of additional individual calibrations may provide further improvement of VOC measurements. Since syringe injections of liquid calibration standards for GC-FID analysis were shown to cause major discrepancies to the specified reference concentration, permeation devices may be a reliable alternative. However, also the utilisation of permeation devices may result in major discrepancies to a reference concentration, since adsorption or desorption effects are neglected. Therefore, implementation of both techniques for the calibration of VOC analysis by GC-FID is encouraged.

This recommendation is moreover strengthened, since the results of the present study demonstrated the importance of potential adsorption and coelution effects. Utilisation of individual calibrations may provide further information with respect to these effects and may moreover help to identify potential adsorption effects on the surface of the applied ozone scrubber assembly.

Potential carry over effects from previous analysis were observed for some compounds evaluated by GC-FID analysis. Therefore, a single desorption step of the adsorbent tubes may be not sufficient for VOC analysis. Longer and/or several desorption steps prior to the next measurement may provide better results.

The evaluation of both DNPH cartridge systems clearly demonstrated the advantage of the silica DNPH system with respect to the analysis of acetaldehyde and acetone. Moreover, due to the low accuracy obtained, the evaluation of acetone measurements using C_{18} silica DNPH cartridges is not recommended.

CHAPTER 3

EMISSION OF ISOPRENE AND MONOTERPENES FROM ENGLISH OAK AND EUROPEAN BEECH

ABSTRACT

Using a dynamic branch enclosure system the emission of isoprene and monoterpenes was investigated under field conditions from sunlit leaves of English oak (*Quercus robur* L.) and European beech (*Fagus sylvatica* L.). English oak was characterised as a strong emitter of isoprene, releasing VOCs as a function of light and temperature. Basal emission rates that were calculated by application of the G97 algorithm, ranged at 75 $\mu g\ g^{-1}\ h^{-1}$.

In contrast to several previous studies, European beech was characterised as a substantial emitter of monoterpenes, with sabinene being the predominant compound released. Basal emission rates measured from sunlit leaves of European beech ranged up to 13 $\mu g\ g^{-1}\ h^{-1}$. Shaded leaves of European beech exhibited an even higher standard emission factor that accounted up to 20 $\mu g\ g^{-1}\ h^{-1}$, but the latter factor was associated with a high uncertainty. Moreover, the monoterpene emission from European beech was shown to be a function of light, temperature, and the respective time of day. During high ambient temperature periods a midday depression of monoterpene emission was observed for one measurement day in June 2002. The night time emission of monoterpene compounds was negligible for the investigated tree individual. According to its broad geographical distribution and its substantial basal emission rate, the specific consideration of European beech demonstrated to have a substantial impact on the European monoterpene budget yielding increases of 16-54% relative to conventional inventories. On a local scale, increases of monoterpene emission exceeded 100%.

INTRODUCTION

The release of biogenic volatile organic compounds (VOCs) represents a substantial input of reactive trace gases into the atmosphere and influences atmospheric chemistry and physics (Went 1960; Fehsenfeld *et al.* 1992; Andreae and Crutzen 1997; Atkinson 2000). Furthermore, the emission of VOCs may represent a substantial loss of carbon for the biosphere (Guenther 2002; Kesselmeier *et al.* 2002b) and the exchange (emission and deposition) of volatile organic compounds, involved in the oxidant cycle, aerosol production, and carbon budget, plays a crucial role in climate forcing but is poorly understood in view of the high number of different VOC species and their exchange regulations.

The emission of isoprenoids, the dominating biogenic VOC fraction consisting mainly of isoprene and monoterpenes, has been investigated intensively during the last decades. However, our knowledge still is full of gaps. Until a decade ago a clear difference between

the emission of isoprene and that of monoterpenes was postulated. Isoprene emission was regarded as dependent on light and temperature, whereas monoterpenes were thought to be produced as storage compounds and to be emitted as a function of temperature only. However, within the course of the EU-project "BEMA, Biogenic Emissions in the Mediterranean Area" (for an overview see Seufert *et al.* 1997), it became obvious that monoterpenes can be released in the same manner as isoprene (see Kesselmeier and Staudt 1999), an observation that has recently been confirmed for the tropical rainforest (Kuhn *et al.* 2002b; Rinne *et al.* 2002). Meanwhile the release of monoterpenes from storage pools solely as a function of temperature is discussed rather as a special case (Kesselmeier 2004).

Light dependence of monoterpene emission is in full agreement with the recent knowledge of biosynthesis of isoprenoids and the close relation between photosynthesis and isoprene/monoterpene production within chloroplasts (see Lichtenthaler 1999). This knowledge has resulted in a substantial number of new questions concerning ecology and evolution (Lerdau and Gray 2003), regulation and controls of production and emission (Peñuelas and Llusia 2001; Niinemets and Reichstein 2003; Wolfertz *et al.* 2003), as well as what the contribution of different carbon sources to isoprenoid biosynthesis are in order to understand production, accumulation and emission (Schnitzler *et al.* 2004).

Several plant species of high importance for regional or global estimations have not been sufficiently investigated yet but are nevertheless included in budget calculations just by assigning emission rates based on plant family relationships (Karlik and Winer 2001). Finally, the seasonal development of VOC emission capacity plays a significant role (Kesselmeier *et al.* 2003; Kuhn *et al.* 2004a; 2004b) and neglecting environmental effects and plant adaptations may lead to a significant under/overestimation of isoprenoid emission.

Within the framework of the German ECHO project (Emission and CHemical transformation of biogenic volatile Organic compounds, AFO 2000, see http://www.fz-juelich.de/icg/icg-ii/echo) we performed enclosure measurements during two intensive field campaigns in the summers of 2002 and 2003 in order to investigate the primary emission of volatile organic compounds from naturally growing English oak (*Quercus robur* L.) and European beech (*Fagus sylvatica* L.).

METHODS

To investigate the exchange of volatile organic compounds from English oak and European beech by enclosure techniques, two intensive field campaigns were conducted in a small

mixed forest stand in the summer of 2002 and 2003. Vertical and horizontal distribution of volatile organics was investigated by simultaneous profile measurements within the forest stand. Table 3.1. gives an overview of the measurements conducted during the field campaigns of 2002 and 2003.

Table 3.1. Measurements conducted during both field campaigns in the summer of 2002 and 2003.

Measurement	Date
Enclosure measurement: European beech, canopy top	12.06. - 19.06.2002 and 23.07. - 07.08.2003
Enclosure measurement: European beech, below canopy	09.08. – 12.08.2003
Enclosure measurement: English oak	25.06. – 01.07.2002
Vertical and horizontal profile measurements	08.07 and 10.07.2002

SITE DESCRIPTION

The measurement site was located in an urban area, nearby the small city of Jülich, Germany, in about 30 km distance from the Dutch and Belgian border at geographical coordinates of 50° 54.321’ N, 006° 25.130’ E. The region is dominated by agricultural land and forests account only for a small percentage of the total area. The measurement site is characterised by moderate climatic conditions, with a mean annual precipitation of 685 mm and an average annual temperature of 10°C.

Beech enclosure- and profile measurements were carried out in a deciduous forest stand of about 3.5 km^2 size that was partially located on the premises of the Research Centre Jülich (RCJ). Predominant soil type of this forest area was luvic stagnosol that provided a moderate supply of nutrients for the growing plants. Three scaffold towers were built by the RCJ within the forest stand in the following referred to as West Tower, Main Tower and East Tower, with heights ranging from 36 to 24 m. For enclosure measurements on English oak, another scaffold tower (in the following referred to as Small Tower) was located outside of the forest area on a small meadow near to an accumulation of several oak trees. Figure 3.1. gives an overview of the measurement site and the location of all scaffolding towers. Enclosure measurements were performed at the East Tower- and at the Small Tower site. The area near-by the East Tower site was dominated by European beech trees of up to 28 m in height. In contrast to the East Tower site, the Small Tower site was dominated by grassland, with only few adult oak trees located on the meadow. To provide an insight to the vertical and horizontal distribution of volatile organic compounds within the forest, VOCs were measured

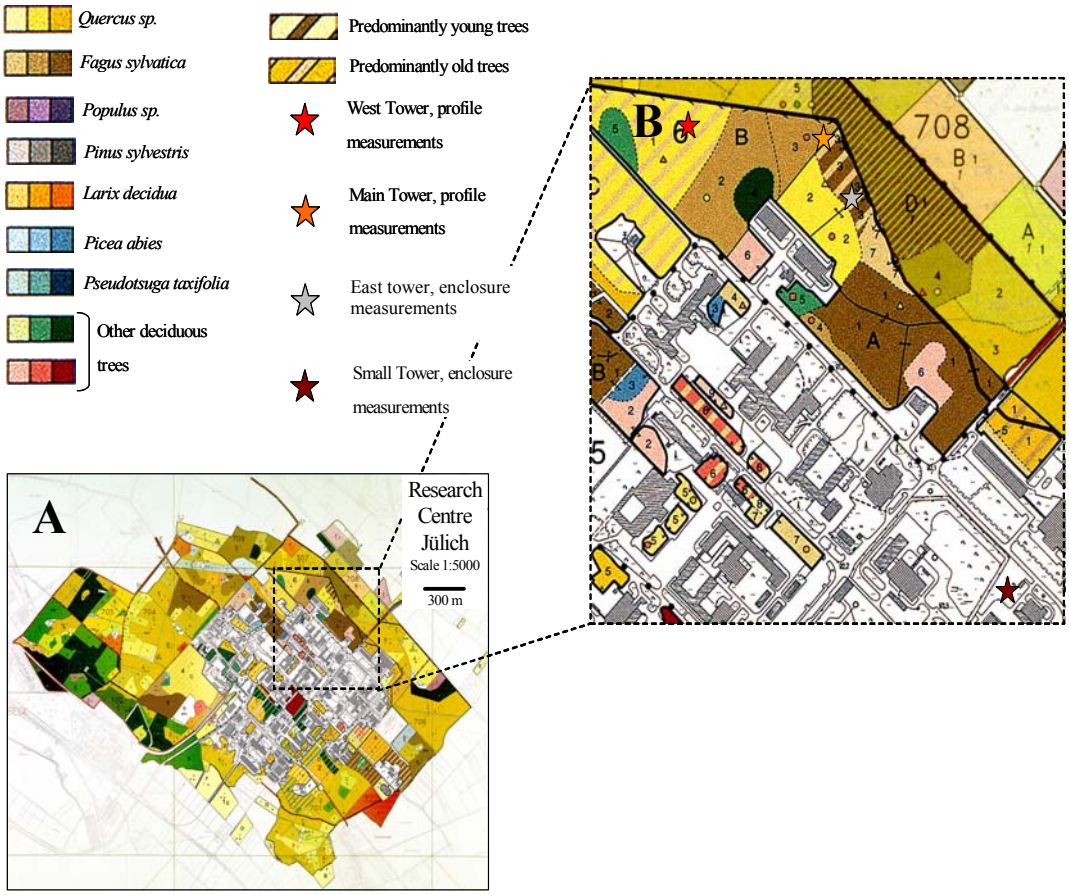

Figure 3.1. Vegetation map of the measurement site. (A) Map of the Research Centre Jülich. (B) Enlargement of the vegetation map showing the four measurement sites. Adapted from Forsteinrichtungsbüro B. Paggenborg, Wietmarschen, Germany.

simultaneously on four different heights at the Main Tower site and on two different heights at the West Tower site. The West Tower site was dominated by a 55 year old stand of English oak and a minor fraction of silver birch. The Main Tower site was dominated by 150 year old European beech and birches. While the forest canopy reached about 30 m at the Main Tower site, the canopy top at the West Tower site was located at a height of 24 -26 m.

ENCLOSURE MEASUREMENTS

Plant material

Enclosure measurements were conducted at the East Tower site on European beech (*Fagus sylvatica* L.), over a period of 8 days in June 2002 and 16 days in July/August 2003. Cuvette measurements were accomplished during both years with the same individual branch located at the canopy top (in ~28 m height) of a ~160 year old European beech tree. A second branch

located below the canopy (in ~18 m height) of the same tree individual was investigated for 4 days in August 2003 including 2 days of VOC measurements. English oak (*Quercus robur* L., pedunculate oak) was investigated for 8 days in June 2002. However, VOC measurements by GC-FID analysis were performed only for 2 days. The measurements were performed at the small tower site on a sunlit branch of an adult oak tree in ~4 m height.

In general, both deciduous tree species belong to the family *Fagaceae*. However, *Fagus sylvatica* L. is known to be a monoterpene emitter and *Quercus robur* L. is known to be an isoprene emitting tree species (see Kesselmeier and Staudt 1999). A detailed description of the plant family *Fagaceae* can be obtained from botanical literature (Schmeil and Fitschen 1993; Strasburger *et al.* 1993). In general, the flowers of both tree species are either female or male. While the female flowers follow the overall formula P 3 + 3 G (3), male flowers consist of a changing amount of perianth leaves and stamina. Both tree species produce endosperm-less nut fruits that are generally diffused by rodents. Moreover, both tree species are socialised with mycorrhiza fungi. A main distinctive feature of the tree species is the form of their leaf margins, since *Fagus sylvatica* L. is characterised by its entire, slightly undulated leaf margin and *Quercus robur* L. is characterised by its sinuate leaf margin (see Figure 3.2. A and C). Furthermore, *Quercus robur* L. is characterised by its short petiole and its peduculated fruits.

Both tree species are widely distributed in Europe. As described in detail by Köble and Seufert (2001), *Fagus sylvatica* L. is the dominating deciduous tree species in Europe, covering 7% of the vegetation area. The vegetation coverage of *Quercus robur* L. accounts to 3% on a European scale. Both tree species are not socialised with each other, since European

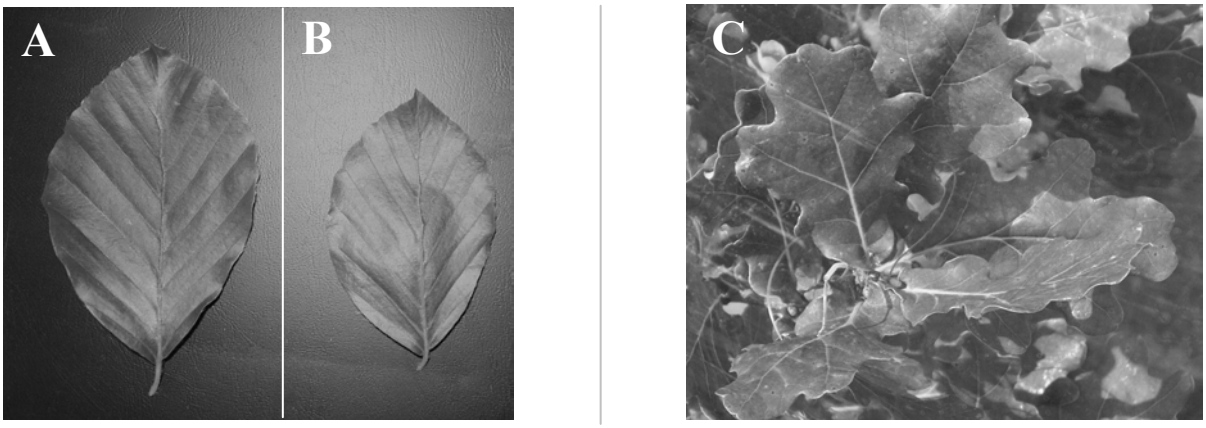

Figure 3.2. Leaves of both measurement trees. Left panel: (A) Adult leaves of European beech picked from the top of the canopy at ~28 m height and (B) below of the canopy at ~18 m height during the summer of 2003. Right panel: (C) Leaves of English oak within the enclosure system during the summer of 2002.

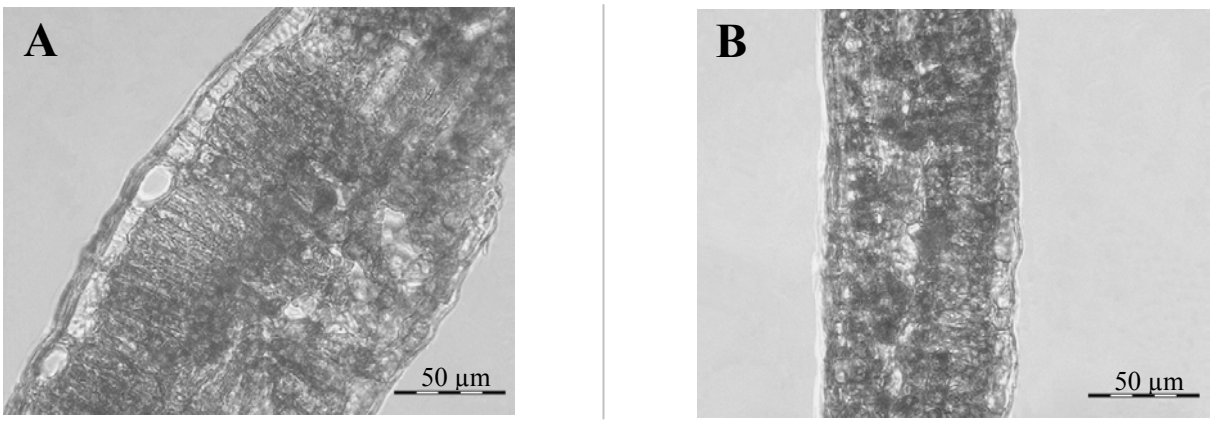

Figure 3.3. Microscopic cross section of European beech leaves. Cross sections of both leaves were cut near the median vein. (A) Leaves picked from the canopy top. (B) Leaves picked from a height of ~18 m.

beech is much more sensitive to drought and heat stress than oak trees (see Strasburger *et al.* 1993; Backes and Leuschner 2000; Thomas 2000).

Both tree species are known to be shade tolerant. Measurements performed on European beech were conducted on leaves from the canopy top (see Figure 3.2.A) and on leaves from below of the canopy (see Figure 3.2.B). As shown by Figure 3.2., the leaves picked from below of the canopy are smaller than the leaves from the canopy top. Moreover, the microscopic analysis of both leaf types demonstrated that leaves from the canopy top showed a higher cross section, than leaves from below of the canopy (see Figure 3.3.).. The latter data are indicative of the formation of sunlit and shaded leaf structures (see Strasburger *et al.* 1993) and are moreover in agreement with the reference data measured at both investigated branches. As shown by Table 3.2., leaves from below of the canopy developed a lower specific leaf weight than leaves grown at the canopy top. In the following paragraphs leaves investigated at the canopy top will therefore be referred to as sunlit leaves and leaves from below of the canopy will be referred to as shaded leaves.

All reference data were obtained at the end of each experiment. Leaves of the investigated tree were harvested directly from the measurement branch (European beech measurements in 2003) or from a second branch near to the investigated one (English oak measurements and European beech measurements in 2002). In either case, the leaf area (single side plus petiole) was copied or drawn from the original branch and was calculated by use of a calibrated scanner system [ScanJET IIX with DeskScan II, Hewlett Packard, USA and the software SIZE, Mueller, Germany]. Fresh and dry weight of the original or reference leaves were determined by a microbalance [PM 400, Mettler-Toledo, Germany] before and after drying in

an oven [Heraeus, Germany] at 70°C for several days. Thus, fresh and dry weight of the measurement branch were determined either directly or were calculated by use of the specific leaf weight of the reference branch.

Table 3.2. Reference values for branch enclosures. Abbreviations: [a] from originally enclosed leaves, [b] calculated by use of the specific leaf weight of the reference branch.

Measurement	Enclosed leaf area [m^2]	Enclosed fresh weight [g]	Enclosed dry weight [g]	Water content of enclosed branch [%]	Enclosed leaf dry mass per area [g m^{-2}]
Fagus sylvatica L.					
Sunlit branch 2002	0.17 [a]	32.62 [b]	18.35 [b]	44	108
Sunlit branch 2003	0.14 [a]	21.33 [a]	10.73 [a]	50	77
Shaded branch 2003	0.06 [a]	5.14 [a]	2.14 [a]	58	33
Quercus robur L.					
Sunlit branch 2002	0.30 [a]	49.71 [b]	27.01 [b]	46	90

Enclosure system

All experiments were conducted by the use of an open, dynamic (flow through) enclosure system consisting of two identical cuvettes of 75 l volume each, that were made from FEP Teflon foil [Norton, 50 µm thickness, Saint-Gobain Performance Plastics, Germany], that was fully light permeable in the spectral range of 300-900 nm (Schäfer *et al.* 1992). Figure 3.4. gives an overview of the basic components of the enclosure system. The system was used for several field campaigns and is described in detail by Kesselmeier *et al.* (1996) and Kuhn *et al.* (2002a).

As shown by Figure 3.4., ambient air was filtered at the inlet of the enclosure system from small particles by utilisation of four Teflon filters [Zeflour Teflon filters, 2 µm pore size, Gelman Science, USA]. Moreover, to prevent oxidant interferences inside of the enclosure system, ozone was scrubbed from the inlet air by two ozone scrubbers [~0.04 m^2 each, MnO_2 covered copper screens, Ansyco, Germany]. The filtered air was pumped by four Teflon membrane pumps [Vakuubrand, Germany] to both cuvettes. The flow rate to each enclosure was monitored by flow meters [EL-Flow, 50 l min^{-1}, Bronkhorst Hi-Tec, Germany] and was typically adjusted to constant flow rates of 25-35 l min^{-1} by use of a needle valve, resulting in a total exchange of the enclosure volume every 2 to 3 minutes. To prevent contamination and/or the loss of volatiles all tubings and fittings were made from PFA Teflon. To offer a

minimum resistance to the inlet air flow, most tubings prior to both enclosures were made from ½" tubing. The filtered air entered both enclosures by a u-shaped ½" tubing. The air inside of the enclosures was well mixed by a Teflon covered propeller (for details of the construction see Kuhn *et al*. (2000)), leading to an aerodynamic resistance of about 30 s m^{-1} (Gut *et al*. 2002). To obviate condensation of water, all Teflon tubings starting at the cuvette outlets were heated to 35°C by use of anti-condensation heating tape [RS components GmbH, USA] that was fixed together with the Teflon tubing in a conventional insulation hose. The Teflon lines had a length of 6 m and an outer diameter of ¼" (for the CO_2 and H_2O measurements) or ⅛" (for the VOC measurements). As demonstrated earlier, the enclosure system can be regarded as inert for the relevant volatile organic compounds and allows the investigation of an enclosed branch for several days without visible effects of stress (e.g. Kesselmeier *et al.* 1996; 1997; 1998a; Kuhn *et al.* 2002b).

Micrometeorological parameters:
For the adequate evaluation of VOC emission rates it is necessary to record micrometeorological parameters during the measurement period. Photosynthetic active radiation (PAR) was measured outside of the enclosures by use of two quantum sensors [Model SB 190, Licor, USA] that were mounted in horizontal arrangement on top of the branch cuvette but not shading the leaves (only one sensor in 2003). Enclosure temperatures in the reference and sample cuvette were measured by Teflon covered thermocouples [0.005", Chromel-Constantan, Omega, UK]. Ambient temperature was measured outside but next to the sample cuvette. Leaf temperatures were measured on the upper- and lower side of two representative leaves inside of the sample cuvette by application of the same type of thermocouples. Relative humidity for ambient and sample cuvette conditions was monitored by the use of two combined temperature/relative humidity sensors [T/rH sensor, see Figure 3.4., Model Rotronics YA-100F, Walz, Germany] that were mounted near to the ambient air inlet system and at the outlet of the sample cuvette.

Meteorological parameters:
Ambient temperatures and rainfall preceding the enclosure measurements were monitored by the meteorological station of the Research Centre Jülich on a meteorological tower located in about 470 m distance from the East Tower site. Photosynthetic active radiation, temperature, and wind direction monitored during the measurement of VOC profiles were recorded at the West Tower site by the meteorology group of the Max Planck Institute for Chemistry, Mainz.

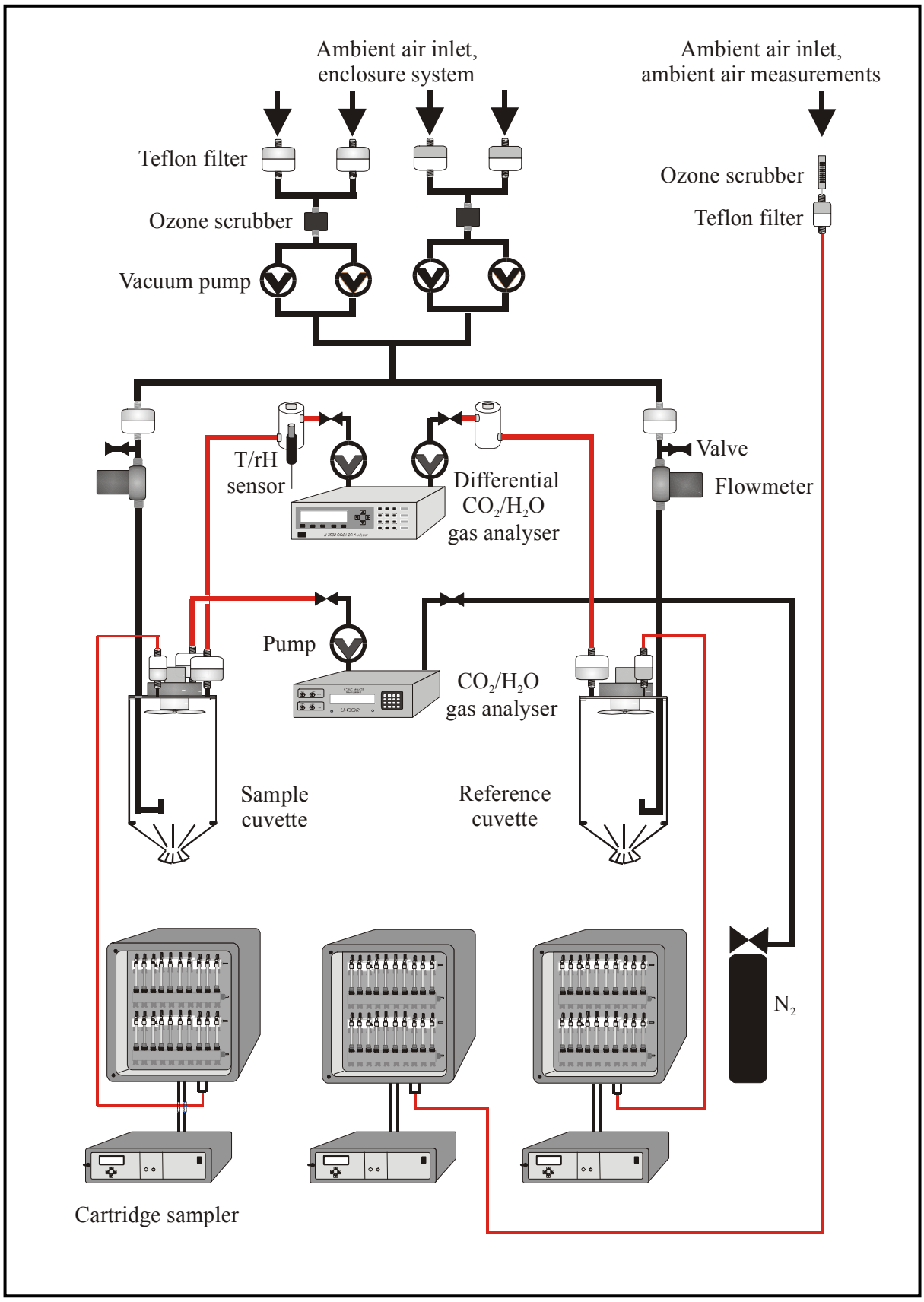

Figure 3.4. General setup of the enclosure system used for the measurement of European beech and English oak. Electrical connections, thermocouples and PAR sensors are not shown. Black lines indicate Teflon tubing. Red lines indicate Teflon tubing that was heated above ambient temperatures. For a detailed description see text.

CO_2 and H_2O concentration inside the sample cuvette:

CO_2 and H_2O concentrations inside the sample cuvette were measured permanently by use of an infrared gas analyser [CO_2/H_2O gas analyser, see Figure 3.4., Model Li-6262, incubated at constant temperature, Licor, USA]. A detailed description of the instrument is given in chapter 4. For the measurement of CO_2 and H_2O concentrations the instrument was operated in an absolute mode with Nitrogen [N_2 5.0, Messer Griesheim, Germany] as a reference gas. The sample gas flow to the instrument was adjusted to 0.5 l min^{-1} by use of a small custom made pump unit that was installed in front of the analyser inlet. The N_2 gas flow to the reference was adjusted to 50 ml min^{-1} by use of a needle valve. Calibration of the analyser was accomplished prior to the experiments by use of a calibration gas standard (347 ppm CO_2 in synthetic air) and a dew point generator. At the end of each experiment the calibration of the analyser was checked and the signal response was corrected for sensitivity and zero drifts as a function of time.

Physiological parameters:

Plant physiological activity and parameter calculations such as photosynthesis, transpiration and stomatal conductance were based on CO_2 and H_2O differences between sample and reference enclosure. CO_2 and H_2O differences were measured by the use of an infrared gas analyser [differential CO_2/H_2O gas analyser, see Figure 3.4., Model Li-7000, incubated at constant temperature, Licor, USA] that was operated in a differential mode (receiving air from both enclosures). The gas flow to the instrument was supplied by a similar pump unit as was used for absolute CO_2 and H_2O measurements. The flow rates were adjusted to 0.5 l min^{-1}. Calibration of the gas analyser was accomplished in analogy to the absolute CO_2 and H_2O measurements and sensitivity and zero drifts were corrected accordingly. Furthermore, the signal response of the instrument was corrected for temperature effects and with regard to the offset of specified and measured reference concentrations. All continuous measured micrometeorological and physiological parameters were recorded by a micrologger [Model CR23X, Campbell Scientific Inc., UK] as 5 minute averages.

Sampling and analysis of volatile organic compounds:

Measurement of volatile organic compounds was performed by the use of solid adsorbents and subsequent analysis of the sampled compounds by GC-FID. The sampling and analysis of volatile organics was performed in agreement with the experiments of intercomparison I and II and is described in detail in chapter 2. The samples were collected simultaneously by the

use of three automated cartridge samplers from the reference cuvette, the branch cuvette, as well as from ambient air. As shown by Figure 3.4., ambient air samples were collected from a second air inlet mounted next to the inlet of the enclosure system. The second inlet was equipped with an identical ozone scrubber assembly as used during the intercomparison experiments. All samples were collected for 30 minutes at flow rates of 150 ml min^{-1} resulting in a total sampling volume of 4500 ml. Analysis of the samples by GC-FID was performed at the end of each experiment by the GC-FID laboratory at the Max Planck Institute in Mainz as described in detail in chapter 2. The calibration of the system was accomplished by use of a gaseous standard containing isoprene and several n-alkanes.

In addition to isoprene and other volatile organics, 10 different monoterpene compounds were evaluated from these analyses: camphene, Δ3-carene, p-cymene, limonene, myrcene, α-pinene, β-pinene, sabinene, α-terpinene, and γ-terpinene. The detection limit of the system was 30 ppt for isoprene and < 10 ppt for monoterpenes (see Kuhn *et al.* 2002b). Unless indicated otherwise, the following paragraphs will report on the total sum of monoterpene compounds measured by GC-FID.

VERTICAL AND HORIZONTAL PROFILE MEASUREMENTS

To provide an insight to the vertical and horizontal distribution of volatile organic compounds within the forest, VOCs were measured simultaneously on four different heights on the Main Tower site and on two different heights on the West Tower site over a time period of 2 days in July 2002.

As shown by Figure 3.5., the inlets were mounted in an easterly direction at 9, 18, 27, and 36 m on the Main Tower and at 24 and 36 m on the West Tower. Since the forest canopy height was different at both towers sites (~30 m at the Main Tower and ~24-26 m at the West Tower), the second highest measurement level was either located at the canopy top (West Tower) or within the canopy (Main Tower). However, the uppermost level was always located above the canopy.

All measurements were conducted by utilisation of 3 automatic cartridge sampler units mounted at both tower sites, with each sampler covering two sampling heights. VOCs were sampled on solid adsorbents and analysed in analogy to the enclosure and intercomparison experiments by the GC-FID laboratory in Mainz. Sampling was conducted in 2 hour intervals by utilisation of PFA Teflon lines (⅛" outer diameter, 5 or 6 m length at the Main Tower and at the West Tower, respectively) for 30 min at flow rates of 150 ml min^{-1}. To prevent a con-

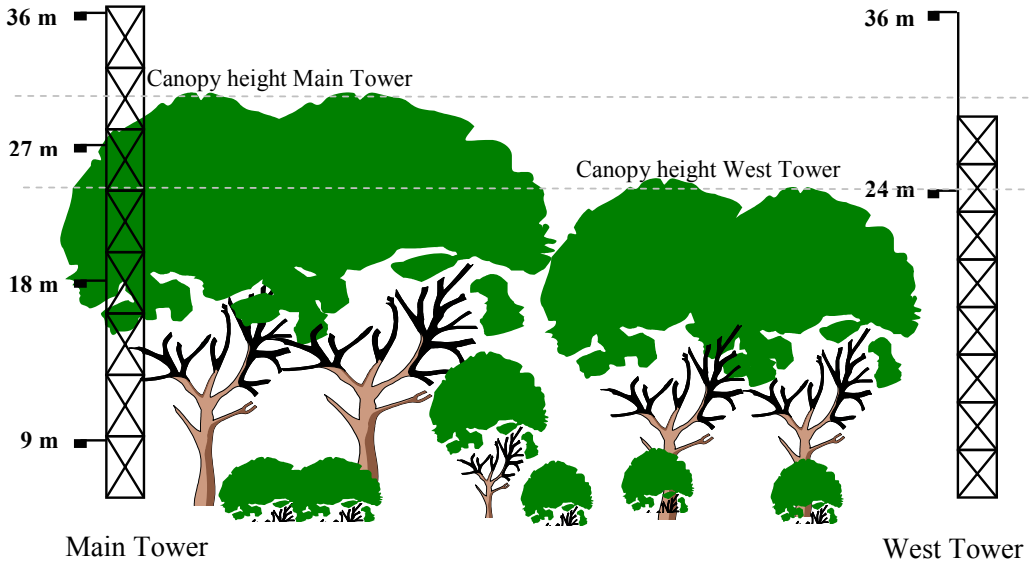

Figure 3.5.. Setup of the vertical and horizontal profile measurements performed during two days in July 2002.

densation of water vapour, the inlet tubings were heated slightly above ambient temperatures as described for the experiments of intercomparison I and II. Furthermore, to eliminate oxidant interferences each sampling inlet was equipped with an ozone scrubber assembly as reported in detail in chapter 2. Each inlet, was mounted in a head first position at the respective inlet height. Meteorological parameters were monitored at the West Tower site by meteorology group of the MPI for Chemistry.

CALCULATION OF VOC CONCENTRATION, PHYSIOLOGICAL PARAMETERS, AND EXCHANGE RATES

Calculation of VOC concentrations

VOC concentrations were calculated by application of Formula 2.2. as described in detail by chapter 2 for the experiments of intercomparison I and II. VOC concentrations were calculated for the reference and sample cuvette as well as for the ambient air measurements.

Calculation of exchange rates

Photosynthesis, respiration, and transpiration were calculated based on CO_2 and H_2O concentration differences between both enclosures. Application of Formula 3.1. calculates the CO_2 and H_2O exchange rates that are normalised to the investigated leaf area or dry weight at standard conditions of 0°C. Negative values indicate deposition of the respective compound, positive values indicate an emission. VOC exchange rates were calculated accordingly.

$$\text{Exchange Rate} = \frac{(MR_{Sample} - MR_{Reference}) \cdot Q}{MV \cdot A} \quad 3.1.$$

Formula 3.1.: A = reference value of the measurement branch, e.g. leaf area [m^2] or dry weight [g], Exchange rate = exchange rate of the respective compound [e.g. µmol g^{-1} min^{-1}], $MR_{Reference}$ = mixing ratio in reference cuvette [e.g. ppm], MR_{Sample} = mixing ratio in sample cuvette [e.g. ppm], MV = mole volume of an ideal gas [22.4 l mol^{-1}, 0°C, 1 bar], Q = chamber flush rate normalised to 0°C [e.g. l min^{-1}]

Calculation of stomatal conductance

The stomatal conductance represents a relative measure of the average opening amplitude of all stomata present on the investigated leaf area. The stomatal conductance is calculated based on the measured transpiration rate and the difference of absolute humidity between the sample cuvette and the leaf. Application of Formulas 3.2. to 3.4. calculates the stomatal conductance for water vapour corrected for the mass flux of water according to Pearcy *et al*. (1989). Conversion to the stomatal conductance for other trace gases can be obtained by application of the respective correction factors (e.g. 1.6 for CO_2).

The absolute humidity inside of the sample cuvette that has to be inserted in Formula 3.2., was calculated by application of Formula 3.3.. The absolute humidity inside of the leaf was calculated accordingly under the assumption that the relative humidity inside of the leaf is 100%. The saturation vapour pressure that has to be inserted in Formula 3.3., was calculated by application of Formula 3.4..

$$\text{Stomatal cond}_{H2O} = \frac{(TR \cdot (1 - aH_{Mean}))}{(aH_{Leaf} - aH_{Cuvette})} \quad 3.2.$$

$$aH = \frac{E \cdot rH \cdot MW}{((R \cdot 1000) \cdot (N_T + T))} \quad 3.3.$$

$$E = 6.1078 \cdot e^{\frac{(17.08085 \cdot T)}{(234.175 + T)}} \quad 3.4.$$

Formula 3.2. to 3.4.: aH = absolute humidity inside of the sample cuvette or leaf [kg m^{-3}], $aH_{Cuvette}$ = absolute humidity inside of the sample cuvette [kg m^{-3}], aH_{Leaf} = absolute humidity inside of the leaf [kg m^{-3}], aH_{Mean} = average of absolute humidity in cuvette and leaf [kg m^{-3}], E = saturation vapour pressure of the sample cuvette or leaf [mbar], MW = molecular weight of water [18 g mol^{-1}], N_T = conversion factor for the Kelvin temperature scale [273.14], R = universal gas constant [8.314 J mol^{-1} K^{-1}], rH = relative humidity inside of the sample cuvette or leaf [%], Stomatal $cond_{H2O}$ = stomatal conductance for water [m h^{-1}], T = Cuvette temperature or leaf temperature [°C], TR = transpiration rate [kg m^{-2} h^{-1}]

APPLIED STATISTICS

The measured trace gas concentrations were evaluated by the utilisation of several statistical procedures that are described in detail in chapter 2.

PRECISION OF VOC CONCENTRATION AND EXCHANGE RATES

The precision of VOC concentration was calculated by conventional Gaussian error propagation as described in detail for the intercomparison experiments (see Formula 2.13.). The calculation of the precision of exchange rates followed the same approach and is given by Formula 3.5..

$$\text{Precision}_{ER} = \sqrt{\left(\left(\frac{\left(\sqrt{P_{MRsample}{}^2 + P_{MRreference}{}^2}\right)}{\left(MR_{Sample} - MR_{Reference}\right)}\right)^2 + P_Q{}^2 + P_A{}^2\right)} \qquad 3.5.$$

Formula 3.5.: $MR_{Reference}$ = mixing ratio in the reference cuvette [ppb], MR_{Sample} = mixing ratio in the sample cuvette [ppb], P_A = precision of leaf reference data (e.g. dry weight) [%], Precision_{ER} = precision of exchange rate [%], $P_{MRreference}$ = precision of mixing ratio measured in the reference cuvette [ppb], $P_{MRsample}$ = precision of mixing ratio measured in the sample cuvette [ppb], P_Q = precision of chamber flush rate [%]

For terms that were liked by multiplication or division during the calculation of exchange rates, relative uncertainties were used. Formula 3.5. combines the measured precision of the chamber flush rate with the precision that arose from the determination of the investigated leaf area or dry weight. The relative uncertainty of the chamber flush rate was specified by the manufacturer and accounted to 0.1%. The uncertainty of the dry weight determination accounted to 0.001 g (e.g. yielding a relative precision of 0.09‰ for the measurement of European beech in 2003). Since mixing ratio differences between the branch enclosure and the empty reference were used for the exchange rate calculation, the precision of these mixing ratios were inserted on an absolute basis.

EMISSION ALGORITHMS

To describe the emission of isoprene and monoterpenes from European beech and English oak, VOC emissions were compared to two algorithms that calculate the VOC emission as a function of short term changes in light and temperature.

The first algorithm (in the following referred to as G97) was basically developed for isoprene emission by Guenther *et al.* (1993; 1995; 1997). In general, isoprene emissions have been shown to be triggered by light as a result of the close link between isoprene emission and its production from photosynthetic precursor compounds. However, several authors demonstrated that the latter algorithm may also be used to calculate light and temperature dependent monoterpene emissions from several tree species (e.g. see Ciccioli *et al.* 1997; Kuhn *et al.* 2002b; Kuhn *et al.* 2004a).

The G97 algorithm assumes a hyperbolic increase of VOC emission with light intensity leading to a saturation (similar to the function of CO_2 assimilation versus light intensity, see Figure 3.6. A). In correlation to leaf temperature the algorithm assumes enzymatic processes leading to a temperature optimum of VOC emission at 39°C (see Figure 3.6. B). Higher temperatures are assumed to lead to a deactivation of the relevant enzyme. The light dependent term of the G97 algorithm is specified by Formula 3.6., the temperature dependent term by Formula 3.7. On a first approach the empirical factor C_{T3} of Formula 3.7. was set to a value of 1 (Guenther *et al.* 1993). In a latter version of the model this empirical coefficient was corrected to a value of 0.961 (Guenther 1997).

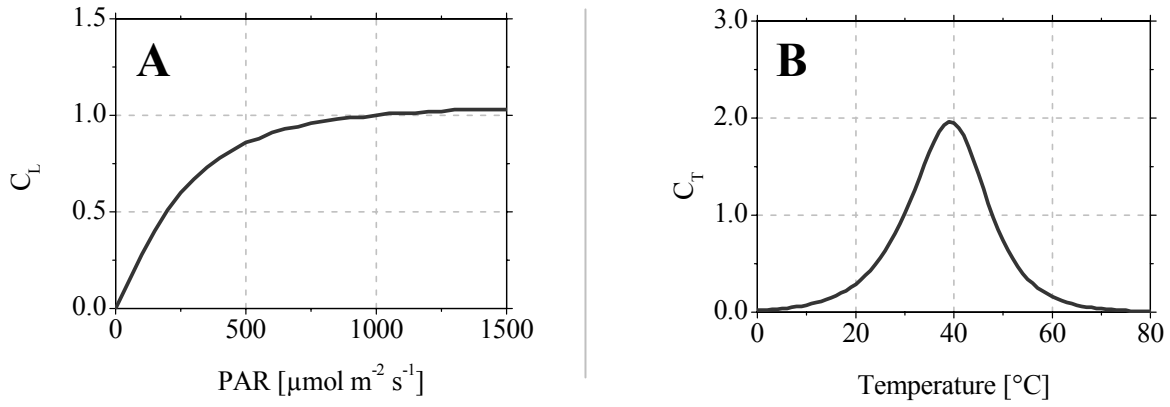

Figure 3.6. Light and temperature dependence of the G97 algorithm. (A) Light dependent function of the G97 algorithm. (B) Temperature dependent function of the G97 algorithm.

To calculate the actual VOC emission, both terms (C_L and C_T) were linked by multiplication with a standard emission factor (SEF) that describes the basal VOC emission at standard conditions (1000 µmol m^{-2} s^{-1}, 30°C, see Formula 3.8.). The standard emission factor can be derived from the slope of linear regression of the measured VOC emission versus the product of the terms C_L and C_T.

$$C_L = \frac{\alpha \cdot C_{L1} \cdot L}{\sqrt{1 + \alpha^2 \cdot L^2}} \qquad 3.6.$$

$$C_T = \frac{\exp\left(\frac{C_{T1} \cdot (T - T_S)}{R \cdot T_S \cdot T}\right)}{C_{T3} + \exp\left(\frac{C_{T2} \cdot (T - T_M)}{R \cdot T_S \cdot T}\right)} \qquad 3.7.$$

$$\text{VOC emission} = SEF \cdot C_L \cdot C_T \qquad 3.8.$$

Formulas 3.6. to 3.8.: α = empirical coefficient = 0.0027, C_{L1} = empirical coefficient = 1.066, C_L = light dependent term of the G97 function, C_T = temperature dependent term of the G97 function, C_{T1} = empirical coefficient = 95000 [J mol^{-1}], C_{T2} = empirical coefficient = 230000 [J mol^{-1}], C_{T3} = empirical coefficient = 0.961, L = photosynthetic active radiation, PAR [µmol m^{-2} s^{-1}], R = universal gas constant = 8.314 [J K^{-1} mol^{-1}], SEF = standard emission factor [µg g^{-1} h^{-1}], T = leaf temperature [°K], T_M = empirical coefficient = 314 [°K], T_s = leaf temperature at standard condition = 303 [°K], VOC emission = VOC emission rate [µg g^{-1} h^{-1}]

The second algorithm (in the following referred to as S97) was basically developed to describe the emission of monoterpenes as a function of light and temperature (Schuh *et al.* 1997). In comparison to the G97 function the S97 algorithm assumes also a saturation effect at high light intensities. However, at lower light levels it assumes an allosteric enzyme regulation leading to a sigmoid increase of the VOC emission which is described by Formula 3.9.. Moreover, in addition to the enzymatic processes that lead to a temperature optimum (described by Formula 3.7.), the S97 function assumes an additional VOC emission from storage pools which is solely temperature controlled and is described by Formula 3.10..

$$C_{L(S)} = C_{L1} \cdot \left(\frac{\alpha \cdot L}{\sqrt{1 + \alpha^2 \cdot L^2}}\right)^2 \qquad 3.9.$$

$$C_{P(S)} = \exp\left(\frac{C_{TP}}{R} \cdot \left(\frac{T - T_S}{T \cdot T_S}\right)\right) \qquad 3.10.$$

All terms ($C_{L(S)}$, C_T, and $C_{P(S)}$) were linked with basal emission rates resulting from an actual production (Φ_{LT}) or from storage pools (Φ_P). The actual VOC emission is described by Formula 3.11., or if storage pools are neglected, by Formula 3.12.

$$\text{VOC emission} = \Phi_P \cdot C_{P(S)} + \Phi_{LT} \cdot C_{L(S)} \cdot C_T \qquad 3.11.$$

$$\text{VOC emission} = \Phi_{LT} \cdot C_{L(S)} \cdot C_T \qquad 3.12.$$

Formulas 3.9. to 3.12.: α = empirical coefficient = 0.0027, C_{L1} = empirical coefficient = 1.066, $C_{L(S)}$ = light dependent term of the S97 function, $C_{P(S)}$ = storage pool dependent term of the S97 function, C_{TP} = empirical constant (equivalent to enthalpy of VOC vaporisation, see Schuh *et al.* (1997)), L = photosynthetic active radiation, PAR [µmol m^{-2} s^{-1}], Φ_{LT} = basal emission factor (light and temperature) [µg g^{-1} h^{-1}], Φ_P = basal emission factor (storage pools) [µg g^{-1} h^{-1}], R = universal gas constant = 8.314 [J K^{-1} mol^{-1}], T = leaf temperature [°K], T_s = leaf temperature at standard condition = 303 [°K], VOC emission = VOC emission rate [µg g^{-1} h^{-1}]

CALCULATION OF EUROPEAN VOC EMISSION

To assess the potential implication of monoterpene emissions from *Fagus sylvatica* L. on a European scale, an offline version of the Guenther *et al.* (1995) VOC emission algorithm was applied by the modelling group of the MPI for Chemistry. The latter offline version of the algorithm that is normally used for global scale studies (Ganzeveld *et al.* 2002), uses the Olson (1992) global ecosystem database, which distinguishes 72 ecosystems at a 0.5 x 0.5 grid resolution, combined with a 5-year climatology of monthly NDVI (Normalized Differential Vegetation Index) satellite data (Gutman *et al.* 1995) to infer global surface cover properties. VOC emissions were calculated as a function of ecosystem specific emission factors, surface radiation, temperature, foliar density and its vertical distribution. The latter is required to calculate the within-canopy profiles of photosynthetic active radiation (Weiss and Norman 1985) and distinguishes four canopy layers based on the sensitivity of the emissions on the vertical resolution (Ganzeveld *et al.* 2002). Normally, the emission algorithm is applied in the chemistry-climate model ECHAM to calculate the biogenic VOC emissions and their role for atmospheric chemistry online from the model's surface temperature and net radiation. However, for the offline calculations presented, the temperature and net radiation output fields of an ECHAM T106 (~125 km resolution) simulation were applied for the month of July at 6-hour time intervals. For a comparison with the global scale algorithm, a dataset that describes the European distribution of *Fagus sylvatica* L. at a 1 x 1 km grid resolution (Köble and Seufert 2001) was used and was combined with an average monoterpene emission factor.

SAMPLING PROCEDURES AND PROTOCOL

Enclosure measurements were carried out over a period of 8 days in June 2002 and 16 days in July/August 2003 with the same branch of a ~160 year old beech tree. The tree was located in north-north-westerly direction of the tower and was sunlit for the whole sunshine period of

the day. Moreover, measurements were conducted for 4 days in August 2003 with a shaded branch of the same tree individual located below the canopy. Enclosure measurements on English oak were conducted in June 2002 over a period of 8 measurement days.

Measurements of the empty cuvette system were conducted prior or after each experiment but showed no significant bias between the both enclosures. CO_2 concentration differences of the empty system measured prior to the enclosure of *Fagus sylvatica* L. ranged < 2% (in 2002) and < 5% (in 2003) of the daytime CO_2 concentration differences. The H_2O concentration differences of the empty system ranged < 10% and < 2% accordingly. Monoterpene differences ranged at 0.0 ± 0.5 ppb and 0.0 ± 0.1 ppb in 2002 and 2003, respectively. Isoprene differences ranged at 0.0 ± 0.0 ppb. The latter mixing ratio differences ranged < 1% of the daytime monoterpene emission measured from European beech and < 1% of the daytime isoprene emission measured from English oak.

For the cuvette measurements a representative branch of the respective tree individual was enclosed in the sample cuvette as shown by Figure 3.7., while the other cuvette remained empty (reference cuvette). Except for the measurement of the shaded branch of *Fagus sylvatica* L. both enclosures were mounted at the same height. For the measurements conducted on the shaded branch, only the branch cuvette was moved below the canopy. Prior to the first VOC measurements were conducted on each plant, at least 5.5 hours of acclimatisation time was allowed, to prevent the impact of stress effects on the measured VOC exchange. After this time VOCs were sampled on several measurement days by utilisation of the automated cartridge sampling device in one or two hour intervals during day and night time conditions. The sampled cartridges were stored at ambient temperatures in airtight containers until their analysis at the Max Planck Institute for Chemistry in Mainz.

In addition to the GC-FID analysis performed by the MPI for Chemistry, samples for GC-MS analysis were collected occasionally on glass tubes (6 mm OD, 160 mm length) that were packed sequentially with 118 mg Carbograph 2 (12 m^2 g^{-1}), 60 mg Carbograph 1, and 115 mg Carbograph 5 [20-40 mesh each, Lara s.r.l., Italy]. Analysis of these cartridges was carried out by the Italian Research Council (CNR) in Rome, Italy. Monoterpene compounds that were evaluated from these analyses were camphene, Δ3-carene, p-cymene, limonene, myrcene, α-phellandrene, β-phellandrene, α-pinene, β-pinene, sabinene, α-terpinene, γ-terpinene, terpinolene, α-thujene, and tricyclene. A detailed overview of the method used for GC-MS analysis is given by Ciccioli *et al*. (1992) and Brancaleoni *et al*. (1999). According to the results of subsequent laboratory tests, it was shown that sabinene partially decomposed on the GC-MS cartridges to p-cymene, α-phellandrene, β-phellandrene, α-terpinene, γ-terpinene,

terpinolene, and α-thujene during the storage time of these cartridges. Therefore, a correction factor was applied to the relevant compounds.

Measurements of English oak were also performed by utilisation of on-line PTR-MS analysis that was conducted by the Swiss Federal Research Station for Agroecology and Agriculture (FAL), Zurich, Switzerland. The PTR-MS instrument was connected to the sample and reference enclosure by a Teflon valve alternating the air flow to the instrument between both cuvettes in regular intervals.

Vertical and horizontal profile measurements were conducted for 2 days in July 2002. VOC samples were collected in 2 hour intervals during day and night time conditions. Until their analysis by GC-FID at the end of the experiments they were stored at ambient temperatures in airtight containers. To eliminate potential interferences of the different cartridge sampler units applied, all VOC samplers were mounted at identical heights sampling ambient air from one common source. The latter experiment that preceded the profile measurements showed only small differences between the VOC samplers (isoprene < 0.1 ppb, monoterpenes < 0.1 ppb). Therefore, VOC concentration differences of > 0.1 ppb measured by the different VOC samplers were demonstrated to be derived from differences in ambient VOC concentrations at different heights and/or locations. All data measured by enclosures and gradient techniques were assigned to Central European Time (CET, i.e. 1 hour earlier than local time).

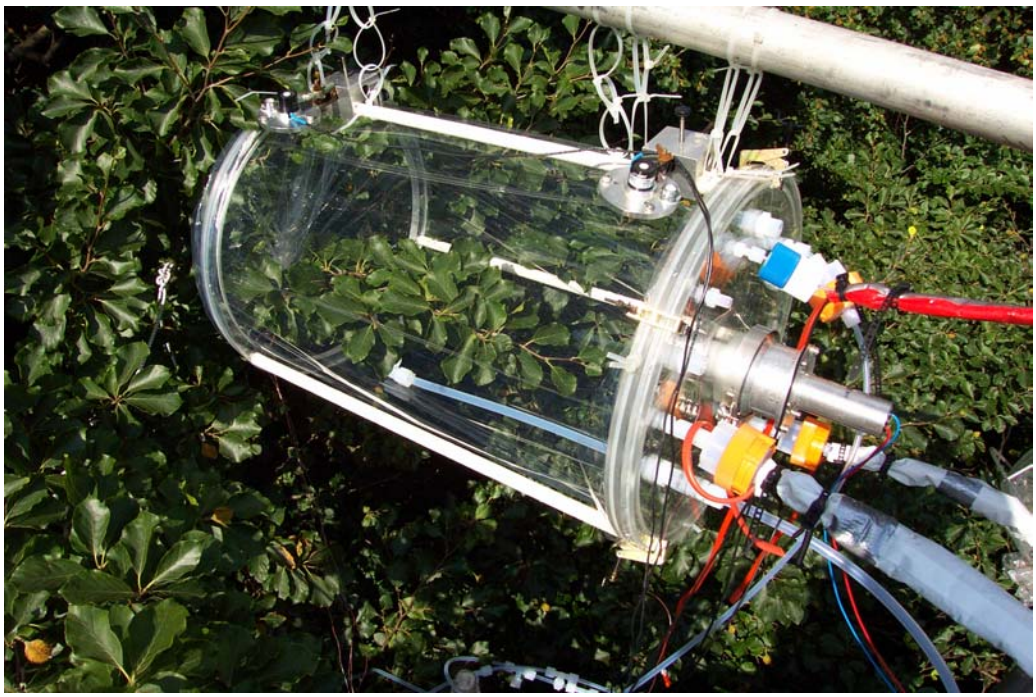

Figure 3.7.. Enclosure of European beech (*Fagus sylvatica* L.) during the experiments performed in June 2002.

RESULTS

VOC EMISSION AS A FUNCTION OF LIGHT AND TEMPERATURE

English oak (*Quercus robur* L.)

The experiments on English oak (*Quercus robur* L.) were conducted over a period of 8 measurement days. VOC exchange rates, investigated by GC-FID analysis, were measured on the first two days of the experiment in intervals of 1 to 2 hours. GC-MS samples were collected occasionally and were analysed by the laboratory of CNR in Rome. Moreover, the measurements were accompanied by PTR-MS analysis that was conducted by the FAL group and focussed on the exchange of isoprene and methanol from the investigated tree species. The PTR-MS measurements were also conducted during the third day of measurement during an artificial shading experiment that demonstrated the light dependency of isoprene emission under a daytime temperature regime (data not shown). However, GC-FID samples were not collected during the latter experiment and the residual five measurement days were assigned only to the measurement of plant physiology and ozone deposition (data not shown). An overview of the micrometeorological and physiological parameters measured during the complete measurement period is given in Table A1 and A2 in Appendix 1.

Figure 3.8. shows the evolution of micrometeorological and physiological parameters measured during the first two days on *Quercus robur* L.. As shown by the figure, both days were sunny and the photosynthetic active radiation (PAR) reached intensities of 1564 and 1722 µmol m^{-2} s^{-1}. Ambient temperatures reached maxima of 26 and 28°C during both days. Temperatures inside of the branch enclosure exceeded the ambient temperatures slightly and accounted up to 28 and 29°C, respectively. As a consequence, leaf temperatures reached maxima of 30 and 32°C, but accounted to 18 and 20°C on average. As shown by Figure 3.8., net CO_2 and H_2O exchange rates exhibited a pronounced diurnal cycle. Net CO_2 exchange rates reached values of -13 mg g^{-1} h^{-1} (note, that negative values indicate deposition and that CO_2 deposition = photosynthesis). H_2O exchange rates (= transpiration rates) accounted up to 1201 mg g^{-1} h^{-1}. Ambient VOC concentrations were measured only during the first measurement day. Ambient isoprene concentrations ranged ≤ 1.1 ppb, ambient monoterpene concentrations ranged ≤ 0.3 ppb. As shown by Figure 3.8. isoprene exchange rates measured by GC-FID analysis exhibited a pronounced diurnal cycle that followed closely the course of ambient light intensities and leaf temperature. Isoprene emission started at about 06:00 h in the morning and ceased again at about 20:00 h in the evening. Under daytime conditions, isoprene exchange rates reached maximum values of up to 87.5 µg g^{-1} h^{-1}. Night time

exchange rates ranged ≤ 0.1 µg g^{-1} h^{-1} (detection limit of the GC-FID analysis corresponds to 14 ng g^{-1} h^{-1}). Due to the high loading of isoprene on the adsorbent cartridges under daytime conditions, three samples had to be eliminated from the dataset, since the isoprene peak was out of the measurement range during the analysis. After adjustment to a decreased sensitivity the analysis was conducted for all other samples in conventional fashion.

The isoprene measurements conducted by the PTR-MS analysis supported the strong light and temperature dependency of isoprene emission but underestimated the GC-FID measurements. Consequently, maximum exchange rates ranged up to 63.1 µg g^{-1} h^{-1}. The difference between both analyses may be attributed to a sensitivity drift of the secondary electron multiplier (SEM) response curve as a consequence of the venting of the vacuum sec-

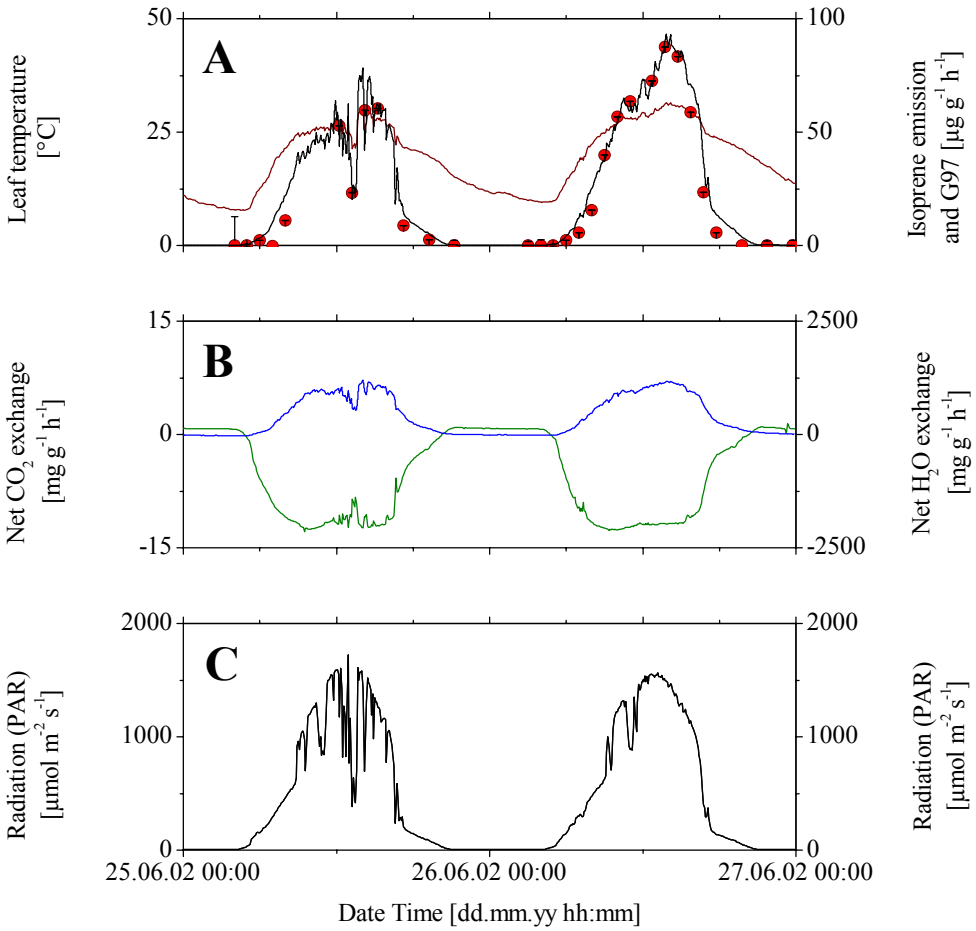

Figure 3.8. Diurnal course of micrometeorological and physiological parameters measured over a period of two days on English oak in June 2002. (A) Development of leaf temperatures (red line) and isoprene emission. Isoprene emission measured by GC-FID analysis is indicated by the red cycles, isoprene emission calculated by the G97 algorithm is indicated by the black line. (B) Diurnal course of net CO_2 exchange (green line) and H_2O exchange (blue line). (C) Course of photosynthetic active radiation (black line) during the respective measurements days.

tion of the PTR-MS instrument (for details see Ammann *et al.* 2004). However, also an overestimation by the GC-FID measurements due to coelution effects may be possible. The latter is supported by fact that the GC-MS analysis performed by CNR also underestimated the GC-FID measurements by 45% on average. Monoterpene measurements performed by GC-FID analysis showed only small emission rates that ranged at a maximum value of up to 76 ng g^{-1} h^{-1} (detection limit of GC-FID analysis corresponds to 5 ng g^{-1} h^{-1}). Even though the diel course of monoterpene exchange may point to a light and temperature dependent release of monoterpenes, scattering of the present dataset was high and the calculated errors of the exchange rates exceeded the measured exchange rates by far (data not shown).

European beech (*Fagus sylvatica* L.)

The experiments on sunlit leaves of European beech (*Fagus sylvatica* L.) were conducted over a period of 8 days in June 2002 and 16 days in July/August 2003. An overview of the daily maxima and average values of micrometeorological and physiological parameters is given by the Tables A3 to A6 in Appendix 1. Figure 3.9. shows the evolution of micrometeorological and physiological parameters that were measured during the enclosure of *Fagus sylvatica* L. during both years. As shown by the graph, most of the measurement days were sunny, yielding maximum radiation intensities of > 1000 µmol m^{-2} s^{-1}. Ambient temperatures ranged between 17 to 36°C in June 2002 and 24 to 42°C in July/August 2003. As shown by Figure 3.9., irradiation and leaf temperatures increased particularly in June 2002 as a result of a short high ambient temperature period (the first high ambient temperature period of the respective growing season). Cuvette temperatures exceeded the ambient temperatures to ≤ 5°C. Leaf temperatures ranged between maxima of 20 to 44°C in 2002 and 27 to 44°C in 2003. Regarding the course of net CO_2 and H_2O exchange, all parameters exhibited pronounced diurnal characteristics. Net photosynthesis rates reached values of -14 mg g^{-1} h^{-1} in 2002 and 2003. Transpiration reached maximum exchange rates of 1471 mg g^{-1} h^{-1} in 2002 and 1650 mg g^{-1} h^{-1} in 2003.

Ambient isoprene and monoterpene concentrations exhibited pronounced diel courses during the majority of measurement days. Ambient isoprene concentrations ranged ≤ 7.9 ppb in 2002 and ≤ 6.4 ppb and 2003. Ambient monoterpene concentrations ranged ≤ 1.8 ppb in 2002 and ≤ 1.1 ppb in 2003.

As shown by Figure 3.9., monoterpene exchange rates were measured typically in 1-2 h intervals during three and six days in June 2002 and July/August 2003, respectively. Monoterpene emission exhibited pronounced diel cycles during both measurement years and

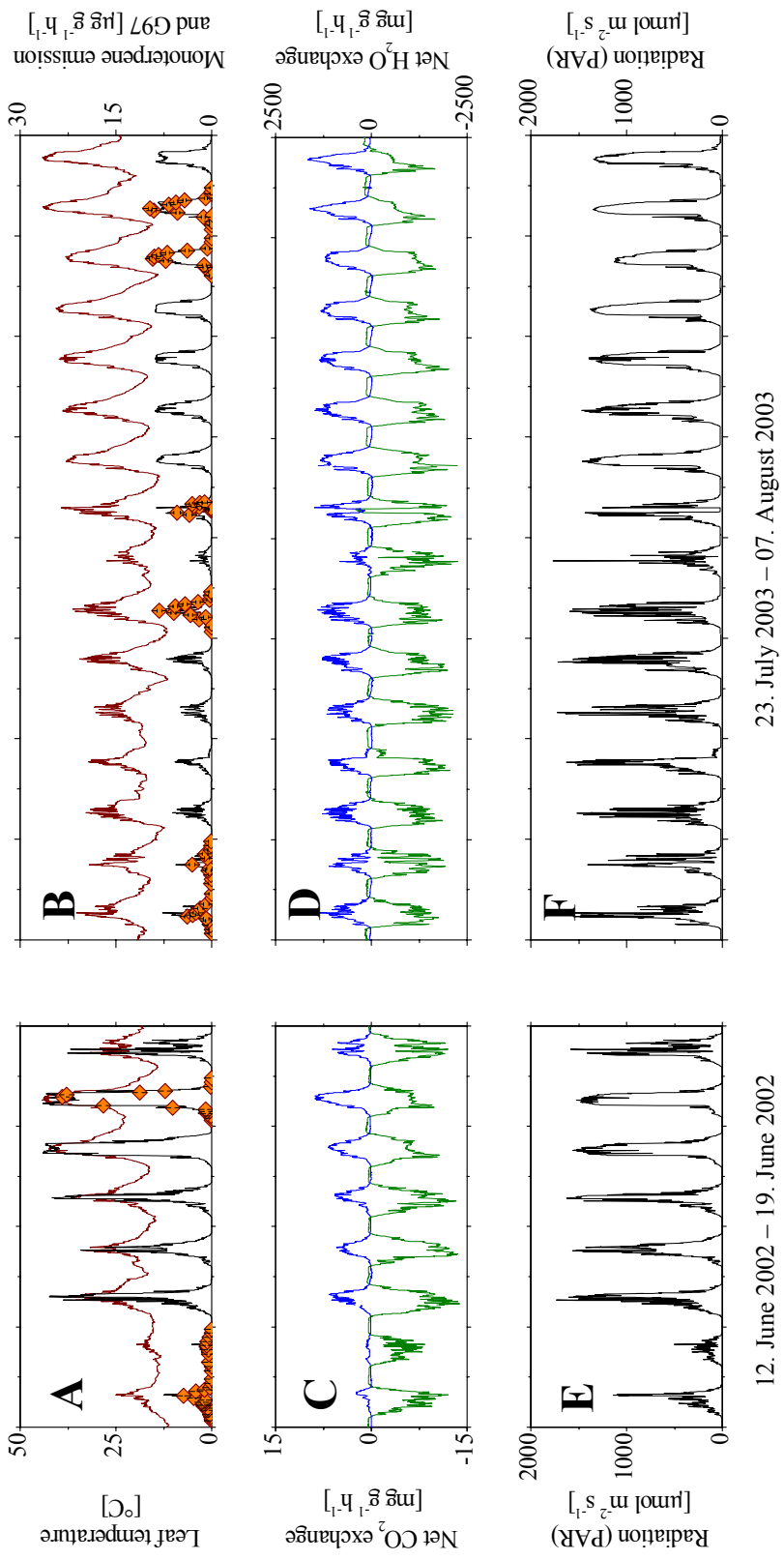

Figure 3.9. Diurnal course of micrometeorological and physiological parameters measured on European beech during both field experiments in June 2002 (left panel) and July/August 2003 (right panel). (A, B) Development of leaf temperature (red line) and monoterpene emission. Monoterpene emission that was measured by GC-FID analysis is indicated by the orange diamonds. Monoterpene emission that was calculated by application of the G97 algorithm is indicated by the black line. The calculated error of monoterpene mixing ratios is given by the error bars. If no error bars are visible, they reside within the diameter of the plotted symbol. (C, D) Diurnal course of net CO_2 exchange (green line) and net H_2O exchange (blue line). (E, F) Photosynthetic active radiation (black line).

followed closely the course of photosynthetic active radiation and leaf temperature. Monoterpene emission increased in the early morning at about 06:00 - 07:00 h and ceased in the evening at about 20:00 h. The daytime emission reached maximum exchange rates of up to 33.2 µg g^{-1} h^{-1} in June 2002 and 9.6 µg g^{-1} h^{-1} in July/August 2003. Night time exchange rates ranged ≤ 93 ng g^{-1} h^{-1} for both experiments and scattered between deposition and emission of the respective compounds (detection limit of GC-FID analysis corresponds to 7 ng g^{-1} h^{-1} (2002) and 12 ng g^{-1} h^{-1} (2003)). GC-MS samples (analysed by CNR, Rome) that were collected under daytime conditions in parallel to the GC-FID samples exceeded the emission rates measured by the MPI analysis by 24 to 112%.

Isoprene exchange rates measured by GC-FID ranged ≤ 0.3 µg g^{-1} h^{-1} in the year of 2002 and ≤ 0.9 µg g^{-1} h^{-1} in the year of 2003 and scattered between emission and deposition. During the high ambient temperature period observed in June 2002 a diel course of isoprene emission was detectable by the GC-FID measurements (data not shown). However, this result was not supported by the GC-MS sample collected during the respective measurement day. Therefore it remains unclear, if the observed diurnal exchange was triggered by a light and temperature dependent isoprene release or if these measurements were influenced by sampling artefacts on the GC-FID cartridges.

Light saturation and temperature optimum of net CO_2 exchange

As shown by Figure 3.10., the correlation of net CO_2 exchange rates (multiplied by a factor of -1) to radiation exhibited typical saturation curves for all experiments conducted on English oak (Figure 3.10. A) and European beech (Figure 3.10. C and E). Saturation was reached at radiation intensities of > 400-500 µmol m^{-2} h^{-1}. Since the net CO_2 exchange rates were measured under a simultaneous change of environmental conditions (i.e. radiation and leaf temperature), the second parameter was encoded by the respective colour scale in Figure 3.10..

However, considering solely leaf temperatures in the range of 20–30°C net CO_2 exchange rates exhibited a full saturation curve as well (see orange symbols in Figure 3.10. A, C, and E). At higher leaf temperatures, net CO_2 exchange rates decreased (see the red and dark red symbols). In correlation to leaf temperature, optimum curves were obtained for European beech if all data points were considered (Figure 3.10. D and F, optimum at 25 to 27°C). Regarding the measurements performed on English oak (Figure 3.10. B), no optimum curve was observed since maximum leaf temperatures reached only 32°C. As shown by Figure 3.10. B, D, and F, the increase of photosynthesis with leaf temperature was accompanied by an in-

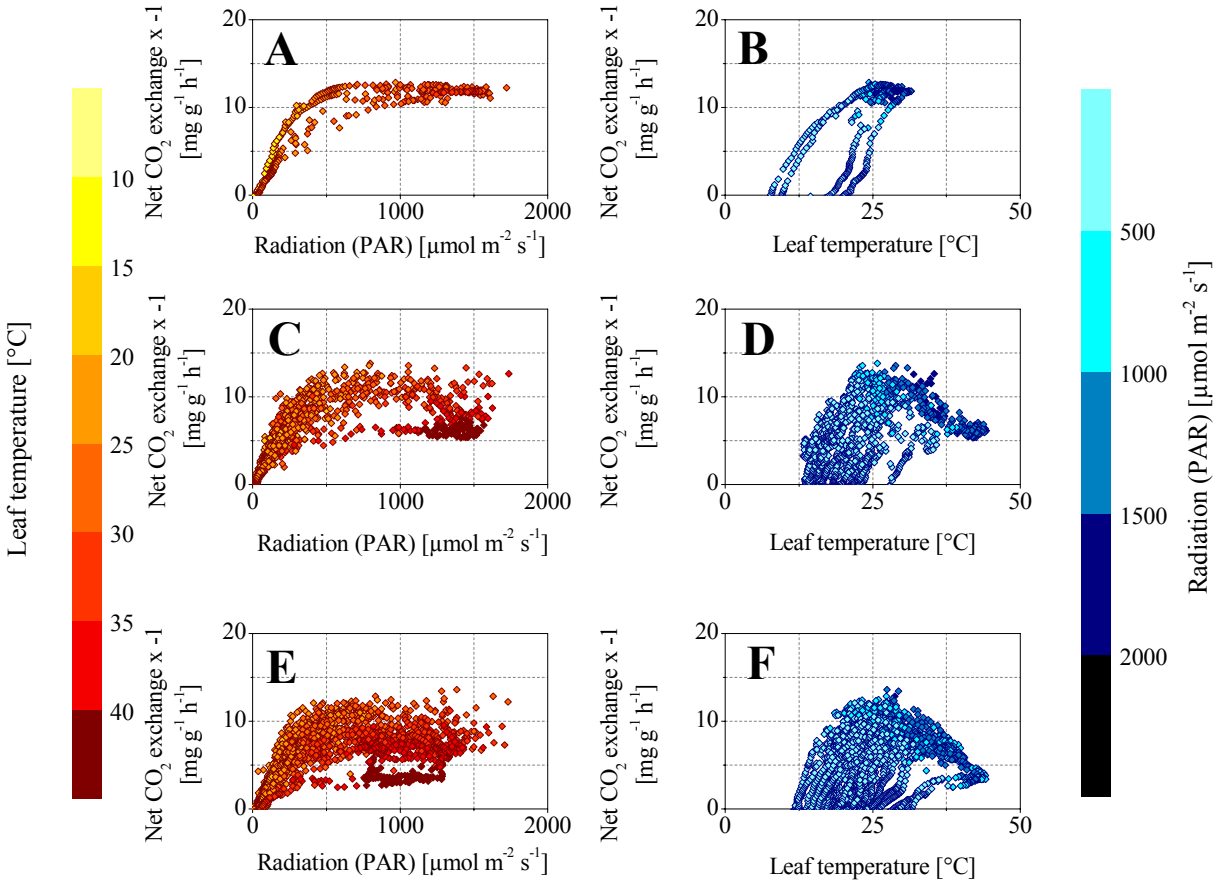

Figure 3.10. Light (left panel) and temperature dependence (right panel) of net CO_2 exchange. (A, B) Data measured on *Quercus robur* L. in June 2002. (C, D) Data measured on *Fagus sylvatica* L. in June 2002 and (E, F) in July/August 2003. Note that net CO_2 exchange rates are multiplied by a factor of -1 (i.e. photosynthesis rates are given as positive numbers). Since light saturation curves are measured at different temperatures and temperature optimum curves are measured at different radiation intensities, both parameters are encoded by the colour scale at the respective graphs.

increase of photosynthetic active radiation. Considering only radiation intensities of > 500 µmol m^{-2} s^{-1} for the correlation of net CO_2 exchange rates to leaf temperature (see the blue and dark blue symbols in Figure 3.10. B, D, and F), the increase of net CO_2 exchange rates with leaf temperature was not observable. Therefore, the increase of net CO_2 exchange with leaf temperature as observed regarding all measured data points may also be attributed to a simultaneous increase of light intensity. The decrease of net CO_2 exchange rates with leaf temperature was accompanied by high radiation intensities (> 1000 µmol m^{-2} s^{-1}, see the dark blue symbols). Since these high radiation intensities caused no stress induced decrease of photosynthesis (see e.g. Figure 3.10. E), the decrease of net CO_2 exchange rates with leaf temperatures of > 28°C may be attributed only to temperature effects.

Artificial shading experiment on European beech (*Fagus sylvatica* L.)

A variety of physiological functions is influenced by diurnal rhythms of the plant. Whereas endogenous (circadian) rhythms are characterised mainly by the fact that they obtain periodicity even if environmental factors remain constant, exogenous rhythms are triggered by ambient conditions. Monoterpene emission from European beech was shown to have a diurnal periodicity that correlates to light and temperature. However, since light intensity and temperature exhibited a coupled diurnal periodicity by themselves, a pseudo correlation of monoterpene emission to both factors might be possible. To exclude this and to demonstrate the light dependency of monoterpene emission under a daytime temperature regime, an artificial shading experiment was conducted during one measurement day in the year of 2003 (see Figure 3.10.). The artificial darkening of the enclosure started at noon and was completed within 30 min (remaining light intensity 20-21 µmol m^{-2} s^{-1}). Two hours later the artificial plant cover was removed again and irradiation progressed in a conventional daily pattern. When the plant cuvette was coated by a dark cover, cuvette temperature (and as a consequence leaf temperature) decreased after darkening but increased again in the course of

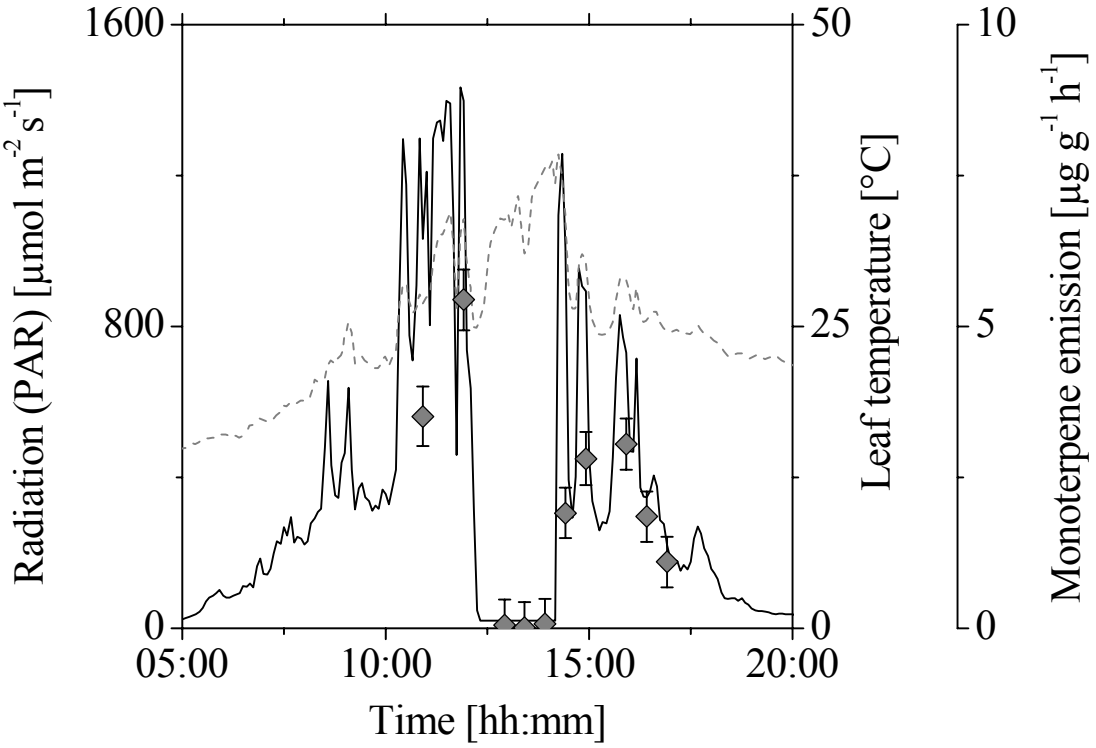

Figure 3.11. Artificial shading experiment. Course of photosynthetic active radiation (black solid line) and leaf temperature (grey dashed line) during the artificial shading of the branch enclosure in July 2003. Monoterpene emission measured prior, during and after the artificial darkening is indicated by the grey diamonds. The calculated error of the monoterpene exchange rates is given by the error bars.

the shading period (max. difference in leaf temperature during shading 13°C). VOC exchange measured prior to the artificial shading ranged at exchange rates of 3.5 and 5.4 µg g^{-1} h^{-1}. 30 min after complete coverage of the cuvette monoterpene exchange rates ≤ 0.1 µg g^{-1} h^{-1} were observed. As soon as the artificial darkening was removed, monoterpene emission progressed with its conventional diurnal characteristics, yielding exchange rates ranging between 1.9 and 3.0 µg g^{-1} h^{-1}.

Standard emission factor of English oak and European beech

According to the diel characteristics of isoprene and monoterpene emission and the results obtained by the artificial shading experiment conducted on European beech, a dependence of isoprene and monoterpene release to irradiation and leaf temperature is evident. Moreover, night time exchange rates near the detection limit eliminate an exclusive role of leaf temperature as a controlling factor for the release of both compounds.

In analogy to the net CO_2 exchange rates observed from English oak and European beech, isoprene and monoterpene exchange rates were correlated to photosynthetic active radiation and leaf temperature (see Figure 3.12.. Note, that due to the simultaneous change of irradiation and temperature, isoprene and monoterpene exchange rates were normalised with the respective function of the G97 algorithm). As shown by Figure 3.12. A, C, and E, the light dependence of isoprene and monoterpene emission exhibited a similar function as observed for the net CO_2 exchange rates, yielding a saturation trend at > 500 µmol m^{-2} s^{-1}. However, scattering of the present dataset (including all morning and afternoon exchange rates) does not allow clear conclusions as to whether the increase of isoprene and monoterpene emission with light intensity was hyperbolic (corresponding to the G97 function) or sigmoid (corresponding to the S97 function). Considering the progression of monoterpene emission during single, sunny measurement days in 2003 a hysteretic structure was observable that was shown to be a function of daytime (see Figure 3.16. and the respective paragraph). In correlation to leaf temperatures, isoprene and monoterpene emission showed no optimum curve and increased exponentially with leaf temperature up to maximum temperatures of 31°C (*Quercus robur* L., see Figure 3.12. B) and 43°C (*Fagus sylvatica* L., see Figure 3.12. D and F). However, comparison to the G97 function resulted in reasonable agreement regarding the light and temperature dependence of isoprene and monoterpene emission.

As the results show the correlation of isoprene and monoterpene emission to light and temperature, standard emission factors (SEF, see Formula 3.8.) were calculated by application of the G97 algorithm from the slope of linear regression of the measured VOC emission

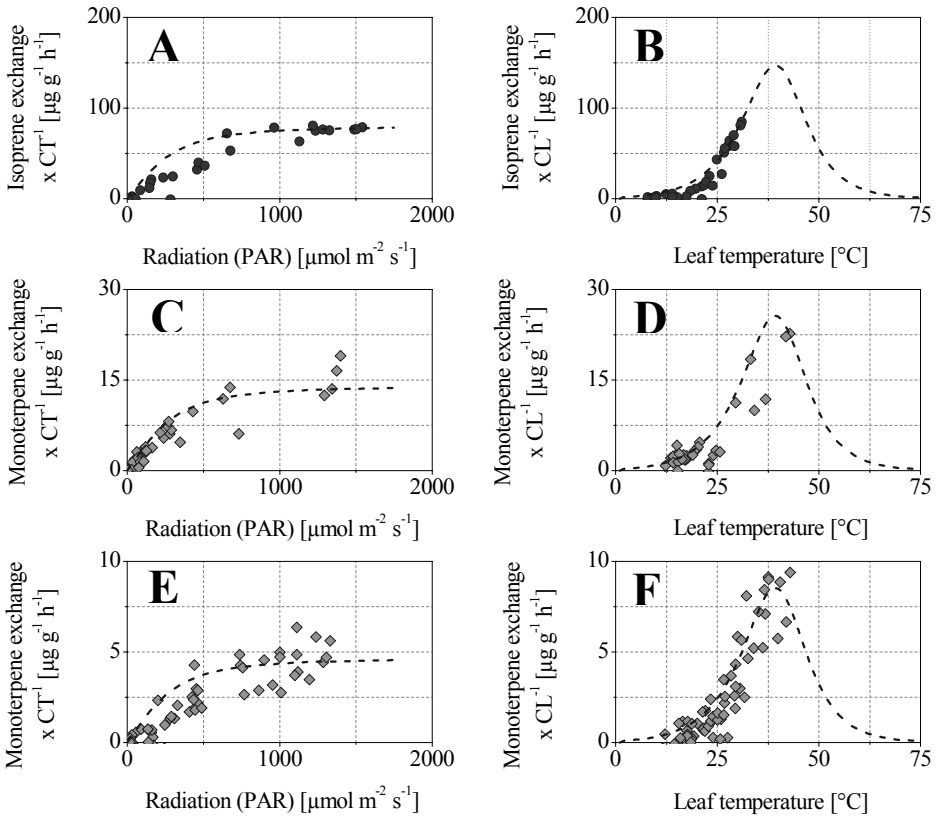

Figure 3.12. Light (left panel) and temperature dependence (right panel) of isoprene (grey circles) and monoterpene exchange (grey diamonds). (A, B) Isoprene exchange measured on *Quercus robur* in June 2002. (C, D) Monoterpene exchange measured on *Fagus sylvatica* in June 2002 and (E, F) in July/August 2003. Note, that the respective exchange rates are normalised with the relevant function of the G97 algorithm (i.e. the light dependence of VOC emission is normalised with the temperature function and vice versa, see function 2.6. and 2.7.). The respective function of the G97 algorithm is given by the dashed line.

versus the product of C_L and C_T. For comparison a standard emission factor (Φ_{LT}) was also calculated by application of a modified version of the S97 algorithm that neglected the storage pool term of the algorithm (as recommended for sabinene emission by Schuh *et al.* (1997), see Formula 3.12.). Figure 3.13. shows the linear correlation of VOC emission to the respective algorithm on the right panel and the respective function of the linear fit on the left panel. Outliers from this correlation were often caused by temperature effects (e.g. midday depression).

In general, the standard emission factors that were calculated by application of the modified S97 function exhibited higher values than the standard emission factors that were calculated from the G97 function. Standard emission factors obtained for isoprene emission from English oak ranged at 75.1 µg g^{-1} h^{-1} for the G97 function and 76.7 µg g^{-1} h^{-1} for the S97

A

Quercus robur L. (2002):

G97: y = 75.08 x - 3.26

$r^2 = 0.97$

S97: y = 76.66 x – 0.82

$r^2 = 0.98$

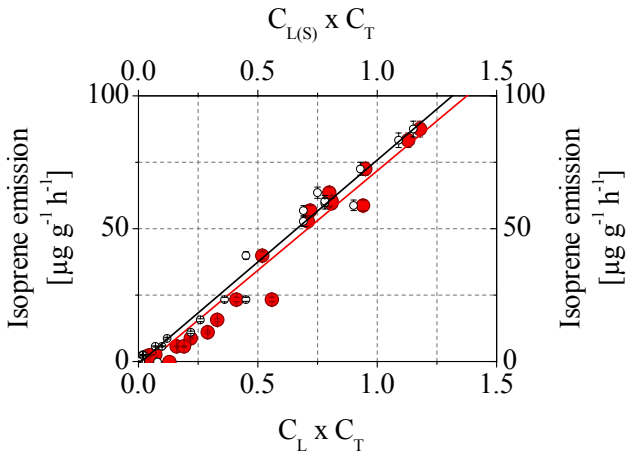

B

Fagus sylvatica L. (2002):

G97: y = 13.11 x - 0.31

$r^2 = 0.89$

S97: y = 14.05 x + 0.17

$r^2 = 0.92$

C

Fagus sylvatica L. (2003):

G97: y = 4.36 x - 0.30

$r^2 = 0.92$

S97: y = 4.59 x – 0.06

$r^2 = 0.94$

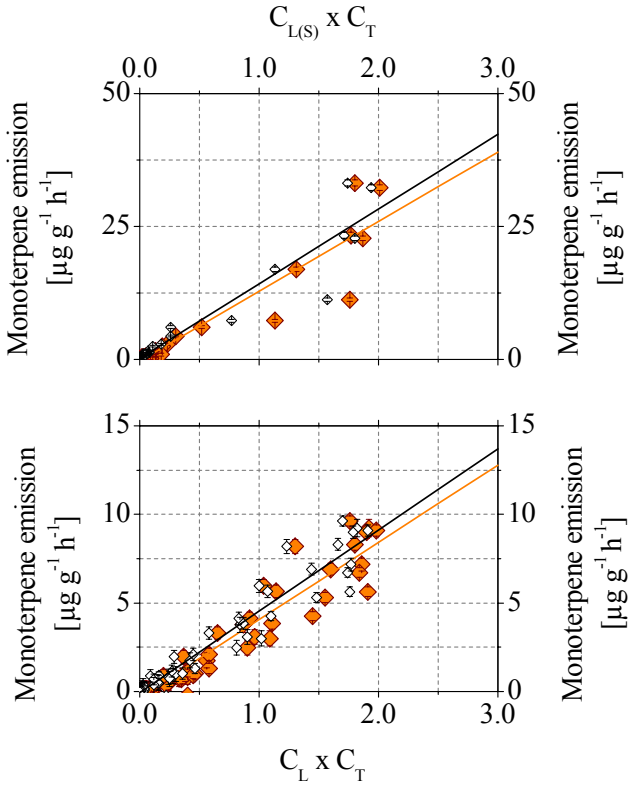

Figure 3.13. Isoprene and monoterpene emission as a function of the G97 and the modified S97 algorithm. (A) Isoprene emission from *Quercus robur* L. measured in June 2002. Red filled circles indicate the regression of isoprene emission versus the product of the light and temperature function of the G97 algorithm (bottom x-axis (C_L x C_T)). The red line gives the linear fit of the respective regression. Black circles indicate the regression of isoprene emission versus the light and temperature function of the modified S97 algorithm (top x-axis ($C_{L(S)}$ x C_T)). The black line indicates the linear fit of the regression. The function of the respective linear regression is given on the left panel. (B) Monoterpene emission from *Fagus sylvatica* L. measured in 2002 and (C) 2003. Orange filled diamonds and the orange line indicate the regression of monoterpene emission versus the G97 function and the respective linear fit. Black diamonds and the black line indicate the regression versus the modified S97 function and the relevant linear fit. The respective functions are given on the left panel.

function. According to the lower response of the PTR-MS instrument, the standard emission factors that were calculated from the G97 function and 1 hour averages of the observed isoprene emission measured by the PTR-MS analysis ranged up to 46.3 µg g^{-1} h^{-1}. However, the correlation coefficient obtained by the PTR-MS analysis was good (r^2 = 0.90).

For monoterpene emission measured by GC-FID from European beech, standard emission factors of 13.1 and 4.4 µg g^{-1} h^{-1} were obtained for the experiments conducted in 2002 and 2003 by application of the G97 function. By application of the S97 function standard emission factors of 14.1 and 4.6 µg g^{-1} h^{-1} were calculated. Correlation coefficients that were obtained from the linear fit of the VOC emission versus the S97 function showed better results than the correlation to the G97 function.

The standard emission factors that were obtained for the monoterpene emission from European beech differed by a factor of 3 between both years. However, the differences observed for individual days during one growing season were smaller. Table 3.3. gives an overview of the minimum, maximum, and average standard emission factors that were calculated by application of the G97 and S97 function. Comparison to the GC-MS data (measured by CNR, Rome) that were obtained for one day in August 2003, revealed a difference in the standard emission factor of 25% (calculated by the G97 function, GC-FID = 4.7 µg g^{-1} h^{-1}, GC-MS = 5.9 µg g^{-1} h^{-1}).

Table 3.3. Standard emission factors calculated for isoprene and monoterpene emission from English oak and European beech. Standard emission factors were calculated by application of the G97 function and the modified S97 function (data in parenthesis). Standard emission factors were calculated for single measurement days (minimum and maximum values) as well as for the complete measurement period on one measurement tree (average, n = 30 (*Quercus robur* L. 2002), n = 44 (*Fagus sylvatica* L. 2002) and n = 65 (*Fagus sylvatica* L. 2003).

	Standard emission factor [µg g^{-1} h^{-1}]		
Measurement	Minimum	Maximum	Average
Isoprene			
Quercus robur L. 2002	74.7 (76.4)	75.9 (77.0)	75.1 (76.7)
Monoterpenes			
Fagus sylvatica L. 2002	9.0 (14.2)	13.5 (22.0)	13.1 (14.0)
Fagus sylvatica L. 2003	3.1 (3.4)	5.6 (5.8)	4.4 (4.6)

Composition of monoterpene compounds emitted from European beech

Figure 3.14. shows the diurnal course of individual monoterpene emission measured by GC-MS (analysed by CNR, Rome) for one of the measurement days in August 2003 that was conducted on the sunlit branch of European beech. Light and temperature dependency of monoterpene emission was observed for all analysed compounds with exception of tricyclene that scattered at exchange rates < 1 ng g^{-1} h^{-1}. Sabinene was the predominant monoterpene compound emitted (max. 8.1 µg g^{-1} h^{-1}). Standard emission factors that were calculated for the sum of all monoterpenes for this respective day reached 7.1 µg g^{-1} h^{-1} (G97, sum of 15 individual monoterpene compounds) or 5.9 µg g^{-1} h^{-1} (G97, sum of 10 individual monoterpene

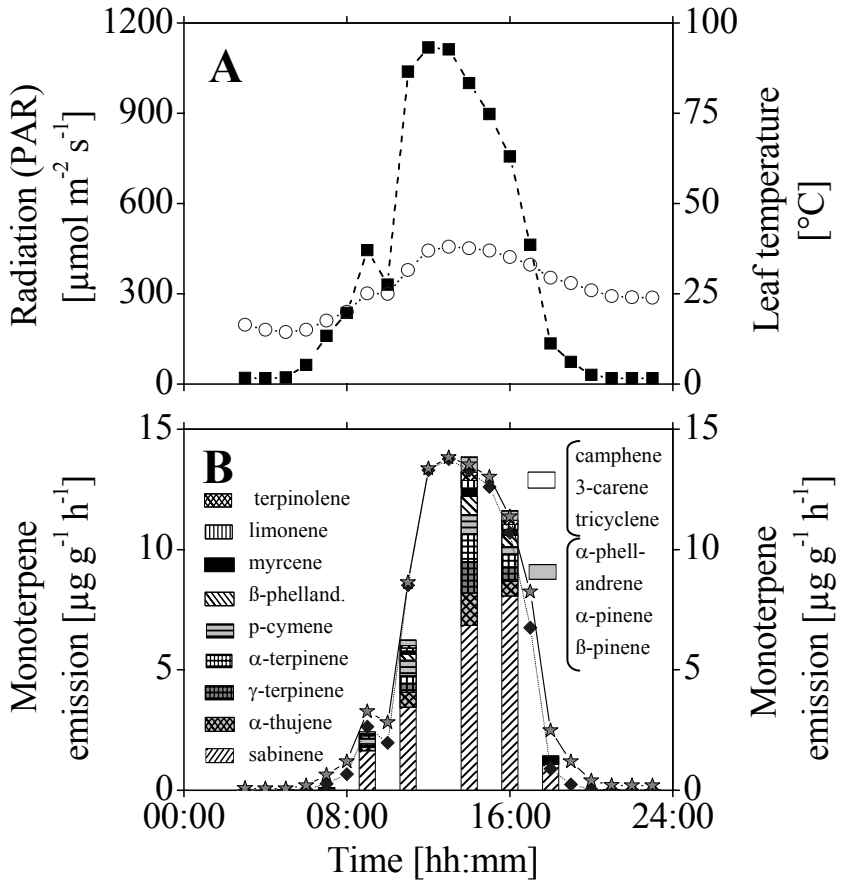

Figure 3.14. Course of photosynthetic active radiation (PAR), leaf temperature, and monoterpene emission measured during one single day in August 2003. (A) Diurnal course of PAR (black squares plus dashed line) and leaf temperature (hollow circles plus dotted line). Data show the respective 30 min average during which VOC cartridges were collected. (B) Diurnal course and composition of monoterpene emission. Data show monoterpene emission measured by GC-MS analysis (stacked bars, for caption see graph), the respective emission calculated by the G97 algorithm (grey stars plus solid line), and the modified S97 function (grey diamonds plus dotted line).

compounds, see GC-FID analysis). Monoterpene emission calculated by the G97 algorithm fitted well to midday and afternoon values but morning and evening monoterpene emission was lower than calculated by the algorithm. Thus integration of measured and calculated emission for the respective day resulted in an overestimation of +13% by the calculated data. Application of a sigmoid increase of monoterpene emission with light intensity (as assumed by the modified S97 function) resulted in a better reproducibility of the observed data in the morning hours. However, both algorithms still overestimated monoterpene emission in the morning and underestimated midday and afternoon emission to a various extent.

In order to determine the contribution of different monoterpene species to the sum of monoterpene emission, standard emission factors for different monoterpene compounds were calculated as shown in Table 3.4. As described previously, sabinene was shown to be decom-

Table 3.4. Standard emission factors (G97) for 15 monoterpene compounds measured by GC-MS during one single day in August 2003. Abbreviations: [a] partially decomposed, [b] partial decomposition product.

Monoterpene species	Monoterpene emission SEF [ng g^{-1} h^{-1}]	Monoterpene emission SEF [%]
sabinene [a]	4036	57
α-thujene [b]	584	8
γ-terpinene [b]	541	8
α-terpinene [b]	483	7
p-cymene [b]	365	5
β-phellandrene [b]	336	5
myrcene	166	2
limonene	154	2
terpinolene [b]	142	2
α-phellandrene [b]	113	2
α-pinene	99	1
β-pinene	73	1
camphene	6	0
Δ3-carene	3	0
tricyclene	1	0

posed on the GC-MS cartridges as a function of storage time. Sabinene decomposition reached a saturation effect after 7 days. At this time 45% of the sabinene was decomposed to p-cymene (7%), α-phellandrene (2%), β-phellandrene (6%), α-terpinene (8%), γ-terpinene (9%), terpinolene (3%), and α-thujene (10%). Since all samples that were analysed during the ECHO campaign were stored longer than 7 days before GC-MS analysis was performed, sabinene concentrations as well as the concentrations of the relevant decomposition products were multiplied by the respective correction factor. As shown by Table 3.4., sabinene was the major monoterpene compound emitted from European beech, even if no correction factor would have been applied. However, this result was not supported by the GC-FID analysis. Here sabinene was the second common monoterpene compound (major monoterpene compound for GC-FID analysis p-cymene).

EFFECT OF HIGH AMBIENT TEMPERATURES

Midday depression of net CO_2 exchange from European beech

Increasing leaf temperature and water vapour pressure deficit have a severe effect on the water loss of the leaf epidermis which is an important factor for stomatal aperture (for a detailed overview see Schulze (1986)). According to Backes and Leuschner (2000) *Fagus sylvatica* L. evolved a very sensitive stomatal regulation that allows maintenance of leaf turgor during dry, high temperature conditions. Consequently, on days with high ambient temperature European beech, due to its sensitive stomatal regulation, exhibited a distinct midday depression of net CO_2 assimilation as observed two times in June 2002 and five times in July/August 2003. Figure 3.15. gives an overview of the daily course of leaf temperature, as well as the correlation of stomatal conductance and net CO_2 exchange to PAR during the measurement period in June 2002 that included the first high ambient temperature period of the respective growing season.

As shown in Figures 3.15. A, B, C, D, and E the net CO_2 exchange exhibited a typical saturation curve in correlation to photosynthetic active radiation. Moreover, with exception of the first measurement day, stomatal conductance followed this trend at lower light intensities (< 100 μmol m^{-2} s^{-1}) but decreased at high light conditions. During the 6^{th} and 7^{th} day of measurement (see Figure 3.15. F and G) a midday depression of the net CO_2 exchange was observed as midday leaf temperatures increased to more than 41°C. Here, higher net CO_2 exchange rates were measured during the morning hours and lower net CO_2 exchange rates were measured in the afternoon. Regarding the stomatal conductance the depression was not

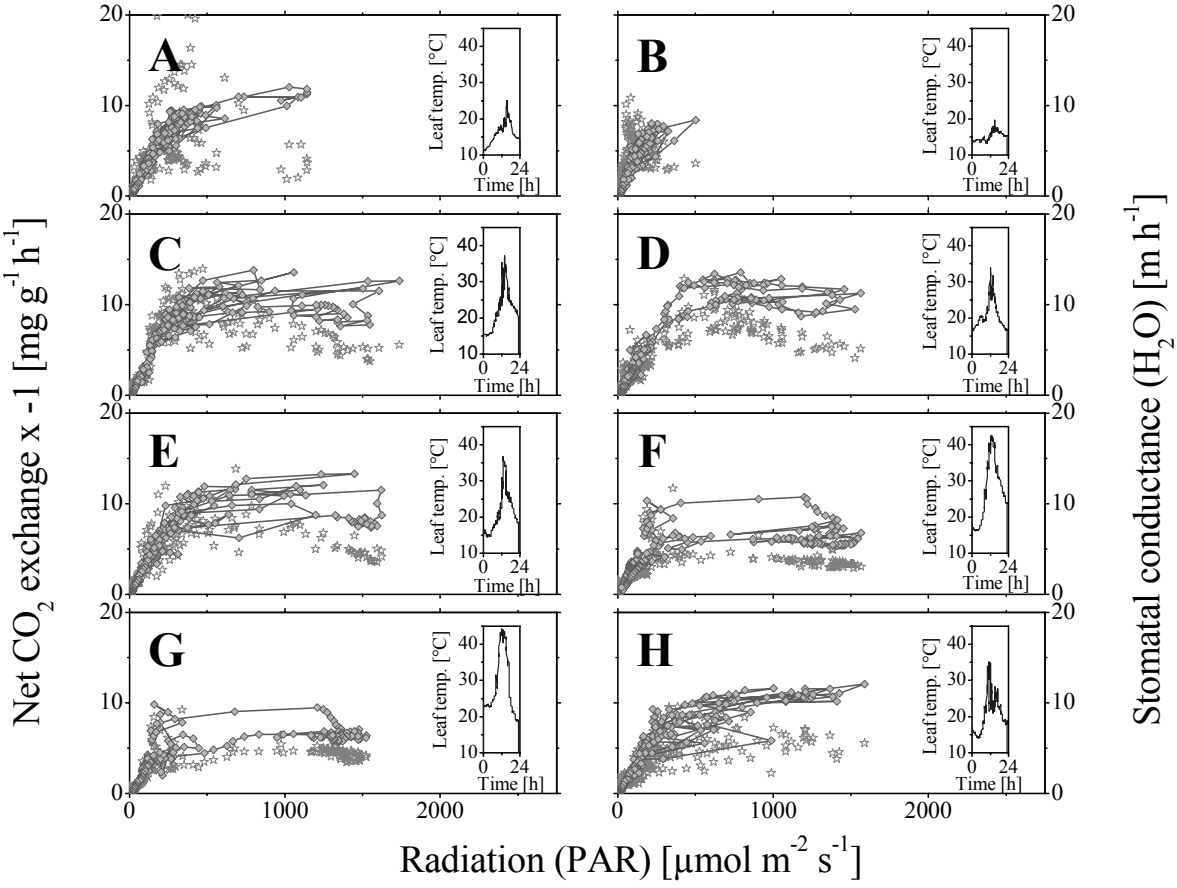

Figure 3.15. Midday depression of plant physiology in June 2002. Figures A to H show the correlation of net CO_2 exchange (grey diamonds) and stomatal conductance (grey stars) to photosynthetic active radiation (PAR) for each single day of the measurement period (12-19. June 2002). Note that the CO_2 exchange rates are multiplied by a factor of -1 (i.e. net CO_2 deposition (= photosynthesis) is shown as positive numbers). The development of the respective daily leaf temperature is indicated by the small graphs as a function of time.

as pronounced as the midday depression of net CO_2 exchange, but still observable. Transpiration rates (i.e. net H_2O exchange rates) exhibited no temperature induced decrease during the respective high ambient temperature period. However, as soon as midday leaf temperatures decreased and were below 28°C the next day (see Figure 3.15. H), midday depresssion was not observed and plant's stomatal conductance and net CO_2 exchange rates progressed in a conventional pattern resulting in a typical saturation curve.

Midday depression of monoterpene emission from European beech

As discussed above, monoterpene emission exhibited a saturation trend in correlation to light intensity. However, considering single sunny days, the correlation revealed a typical hysteretic structure that was observed to be a function of time (lower monoterpene emission

in the morning, see Figure 3.16. A). The hysteresis was attributed to a time lag phase of monoterpene emission in the early morning. Since the morning increase of monoterpene emission with radiation intensity was less pronounced than the decrease in the early evening, the correlation of monoterpene emission to PAR resulted in a hysteretic structure that was observed several times during the measurement period in July/August 2003.

In contrast, during hot sunny days, midday depression of net CO_2 exchange and stomatal conductance may lead to a hysteretic course of monoterpene emission that follows the time of day in an opposite direction (lower monoterpene emission in the afternoon). Indeed, this effect was observed once, during the measurement period in June 2002 as monoterpene emission was very high and the plant experienced its first high temperature period of the respective growing season (see Figure 3.16. B). Furthermore, a similar hysteresis was also observed in correlation to leaf temperature during the respective measurement day.

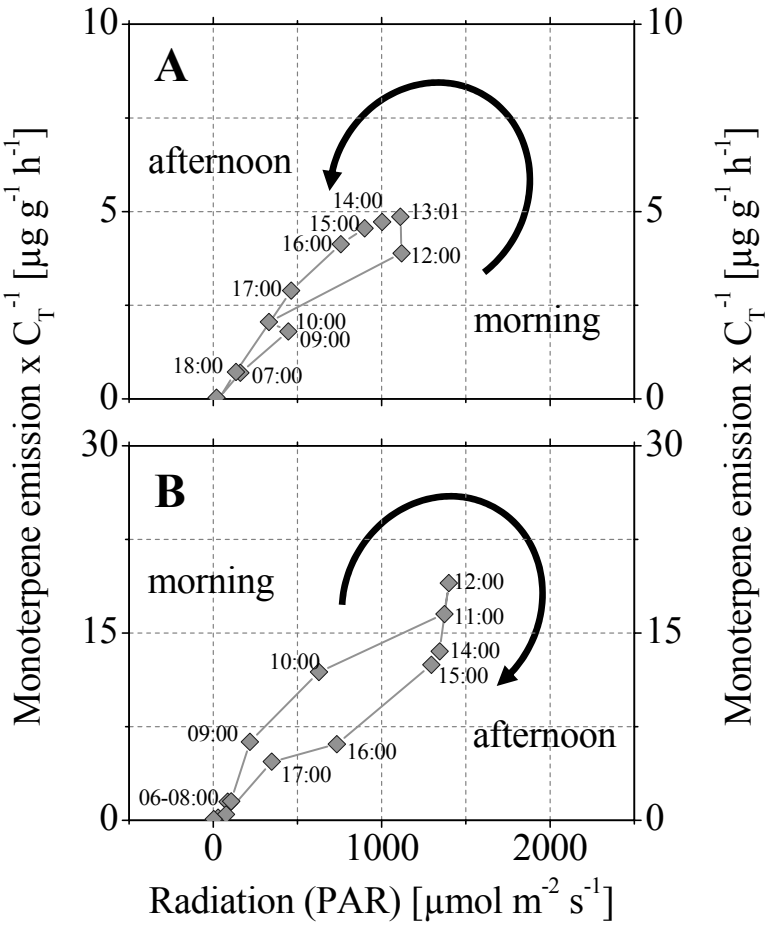

Figure 3.16. Monoterpene emission as a function of photosynthetic active radiation (PAR). (A) during a typical day in August 2003 and (B) during midday depression in June 2002. Monoterpene emission is indicated by the grey diamonds. Note that the monoterpene emission was normalised with the temperature function (C_T) of the G97 algorithm. The respective time of day is indicated for each data point.

VOC EMISSION FROM SHADED LEAVES OF EUROPEAN BEECH

In addition to the sunlit leaves of *Fagus sylvatica* L. that were investigated at the canopy top during the measurement period of June 2002 and July/August 2003, shaded leaves of the same tree individual were investigated for 4 days in August 2003. VOC samples were collected in 1-2 h intervals during the first two measurement days. According to the lower measurement height, radiation intensities reached maximum values of only 63 and 79 µmol m^{-2} s^{-1}. Leaf temperatures ranged < 30°C during both VOC measurement days. An overview of micrometeorological and physiological parameters measured from this shaded branch is given in Table A7 and A8 in Appendix 1.

Despite of the low radiation intensities that were measured at the respective height of the shaded branch, net CO_2 exchange rates reached values of -6 mg g^{-1} h^{-1} during both days. Due to technical problems, H_2O exchange rates and the stomatal conductance for water vapour are missing for these experiments. Monoterpene emission exhibited a diel progression with maximum exchange rates of 1.5 and 1.4 µg g^{-1} h^{-1} during the first and second measurement day. Night time exchange rates ranged ≤ 0.2 µg g^{-1} h^{-1} and exhibited also negative values. The standard emission factor ranged at 20.0 µg g^{-1} h^{-1} (calculated by application of the G97 function), but the correlation coefficient reached only a value of 0.69. Application of the S97 function resulted in even inferior results.

HORIZONTAL AND VERTICAL PROFILES OF ISOPRENE AND MONOTERPENES

Horizontal and vertical profiles of isoprene and monoterpene concentrations were measured during a sunny and a cloudy/rainy day in July 2002. Figure 3.17. A gives an overview of the diurnal course of photosynthetic active radiation (PAR) and ambient temperature that were measured during the sunny measurements day at a height of 28 and 38 m at the West Tower site (radiation intensity and ambient temperature recorded by the meteorology group of the MPI for Chemistry, Mainz). The measured radiation intensities reached maximum values of up to 2194 µmol m^{-2} s^{-1} and followed a pronounced diurnal course. Ambient temperatures reached maxima of 27°C during the respective measurement day.

Isoprene and monoterpene concentrations were recorded simultaneously at the West Tower and the Main Tower site. As shown by Figure 3.17. B and C, isoprene concentrations exhibited a pronounced diurnal course with maximum concentrations measured at 15:15 h at both tower sites. Isoprene mixing ratios measured at the West Tower site reached 4.0 ppb (see

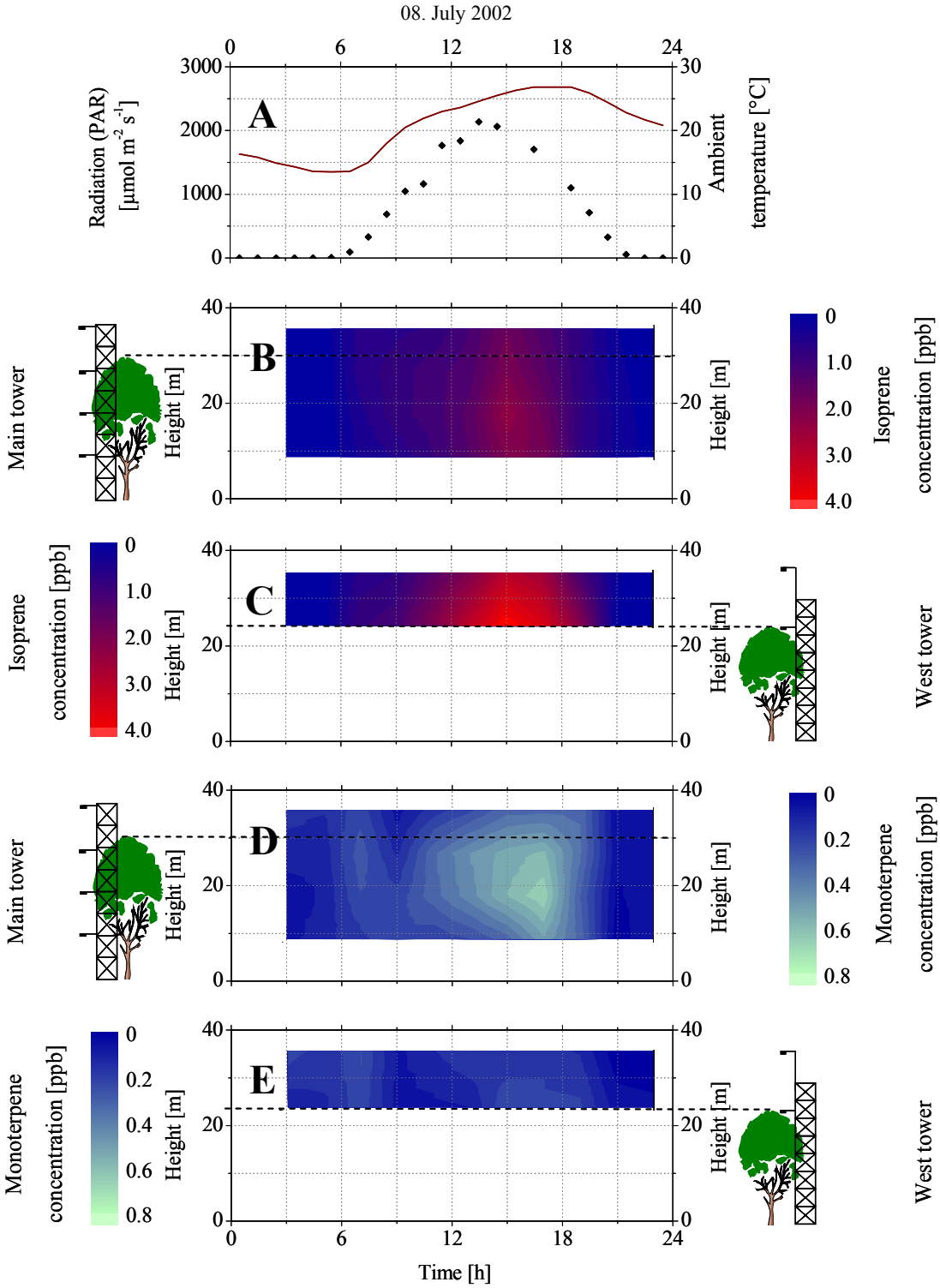

Figure 3.17. Vertical and horizontal profile measurements conducted on one sunny day in July 2002. VOC measurements were conducted simultaneously at 4 different heights at the Main tower site and at two different heights at the West tower site. The canopy height at the respective measurements site is indicated by the dashed black line. (A) Photosynthetic active radiation (black squares) and ambient temperature (wine line) measured on top of the West tower. Isoprene (B, C) and monoterpene (D, E) concentrations were measured in two hour intervals. Intermediate data points were interpolated from these measurements. The relevant VOC concentrations are indicated by the colour code.

Figure 3.17. C) and exceeded the ones measured at the Main Tower site (see Figure 3.17. B) by a factor of up to 1.7. The maximum isoprene concentration that was recorded at the West Tower site was collected at the lowest measurement level at a height of 24 m. Maximum isoprene concentrations that were measured at the Main Tower site were recorded at a height of 18 m.

Monoterpene concentrations exhibited only a diurnal course at the Main Tower site (see Figures 3.17. D). Maximum monoterpene mixing ratios of 0.6 ppb were collected at a height 18 m. Monoterpene concentrations measured at the West Tower site ranged ≤ 0.3 ppb and showed no diurnal characteristics (see Figures 3.17. E). In comparison to the isoprene concentrations measured at both tower sites, maximum monoterpene concentrations were recorded later in the afternoon at 17:14 h.

In contrast to this sunny measurement day, radiation intensities measured during the cloudy and rainy day reached maximum values of 740 μmol m^{-1} s^{-1} and ambient temperatures ranged ≤ 19°C. Consequently, isoprene and monoterpene mixing ratios exhibited no pronounced diurnal course with isoprene concentrations ranging ≤ 0.1 ppb and 1.0 ppb at the Main Tower and West Tower site, respectively. Monoterpene concentrations ranged ≤ 0.2 ppb at the Main Tower site and ≤ 0.3 ppb at the West Tower site.

EFFECT OF MONOTERPENE EMISSION FROM *FAGUS SYLVATICA* L. ON EUROPEAN VOC EMISSIONS

According to Guenther *et al.* (1995; 1997), there are two approaches to assign emission factors at an ecosystem scale.

(i) The first method assigns a landscape type to each location within the model domain. An emission potential, derived by micrometeorological measurement techniques or from general assumptions of species distribution, is associated with each landscape type.

(ii) The second approach requires an estimate of the composition of plant species for each location in the model domain, as well as a database of specific emission potentials that are derived e.g. by enclosure measurements for each plant species. A landscape average emission potential can then be assigned as the weighted average of all species at each location.

In the global model of Guenther *et al.* (1995) distinct emission factors have been assigned to various ecosystem types following the first approach described above.

Figure 3.18. A shows the mean European monoterpene emission flux (domain 10°W-30°E and 35°N-60°N) for the month of July that was calculated with the default monoterpene emission factors assigned to the Olson ecosystems as described by Guenther *et al.* (1995, henceforth G95Ols) for a 0.5 x 0.5 grid resolution.

Figure 3.18. B shows the relative increase of monthly mean monoterpene emission in relation to the G95Ols assumption if the spatial distribution of *Fagus sylvatica* L. is specifically considered (henceforth G95FS). The G95FS flux is calculated from the flux using the default emission factor of the G95Ols assumption and the flux based on an average monoterpene emission factor for European beech. The latter average factor of 15 μg g^{-1} h^{-1} was calculated from the standard emission factors reported by Moukhtar *et al.* (2005), Spirig *et al.* (2005) and the present study. Moreover basal emission rates specified by Schuh *et al.* (1997) and Kahl *et al.* (1999) were used for the calculation. The basal emission rates reported by Schuh *et al.* (1997) and Kahl *et al.* (1999) were normalised to standard conditions of 1000 μmol m^{-2} s^{-1} and 30°C by application of the G97 function. Conversion to a leaf dry weight basis was performed by application of the average specific leaf weight measured during the present study (i.e. 93 g m^{-2}). In this way weighted average fluxes were calculated, specifically taking into consideration the fraction of *Fagus sylvatica* L. area coverage in every 0.5 x 0.5 grid. The relative difference to the default G95Ols model (see Figure 3.18.B) is calculated according to Formula 3.13..

$$100 \times \frac{G95FS - G95Ols}{(G95FS + G95Ols)/2} \qquad 3.13.$$

The spatial distribution of the differences reflects moreover the European distribution of *Fagus sylvatica* L., which makes up about 7.1% of the European forest area. Despite the relatively small area covered by European beech there is a significant carbon increase in the European monoterpene emission for the month of July from 695 to 1067 Gg $month^{-1}$ if the average standard emission factor and the spatial distribution of *Fagus sylvatica* L. are taken into account.

However, in both simulations (G95Ols and G95FS) monoterpene emission was calculated only as a function of temperature. By also considering the role of light as a controlling parameter of monoterpene emission from *Fagus sylvatica* L. (henceforth FSlight), the total

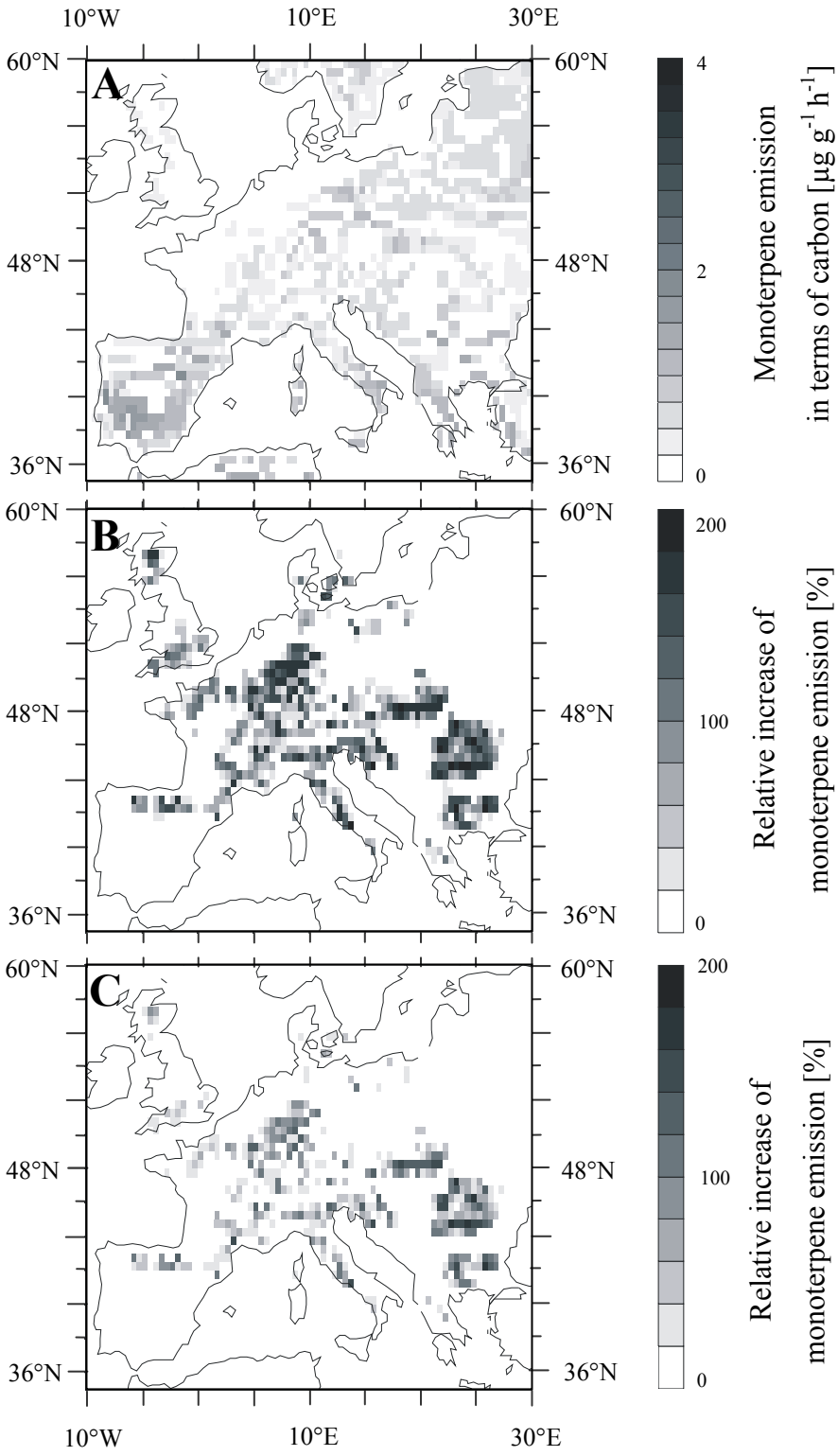

Figure 3.18.. Mean European monoterpene emission fluxes for the month of July. (A) Monoterpene emissions were calculated by the default monoterpene emission factors, considering temperature dependence only. (B) Relative increase of mean monoterpene emission if an average standard emission factor and the spatial distribution of European beech are considered as a function of temperature. (C) Relative increase of mean monoterpene emission if an average standard emission factor and the spatial distribution of European beech are considered as a function of light and temperature.

amount of monoterpene release is reduced significantly. In the latter assumption, relative increases of > 100% between the FSlight and the G95Ols were estimated on a local scale, when relative changes are calculated in analogy to Formula 3.13.. Note, that the FSlight results reflect a simulation where only the light and temperature attenuation functions for *Fagus sylvatica* L. are applied, whereas the monoterpene emissions for the remaining fraction in each 0.5 x 0.5 grid are calculated considering only the role of temperature.

DISCUSSION

ISOPRENE EMISSION FROM ENGLISH OAK

Isoprene was shown to be the predominant compound emitted by *Quercus robur* L.. In agreement with previous studies (see the review of Sharkey and Yeh 2001), isoprene emission followed clearly the diurnal course of ambient light intensity and leaf temperature. The standard emission factor that was calculated by application of the G97 function ranged up to 75 µg g^{-1} h^{-1}, which is in agreement with previous studies that specified the isoprene emission factor of English oak to 76.6 µg g^{-1} h^{-1} (Isidorov *et al.* 1985). Experiments that were performed by applying micrometeorological techniques and a top down model approach at the same measurement site specified standard emission factors of 60 µg g^{-1} h^{-1} for the emission of isoprene from *Quercus robur* L. (Spirig *et al.* 2005).

MONOTERPENE EMISSION AS A FUNCTION OF LIGHT AND TEMPERATURE

In analogy to the monoterpene emission pattern that was observed for other tree species of the plant family *Fagaceae* (e.g. Staudt and Seufert 1995; Bertin and Staudt 1996; Loreto *et al.* 1996; BEMA-Project 1997; Ciccioli *et al.* 1997; Staudt and Bertin 1998; Niinemets *et al.* 2002a; Owen *et al.* 2002) and the laboratory experiments conducted by Schuh *et al.* (1997), monoterpene emission from European beech was demonstrated to be a function of light and temperature. Moreover, the experiments performed during the present study demonstrated that monoterpene emissions vary with the respective time of day (i.e. morning and afternoon). Regarding the correlation of monoterpene emission with light intensity, a saturation trend was reached at radiation intensities of > 500 µmol m^{-2} s^{-1}. The results are in good agreement with previous studies that demonstrated that monoterpene emission from the Mediterranean tree species *Quercus ilex* L. was a function of radiation intensity (e.g. Ciccioli *et al.* 1997).

Moreover, they agree with the saturation trend of photosynthesis that was observed at light intensities of 400–500 μmol m^{-2} s^{-1}, an effect that has been studied in detail for isoprene emission (see the review published by Sharkey and Yeh 2001).

A temperature optimum was not reached and monoterpene emission increased exponentially up to a maximum leaf temperature of 43°C during both campaigns. According to the laboratory experiments conducted by Fischbach *et al.* (2000; 2002) temperature optima for monoterpene synthase from *Quercus ilex* L. ranged between 30 to 40°C (in vitro) and enzyme activity was measurable up to 60°C. Staudt and Bertin (1998) reported in vivo optima at 42°C for a variety of monoterpene compounds that were emitted by *Quercus ilex* L.. Similar optima (~40°C) were obtained by Niinemets *et al.* (2002b) with *Quercus ilex* L. and *Quercus coccifera* L. (in vivo), who demonstrated that the shape of in vitro and in vivo temperature dependencies differ. They concluded that monoterpene synthase activity was influenced by the chloroplastic (stromal) pH. As a decrease in photosynthetic activity at temperatures above the optimum of photosynthesis lead to an acidification of the stromal pH, a decrease in photosynthesis should favour the emission of monoterpenes, since the pH optima of monoterpene synthase are reported to be shifted to the acidic range (Bohlmann *et al.* 1998; Fischbach *et al.* 2000; Niinemets *et al.* 2002b).

Moreover, several authors discussed the relevance of unspecific storage pools for the emission of monoterpenes from *Quercus sp*. (Loreto *et al.* 1996; Ciccioli *et al.* 1997; Delfine *et al.* 2000; Loreto *et al.* 2000; Niinemets *et al.* 2002b; Niinemets and Reichstein 2002; Niinemets *et al.* 2004). We cannot exclude a relevance of such storage pools for the emission of monoterpenes from *Fagus sylvatica* L., particularly since Schuh *et al.* (1997) reported significant night time emission of α-pinene at emission rates of 24.5 μg m^{-2} h^{-1} (Φ_P at 25°C). However, comparable night time emissions should have been detectable in the present study but were not observed. Moreover, the artificial darkening experiment demonstrated a cessation of monoterpene emission in the absence of light. Assuming the existence of unspecific storage pools for monoterpenes in European beech as reported by Schuh *et al.* (1997), storage pools must have been emptied after darkening in a time period of 30 min, since proceeding monoterpene emissions should have been detectable. On the other hand, this is not consistent with the analysis performed by Niinemets and Reichstein (2002) who demonstrated that the decrease of monoterpene emission from storage pools follows a double exponential function. Other authors have also reported a persistence of monoterpene emission from unspecific storage pools of *Quercus sp.*, for several hours to days (Loreto *et al.* 1996; 2000; Ciccioli *et al.* 1997; Niinemets *et al.* 2002a). However, if storage pools would have

existed for the present tree individual and were not depleted by the time the artificial cover was removed, a typical burst of monoterpene emission as reported earlier for *Quercus ilex* L. (Loreto *et al.* 2000) should have been observed for European beech as well (which was not the case). Furthermore a rapid depletion of potential storage pools would explain the lack of night time emission in the present study, since the time resolution of monoterpene measurements was typically 1-2 h. Hence, the experiments clearly demonstrated that monoterpene emission from storage pools may be negligible for the present tree individual.

According to the latter results, the measured monoterpene emission was compared to the G97 algorithm (Guenther *et al.* 1993; 1995; Guenther 1997) that simulates monoterpene emission as a function of light and temperature. Moreover, monoterpene emission was simulated by a modified version of the S97 algorithm (Schuh *et al.* 1997) that neglected the storage pool term of the original S97 function. In general, both algorithms generated a good agreement with the measured monoterpene emission. Correlation coefficients of the measured monoterpene emission to the product of C_L and C_T, ranged from 0.89 to 0.94. However, the S97 provided a better fit to the measured monoterpene exchange. Average standard emission factors that were calculated from the linear regression of monoterpene emission to the respective function ranged from 13.1 to 4.4 µg g^{-1} h^{-1} for the G97 function in June 2002 and July/August 2003, respectively. Emission factors for the S97 function ranged at 14.0 and 4.6 µg g^{-1} h^{-1} for the respective field experiments.

Although the comparison of measured monoterpene emission to the simulated exchange (G97 and S97 function) resulted in good results, major discrepancies were recognised:

(i) During the morning hours the calculated monoterpene emissions were overestimated by the G97 and to a minor extent also by the S97 function.

(ii) During midday and afternoon both algorithms underestimated the measured monoterpene emission.

Regarding the correlation of measured monoterpene emission to light intensity for each single measurement day showed that monoterpene emission was a function of the respective time of the day. Under clear sky conditions, with a rapid increase of light intensity in the early morning, a significant delay of monoterpene emission (in relation to the onset of photo-synthesis) was observable, a phenomenon that has previously been described for other monoterpene emitting broad leaf tree species (e.g. Ciccioli *et al.* 1997). The latter delay in the

onset of monoterpene emission resulted in a typical hysteretic structure regarding the correlation of monoterpene emission to light intensity (see Figure 3.16.). Therefore, the sigmoid increase of the S97 algorithm resulted in a better fit to monoterpene emissions measured during the morning hours. However, a sigmoid decrease in the afternoon was not observable by the measured monoterpene emission. Therefore the simulated emission (S97) underestimated the measured monoterpene exchange in the afternoon.

COMPOSITION OF MONOTERPENES EMITTED BY EUROPEAN BEECH

As measured by the GC-MS samples that were analysed by CNR, sabinene was shown to be the predominant compound emitted from the sunlit leaves of *Fagus sylvatica* L.. This result is consistent with several previous studies that reported sabinene as being the predominant compound released from European beech (see Tollsten and Müller 1996; Schuh *et al.* 1997; Kahl *et al.* 1999). However, in a subsequent laboratory study performed by CNR, sabinene was shown to be decomposed to several other monoterpene compounds during the storage time of the GC-MS cartridges. According to the results of the test, 45% of the initial sabinene concentration was decomposed, yielding the monoterpene α-thujene as a major product. The decomposition, as well as the correction factor applied in the present study, may introduce several uncertainties regarding the apportionment of the relevant compounds (i.e. p-cymene, α-phellandrene, β-phellandrene, sabinene, α-terpinene, γ-terpinene, terpinolene, α-thujene). Moreover, the comparison to the GC-FID samples revealed major discrepancies for the apportionment of the three monoterpenes sabinene, limonene, and p-cymene. Laboratory experiments evaluating the stability of these compounds on the GC-FID samples were not performed during the present study but are strongly encouraged. In total, the discrepancy in basal emission accounted to 25%. Therefore, it may be possible that monoterpene exchange rates specified for the GC-FID system underestimate the monoterpene emission.

Regarding the sum of sabinene and its decomposition products an apportionment of 94% on the total monoterpene emission was calculated. The apportionment of myrcene and limonene was in reasonable agreement with previous studies (see Tollsten and Müller 1996). The results reported for α-pinene emissions are inconsistent between the previous studies, since α-pinene was reported to be released to a major (Schuh *et al.* 1997; Kahl *et al.* 1999), moderate (König *et al.* 1995), or minor (this study and Tollsten and Müller 1996) extent by European beech. Similar contradictory results were obtained for the emission of β-pinene that was reported to be released as a major (König *et al.* 1995) or minor (this study and Tollsten

and Müller 1996) compound. However, as discussed by König *et al.* (1995) temperature effects can be an important factor for the apportionment of monoterpene emission from European beech, resulting in the dominance of different compounds depending on preceding enclosure or ambient temperatures. Moreover, seasonal effects may play an important role. Hence, inconsistencies between the different studies mentioned above might not be surprising, since most of them were conducted at different temperatures (see Table 3.5.).

MIDDAY DEPRESSION OF MONOTERPENE EMISSION

The clear light dependence of monoterpene release reflects the close link of monoterpene production with CO_2 assimilation. A midday depression of net CO_2 assimilation and stomatal conductance was observed several times during the experiments performed in June 2002 and July/August 2003 and reflects the sensitive stomatal regulation that has been evolved by *Fagus sylvatica* L. in response to dry, high temperature conditions (Backes and Leuschner 2000). According to Parry *et al.* (2002), drought effects may lead to a down regulation of ribulose-1,5-bisphosphate-carboxylase (RUBISCO) by tight binding inhibitors, a mechanism that was discussed recently as a central effect of the midday depression of photosynthesis (Griffith and Parry 2002).

Within the course of the experiment conducted in June 2002 a midday depression of monoterpene emission was observed for one measurement day as the plant experienced its first high ambient temperature period of the respective growing season. The midday depression of monoterpene emission was accompanied by a depression of photosynthesis and stomatal conductance. As reported by Loreto *et al.* (1996) and discussed in detail by Niinemets and Reichstein (2003) monoterpenes are emitted through stomata but are not controlled by stomatal aperture. Therefore, other physiological processes such as photosynthesis should have limited monoterpene emission during the respective day. As discussed above, a decrease in photosynthesis and consequently in stromal pH, should favour the emission of monoterpenes (Bohlmann *et al.* 1998; Fischbach *et al.* 2000; Niinemets *et al.* 2002b). However, midday depression of monoterpene emission from *Quercus ilex* L. has been observed by other studies as well (Bertin *et al.* 1997; Kesselmeier *et al.* 1997; Peñuelas and Llusia 1999b). The DOXP Pathway with its substrates glycerine-aldehyde-3-phosphate and pyruvate is known to represent the major source for plastidic isoprenoids (Lichtenthaler 1999). Therefore, a restriction of RUBISCO during midday depression of photosynthesis may lead to a substrate limitation under high monoterpene production rates. Experiments performed by Kahl *et al.* (1999) on European beech indicated that 90% of the total sabinene

emission was formed de novo from photosynthetic intermediates. Since sabinene was the predominant compound emitted by *Fagus sylvatica* L. (fraction of 57%) a decrease of the photosynthetic activity may consequently lead to a decrease in the emission of monoterpenes. During the midday depression of monoterpene emission the carbon balance (carbon loss in form of monoterpenes per photosynthetic fixed carbon) exceeded the 1% level (up to 1.7%), while under normal environmental conditions the carbon loss was typically below 0.5%. Therefore, monoterpene emission might have been limited by the substrate availability during the respective measurement day. However, the number of measurements performed during the present study is rather small and midday depression of monoterpene emission could not be replicated during the measurements conducted in June 2002 and July/August 2003.

VARIABILITY OF STANDARD EMISSION FACTORS OBSERVED FOR MONOTERPENE EMISSION FROM EUROPEAN BEECH

Standard emission factors that were calculated by application of the G97 algorithm on a dry weight basis differed by a factor of 3 between both years. However, the lower standard emission factors calculated for 2003 were confirmed by contemporaneous canopy scale flux measurements performed by Spirig *et al.* (2005).

The importance of variations in developmental stages, seasonality, growth conditions, and habitat for monoterpene emission from *Quercus ilex* L. has been reported recently (e.g. Street *et al.* 1997; Peñuelas and Llusia 1999a; Llusia and Peñuelas 2000; Sabillon and Cremades 2001; Fischbach *et al.* 2002; Niinemets *et al.* 2002a; Staudt *et al.* 2002; Staudt *et al.* 2003). Also, European beech is known to develop ecotypes that are adapted to the climatic conditions of the habitat they live in (Peuke *et al.* 2002). The location selected for the measurement of European beech is characterised by temperate climatic conditions. However, temperatures can display strong variations as observed during the measurement period of 2002 and 2003.

Figure 3.19. gives an overview of ambient temperature and rainfall that were measured prior and during the enclosure of European beech in the summers of 2002 and 2003. Average ambient temperatures measured 30 days preceding the enclosure measurements ranged from moderate temperatures of 16°C in Mai/June 2002 to higher temperatures of 20°C in June/July 2003. As observed by Staudt *et al.* (2003), the acclimatisation time of standard emission factors to previous temperatures was highly variable and ranged between 3 days and 3 weeks for *Quercus ilex* L.. However, these experiments are not in agreement with our results from European beech, as higher daytime temperatures were observed in days preceding the mea-

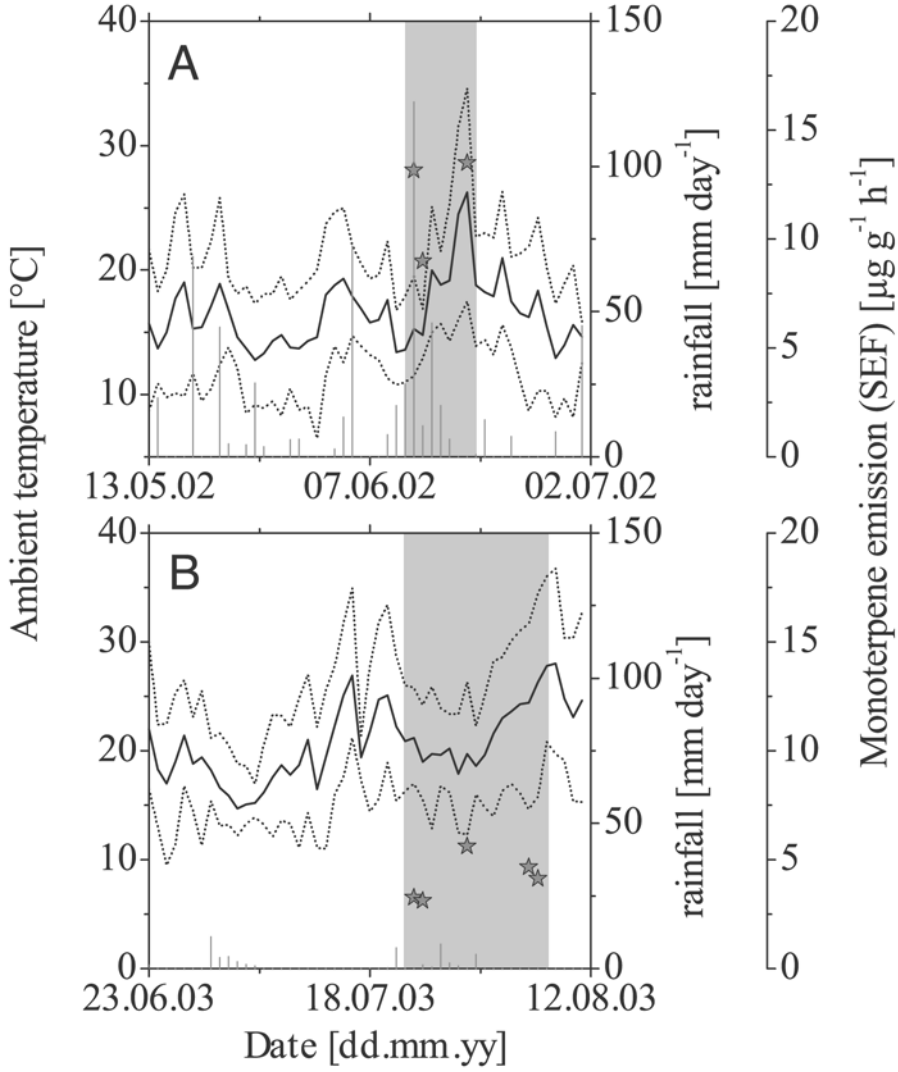

Figure 3.19. Ambient temperature and rainfall prior and during the enclosure measurements of European beech in the years of 2002 (A) and 2003 (B). Grey areas indicate the respective measurement period of each year. Solid lines represent the daily average temperature. Dashed lines show the daily minimum and maximum temperature. Grey bars indicate the respective amount of rainfall. Standard emission factors (SEF) for monoterpene emission rates from sunlit leaves were calculated for single measurement days and are indicated by the grey stars.

surements in 2003, when exchange rates were much smaller. On the other hand lower daytime temperatures were observed preceding the measurements in 2002, when the measured standard emission factors reached high values. Thus, other effects may have dominated the observed variability in standard emission between the experiments conducted in 2002 and 2003.

One of these effects might have been a long lasting drought period that preceded the measurements in 2003 and resulted in a significant reduction of the average photosynthesis during the latter campaign. In comparison, during the summer of 2002 no drought period was

observed and the high ambient temperature episode measured during the course of the experiments of 2002 was only short.

Since a reduction of photosynthesis and transpiration have been reported to be indicators of drought to European beech (Peuke *et al.* 2002; Thomas 2000), we can assume long term effects of drought in 2003. However, transpiration reached significant (t = 99.9%) higher rates during July/August 2003 and increased on average by 48% in July/August 2003. Bertin and Staudt (1996) demonstrated that long periods of drought restricted monoterpene emissions from *Quercus ilex* L. by two orders of magnitude as the daily net carbon balance approached zero. Likewise, Staudt *et al.* (2002) reported a reduction of photosynthesis and transpiration, paralleled by a reduction of monoterpene emission of at least 25% due to drought effects. As reported by Backes and Leuschner (2000) and Thomas (2000), physiological properties of European beech are much more sensitive to drought than physiological properties of oak trees. Hence, this sensibility provides a reasonable explanation for the stronger reduction of monoterpene emission observed during the present study.

Furthermore, as measurements started in June during the first campaign but were conducted in July/August in 2003, seasonal effects on monoterpene emission have to be taken into account. According to Schuh *et al.* (1997), monoterpene emission from *Fagus sylvatica* L. decreased by a factor of 16 between spring and autumn. Also König *et al.* (1995), who investigated beech trees in Austria in late August and early September, reported a decrease of monoterpene emission. For a detailed overview of the seasonal development of monoterpene emission from European beech see Holzke *et al.* (2005), who monitored monoterpene emission from *Fagus sylvatica* L. for a time period of 2 years and reported a temperature independent decline of emissions in the late summer period.

In contrast to older literature data, the present study revealed *Fagus sylvatica* L. as being a strong emitter of monoterpenes. As presented in the review published by Kesselmeier and Staudt 1999, only a few plant species of the plant family *Fagaceae*, exhibited substantial monoterpene emission rates.

Standard emission factors that were calculated for the shaded branch of European beech ranged at 20.0 µg g^{-1} h^{-1} and therefore exceeded the standard emission factors measured for the sunlit leaves. These experiments are not in agreement with experiments performed by Sharkey *et al.* (1991) who demonstrated that shaded leaves exhibited lower basal emission rates for isoprene than sunlit ones. Staudt *et al.* (2003) reported that the effect of previous growth conditions (temperature and light intensity) on *Quercus ilex L.* was influenced by the respective reference dimension that was used for the calculation of standard emission factors

(leaf area or leaf dry weight). Regarding different light conditions, standard emission factors that were normalised to leaf dry weight, exhibited only minor variations during the latter study. However, since the correlation coefficient of the linear fit of monoterpene emission to the G97 function yielded a value of only 0.69 for the shaded branch, it may limit the conclusions that can be derived from the measurements of the present experiment and may therefore explain the observed differences to previous studies. Table 3.5. gives an overview of experi-ments that were conducted earlier to examine monoterpene emission from European beech. Several of these experiments reported, that *Fagus sylvatica* L. emitted only low amounts of monoterpenes. However, these effects may in part be explained by application of different measurement and analytical techniques.

Table 3.5. Monoterpene emission from European beech as reported by several authors. Abbreviations: [a] age of tree, [bdl] below detection limit, [e] enclosure , [ec] eddy covariance flux measurement, [f] field experiment, [l] laboratory experiment, [ldm] leaf disc method, [max] maximum, [norm] normalised to, [par] photosynthetic active radiation, [r] radiation, [t] temperature, [-] not specified, [*] normalised to the average specific leaf weight measured during the present study and by the G97 algorithm to standard conditions of 1000 µmol m^{-2} s^{-1} and 30°C.

Reference	Monoterpene emission [µg g^{-1} h^{-1}]	[µg m^{-2} h^{-1}]	Comment
Hewitt and Street (1992)	bdl	bdl	ldm, a (young/adult), t (-), par (max. 900 µmol m^{-2} s^{-1})
Steinbrecher *et al.* (1993)	-	~0.49	e, l, a (2 years), t (2-14°C), par (max. 600 µmol m^{-2} s^{-1})
König *et al.* (1995)	0.19	-	e, f, a (adult), T (20°C), par (-)
Tollsten and Müller (1996)	0.25	-	e, f, a (adult), T(-), par (-)
Schuh *et al.* (1997)	8*	414	e, l, a (-), Φ_{LT} at t (norm. 25°C), par (norm. 1000 µmol m^{-2} s^{-1})
Kahl *et al.* (1999)	8*	284	e, l, a (6 years), t (norm. 25°C), r (norm. 300 µmol m^{-2} s^{-1})
Spirig *et al.* (2005)	10	930*	ec, f, a (~160 years), t (norm. 30°C), par (norm. 1000 µmol m^{-2} s^{-1})
Moukhtar *et al.* (2005)	44	4092*	e, f, a (~80 years), t (norm. 30°C), par (norm. 1000 µmol m^{-2} s^{-1})
This study	4-13	334-1415	e, f, a (~160 years), t (norm. 30°C), par (norm. 1000 µmol m^{-2} s^{-1})

In general, the physiological data measured by application of a branch enclosure technique (like in the present study) represent the average of a heterogeneous group of leaves (including several developmental leaf stages, physiological leaf types, and/or effects introduced by partial shading of different leaves to one another). Therefore emission factors derived from single leaf level measurements are typically 75% higher than emission factors derived from branch enclosure techniques (Guenther *et al.* 1994). Regarding the laboratory experiments performed by Hewitt and Street (1992) and Steinbrecher *et al.* (1993), monoterpene emission from European beech was below or near the detection limit of the analytical system. Also König *et al.* (1995) and Tollsten and Müller (1996) who examined European beech trees under field conditions in Austria and Switzerland found only low emission of monoterpenes at 0.2 and 0.3 $\mu g\ g^{-1}\ h^{-1}$, respectively. On the other hand, laboratory experiments conducted by Schuh *et al.* (1997) and Kahl *et al.* (1999) revealed substantial monoterpene emissions at exchange rates of 414 and 284 $\mu g\ m^{-2}\ h^{-1}$ (at 25°C). Monoterpene emissions that were measured during the first year of the present study significantly exceeded the latter emission rates reported. However, recent studies that were conducted by Spirig *et al.* (2005) in July 2003 at the same forest site like in the present study indicated higher standard emission factors for *Fagus sylvatica* L. than found by the present study. Moreover Moukhtar *et al.* (2005) reported standard emission factors that exceeded the ones calculated by the present study by a factor of 3. These experiments clearly indicate the variability of monoterpene standard emission factors that can be observed from European beech.

ISOPRENE EMISSION FROM EUROPEAN BEECH

Even though European beech was characterised as monoterpene emitter by this and other studies, the field experiments revealed potential isoprene emissions from *Fagus sylvatica* L.. Typically isoprene exchange rates ranged $\leq 0.4\ \mu g\ g^{-1}\ h^{-1}$ and exhibited no clear diurnal cycles, i.e. scattered between emission and deposition. However, during the high ambient temperature period observed in June 2002 a diurnal course of isoprene emission was detectable. As outlined by Sharkey and Yeh (2001), nearly all plant species emit isoprene at very low levels. Previous studies reported isoprene exchange rates from European beech to range below the emission detected during the present study (see Hewitt and Street 1992; Steinbrecher *et al.* 1993; König *et al.* 1995; Moukhtar *et al.* 2005). The reason for this discrepancy between previous studies and the present experiment remains unclear. Isoprene (and also monoterpene) emission from plants was discussed to increase the temperature tolerance of thylakoid membranes by enhancing hydrophobic interactions. Therefore

temperature effects may play an important role regarding the different studies. According to Havaux (1998), isoprene is dissolved within the thylakoid membrane similar to carotenoid molecules and increases the fluidity of these membranes. Therefore, it may prevent low temperature stress. On the other hand Sharkey and Yeh (2001) discussed isoprene as a protective to repeated heat stress that prevented the formation of water channels within the thylakoid membrane and/or protect large membrane bound protein complexes from fragmentation. Moreover, several studies demonstrated the effect of previous ambient temperatures on isoprene emission (see Sharkey and Yeh 2001 for review). However, the detected isoprene emission was not supported by the single GC-MS cartridge sampled during the respective period. Therefore, it may be also possible that this finding was caused by an analytical artefact (e.g. coelution of other volatile organics).

CARBON BENEFIT OF ENGLISH OAK AND EUROPEAN BEECH

Micrometeorological and physiological parameters were measured during June 2002 and July/August 2003 on sunlit and shaded branches of English oak and European beech. Due to a short high ambient temperature period that was observed within the course of the first measurement campaign, ambient temperatures and radiation intensities monitored on top of the East Tower and at the Small Tower site reached similar values within both field experiments. Measured photosynthesis of the sunlit leaves of *Fagus sylvatica* L. yielded a CO_2 benefit ranging between 4 and 2 mg g^{-1} h^{-1} on a net daily average. Average photosynthesis of *Quercus robur* L. yielded a CO_2 benefit of 5 mg g^{-1} h^{-1}. The data are in reasonable agreement with literature values published by Larcher (1994), that specify the net CO_2 exchange of sunlit *Fagus sylvatica* L. leaves to -350 mg m^{-2} h^{-1} (corresponding to -3.2 mg g^{-1} h^{-1} (*Fagus sylvatica* L., 2002) and -4.5 mg g^{-1} h^{-1} (*Fagus sylvatica* L., 2003)). The net CO_2 exchange rates measured from European beech in June 2002 reached significant higher values than in July/August 2003 (likelihood of T-Test = 99%).

According to the lower light intensity that was available for leaves located below the canopy of European beech, the CO_2 benefit of the shaded branch ranged at values of 0.1 to 0.5 mg g^{-1} h^{-1}. Literature data predicted the net CO_2 exchange rates of shaded leaves of *Fagus sylvatica* L. to at least ⅓ of the carbon gain of sunlit leaves (Larcher 1994). However, the observed difference of carbon benefit from sunlit and shaded leaves was much more pronounced during the present study, since the CO_2 benefit of shaded leaves ranged only at 5 to 13% of the CO_2 benefit of sunlit leaves. Monoterpene emission from sunlit *Fagus sylvatica* L. leaves reached maximum exchange rates of 33.2 µg g^{-1} h^{-1} in June 2002 and 9.6 µg g^{-1} h^{-1}

in July/August 2003 and exhibited pronounced diurnal cycles during both years. Monoterpene emission from shaded leaves of European beech exhibited also a diurnal cycle but ranged at a maximum of 1.5 µg g^{-1} h^{-1} in August 2003, i.e. 16% of the maximum monoterpene emission measured from sunlit leaves in 2003. Considering the percentage loss of photosynthetic fixed carbon in form of the measured monoterpene emission, the sunlit leaves of European beech exhibited pronounced diurnal cycles. No clear diurnal cycle of carbon loss was detectable for the shaded leaves. However, a diurnal cycle of carbon loss might have been present for the shaded branch as well, but was not resolved due to a high analytical uncertainty associated with the small concentration differences measured from the sample and reference enclosure.

On a daily average the carbon loss of sunlit leaves ranged at 0.2 to 0.1% in 2002 and 2003, respectively. Daytime maximum loss rates reached 1.7% in 2002 but only 0.6% in 2003. The average carbon loss of shaded leaves was only 0.1%, indicating that a low light regime has a more pronounced influence on the VOC exchange than on photosynthesis. In contrast to the monoterpene emission measured from European beech, isoprene emission detected from English oak exhibited much higher emission rates ranging up to 77.2 µg g^{-1} h^{-1}. The carbon loss measured from *Quercus robur* L. exhibited clear diurnal cycles and even though the carbon benefit obtained by photosynthesis of English oak was also higher than for European beech, the maximum carbon loss in form of isoprene accounted up to 2.4% (0.7% on a daily average). These latter values are in good agreement with literature data that specify the carbon loss induced by isoprene emission to range typically at 2% of photosynthesis (at 30°C, Sharkey and Yeh 2001). Daytime monoterpene emission from *Quercus ilex* L. has been specified to range between 0.7 and 1.9% of photosynthesis (Kesselmeier *et al.* 1997; 2002b) and therefore exceeded even the maximum values reported here for monoterpene emission from European beech.

VERTICAL AND HORIZONTAL PROFILE MEASUREMENTS

Vertical and horizontal profile measurements conducted during a sunny day in June 2002 showed a diurnal characteristic of isoprene and monoterpene concentrations. As outlined by Atkinson (2000), isoprene and monoterpenes exhibit relatively short lifetimes (~1h). Therefore, the concentration pattern that can be observed for both biogenic VOC follows the emission patter of the surrounding vegetation and should be less influenced by advection processes (Ammann *et al.* 2004). Consistent with our results measured at both tower sites, Spirig *et al.* (2005) reported a diurnal pattern of isoprene and monoterpene concentrations recorded at the Main Tower and at the West Tower site. Moreover the latter study revealed

that isoprene concentrations measured at the West Tower site exceeded the ones recorded at the Main Tower and that monoterpene concentrations exhibited higher values at the Main Tower site. Both observations are consistent with the results obtained during the present study that showed higher monoterpene concentrations at the Main Tower and higher isoprene concentrations at the West Tower site. The results point to the light and temperature dependent release of isoprene and monoterpenes from the different forest sites. Moreover, the concentration differences observed for isoprene and monoterpenes at both tower sites may reflect the distribution of tree species at this forest site, with oaks (i.e. isoprene emitters) predominantly located at the West Tower site and beech and birches (i.e. monoterpene emitters) predominantly located at the Main Tower site.

IMPLICATIONS FOR THE EUROPEAN BUDGET OF MONOTERPENE EMISSION

The results obtained by the various model simulations that were applied demonstrated that consideration of the higher standard emission factor measured for European beech in June 2002 resulted in a significant increase regarding the European budget of monoterpene emissions. Currently monoterpene emission factors that are assigned to temperate forest ecosystems account only to 0.7 to 0.9 µg g^{-1} h^{-1} (see Olson 1992; Guenther *et al.* 1995; Simpson *et al.* 1999). Since *Fagus sylvatica* L. is the dominating deciduous tree species in Europe (vegetation coverage of 7%) its significant impact on the European monoterpene budget is evident. Regarding the latter budget, the consideration of European beech generated an increase of 54% from values of 695 to 1067 t C $month^{-1}$, when only temperature is considered as a controlling parameter. On a local scale, the consideration of the detailed spatial distribution of European beech resulted in significant changes of > 100%, which is in agree-ment with previous studies that demonstrated the impact of a more detailed spatial distribution of a specific land cover type (Guenther 1997; Lenz *et al.* 2001; Solmon *et al.* 2004). However, the applied simulation considering only temperature was still performed in a conservative form, since not the original G95Ols simulation was specified as a reference, but the average of G95Ols and the G95FS simulation (see also the FSlight simulation). Consideration of the G95Ols simulation as a reference led to even higher relative increases in the European monoterpene emission.

Considering moreover radiation intensity as a controlling parameter resulted only in an increase of 16% in the European budget, since night time emission is neglected by the latter simulation. However on a local scale increases of > 100% are still observable. In addition to

the conservative form regarding the selection of the reference value (see above), it has to be noted, that in the FSlight simulation, *Fagus sylvatica* L. was the only tree species that was assigned to light dependent monoterpene emissions. Taking into account, that other tree species may emit monoterpenes as a function of light and temperature as well, also the reference value would decrease, yielding a higher relative impact of the light triggered monoterpene emissions that were released by beech. However, for the European budget the latter increase is small considering all uncertainties involved such as biomass estimates and using the surface- versus the actual canopy or leaf temperature. In addition, the results reflect the simulations for the month of July with high radiation intensity and temperature using the high emission flux measured in 2002. Consequently, the results may reflect an upper range impact of the observed *Fagus sylvatica* L. emission rate and light dependence for the European budget.

CONCLUSION

The results obtained in the present study clearly demonstrated the impact of a more detailed spatial distribution of a specific land cover type for the European VOC budget. As European beech is the predominant deciduous tree species in Europe, its broad geographical distribution led to changes in the local European monoterpene emission of > 100%. Considering only temperature effects the European VOC budget increased by 54%. Taking also the light dependence of monoterpene emission from *Fagus sylvatica* L. into account, the latter increase was calculated to 16%. Considering that a variety of other deciduous tree species may emit substantial amounts of monoterpenes as a function of light and temperature as well, will decrease the amount of monoterpenes emitted in total and will therefore increase the relative impact of European beech on the European VOC budget. However, the uncertainties regarding the calculation of European VOC budgets are high. Moreover, European beech was shown to emit monoterpenes at variable basal emission rates ranging from 4 to 13 $\mu g\ g^{-1}\ h^{-1}$. Basal emission rates of European beech reported by several other studies even exceeded the range reported by the present study. Within this context, drought and temperature effects may play an important role for monoterpene emission, since short term effects of high ambient temperatures were shown to decrease the actual monoterpene emissions (midday depression), while long term drought effects may decrease also basal emission rates.

CHAPTER 4

MEASUREMENT OF TOTAL NONMETHANE ORGANIC CARBON

ABSTRACT

Most of the organic carbon that is present in the atmosphere is found in form of volatile and semivolatile organic compounds. Since vegetation represents the dominant source of volatile organics in the atmosphere it also represents a dominant source of atmospheric organic carbon. One of the major limitations in advancing the understanding of tropospheric ozone and aerosol generation is the technical ability to accurately measure these volatile organics. Within this context, a great variety of analytical techniques enabling the measurement of some specified organics has been developed in the past. However, the integration of these single compound measurements to the sum of organic carbon will only represent a lower limit of atmospheric carbon concentrations, since none of these methods is able to analyse all organic compounds that are present in the atmosphere. Consequently only few studies reported on the measurement of total NMOC concentrations in ambient air. Studies considering the exchange of total carbon between vegetation and the atmosphere are absent. The following chapter will describe the experimental setup of a total NMOC analyser adapted for the performance of plant enclosure measurements to investigate the exchange of total NMOC between plants and the atmosphere. The instrument was tested under laboratory conditions and was evaluated versus an independent analytical technique performing branch enclosure measurements on European beech (*Fagus sylvatica* L.). The instrument is based on general methodologies of elementary analysis and techniques developed by previous studies. The core elements of the analyser are:

(i) a solid adsorbent preconcentration unit, that enabled the adsorption of volatile organics as well as their separation from CO, CO_2, and CH_4,

(ii) an oxidation tube, that converted these volatile organics to CO_2, and

(iii) a CO_2 adsorption trap followed by an infrared gas analyser for the detection of the previously formed CO_2.

The detection limit of the instrument was 0.5 ng carbon and the reproducibility ± 0.5%. Oxidation efficiencies of different volatiles ranged between 91 and 101%. However, recovery rates of several NMOC compounds were as low as 48% and represent the strongest source of uncertainty. Intercomparison of diel courses of the NMOC exchange of European beech

measured by means of enclosures showed a perfect agreement between the total NMOC analyser and a GC-FID approach as an independent method.

INTRODUCTION

Carbon compounds are extensively recycled in the earth's system including processes taking place in the atmosphere, in the biosphere, as well as in the oceanic compartment. The majority of carbon that is present in the atmosphere is found in form of inorganic compounds like the ubiquitous volatiles carbon monoxide (CO) and carbon dioxide (CO_2). In contrast to these inorganic molecules that exhibit tropospheric mixing ratios of ~1.0 and ~350 ppm (Seinfeld and Pandis 1997; Finlayson-Pitts and Pitts 2000; Park 2001), the fraction of volatile and semivolatile organic molecules represents a much smaller pool of carbon in the atmosphere. Methane (CH_4) is known to represent the predominant component of these volatile organics exhibiting tropospheric mixing ratios of ~1.7 ppm (Park 2001). However, CO, CO_2, and CH_4 exhibit atmospheric lifetimes that range between months to years (Finlayson-Pitts and Pitts 2000; Park 2001; Roberts *et al.* 1998). To distinguish the latter molecules from highly reactive organic compounds, which impact atmospheric chemistry on short distances and timescales, the term nonmethane organic carbon was defined (NMOC, i.e. organic carbon other that methane, lifetimes range between several minutes to days). Major characteristic of all NMOC compounds is their great variety in structure and molecular weight (e.g. saturated and non-saturated hydrocarbons or oxygenated volatiles). Since terrestrial vegetation was identified being the predominant source of global NMOC emissions (Guenther *et al.* 1995; 1997; Finlayson-Pitts and Pitts 2000), investigation of the NMOC exchange between plants and the atmosphere was extensively studied in the past (see e.g. the reviews of Kesselmeier and Staudt 1999; Sharkey and Yeh 2001; Lerdau and Gray 2003).

However, previous studies focussed on the detection of a limited, but well defined set of NMOC compounds, e.g. detectable by gas-chromatography coupled to a flame ionisation detector or a mass spectrometer (GC-FID or GC-MS, see also chapter 2 and 3). Measurements of the total NMOC exchange between vegetation and the atmosphere are not reported hitherto and only very few studies reported on total NMOC concentration measurements in ambient air (Roberts *et al.* 1998; Chung *et al.* 2003; Maris *et al.* 2003). Even though summation of reported measurements results in carbon concentrations of up to hundreds of ppb in urban areas (Singh and Zimmermann 1992), yet unidentified organic compounds resulting from primary emissions as well as oxidation processes may represent a major share of total NMOC

concentrations. To acquire the total NMOC concentration of air samples, different techniques have been applied. The most common instrument supplied by several manufac-turers (e.g. J.U.M. Engineering, Germany, Environment S.A, France, Baseline-Mocon Inc., USA) employs a continuous flow FID device that responds to methane and NMOCs. Even though the handling of these instruments is quite comfortable, the latter technique exhibits a different carbon response for several functional groups and is affected by varying levels of O_2. Moreover, a discrimination of the FID response between CH_4 and NMOCs is not possible. Therefore, several of these instruments comprise a selective catalyst to remove all NMOC compounds to measure the amount of NMOCs by difference between the single CH_4 signal and the total CH_4 + NMOC response. However, since atmospheric CH_4 concentrations exceed the atmospheric NMOC mixing ratios by far, large uncertainties are associated with the latter technique and its prevalent application is set in industrial process and safety monitoring.

To determine the total NMOC concentration of ambient air samples, recent studies attempted to separate CO, CO_2, and CH_4 from the NMOC fraction after or during a NMOC preconcentration step. Based on this concept Roberts *et al.* (1998) developed a complex instrument for the measurement of total NMOC mixing ratios in ambient air. The latter technique comprised the cryogenic collection of NMOCs by use of stainless steel tubing that was immersed in liquid nitrogen. CO, CO_2, and CH_4 were separated from the sample by a chromatographic column that was operated alternatively in a flush- and backflush mode. To achieve an equal FID sensitivity per carbon atom of the remaining total NMOC fraction, all carbon compounds were catalytically converted to CO_2 and, in a second step, to the FID sensored CH_4. A similar technique that was developed by Maris *et al.* (2003) provided also good results for the measurement of total organic carbon. Here separation of CO, CO_2, and CH_4 from the NMOC fraction was achieved by cryotrapping of the NMOCs on fused silica beads cooled by liquid nitrogen. Under these conditions CO, CO_2, and CH_4 were co-collected only at low amounts.

Even though both systems provided good results for the measurement of total NMOC concentrations (detection limits ranged between carbon mixing ratios of 5 and 35 ppb), Roberts *et al.* (1998) and Maris *et al.* (2003) discovered that the FID detection was interfered by different water concentrations of the ambient air samples. Since this sensitivity would cause serious interferences applying plant enclosure techniques, several adaptations to the latter techniques had to be established in order to investigate the exchange of NMOC compounds between plants and the atmosphere. The following chapter will describe the setup of a total NMOC analyser adapted for the performance of plant enclosure measurements.

METHODS

GENERAL SETUP

The present NMOC analyser was based on the general methodologies of elementary analysis (Roth, 1958) and the techniques developed by Roberts *et al.* (1998) and Maris *et al.* (2003). Figure 4.1. gives a small overview of the analyser setup. For a better lucidity, all elements of the NMOC system are characterised by a specific number that is referred to in the following paragraphs (italic number in parenthesis).

In general the analysis of NMOC concentrations that are present in various air samples was performed by collecting these compounds on a solid adsorbent trap, followed by their thermal desorption, oxidation of these organic volatiles to CO_2, a subsequent adsorption of CO_2 on a second preconcentration unit, its thermal desorption, and its detection by an infrared gas analyser. As shown by Figure 4.1., the system was operated with helium carrier gas [[*1*], He 6.0, Messer Griesheim, Germany] that was filtered from CO_2 by utilisation of purifier cartridges [*3, 4*] mounted prior to the carrier/dilution gas inlet and prior to the reference cell of the CO_2 detector [*23*]. After sequentially passing a calibration [*16*] and an identical sampling valve [[*17*], 6 way, 2 position, model ET46 UWE, $Vici_{AG}$, Gamma Analysen Technik GmbH, Germany], the carrier gas was either directed to an oxidation tube [*21*] or, using two bypass valves [[*14 and 15*], 3 way, 2 position, model SP764.0282, Elementar Analysensysteme GmbH, Germany], directly to a dryer cartridge [*5*] that removed excessive water molecules from the carrier gas stream. In both cases, detection of the CO_2 amount was accomplished by an infrared gas analyser [*23*]. This way, determination of the basic CO_2 amount as well as the CO_2 plus NMOC content was possible. To prevent peak broadening during detection, CO_2 was focussed using a trapping system filled with a CO_2 adsorbent material [*22*]. CO_2 was released upon heating and was detected by infrared gas analysis.

Sampling of NMOC compounds was performed by a NMOC solid adsorbent unit [*19*] that was connected to the sample valve [*17*] of the instrument. The latter unit provided the possibility to sample volatile organics at various flow rates and temperatures on solid adsorbents. Due to the special characteristics of the utilised adsorbents a separation of the stable gases CO, CO_2, and CH_4 from the volatile NMOC fraction was achieved. By subsequent heating of the NMOC adsorbent trap the volatiles were desorbed and oxidised in the oxidation tube.

Calibration of the system was achieved by utilisation of a CO_2 gas standard [[*2*], 347 ppm CO_2 in synthetic air, Messer Griesheim, Germany] that was mixed with the carrier/dilution gas in the sampling loop of the calibration valve [*16*]. Gas flow of the instrument was regulated by 4 flow controller units [MKS Instruments, USA], controlling the carrier gas flow ([*9*], size of 500 sccm), the CO_2 calibration gas flow ([*6*], size of 10 sccm), the dilution gas flow ([*7*], size 50 sccm), and the sample gas flow ([*8*], size of 500 sccm). To prevent contamination of the carrier gas stream with ambient CO_2, the majority of tubing materials downstream of the purifier cartridges were made from 1/8" stainless steel tubing (see Figure

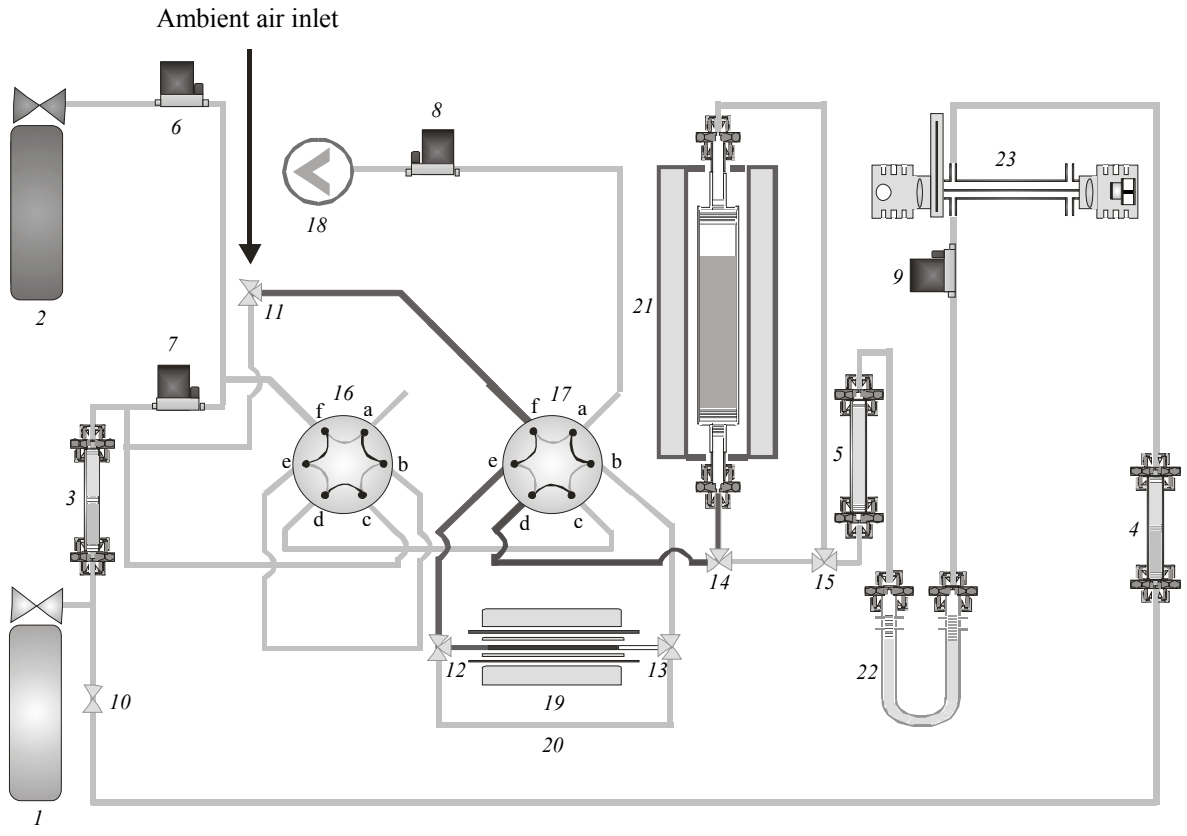

Figure 4.1. General setup of total NMOC analysis. Electrical connections, controller unit, and the data acquisition system are not shown. Abbreviations: [*1*] carrier gas, [*2*] CO_2 calibration gas, [*3*] purifier cartridge for carrier and dilution gas, [*4*] purifier cartridge for reference gas, [*5*] dryer cartridge, [*6*] CO_2 calibration gas flow controller, [*7*] dilution gas flow controller, [*8*] sample gas flow controller, [*9*] carrier gas flow controller, [*10*] needle valve, [*11*] ambient air inlet/flush valve (3 way, 2 position), [*12*] and [*13*] adsorption cartridge valves (3 way, 2 position), [*14*] and [*15*] bypass valves (3 way, 2 position), [*16*] calibration valve (6 way, 2 position), [*17*] sample valve (6 way, 2 position), [*18*] pump, [*19*] NMOC solid adsorbent unit, [*20*] bypass of NMOC sampling/desorption unit, [*21*] oxidation tube and furnace, [*22*] CO_2 adsorption unit, [*23*] infrared gas analyser. Note, that stainless steel tubing is indicated by light grey lines, Silicosteel tubing by dark grey lines, and Teflon tubing by white lines.

4.1., light grey lines). 1/8" Teflon tubing was used only downstream of the NMOC adsorption trap (see Figure 4.1. [*19*]). To prevent adsorption effects of volatile organics within the analyser, tubing upstream of the NMOC adsorption tube and prior to the oxidation step was made from Silicosteel® tubing [1/8", RESTEK, USA, see Figure 4.1., dark grey lines]. Moreover, the Silicosteel® tubing, the sampling valve, and the bypass valve were heated to 130°C by utilisation of an external heating tape and controller unit [model BC8028 HBST, 5 m, 250 W, Horst GmbH, Germany and model TD05F, Heraeus Wittmann, Germany].

To prevent the clogging of analyser valves and detection systems by small particles (derived e.g. from the utilisation of quartz wool in the adsorption and oxidation system), small Teflon filters [Zeflour Teflon filters, 2 µm pore size, Gelman Science, USA] were mounted within several stainless steel reducer units according to Figure 4.2.. The filters were located at the inlet and outlet of each purifier and dryer cartridge, prior to the flow controller units, at each inlet/outlet of the 3 way, 2 position valves, the CO_2 and the NMOC adsorption trap, and at the detector inlets (sample and reference cell).

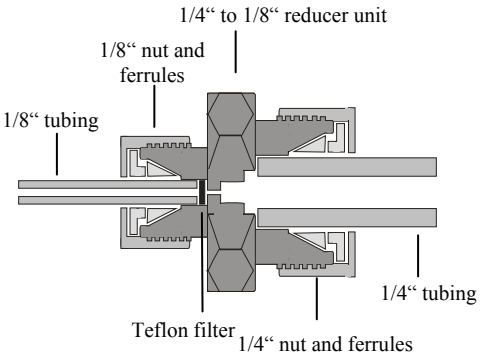

Figure 4.2. Teflon filter assembly as mounted in the 2 way, 3-position valves, in front of each flowcontroller unit, at the inlet and outlet of each purifier cartridge, and in front of the detector unit. The assembly consisted of a small Teflon filter that was inserted in a commercial available straight reducer fitting or a straight maile reducer unit. By attaching a tubing to the connector unit, the Teflon filter was kept in place.

The majority of subunits were under control of an external controller device. The detector output was recorded by conventional chromatographic software [E-lab™ Chromatography system, OMS Tech Inc., USA]. The following paragraphs will give a detailed description of all subunits of the total NMOC analyser.

DETECTOR OF TOTAL NMOC ANALYSIS [*23*]

Detection of the carbon content released by the CO_2 adsorption trap [*22*] was achieved by utilisation of a commercially available infrared gas analyser [model Li 6262, Li-COR, USA]. The system was placed in a tempered aluminium box to prevent signal fluctuations induced by the detector's temperature sensitivity. Constant detector temperatures of 38°C were enab-

led by combination of the heat output of the infrared gas analyser itself and the use of two ventilator units [24 V, 2.4 W] that were controlled by the external controller device.

In general the detector was based on non-dispersive infrared gas analysis (NDIR). As shown by Figure 4.3., it consisted from a gold plated sample cell and a reference cell. Radiation emitted by a vacuum sealed infrared source was transmitted alternately to the latter sample and reference cell by a chopping shutter disc that rotated at 500 Hz. To eliminate the interference from ambient CO_2 and water vapour, the optical path between the infrared source and the optical bench was continuously purged by a low flow of air passing a small desiccant tube containing sodalime (to remove CO_2) and manganese perchlorate (to remove water vapour). CO_2 detection was achieved at a wavelength of 4.26 μm by measuring the adsorptive difference between the sample and the reference cell (reference gas He 6.0). Since the detector was a solid state device (i.e. a device that changes its electrical conductivity in response to infrared radiation) it was insensitive to vibration. Flow rates to the sample cell were adjusted to 100 ml min^{-1} (at standard conditions of 0°C) by use of a flow controller unit [*9*]. Flow rates to the reference cell were adjusted to ~20 ml min^{-1} by use of a needle valve [*10*]. As water vapour was removed from the sample and reference gas, cross sensitivities of H_2O molecules were eliminated. Therefore pressure broadening and dilution corrections were not accounted for by the detector device (function 76 = off).

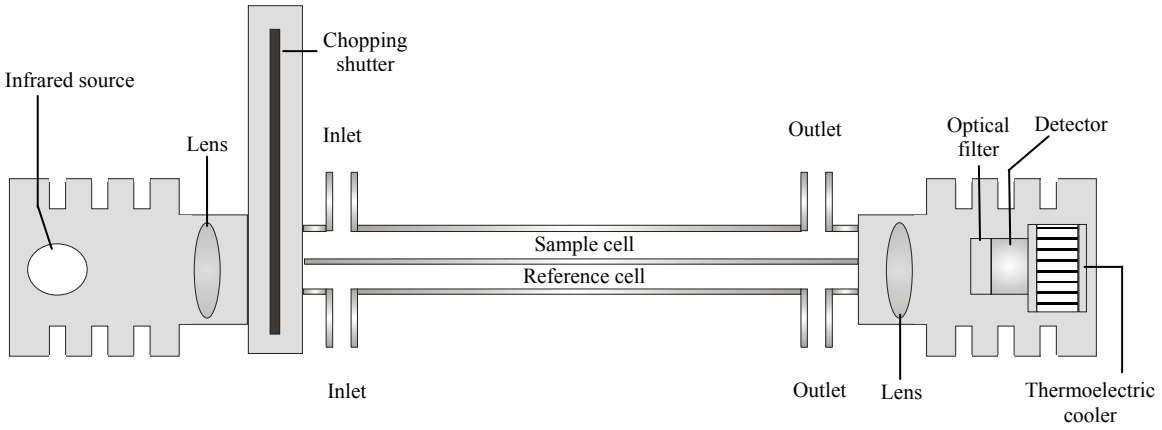

Figure 4.3. Infrared gas analyser. Modified according to LI-COR.

Calibration of the detector was achieved by a CO_2 gas standard [*2*] and Helium 6.0 [*1*] in regular intervals following the default procedure. Storage of the CO_2 signal was obtained by connecting the voltage output of the detector (DAC, 5000 mV) via a potential divider (reduction to 1000 mV) to an external computer device running chromatographic software (E-lab™). Concurrently the detector response was recorded by the external controller device.

The maximum detector response was typically set to mixing ratios of 25 ppm CO_2. As CO_2 was released by the CO_2 adsorption trap it resembled a chromatographic peak that was detectable by the standard chromatographic software. Control of the latter software was achieved by the external controller device that generated a trigger signal to start each chromatogram. Typical run times of a chromatogram were set to 15 min for calibration of the NMOC analyser and 20 min for the sampling of ambient air. Typical settings of the chromatography software are given in Appendix 2.

CO_2 ADSORPTION TRAP [*22*]

Sampling of CO_2 prior to detection by infrared gas analysis was achieved by a CO_2 adsorption trap that was used by courtesy of Elementar Analysensysteme GmbH, Germany. As shown by Figure 4.4. A, the system consisted of an U-shaped copper tubing (8 mm in diameter, terminal connection 1/4" stainless steel) that was mounted in a support frame and was connected to the NMOC analyser by 1/4 to 1/8" reducer units. Heating of the system was achieved by a heating coil fixed to the surface of the copper tubing. The power supply of the heating coil was either controlled directly by the external controller device or via a transformer unit [in: 220, out: 24 V, 5.43 A] that was connected to the 220 V supply. Cooling was enabled by utilisation of a conventional ventilator [24 V, 0.15 A] mounted at the back panel of the support frame. The temperature was controlled by a thermocouple that was fixed to the outer

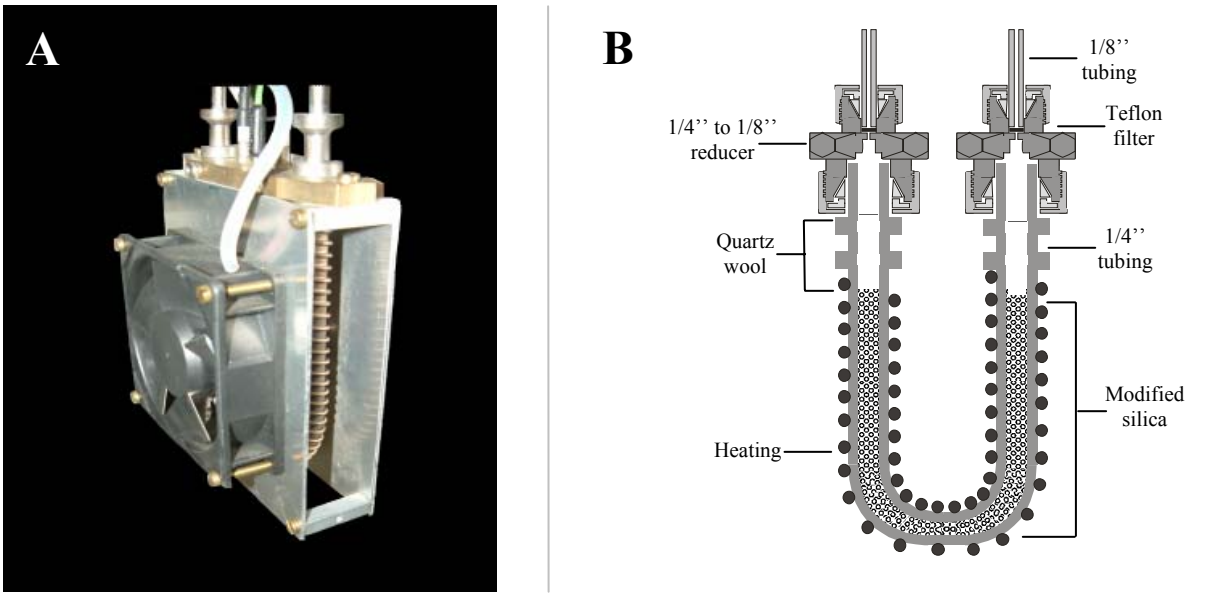

Figure 4.4. CO_2 adsorption trap. (A) Assembly of CO_2 adsorption trap, heating and ventilator as mounted in the NMOC analyser. (B) Schematic drawing of the adsorption trap filled with CO_2 adsorbents.

surface of the copper tubing and generated a permanent temperature input to the controller device. As shown by Figure 4.4. B, the copper tubing was filled with CO_2 adsorbent material up to its maximum fill up quantity. On a first attempt, the CO_2 adsorption trap contained 4 g of a molecular sieve [5 Å, 30/40 mesh, SUPELCO, Germany] and quartz wool [Roth, Germany]. In a later approach the molecular sieve was replaced by 7 g of modified silica [silica type 175, 0.5–1 mm, Elementar Analysensysteme GmbH, Germany].

CALIBRATION OF TOTAL NMOC ANALYSIS

Calibration of the total NMOC analyser was achieved by utilisation of a CO_2 gas standard ([*2*], 347 ppm CO_2 in synthetic air) that was mixed with variable amounts of He dilution gas ([*1*], He 6.0). Purification of the latter dilution gas from CO_2 and H_2O was achieved by purifier cartridges that contained NaOH coated carrier material [sodium hydroxide on support, granulated 0.8-1.6 mm, for elementary analysis, Merck, Germany], Sicapent [phosphorous pentoxide with indicator, Merck, Germany] and quartz wool (see Figure 4.5. A and B).

The calibration and dilution gas flow was regulated by two flow controller units [*6 and 7*] that were under control of the external controller device. Both gas flows were mixed in a calibration loop of 1 ml volume [1/8“, stainless steel, Gamma Analysen Technik GmbH,

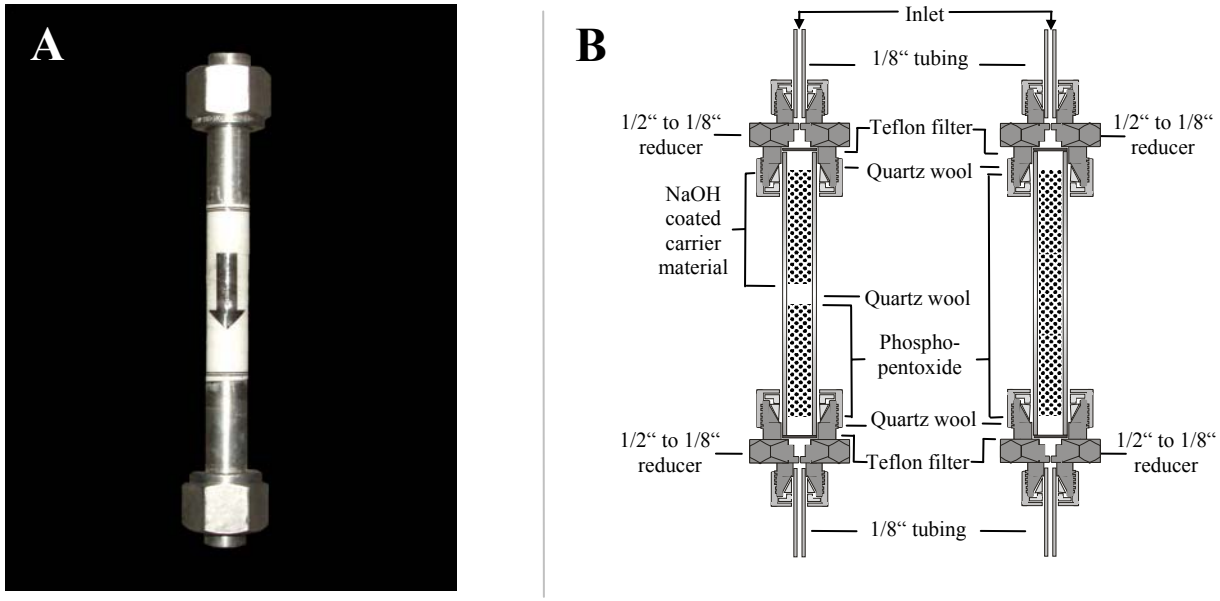

Figure 4.5. Purifier or dryer cartridge. (A) Cartridge as mounted in the NMOC analyser. (B, left panel) Schematic drawing of the purifier cartridge as used for purification of carrier-, dilution-, and reference gas. (B, right panel) Schematic drawing of the drying cartridge as used in the NMOC analyser to remove H_2O prior to CO_2 detection.

Germany] that was connected through ports “b” and “e” (see Figure 4.1.) to the calibration valve [*16*]. In the default configuration the calibration gas inlet was set at port “f” of the calibration valve. The outlet was set at port “a” of the calibration valve. By switching the calibration valve, the calibration loop was connected to the carrier gas stream, transferring the calibration gas to the analyser.

In the default setting the CO_2 amounts utilised for the calibration of the analyser ranged from 0 to 186 ng (at standard conditions of 0°C). Due to the expansion of the calibration gas at higher temperatures, laboratory conditions resulted in a decrease of the carbon amount sampled in the calibration loop. Therefore the calibrated carbon amount was normalised to the respective ambient temperature that was measured by the external controller device. To eliminate potential interference of other trace gases present in the calibration gas, CO_2 samples bypassed the CuO oxidation tube by utilisation of two bypass valves ([*14 and 15*], status “on” = bypass activated). Residual water vapour was trapped by a drier cartridge [*5*] that contained Sicapent in analogy to the purifying cartridges (see Figure 4.5. B). After adsorption and desorption by the CO_2 adsorption trap [*22*] the CO_2 was detected by the infrared gas analyser [*23*].

OXIDATION TUBE [*21*]

Conversion of trapped NMOC compounds to CO_2 was achieved by utilisation of an oxidation tube made from quartz glass (length 360 mm, external diameter 28 mm) that was manufactured by the workshop of the MPI for Chemistry. On a first approach the oxidation tube was connected to the total NMOC analyser by use of various fitting types and materials (e.g. ball and socket joints or stainless steel fittings with Teflon ferrules). However, the majority of tested materials led to high carbon background values upon heating. Best results were obtained by utilisation of quartz to metal seals [model GMQS050TE, ½” OD, Kurt J. Lesker Company Ltd, UK] that were directly connected to the quartz tube. Connection to the total NMOC analyser was achieved by utilisation of stainless steel reducer units (see Figure 4.6. A and C).

The quartz tube was filled with 250 g CuO [copper oxide, wire fine, 0.65-3 mm, for elementary analysis, surface CuO, core Cu_2O, ≤ 0.002% total carbon, Elementar Analysen-systeme GmbH, Germany, see Figure 4.6. B] and quartz wool as shown by Figure 4.6. C. To convert volatile organics, the tube was placed in a vertical tube furnace that was used by the courtesy of the Johannes Gutenberg University, Mainz and was kept at 800°C. The vertical arrangement of the oxidation tube was crucial for NMOC analysis, since the contact

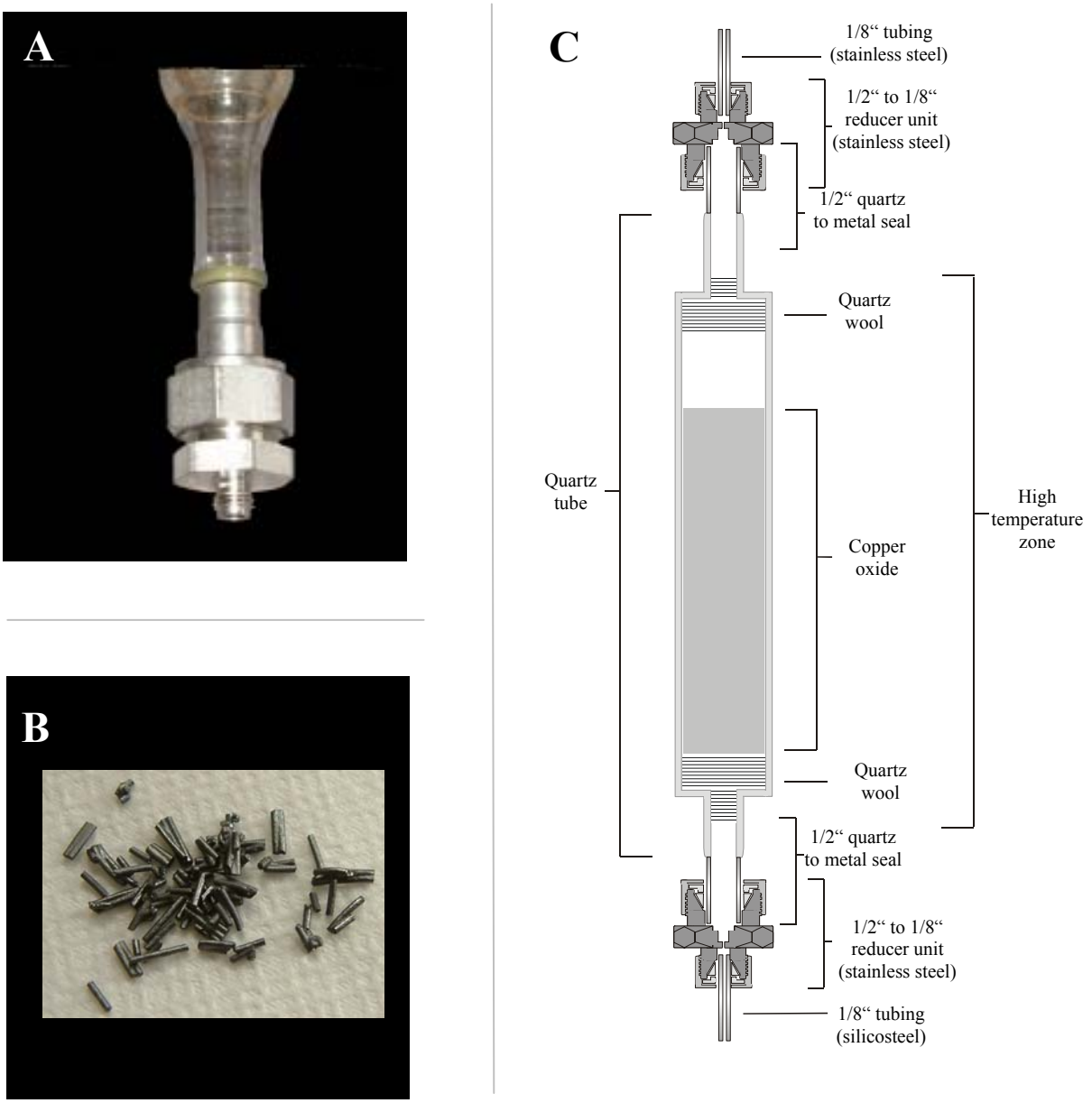

Figure 4.6. Oxidation tube made of quartz. (A) Quartz metal seal as used for the connection of Silicosteel (or stainless steel) tubing with the quartz tube. (B) CuO as used for the oxidation of NMOC compounds. (C) Schematic drawing of the oxidation tube filled with CuO.

time of NMOC compounds and oxidation material was maximised by preventing the formation of small channels within the CuO material. To enable low background values, new CuO needed to be purged with helium carrier gas at flow rates of 50-100 ml min^{-1} for at least 24 h. Further purification and/or regeneration of the oxidation material was enabled by utilisation of ultra pure O_2 [5.5, Messer Griesheim, Germany] that was mixed with He carrier gas to mixing ratios of ~20%. Several tests of the instrument were performed with addition of variable amounts of O_2 to the carrier gas stream to facilitate the oxidation of some volatiles.

To minimize interferences to the NMOC adsorption trap during these experiments, O_2 was added directly prior to the oxidation tube by a T-connector unit (note, the connection of the O_2 gas cylinder is not shown in Figure 4.1.).

NMOC SOLID ADSORBENT UNIT [*19, 20*]

Adsorption of NMOC compounds and separation from CO, CO_2, and CH_4 present in ambient air was achieved by utilisation of a combined sampling/desorption unit that comprised a glass tube filled with solid adsorbents. As shown by Figure 4.1., the unit was connected to the sample valve [*17*] through ports "b" and "e". The complete unit consisted of an aluminium block (length 190 mm, height 70 mm, width 50 mm) that contained 3 drilling holes. While the first drilling hole (32 mm in diameter) contained the cooling probe of a commercially available immersion cooler [model CC-100 with cryotrol, Thermo Neslab, Germany], the second drilling hole (5 mm in diameter) contained the temperature sensor of the latter immersion cooler system (see Figure 4.7.). By cooling the probe to a preset temperature (range -25 to -90°C) the aluminium block was kept at constant temperatures and allowed fast cooling of the heated adsorbent material.

The adsorption tube for NMOC sampling was situated in the third drilling hole (12 mm in diameter) of the aluminium block. To enable heating of the adsorption tube it was enclosed by a heating coil that was connected to the voltage output of the external controller device. Measuring the temperature of the heating coil by utilisation of a thermocouple enabled temperature regulation of the adsorption trap. Electrical isolation of the heating coil to the aluminium block was achieved by a glass tubing (16 mm OD) that surrounded the heating coil as well as by use of two small glass rings that were situated at the upper- and lower side of the adsorbent tubing (see Figure 4.7.B). On a first approach adsorption tubes made from 1/4" Silicosteel® tubing were utilised. However application of glass tubes (6 mm OD, 240 mm length) provided better results, yielding a more efficient energy transfer from the heating coil to the adsorbents. Moreover, temperature differences between surface and adsorbent temperatures were smaller during the heating phase of the quartz glass.

As shown by Figure 4.1. and 4.7., the adsorption tube was connected to the analyser tubing by 1/4 to 1/8" reducer units (made of stainless steel with Teflon ferrules). To allow purging of the tubing material located upstream of the adsorbent material, a bypass-tubing was installed next to the adsorption tube. The latter bypass was connected to the adsorption system by two adsorption cartridge valves [[*12 and 13*], 3 way, 2 position, model SP764.0282, Elementar Analysensysteme GmbH, Germany, status "on" = bypass inactive]. Air was sampled using a

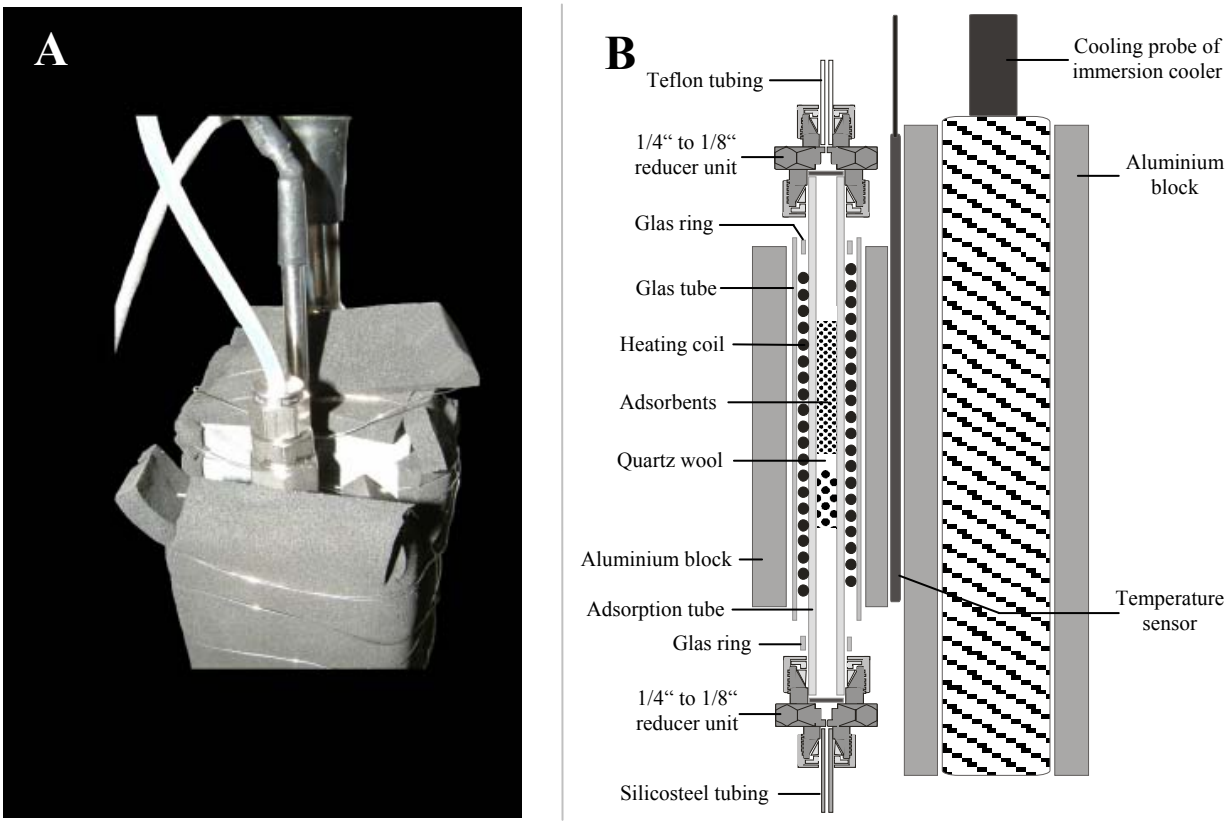

Figure 4.7. NMOC solid adsorbent unit. (A) Adsorption trap as mounted in the NMOC analyser. (B) Schematic cross section of the NMOC adsorption trap.

a flow controller unit ([*8*], size 500 sccm) and a small pump unit [[*18*], model NMP30KNDC, 12 V, 0.5 A, KNF Neuberger] that were connected to port “a” of the sampling valve [*17*]. The gas inlet was connected to port “f” of the sampling valve. To allow the purging of the bypass and adsorption trap with either ambient air or He, a flush valve [[*11*], 3 way, 2 position, model SP764.0282, Elementar Analysensysteme GmbH, Germany] was installed at the air inlet (status “on” = purging with He).

In the default configuration the adsorbent tube was filled with 100 mg Carbograph 1 [90 m^2 g^{-1}, 20-40 mesh, LARA, Italy] and 200 mg Carbograph 5 [560 m^2 g^{-1}, 20-40 mesh, LARA, Italy] that were separated by quartz wool. Vertical arrangement of the adsorbent tube prevented the formation of small air channels within the adsorbent material. However, on some occasions the adsorbent materials were removed slightly from the heating zone by the through flowing sample air and new adsorbent tubes had to be inserted in the NMOC sampling unit. Upon sampling, air first passed the weakest adsorbent material (i.e. Carbograph 1) mounted in the NMOC sampling device. Sampling of NMOC compounds present in ambient air was typically performed for 10 min at 35°C. Flow rates were set to 300 ml min^{-1}.

Removal of excessive air present in the dead volumes of the sample tubing was achieved by subsequent purgation with helium. Desorption of sampled NMOC compounds was achieved for 4 min in a back flush mode at 250°C by switching the sample valve and thus connecting the adsorption tube to the carrier gas flow. NMOC compounds sampled on the adsorbent material were released from the adsorbent material and were transferred to the oxidation tube to be converted to CO_2.

EXTERNAL CONTROLLER DEVICE

Control of the NMOC analyser was achieved by utilisation of an external microprocessor control unit that was built by the electronic department of the Max Planck Institute for Chemistry. The system provided control signals to operate the analyser valves [*11, 12, 13,14, 15, 16, 17*], the flow controller units [*6, 7, 8, 9*], the adsorption and desorption units [*19/20, 22*], the detector temperature, the pump [*18*], as well as the chromatography software. Table 4.1 gives an overview of all parameters that were stored in 1 second intervals by the controller device to a non volatile memory (PCMCIA flash disk). Communication of the controller unit with an external computer device was achieved via a RS-232 connector by the software RPC0700 [Max Planck Institute for Chemistry, electronic department]. Moreover a keypad that was mounted directly at the controller device enabled an easy access of several analyser functions.

Table 4.1. Parameters stored to non volatile memory.

Parameter	
Date and time	Flow rate carrier gas
CO_2 detector signal	Flow rate ambient air
H_2O detector signal	Reference temperature
Detector temperature	Status ambient air inlet/flush valve
Temperature of NMOC adsorption unit	Status bypass valves
Temperature of CO_2 adsorption unit	Status calibration valve
Flow rate dilution gas	Status sample valve
Flow rate CO_2 calibration gas	Status adsorption cartridge valves

Operation of the NMMOC analyser was performed by several files that were stored in the internal memory of the controller unit and were moreover designed by the electronic department of the Max Planck Institute for Chemistry. An overview of these different files is

given in Appendix 2. As shown in the appendix, the general assignment of all instrument subunits to a virtual address number was performed by a configuration file. Furthermore, the latter file comprised a thermistor table that enabled an adequate temperature measurement, defined the overall menu structure, and several analyser functions. A parameter file enabled the calibration of the various flow controller units and comprised the settings of the temperature regulation for the detector, as well as for the ad- and desorption units. To enable rapid variations of the analyser control, the respective subunit status (e.g. valves, flow controllers) was defined by several program files. Finally the chronological progression of these program files was defined by a method file. The power consumption of the external controller device was 1 A at 28 VDC in standby mode.

SETUP OF ENCLOSURE MEASUREMENTS

A test of the NMOC analyser under field conditions was performed within the framework of the ECHO project in August 2003, accompanying the GC-FID measurements performed on a sunlit branch of European beech (*Fagus sylvatica* L.). The setup of the enclosure system and the measurements performed on *Fagus sylvatica* L. are described in detail in chapter 3.

Unlike the automated VOC samplers that were installed on top of the canopy, the NMOC analyser was installed in a ground based mode. Connection of the analyser's air inlet to the sample and reference cuvette was obtained by PFA Teflon tubing (1/4" tubing, 50 m length, 1/8" tubing, 6 m length) that was slightly heated above ambient temperatures by use of a heating tape [model HBRC, 10 W m^{-1}, Horst GmbH, Germany (50 m tubing) and RS components GmbH, USA (6 m tubing)]. As shown by Figure 4.8., the 50 m inlet tubing was directly connected to the sample and reference cuvette of the enclosure system. Two PFA

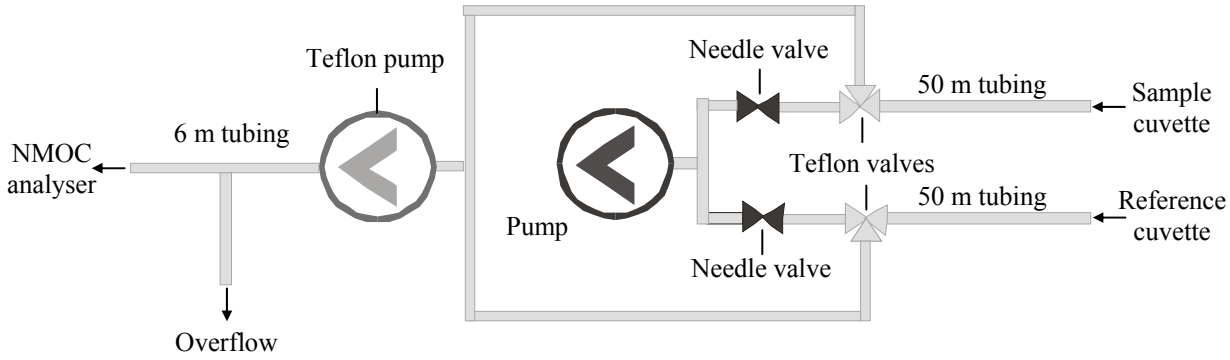

Figure 4.8. Valve and pumping system for the measurement of volatile organic carbon by total NMOC analysis as conduceted during the enclosure measurements performed in August 2003.

Teflon valves [3 way, 2 position, Galtek, USA] (controlled by a data logger [model CR23X, Campbell Scientific Inc., UK], switching interval 40 min) directed the cuvette air either to the NMOC analyser or to a bypass that enabled a continuous purging of the inlet tubing at flow rates of 10 l min^{-1}. Air flow to the NMOC analyser and overflow was enabled by utilisation of a Teflon pump [Laboport, KNF Neuberger, Germany]. Typical sampling flows of the NMOC analyser ranged at 300 ml min^{-1}. Excessive air flow was directed to the overflow outlet.

CALCULATION OF CARBON MIXING RATIOS AND EXCHANGE RATES

The calculation of carbon mixing ratios present in ambient air was performed in analogy to the GC-FID measurements that are described in detail in chapter 2 and 3. Calibration of the analyser was achieved with different calibration gas volumes that were normalised to the respective ambient temperature, yielding the actual carbon amount. The calibration factor was either calculated from the slope of linear regression according to Formula 2.1., or from repeated standard injections of a single calibration gas volume. In any case carbon mixing ratios were calculated according to Formula 4.1. As shown by the formula, different sample/blank types were analysed for the determination of ambient carbon mixing ratios to distinguish the amount of carbon sampled on the adsorption tube ($Area_{NMOCSample}$) from sampled CO_2 ($Area_{CO2Sample}$) as well as from carbon and CO_2 residuals, present in the analytical system ($Area_{NMOCBlank}$).

$$\text{Mixing Ratio} = \frac{MV}{\text{Cal Factor} \cdot MW} \cdot \frac{((\text{Area}_{NMOCSample} - \text{Area}_{CO2Sample}) - \text{Area}_{NMOCBlank})}{SV} \qquad 4.1.$$

Formula 4.1.: $Area_{CO2Sample}$ = area of the CO_2 amount sampled on the adsorbent cartridge [µV s], $Area_{NMOCBlank}$ = area of the total NMOC amount present in the analytical system (e.g. in carrier gas) without sample injection [µV s], $Area_{NMOCSample}$ = area of the total NMOC amount sampled on the adsorbent cartridge [µV s], CalFactor = calibration factor [µV s ng^{-1}], MV = mole volume of an ideal gas [22.4 l mol^{-1}, 0°C, 1 bar], MW = molecular weight of carbon [g mol^{-1}], SV = air volume sampled on the respective cartridge [l], Mixing ratio = mixing ratio of the respective compound [ppb]

Carbon exchange rates were calculated in analogy to the VOC exchange measurements by difference from the sample and reference enclosure. Since the present setup allowed only a consecutive measurement of both enclosures, differences between both cuvette systems were calculated by subtraction of an average reference enclosure value (see Formula 4.2.).

$$\text{Exchange Rate} = \frac{(MR_{Sample} - ((MR_{Reference\_1} + MR_{Reference\_2})/2) \cdot Q}{MV \cdot A} \quad 4.2.$$

Formula 4.2.: A = reference value of the measurement branch, e.g. dry weight [g], Exchange rate = exchange rate of the respective compound [µg g^{-1} min^{-1}], $MR_{Reference\_1}$ = mixing ratio measured in the reference enclosure prior the sample cuvette measurement [ppb], $MR_{Reference\_2}$ = mixing ratio measured in the reference enclosure after the sample cuvette measurement [ppb], MR_{Sample} = mixing ratio measured in the sample cuvette [ppb], MV = mole volume of an ideal gas [22.4 l mol^{-1}, 0°C, 1 bar], Q = chamber flush rate normalised to 0°C [l min^{-1}]

CALCULATION OF OXIDATION EFFICIENCIES

Oxidation efficiencies were calculated according to Formula 4.3. from repeated injection of different test gas mixtures into the NMOC analyser.

$$\text{Efficiency} = \frac{100}{\text{Amount C}} \cdot \left(\frac{((\text{Area}_{NMOCTG} - \text{Area}_{CO2TG}) - \text{Area}_{NMOCBlank})}{\text{Cal Factor}} \right) \quad 4.3.$$

Formula 4.3.: Amount C = amount carbon injected into the NMOC analyser [ng], $Area_{CO2TG}$ = area of the CO_2 amount present in the test gas mixture [µV s], $Area_{NMOCBlank}$ = area of the total NMOC amount present in the analytical system (e.g. in carrier gas) without sample injection [µV s], $Area_{NMOCTG}$ = area of the total NMOC amount present in the test gas mixture [µV s], CalFactor = calibration factor [µV s ng^{-1}], Efficiency = oxidation efficiency of the test gas mixture [%]

APPLIED STATISTICS

The measured carbon mixing ratios were evaluated by utilisation of several statistical procedures that are described in detail in chapter 2.

UNCERTAINTY OF MIXING RATIOS AND EXCHANGE RATES

Accuracy of NMOC mixing ratios

The accuracy of the CO_2 calibration gas standard (347 ppm CO2 in synthetic air) was specified by the manufacturer to range at ± 2%. Consequently the carbon amount of the undiluted CO_2 standard that was sampled in the calibration loop varied up to a maximum of ± 3.4 ng. However, for the determination of the analyser's accuracy other effects have additionally to be taken into account (e.g. different oxidation efficiencies and/or sample efficiencies of various volatile organic compounds). Therefore extensive intercomparison

tests are needed to determine the accuracy of the NMOC analyser for each single NMOC compound.

Precision of NMOC mixing ratios and exchange rates

The precision of the NMOC analyser was calculated in analogy to the GC-FID and HPLC measurements by conventional error propagation, following Formula 4.4. and 4.5.. Since blank values ($Area_{CO2Sample}$ and $Area_{NMOCBlank}$) were typically subtracted from the sample area on an average basis, the standard deviations of these blank values had to be taken into account.

4.4.

$$Precision_{MR} = MR \cdot \left(\frac{\sqrt{\left(Area_{Sample-Blank} \cdot \sqrt{\left(\frac{\left(P_{Analyt} \cdot CalFactor \right)}{Area_{Sample-Blank}} \right)^2 + P_{Flow}{}^2} \right)^2 + s_{AreaCO2Sample}{}^2 + S_{AreaNMOCBlank}{}^2}}{Area_{Sample-Blank}} \right)$$

$$Area_{Sample\text{-}Blank} = \left(Area_{NMOCSample} - Area_{AverageCO2Sample} \right) - Area_{AverageNMOCBlank} \qquad 4.5.$$

Formulas 4.4. to 4.5.: $Area_{AverageCO2Sample}$ = average area of the CO_2 amount sampled on the adsorbent cartridge [µV s], $Area_{AverageNMOCBlank}$ = average area of the total NMOC amount present in the analytical system (e.g. in carrier gas) without sample injection [µV s], $Area_{NMOCSample}$ = area of the total NMOC amount sampled on the adsorbent cartridge [µV s], $Area_{Sample\text{-}Blank}$ = area of the organic carbon amount present in the sample [µV s], CalFactor = calibration factor [µV s ng^{-1}], MR = mixing ratio [ppb], P_{Analyt} = precision of analysis [ng], P_{Flow} = relative uncertainty of flow and volume measurement [%], $Precision_{MR}$ = Precision of carbon mixing ratios [ppb], $S_{AreaNMOCBlank}$ = standard deviation, area of total NMOC amount present in the analytical system (e.g. in carrier gas) without sample injection [µV s], $S_{AreaCO2Sample}$ = standard deviation, area of the CO_2 amount sampled on the adsorbent tube [µV s]

The calculation of the analytical precision (P_{Analyt}) was performed in analogy to Formulas 2.14. to 2.16.. In case the calculation of mixing ratios was performed with a calibration factor derived from the average of multiple injections of only one standard amount, the term ("P_{Analyt} · CalFactor") of Formula 4.4. was replaced by the standard deviation of the calibrated area. The precision of exchange rates derived from the plant enclosure measurements was cal-

culated in analogy to the GC-FID and GC-MS analysis according to Formula 4.6..

$$\text{Precision}_{ER} = \sqrt{\left(\left(\frac{\left(\sqrt{P_{MRsample}{}^2 + \left(\frac{1}{2}\cdot\sqrt{P_{MRreference\_1}{}^2 + P_{MRreference\_2}{}^2}\right)^2}\right)}{\left(MR_{Sample} - \left(\frac{\left(MR_{Reference\_1} + MR_{Reference\_2}\right)}{2}\right)\right)}\right)^2 + P_Q{}^2 + P_A{}^2\right)} \quad 4.6.$$

Formula 4.6.: $MR_{Reference}$ = mixing ratio measured in the reference cuvette [ppb], MR_{Sample} = mixing ratio measured in the sample cuvette [ppb], P_A = precision of leaf reference data (e.g. dry weight) [%], Precision_{ER} = precision of exchange rate [%], $P_{MRreference\_1}$ = Precision of the mixing ratio measured in the reference cuvette prior to the sample cuvette measurement [ppb], $P_{MRReference\_2}$ = Precision of the mixing ratio measured in the reference cuvette after the sample cuvette measurement [ppb], $P_{MRsample}$ = precision of mixing ratio measured in the sample cuvette [ppb], P_Q = precision of chamber flush rate [%]

The precision of the oxidation efficiency of the different test gas mixtures that were injected by the calibration loop in the NMOC analyser was determined according to Formula 4.7. and 4.8.

$$\text{Precision}_{OE} = \frac{100}{\text{Amount C}}\cdot\left(\frac{\left(\sqrt{\left(\frac{S_{AreaCal}}{\text{Area}_{\text{Sample-Blank}}}\right)^2 + S_{AreaNMOCTG}{}^2 + S_{AreaCO2TG}{}^2 + S_{AreaNMOCBlank}{}^2}\right)}{\text{Cal Factor}}\right) \quad 4.7.$$

$$\text{Area}_{\text{Sample-Blank}} = \left(\text{Area}_{\text{AverageNMOCTG}} - \text{Area}_{\text{AverageCO2TG}}\right) - \text{Area}_{\text{AverageNMOCBlank}} \quad 4.8.$$

Formulas 4.7. to 4.8.: Amount C = amount carbon injected into the NMOC analyser [ng], $\text{Area}_{\text{AverageCO2TG}}$ = area of the CO_2 amount present in the test gas mixture [µV s], $\text{Area}_{\text{AverageNMOCBlank}}$ = area of the total NMOC amount present in the analytical system (e.g. in carrier gas) without sample injection [µV s], $\text{Area}_{\text{AverageNMOCTG}}$ = area of the total NMOC amount present in the test gas mixture [µV s], $\text{Area}_{\text{Sample-Blank}}$ = area of the organic carbon amount present in the test gas mixture [µV s], CalFactor = calibration factor [µV s ng^{-1}], Precision_{OE} = Precision of the oxidation efficiency of the test gas mixture [%], $S_{AreaCal}$ = standard deviation, area of calibration standards [µV s], $S_{AreaCO2TG}$ = standard deviation, area of CO_2 amount present in the test gas mixture [µV s], $S_{AreaNMOCBlank}$ = standard deviation, area of total NMOC amount present in the analytical system (e.g. in carrier gas) without sample injection [µV s], $S_{AreaNMOCTG}$ = standard deviation, area of total NMOC amount present in the test gas mixture [µV s]

SAMPLING PROCEDURES AND PROTOCOL

With exception of the branch enclosure measurements, all tests of the total NMOC analyser performance were carried out under laboratory conditions. Calibration of the analyser was performed in regular intervals with various standard amounts. Additional standard injections were performed within each measurement sequence. In general, all measurements were conducted by multiple repetitions (minimum 3 repetitions) of an experiment within one measurement sequence. In case the amount of repetitions exceeded a number of 3, the first analysis performed within the sequence was discarded from the dataset. Therefore, the majority of data that is presented in the following paragraphs was calculated from the average and standard deviation of multiple repetitions of the same experiment.

An evaluation of the NMOC analyser's performance under field conditions was carried out during two consecutive days in August 2003 accompanying the branch enclosure measurements of European beech (*Fagus sylvatica* L.) that are described in detail in chapter 3. For analysis the NMOC analyser was connected to the enclosure system as described above. Samples were collected during day and night time conditions by sampling air alternately from the sample and reference enclosure for a time period of 10 min at flow rates of 300 ml min^{-1} (resulting in a sampling volume 3000 ml). Helium flush volumes of the adsorbent tube were set to 2175 ml at He gas flows of 725 ml min^{-1}.

To grant an efficient oxidation of sampled NMOC compounds, about 6% of ultra pure O_2 were added to the carrier gas flow that was set to flow rates of 100 ml min^{-1}. Measurements of the total NMOC content were performed with a glass adsorbent trap filled with 100 mg Carbograph 1 and 200 mg Carbograph 5 as shown by Figure 4.7.. Calibration of the NMOC analyser was performed directly prior to the measurement period by repeated standard injection. Blank values of the total carbon amount present in the analytical system were measured at the beginning of each measurement sequence. The amount of CO_2 that was collected on the adsorbent cartridges (see Formula 4.1., $Area_{CO2Sample}$) was measured alternately from the sample and reference enclosure directly prior to each total NMOC analysis (see Formula 4.1., $Area_{NMOCSample}$). Blank values of the analytical system (see Formula 4.1., $Area_{NMOCBlank}$) were measured prior to each measurement sequence. All blank values were subtracted from the respective sample area on an average basis.

Measurements of the empty cuvette system were performed by GC-FID analysis and showed no significant bias of the investigated VOC concentrations between the sample and reference enclosure (see chapter 3).

RESULTS

TEMPERATURE DEPENDENCE OF THE DETECTOR RESPONSE

To investigate the temperature dependence of the detector response, the infrared gas analyser was heated and cooled down to temperatures ranging between 20 and 40°C. At each preset temperature, carbon amounts were injected from a CO_2 gas standard by means of a 1 ml calibration loop that was mounted at the calibration valve. After ad- and desorption on the CO_2 adsorption trap, the respective detector response was measured by the chromatographic software. Since the injected carbon amounts varied between 170 and 173 ng (depending on the actual laboratory temperatures), the actual detector response was normalised to the respective amount of carbon, yielding the calibration factor of the NMOC analyser. As shown by Figure 4.9., the calibration factor (and consequently the detector response) increased linearly with increasing detector temperatures up to a maximum of 35°C. At higher detector temperatures no significant increase was observable and the detector response curve followed a saturation trend. According to the results of the latter experiment, a detector temperature of 38°C was set as a default setup of the NMOC analyser. The latter temperature was chosen, as it was located within the range of the saturation trend of the response curve. In this way, small short term variations of the detector temperature resulted in minor variations of the calibration factor. Moreover, the controller unit demonstrated to regulate the preset temperature without major failures indicating that the heat output of the infrared gas analyser generated a sufficient heating effect and that the air flow that was generated by the two small ventilator units (installed at the tempered detector housing) generated an adequate cooling effect.

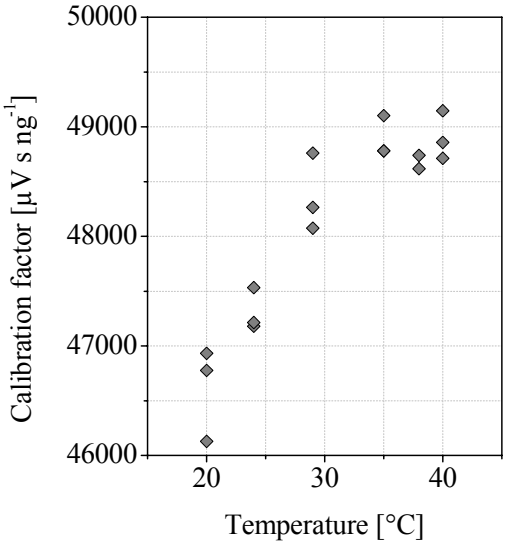

Figure 4.9. Temperature dependence of the detector response. Measurements were performed at detector temperatures of 20, 24, 29, 35, 38, and 40°C. Data show the detector response factors that were achieved with carbon amounts ranging from 170 to 173 ng depending on the respective laboratory temperatures. Carrier gas flow rates were set to 100 ml min^{-1}.

CO_2 ADSORBENT MATERIALS AND COLUMN

For the efficient prefocusing of the CO_2 prior to its detection, two different adsorption materials have been evaluated. On a first approach 4 g of a molecular sieve were chosen as an adsorbent of CO_2. Even though the latter material exhibited a high breakthrough volume for CO_2, it released the sampled CO_2 only at high temperatures (> 200°C). Moreover, the desorption of CO_2 led to broad chromatographic peaks, even if high carrier gas flow rates (up to 1000 ml min^{-1}) were applied. Much better results were achieved by utilisation of 7 g of a modified silica material. As shown by Figure 4.10., the latter material released CO_2 at temperatures of > 125°C (maximum temperature ~200°C). Moreover, the respective chromatographic peak resulted in less peak broadening (peak width ~1 min at 169 ng carbon and 100 ml min^{-1} carrier gas flow rate) than observed for the molecular sieve. Therefore the utilisation of the silica adsorbent material resulted in a much higher detector response given in units of ppm.

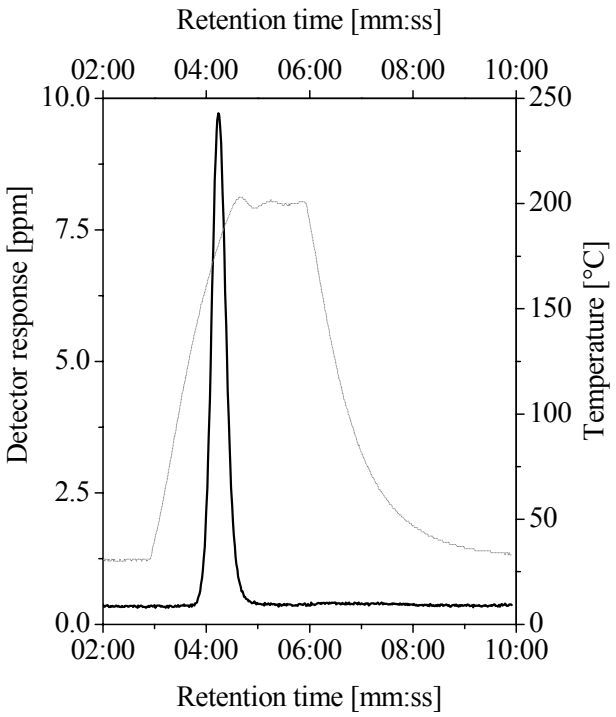

Figure 4.10. Desorption of CO_2 from the silica adsorbent material. The detector response (black solid line) and the temperature profile of the CO_2 adsorbent trap (grey dotted line) were recorded by the controller unit as a function of time. The adsorbent trap was filled with 7 g of modified silica CO_2 adsorbent. The Figure shows the detector response to a carbon amount of 169 ng.

Although the CO_2 breakthrough volume of the silica material was lower than for the molecular sieve, it varied with the amount of sampled CO_2, as well as with the applied carrier gas flow (see Figure 4.11.). Given the default flow rate of 100 ml min^{-1} that was applied for the majority of experiments, breakthrough of sampled CO_2 amounts occurred after 6:44 min (corresponding to 644 ml of carrier gas) if carbon amounts of 169 ng are injected. Injection of

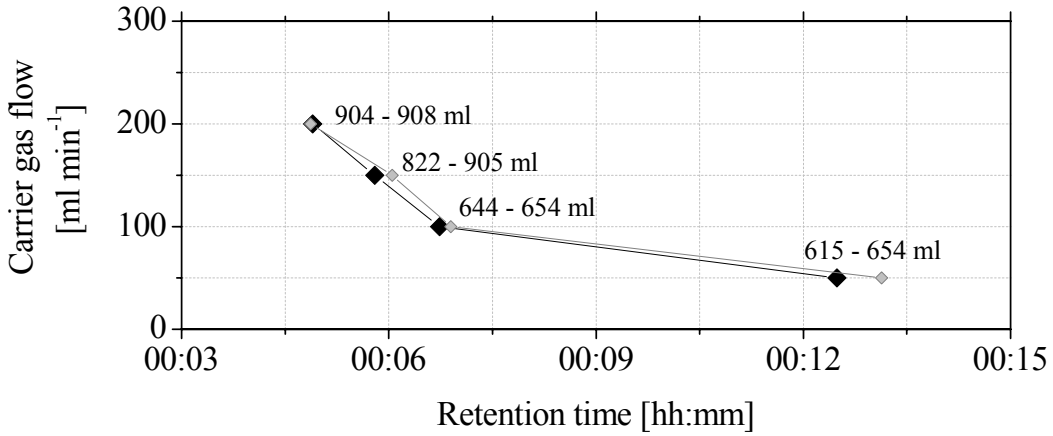

Figure 4.11. Breakthrough of CO_2 as a function of the carrier gas flow rate and carbon amount. Data show the average and standard deviation of 3 repetitive measurements performed at carrier gas flow rates of 50, 100, 150, and 200 ml min^{-1}. The respective breakthrough volumes are indicated in the figure. Carbon amounts were set to 168 - 171 ng (black diamonds) and 84 ng (grey diamonds). If no error bars are visible, they reside within the diameter of the plotted symbol.

lower carbon amounts increased the breakthrough volume only slightly. As shown by Figure 4.11., flow rates of $\leq$ 100 ml min^{-1} resulted in a proportional relationship between breakthrough volume and flow rate, whereas flow rates of $\geq$ 100 ml min^{-1} resulted in a disproportional relation. Consequently, breakthrough times were almost doubled by a reduction of the carrier gas flow from 100 to 50 ml min^{-1}, but were reduced by only ~1/3 if the carrier gas flow was doubled from 100 to 200 ml min^{-1}. These factors have to be taken into account, if different carrier gas flow rates were applied for NMOC analysis.

TOTAL NMOC ANALYSER CALIBRATION

Calibration of the total NMOC analyser was achieved by a CO_2 standard gas mixture (347 ppm CO_2 in synthetic air) that was diluted with helium gas in a calibration loop of 1 ml volume. As specified by the manufacturer of the standard gas mixture the accuracy of the calibration gas was ± 2%, yielding a maximum uncertainty of ± 3 ng (if the pure CO_2 calibration gas standard was injected into the NMOC analyser).

Figure 4.12. gives an overview of a typical calibration that was achieved at carrier gas flow rates of 100 ml min^{-1} (Figure 4.12. A) and 50 ml min^{-1} (Figure 4.12. B). As shown by Figure 4.12., the detector response was directly proportional to the carbon amount that was injected into the NMOC analyser (calibration range 0 to 170 ng carbon, 25 standard injections) and yielded an excellent Pearson product moment correlation coefficient > 0.99. Moreover, these

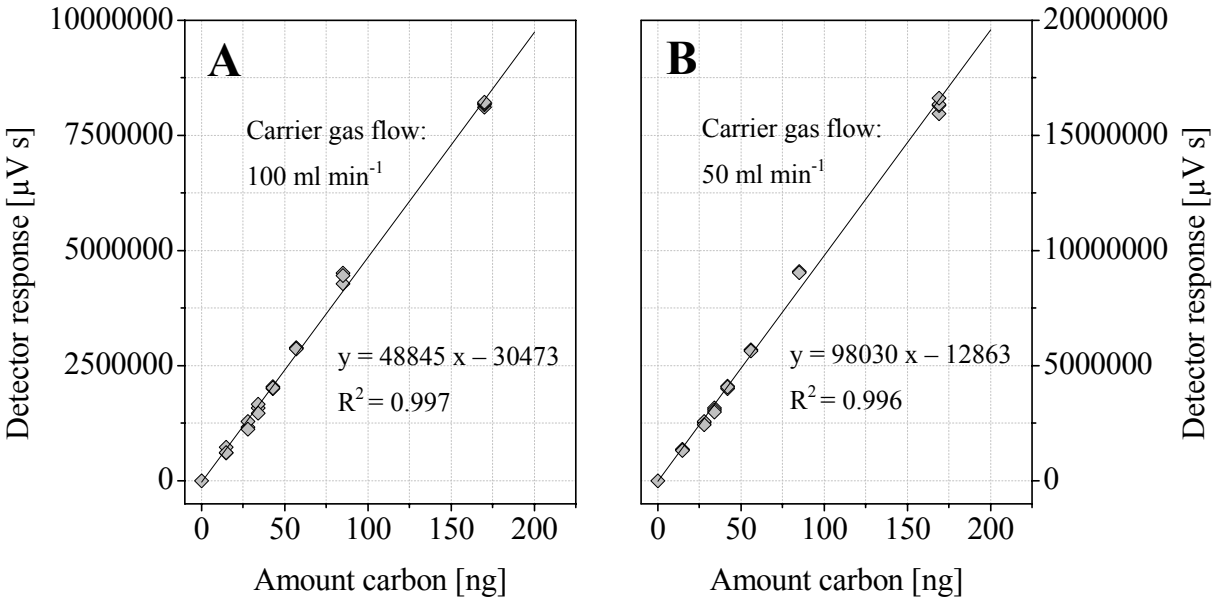

Figure 4.12. Calibration of the NMOC analyser. The calibration was performed with carrier gas flows of 100 ml min^{-1} (A) and 50 ml min^{-1} (B). Standard amount ranged from 0 to 170 ng carbon. The respective function of the linear fit is indicated at each graph. Note the different scales of the detector response measured at both flow rates.

experiments demonstrated that the detector response was directly proportional to the utilised carrier gas flow.

DETECTION LIMIT AND REPRODUCIBILITY

In general, the detection limit is defined as the minimum single result which can be distinguished from a suitable blank value and can be measured from the signal to noise ratio of an instrument. For the present NMOC analyser the detection limit was determined from the carbon blank value of the instrument (see Formula 4.1., $_{AreaNMOCBlank}$). The latter blank value was measured repeatedly (n = 12) at carrier gas flow rates of 100 ml min^{-1} and accounted to 0.1 ng carbon on average. The detection limit was calculated from the decuple of the standard deviation (i.e. the noise ratio) of this average blank value and accounted to 0.5 ng carbon.

The reproducibility of the total NMOC analyser was determined from calibration standards that were injected repeatedly into the system. Calculation of the reproducibility was accomplished according to Formula 2.17.. Using the highest standard amount available (186 ng carbon at 0°C), the reproducibility accounted to ± 0.5%. Lower carbon amounts (17 ng carbon at 0°C) resulted in a lower reproducibility (± 7.3%). In any way the reproducibility measured by peak integration performed with the chromatographic software (E-lab^{TM})

resulted in a better reproducibility than integration of the data that were stored by the external controller device. The latter effect was a result of the higher time resolution achieved by the chromatographic software (20 data points per second). The time resolution of the data stored by the external controller device was set to 1 data point per second, since a higher time resolution would have increased the size of the data files to excess.

OXIDATION EFFICIENCY

The oxidation efficiency of the total NMOC analyser was evaluated by use of two test gas mixtures that were sampled by the 1 ml calibration loop. Each test gas mixture contained either methane (CH_4) or carbon monoxide (CO) in high purity helium gas [1.67 ppm CH_4 (4.5) in He (6.0) and 1.08 ppm CO (4.7) in He (6.0), Messer Griesheim, BRD]. According to the manufacturer specification, the accuracy of both test gas mixtures ranged at ± 2%. Both test gases were injected to the NMOC analyser by repeatedly switching the calibration loop (6 times switching equals to 6 ml test gas volume). Consequently carbon amounts of 5 ng (CH_4) and 3 ng (CO) were injected, corresponding to carbon mixing ratios of 2 ppb (CH_4) and 1 ppb (CO) if typical sampling volumes of 3000 ml were considered.

Oxidation efficiencies for both compounds were calculated according to Formula 4.2., from the average of 3 repeated measurements. The calibration factor was determined directly prior to each measurement sequence from the average of 3 repeated standard injections. The precision of these measurements was calculated according to Formula 4.5. and 4.6..

As shown by Table 4.2. the oxidation efficiency of both compounds ranged at 101 and 91% for methane and carbon monoxide, respectively. The calculated precision of the measured oxidation efficiency exhibited an error of ± 26 and ± 30% and was dominated by the standard deviation that was calculated for the repeated measurements of the test gas mixture.

Table 4.2. Oxidation efficiency of the NMOC analyser for two test gas mixtures containing methane and carbon monoxide, n = 3.

Test gas mixture	Specified carbon amount [ng]	Specified accuracy [ng]	Oxidation efficiency [%]	Precision of oxidation efficiency [%]
Methane (CH_4)	4.9	± 0.1	101	± 26
Carbon monoxide (CO)	3.1	± 0.1	91	± 30

SAMPLING EFFICIENCY (RECOVERY)

Sampling efficiencies of the NMOC adsorption trap that was mounted in the NMOC solid adsorbent unit were performed using several test gas mixtures. On a first approach the sampling efficiencies (i.e. the recovery) of CO_2 and its potential separation from the NMOC fraction were tested for several adsorbent types and adsorbent amounts. In a later approach sampling efficiencies were also tested for other test gas mixtures.

CO_2 sampling efficiency

Variable amounts of the CO_2 standard gas mixture (347 ppm CO_2 in synthetic air) were sampled in glass tubes (6 mm OD, 240 mm length) mounted in the NMOC solid adsorbent unit. The glass tubes were either empty, or filled with 100 mg Carbograph 1, 100 mg Carbograph 5, or 200 mg Carbograph 5. Sampling of CO_2 was performed at flow rates adjusted to 100, 200 or 300 ml min^{-1}, but previous experiments showed that these different sampling flow rates did not influence the sampling efficiency of the test gas. To equilibrate the sampling tubings with the test gas mixture, all tubings were flushed with the standard gas prior to the sampling step. Sampling volumes of the standard gas were set to 50, 100, 200, 500, 1000, and 3000 ml. To remove excessive standard gas from the dead volumes of the inlet tubings and sampling valves, the adsorption trap was flushed with ultra pure helium gas after the preconcentration step. The flush volumes were set at the controller unit to 0.5, 1, 2, and 4 x the CO_2 sampling volume. Since the thermal conductivity of He gas differed from that of CO_2 and ambient air, these flush rates had to be multiplied by the respective gas correction factor specified by the manufacturer of the applied flow controller units (correction factor He= 1.45, MKS Instruments, USA). Consequently corrected flush volumes of 0.73, 1.45, 2.90, and 5.8 x the CO_2 sampling volume were applied. To disable any interference of volatile organics that might be present in the standard gas, all CO_2 samples bypassed the oxidation tube.

Figure 4.13. shows the results of the respective experiments. As shown for all different flush volumes that were observed, the CO_2 sampling efficiency followed a clear inverse hyperbolic trend, yielding lower CO_2 sample efficiencies at higher sampling volumes. Considering the different adsorption materials tested, Carbograph 1 was shown to be the strongest adsorbent for CO_2 with efficiencies ranging < 0.255%. Better results were obtained for Carbograph 5. With the latter adsorbent no significant differences to the empty glass tube were detectable, and sample efficiencies ranged < 0.228%.

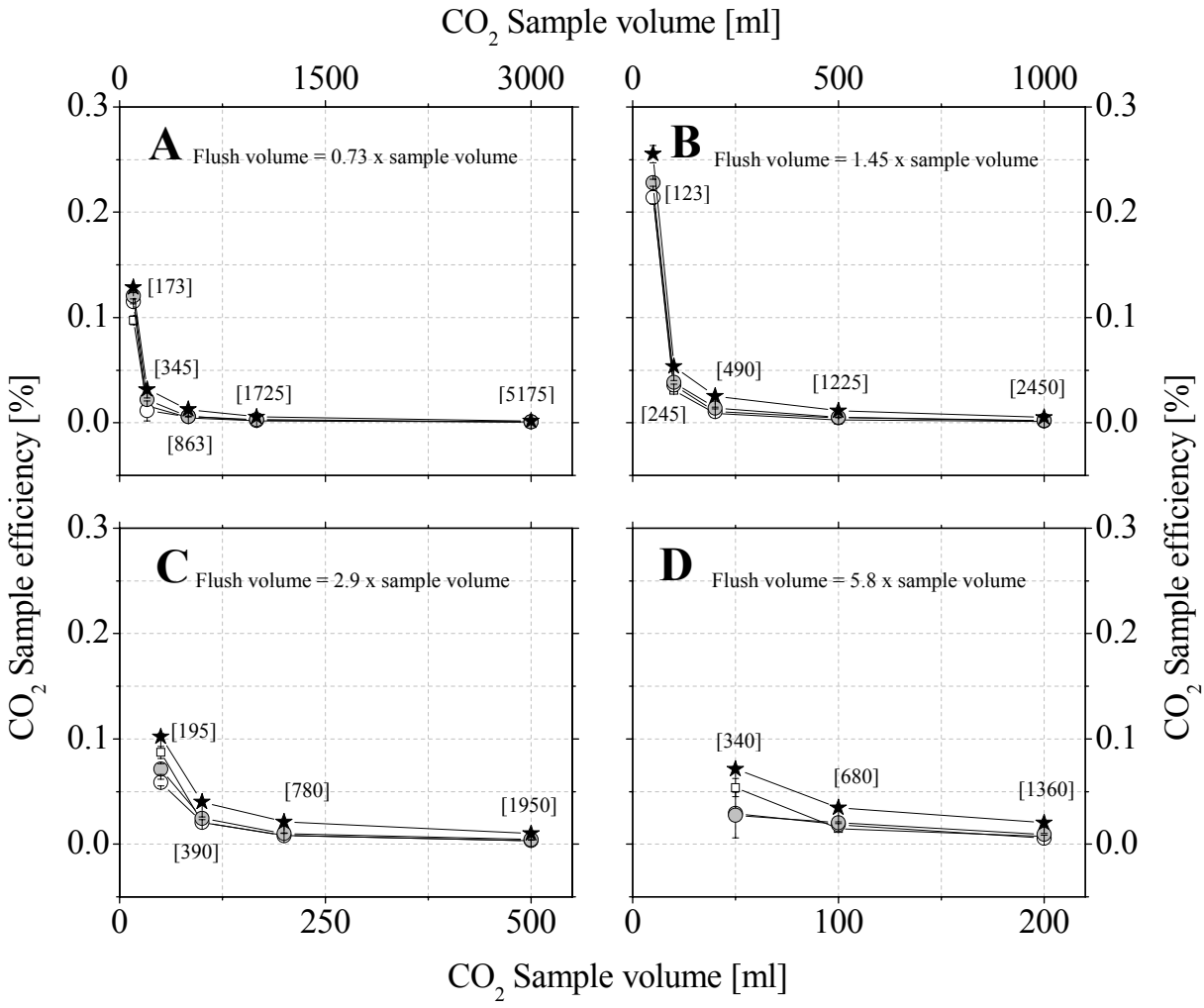

Figure 4.13. Sampling efficiency of CO_2. Carbon samples derived from the CO_2 standard gas mixture were collected on the adsorbent trap with sampling volumes ranging between 50 and 3000 ml. Flush volumes were set to 0.73 x sample volume (A), 1.45 x sample volume (B), 2.90 x sample volume (C), and 5.80 x sample volume (D). Total sampling volumes (i.e. CO_2 sampling volume + flush volume) were indicated in units of ml in the respective graph in parenthesis. Experiments were performed with empty glass tubes (hollow squares, n=3), with 100 mg Carbograph 5 (hollow circles, n=3), 200 mg Carbograph 5 (grey circles, n=3), and 100 mg Carbograph 1 (black stars, n=3). Please note the different scales of each graph.

As shown by Figure 4.13., good results for the desired low sampling efficiency of CO_2 were obtained by application of total sampling volumes (i.e. CO_2 sampling volume + flush volume) of > 1000 ml. On the other hand sampling volumes of ≤ 100 ml resulted in poor results. To obtain an optimum proportion between high CO_2 sampling and low flush volumes, the application of CO_2 sampling volumes of > 1000 ml, combined with a flush volume of 0.73 x this sampling volume is recommended. Given e.g. a sampling volume of 3000 ml the latter approach would result in a sampling efficiency of 0.003% for an adsorbent amount of 200 mg

Carbograph 5, yielding an expected carbon amount of 17 ng at typical CO_2 mixing ratios of 350 ppm. Considering carbon mixing ratios of about 100 ppb, the latter CO_2 blank would account up to 11% of the sampled carbon amount. However, at low carbon mixing ratios the fraction of the CO_2 blank value to the sum of total carbon collected on the adsorbent cartridge may reach substantial values.

Sampling efficiencies of other compounds

Sampling efficiencies of CO_2, CH_4, CO, and NMOCs were tested using a glass adsorbent trap (O.D. 6mm, 240 mm length) filled with 100 mg Carbograph 1 and 200 mg Carbograph 5 as shown by Figure 4.7.. Sampling volumes of the respective test gas mixtures (347 ppm CO_2 in synthetic air, 1.67 ppm CH_4 in He, and 1.08 ppm CO in He, Messer Griesheim, Germany, and 700 ppb NMOC (n-pentane, n-hexane, n-heptane, n-nonane, n-decane, isoprene) in synthetic air, Apel Riemer, USA) were collected for 10 min using a sampling flow rate of 300 ml min^{-1}, resulting in a sampling volume of 3000 ml. Flush volumes were set to 2175 ml of He, yielding a total sampling volume of 5175 ml (see Figure 4.13. A, flush volume = 0.73 x sample volume). He flow rates were set to 300 ml min^{-1}. Table 4.3. gives an overview of the sampling efficiencies that were recorded for the different test gas mixtures. Sampling efficiencies for CO, CO_2, and CH_4 were negligible, indicating the feasible separation of these compounds from the NMOC fraction. Sampling efficiencies of the NMOC standard resulted in poor results of only 8% recovery. By addition of 30% pure oxygen to the carrier gas stream a significant improvement of the recovery rates was obtained. However, the best achieved sampling efficiency for NMOC compounds ranged only at 48%.

Table 4.3. Sampling efficiencies of different test gas mixtures. Annotation: [1] Analysed with pure He carrier gas, [2] Analysed with addition of about 30% oxygen, [3] laboratory experiment, [4] field experiment.

Test gas mixture	Specified carbon amount [ng]	Specified accuracy [%]	Detected amount [ng]	Sampling efficiency [%]
Carbon dioxide (CO_2) [1,3]	557841	± 2	42	0.008
Carbon dioxide (CO_2) [1,4]	< 757185	Not specified	< 30	< 0.005
Methane (CH_4) [1,3]	2685	± 2	2	0.076
Carbon monoxide (CO) [1,3]	1736	± 2	2	0.115
NMOC [1,3]	1125	Not specified	87	8
NMOC [2,3]	1125	Not specified	540	48

BRANCH ENCLOSURE MEASUREMENTS

Branch enclosure measurements of European beech (*Fagus sylvatica* L.) were carried out in August 2003 during two consecutive days accompanying the GC-FID and GC-MS measurements that are described in detail in chapter 3. As shown by Figure 4.14. D and E, micrometeorological and plant physiological parameters yielded pronounced diurnal courses of photosynthetic active radiation, photosynthesis and transpiration, indicating that the branch was in good physiological conditions.

Analysis of the CO_2 amounts that were sampled on the adsorbent trap prior to each NMOC measurement did not show any significant bias between samples that were collected from the reference or branch enclosure. CO_2 amounts sampled on the adsorbent trap ranged between 16 and 30 ng, corresponding to a fraction of 8 - 28% of the sampled NMOC amount. According to the high total sampling volume that was applied (3000 ml sample volume + 2175 ml flush volume) CO_2 sampling efficiencies ranged < 0.005%. To facilitate the oxidation of volatiles, 6% ultra pure O_2 was added to the carrier gas stream. Carbon amounts measured in the reference and sample enclosure by the total NMOC analyser reached up to 396 ng if the low sampling efficiency of different NMOC compounds (48%, see above) is considered as a correction factor. The latter carbon amount corresponds to a maximum carbon mixing ratio of 266 ppb (reference cuvette). However, typical carbon mixing ratios ranged between 53 and 132 ppb for the reference, and 48 and 211 ppb for the sample enclosure (see Figure 4.14. B and C).

Comparison of these mixing ratios to the accompanying GC-FID measurements (carbon mixing ratios were calculated from the sum of 20 analysed compounds: i.e. n-pentane, n-hexane, n-heptane, n-octane, n-nonane, n-decane, isoprene, camphene, Δ-3-carene, p-cymene, limonene, myrcene, α-pinene, β-pinene, sabinene, α-terpinene, γ-terpinene, benzene, toluene, o-xylene) yielded only a reasonable agreement, both in qualitative and quantitative considerations. As shown by Figure 4.14. B and C, the total NMOC mixing ratios measured in the reference and sample enclosure reached always higher concentrations than the summarised GC-FID measurements. However, this should be not surprising, since the summarised GC-FID results might represent only the lower limit of the actual carbon concentration as some yet unidentified compounds might be missing from the GC-analysis.

Unlike the carbon mixing ratios, the carbon exchange rates (that were calculated from the concentration difference measured in both enclosures) measured by the NMOC analyser followed closely the same diurnal courses that were observed for the summarised GC-FID exchange rates. Moreover, these exchange rates agreed quantitatively with each other. Maxi-

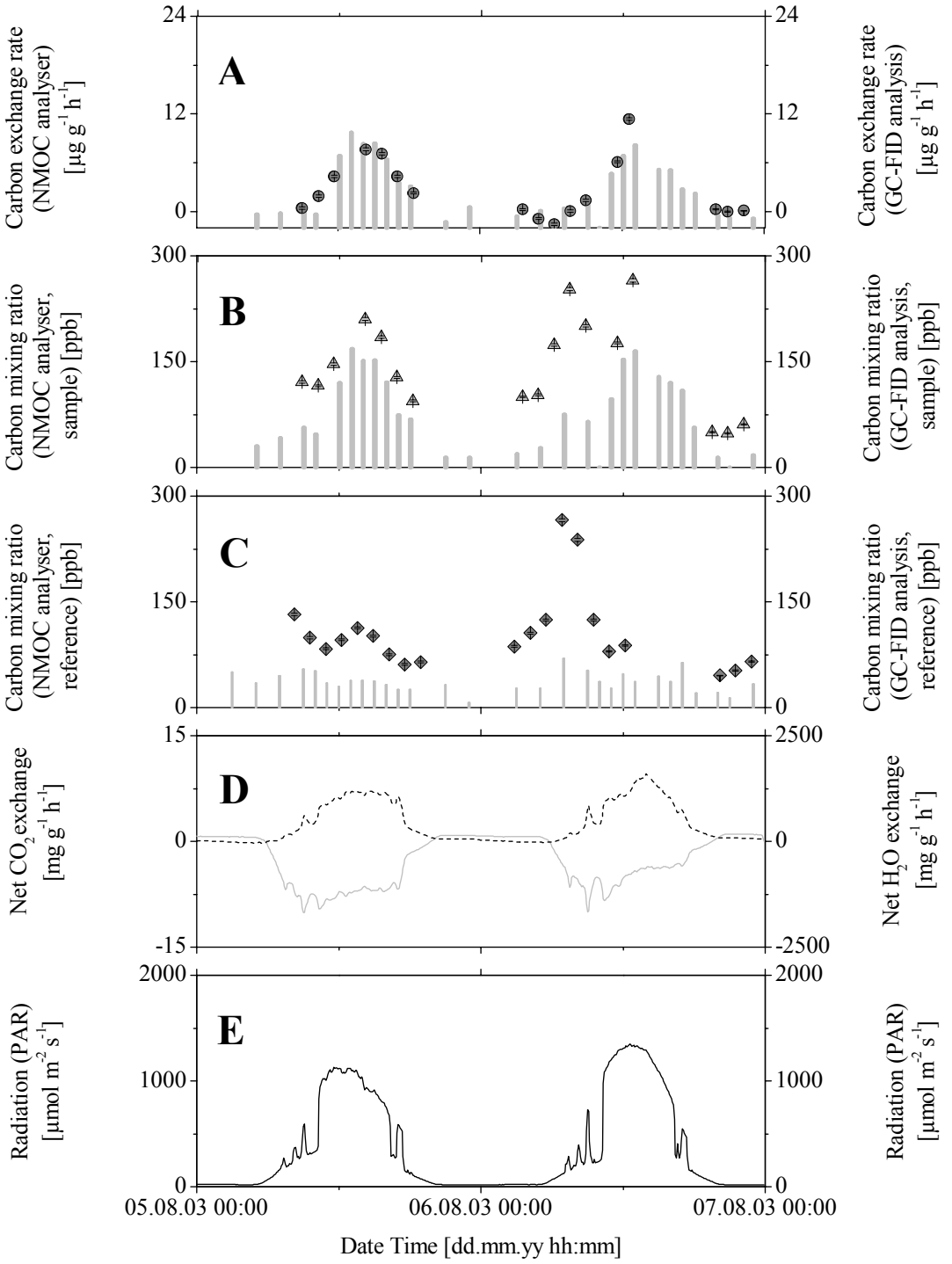

Figure 4.14. Enclosure measurements performed on European beech with the NMOC analyser in August 2003. (A) NMOC exchange of *Fagus sylvatica* L.. NMOC exchange measured by total NMOC analysis is indicated by grey circles and its calculated error by the black error bars. NMOC exchange measured by GC-FID analysis is indicated by the grey bars. (B) Carbon mixing ratios measured in the sample enclosure by total NMOC analysis (grey triangles and error bars) and by GC-FID analysis (grey bars). (C) Carbon mixing ratios measured in the reference enclosure by total NMOC analysis (grey diamonds and error bars) and by GC-FID analysis (grey bars). (D) Photosynthesis (grey solid line) and transpiration (black dashed line) of European beech. (E) Course of photosynthetic active radiation (black solid line) during the respective measurement days.

mum exchange rates measured by the total NMOC analyser reached values of 11 µg g^{-1} h^{-1}, while carbon exchange rates measured by GC-FID analysis accounted to 10 µg g^{-1} h^{-1}. According to the GC-FID analysis, monoterpenes were shown to be the predominant carbon species released from European beech.

DISCUSSION

GENERAL SETUP AND DESIGN OF THE TOTAL NMOC ANALYSER

Dynamic cuvette air samples obtained from enclosed plants are characterised by high, but variable concentrations of NMOC compounds and water vapour. Considering the typical monoterpene emission data for European beech (see chapter 3, average standard emission factor of 15 µg g^{-1} h^{-1}, cuvette flow rates of 35 l min^{-1}, and a leaf dry weight of 10 g) carbon mixing ratios of 118 ppb are expected at standard conditions of 1000 µmol m^{-2} s^{-1} and 25°C. By also considering the additional introduction of background VOC concentrations in ambient air, carbon mixing ratios may even exceed this range.

This way, the high NMOC mixing ratios that can be found in a plant enclosure enable the utilisation of detection systems with low sensitivity such as infrared gas analysis. Even though the latter method is less sensitive than FID detection, yielding detection limits in the range of 200 ppb in the default "flow through" setup (see detector manual, Li 6262, Li-COR, USA), the detection limit of the applied NMOC analyser was much smaller, yielding detection limits of 0.5 ng carbon or 311 ppt (at typical sampling volumes of 3000 ml). The increase in sensitivity compared to the default "flow through" setup, was attributed to the second preconcentration step (i.e. ad/desorption of CO_2) that was applied in the present NMOC analyser. The latter preconcentration step led to a detector signal of > 9 ppm CO_2 in response to the injection of 169 ng carbon (see Figure 4.10.). In comparison, detection limits of GC-FID analysis were only about 2-fold smaller (detection limit of 30 ppt isoprene = 150 ppt carbon, see Kuhn *et al.* 2002b).

As described in detail in chapter 2, preconcentration on solid adsorbents followed by gas chromatographic separation and flame ionisation detection, is still the most versatile and well accepted method for measuring volatile organics. Also the total NMOC analyser setup described by Roberts *et al.* (1998) and Maris *et al.* (2003) comprised NMOC detection by FID. Consequently their setup included two NMOC conversion steps (first: oxidation to CO_2 to guarantee an equal per carbon response of different NMOC compounds and second: conversion to CH_4 since the FID detector is insensitive to the previously formed CO_2).

Application of an infrared gas analyser as performed by the present setup enabled the utilisation of only one NMOC conversion step and therefore minimised the risk of a decreased recovery of NMOC compounds that is associated with every conversion step. Moreover, Roberts *et al.* (1998) and Maris *et al.* (2003) reported, that FID detection interfered with variable amounts of water vapour that were present in the ambient air. This sensitivity would provide major interferences applying plant enclosures, due to the high amounts of water vapour that are emitted by the investigated organisms.

For the present NMOC analyser, the sampling of volatile organics was performed in analogy to the experiments performed by Maris *et al.* (2003) who applied the sampling and preseparation of NMOCs from CO, CO_2, and CH_4 within one combined step. However, the high relative humidity that is present in a plant enclosure limited also the utilisation of a cryogenic trapping step as performed by the latter authors. Therefore, sampling of volatiles was achieved by utilisation of graphitised carbon blacks as performed for the GC-FID analysis within the framework of the ECHO project (see Chapter 2 and 3). Due to the hydrophobic character of the latter adsorbents, clogging of the sampling unit by small ice particles was prevented. Moreover, the latter adsorbents were characterised as non-specific and therefore guaranteed the collection of a wide variety of NMOC compounds. Due to their specific adsorption characteristics (for a detailed description, see chapter 2) they adsorbed volatile organics as a function of molecular weight and structure. Therefore, low molecular weight compounds like CO, CO_2, and CH_4 were only collected at small amounts and preseparation of the latter compounds from the NMOC fraction was achieved. However, the applied setup holds the risk of loosing other low molecular weight organics as well, such as the widely emitted compound methanol.

CALIBRATION, DETECTION LIMIT, AND REPRODUCIBILITY

As reported in detail by Slemr *et al.* (2002), the different behaviour of various hydrocarbons within an analytical system is a common error source in NMOC gas analysis. Therefore, the latter authors reported an improved performance of VOC analysis performed by GC-FID and GC-MS by utilisation of a multicomponent gas standard. However, for the application of a total carbon analysis the latter technique is not recommendable since the manifoldness of different NMOC compounds analysed by the present setup could not be displayed by a single multicomponent gas standard. Nevertheless, the carbon recovery of VOC mixtures was investigated (see above). In analogy to the experiments performed by Maris *et al.* (2003) who referred to a n-hexane gas standard, the calibration of the present NMOC analyser was

performed by utilisation of CO_2 calibration gas that was diluted with variable amounts of ultra pure He. CO_2 was chosen as a reference for the present setup, since all carbon compounds were finally detected in form of CO_2 by an infrared gas analyser. Moreover adsorption and outgassing effects are negligible for the CO_2 reference. Therefore, the calculated calibration factors do not account for errors that may be introduced e.g. by a reduced recovery of the standard compound. This way, adsorption and/or desorption effects of different volatile organics can be identified within the analytical system. A further advantage of the utilisation of a CO_2 reference gas for the calibration of the total NMOC analyser is its extreme inertness and stability in comparison to the analysed NMOC compounds. Therefore storage of the calibration gas cylinders (concentration at ppm range) can be maintained for several years.

The detection limit of the present NMOC analyser accounted to carbon amounts of 0.5 ng (corresponding to carbon mixing ratios of 311 ppt at typical sampling volumes of 3000 ml) and was only 2-fold smaller than detection limits observed for GC-FID analysis (Kuhn *et al.* 2002b). The latter effect was attributed to the second preconcentration step of the present analyser setup that led to an extreme increase of the detector response. Small background concentrations of the purified He carrier gas ensured detection limits that were about 10 to 100-fold smaller than the detection limits reported previously for other total NMOC instruments (Roberts *et al.* 1998; Maris *et al.* 2003).

The observed different reproducibility of the NMOC analyser in response to variable carbon amounts (± 0.5% at 186 ng carbon and ± 7.3% at 17 ng carbon) may indicate an increasing influence of carbon background concentrations to the accurate integration of the chromatographic peaks. Moreover the observed different reproducibility measured by the two investigated data acquisition systems (integration performed by the external controller unit or by the chromatographic software E-Lab^{TM}) revealed the superiority of the chromatographic software applying a maximum of 20 integration steps per second. Application of chromatographic software capable to perform even more integration steps per second, may even improve the actual reproducibility of the NMOC instrument.

OXIDATION EFFICIENCY

According to Ehrenberger (1991) CuO is still the most reliable oxidation catalyst for the quantitative determination of carbon. Due to its high activity, stability, and availability it has been widely used as an oxidation/reduction catalyst (Bauer *et al.* 1993; Wang *et al.* 2004). Also for the present setup CuO was utilised as a catalyst for the oxidation of volatile organics. The oxidation efficiency of the NMOC analyser was investigated by direct injection of two

test gas mixtures to the NMOC instrument. On a first approach the oxidation efficiency of CuO was tested by injection of 4.9 ng carbon in form of CH_4, yielding an excellent oxidation efficiency of 101 ± 26%. A second approach investigating the oxidation efficiency of CuO by injection of 3.1 ng carbon in form of CO resulted in lower efficiencies of 91 ± 30%.

According to Roberts *et al.* (1998), CH_4 is thermodynamically the most difficult reduced carbon species to be converted to carbon dioxide. Consequently, the latter authors observed methane oxidation efficiencies of > 98% by utilisation of a Pd/Alumina catalyst (kept at 350°C), while C_2-hydrocarbons were converted at efficiencies of 100%. Following this observations, the reduced recovery observed during the present study for the CO test gas mixture, may also result from the low carbon amounts that were applied and must therefore not necessarily point to a reduction of oxidation efficiencies. However, all observed oxidation efficiencies are still within an acceptable range, but experiments injecting higher carbon amounts to the NMOC instrument are strongly encouraged.

SAMPLING EFFICIENCY (RECOVERY)

Unwished carbon containing compounds dominating in the air samples may significantly influence the measured NMOCs. Therefore, CO, CO_2 and CH_4 test gas mixtures were investigated. Experiments evaluating the sample efficiency (recovery) of these compounds on the applied adsorbent traps demonstrated that they were collected only at small amounts. Given the default instrument setup (adsorbent trap filled with 100 mg Carbograph 1 and 200 mg Carbograph 5, sample volumes of 3000 ml and flush volumes of 2175 ml He), CO_2 sample efficiencies were specified to range between 0.008 and 0.005% for the laboratory and field experiments, respectively. CO and CH_4 sample efficiencies ranged at 0.115 and 0.076%. According to these tests, the present NMOC analyser provided better results regarding the CO_2 sampling efficiency than the NMOC instrument evaluated by Maris *et al.* (2003), who reported CO_2 sampling efficiencies of 0.01 - 0.05%.

In general the low sampling efficiencies of CO, CO_2, and CH_4 observed for the present adsorbent trap were attributed to the special characteristics of the applied graphitised carbon blacks (Carbograph 1 and 5). As described in chapter 2 and reported in detail by Brancaleoni *et al.* (1999), these materials are hydrophobic adsorbents that interact non-specifically with all groups of adsorbates. As demonstrated by the latter author, a combination of Carbograph 5 with lighter adsorbents allowed the sampling of volatile organics with $C_n > 3$ at safe sampling volumes of > 5000 ml. Table 4.4. gives an overview of the safe sampling volumes of

Carbograph 1 and 5 that were specified by the latter authors for several hydrocarbon compounds.

Table 4.4. Safe sampling volumes of various hydrocarbons on Carbograph 1 and Carbograph 5. Adapted from Brancaleoni *et al.* (1999).

Compound	Safe sampling volume of Carbograph 5 (230 mg) [ml]	Safe sampling volume of Carbograph 1 (119 mg) [ml]
Ethane	< 100	< 100
Ethene	< 100	< 100
Propane	200	< 100
Propene	200	< 100
Isobutane	> 5000	< 100
n-butane	> 5000	< 100
Trans-2-butene	> 5000	< 100
1-butene	> 5000	< 100
Cis-2-butene	> 5000	< 100
Isopentane	> 10000	100
n-pentane	> 10000	200
Trans-2-pentene	> 10000	< 100
1-pentene	> 10000	< 100
Cis-2-pentene	> 10000	< 100
n-hexane	> 10000	> 5000
1-hexane	> 10000	> 5000
n-heptane	> 10000	> 5000
Benzene	> 10000	2000

According to the results obtained by the present study and the experiments performed by Brancaleoni *et al.* (1999), discrimination of NMOCs ($C_n > 3$) from CO, CO_2, and CH_4 can be achieved by utilisation of an adsorbent trap consisting of 100 mg Carbograph 1 and 200 mg Carbograph 5. However, sampling of hydrocarbons with $C_n < 3$ is not recommended, since the application of sampling volumes < 100 ml (to prevent breakthrough of volatile organics) would result in relatively high sampling efficiencies of CO_2, yielding a severe interference with the collected hydrocarbons. However, the evaluation of the hydrocarbon (isoprene + alkanes) recoveries using the setup of the present study resulted in sampling efficiencies of only 8%, although the oxidation efficiencies of CO and CH_4 yielded in good results. Addition of oxygen increased the observed recovery to 48%, and is therefore imperative for effective

operation of the NMOC analyser. However, hydrocarbon recoveries are still not sufficient and have to be improved. As reported in detail by O'Malley and Hodnett (1999) who observed the influence of the VOC structure on the oxidation efficiency of Pd catalysts, alkanes were shown to be less reactive than other organic compounds. Thus, increasing the amount of added oxygen for the present setup may lead to enhanced oxidation efficiencies and may improve the results obtained for the NMOC instrument. Moreover, adsorption effects within the analytical system have to be taken into account. An incomplete desorption process may also explain the reduced recovery of the NMOC test gas mixture.

PLANT ENCLOSURE MEASUREMENTS

Cuvette experiments were performed during two days in August 2003 investigating an enclosed branch of European beech (*Fagus sylvatica* L.). Samples were collected consecutively from the reference and branch enclosure and were accompanied by GC-FID measurements. Although the CO_2 amounts collected by the NMOC analyser accounted only up to 0.005% of the actual atmospheric CO_2 concentrations, they still constituted a fraction of up to 28% of the atmospheric carbon collected in form of NMOCs. However, similar interferences of ambient CO_2 concentrations were also reported by other authors (Roberts *et al.* 1998). In contrast, sampling efficiencies of CO and CH_4 resulted only in negligible carbon amounts for the present setup.

Comparison of the carbon concentrations measured from the reference and branch enclosure by total NMOC- and GC-FID analysis resulted in reasonable agreement of both datasets and differed (with exception of the first measurement day at the branch enclosure) by a factor of about two, indicating, that some yet unidentified compounds might be missing from the GC-analysis. According to the location of the measurement site which was situated in a small deciduous forest stand, NMOC concentrations measured from the reference enclosure (which represents the ambient conditions in a first approximation) exhibited high NMOC concentrations during midday, revealing the dominant impact of light dependent carbon emissions that originated from the surrounding tree species. Highest NMOC mixing ratios were observed during the second measurement day, with maximum concentrations of 266 ppb. However, typical carbon mixing ratios ranged between 53 and 132 ppb and were comparable to carbon concentrations that were reported by Roberts *et al.* (1998) for a remote measurement site. However, for urban sites the latter authors reported carbon concentrations of several hundreds of ppb, and Maris *et al.* (2003) reported even higher ambient carbon mixing ratios for the SCAQMD station at Pico Rivera (CA) ranging from several hundreds of

ppb up to 3.8 ppm. Considering the exchange of carbon compounds by European beech, the measurements performed with the total NMOC instrument and by GC-FID analysis are in perfect agreement, yielding exchange rates of up to 11 and 10 μg g^{-1} h^{-1}, respectively. This excellent agreement was moreover confirmed by the pronounced diurnal cycle of carbon exchange rates observed by both analytical techniques.

The good agreement between both strategies, combined with the dominating role of monoterpene emission discovered by the GC-FID analysis, indicates that carbon compounds other that monoterpenes were emitted only at low amounts from the investigated tree species. Moreover, deposition rates may be negligible regarding the total exchange of carbon from European beech. However, extensive laboratory and field experiments are needed to confirm these first measurements applying a total NMOC analyser during a branch enclosure study.

FURTHER IMPROVEMENT OF THE TOTAL NMOC ANALYSER

The NMOC analyser was shown to be operational under laboratory and field conditions performing plant enclosure measurements, but several functions may still be improved. Probably the most important improvement needed for the NMOC analyser, is the enhancement of the NMOC recovery. Therefore, more oxygen should be added to the oxidation catalyst in a default setup.

Moreover, a better recovery may in part be achieved by an extended desorption time of the NMOC adsorbent trap. Typical desorption times applied at present for the NMOC adsorption trap were set to a maximum of 4 minutes. Longer desorption times could not be applied by the present NMOC analyser setup, because they were limited by the break through volume of the CO_2 adsorption unit. To increase the desorption time of the NMOC adsorption unit, a new CO_2 adsorbent trap has to be manufactured, being able to comprise more than 7 g of silica adsorbent (which was the maximum fill-up quantity of the present setup). Further improvement may be also be achieved by a reduction of the carrier gas flow, since lower flow rates:

(i) would enable a longer contact time between the NMOC compounds and the oxidant (CuO) and would therefore increase the oxidation efficiency and

(ii) would lead to less dilution and hence an increase of the detector signal in response to a certain amount of carbon.

Also the dead volumes of the NMOC analyser should be reduced to a minimum. The latter

can be achieved by utilisation of tubing and valves with a decreased inner and outer diameter. Moreover, the dead volumes of the NMOC adsorption trap and the oxidation tube should be reduced, minimising also the actual size of the NMOC instrument. Further enhancement of the recovery of NMOC compounds could also be achieved by application of a Silicosteel® treatment [offered by Restek, USA] for the analyser valves and connector units.

Application of a second adsorption trap within the NMOC adsorption unit would double the instruments sample capacity, since desorption and analysis of an ambient air sample could be performed while collecting a subsequent sample on the second adsorbent trap. Furthermore it would allow simultaneous sampling from two sources, such as the plant and reference cuvette. This would increase the reliability of exchange data by avoiding difference calculations from air samples potentially influenced by concentration changes over time. To prevent the migration of adsorbent materials within the adsorbent glass tube, utilisation of glass tubes comprising a smaller inner diameter at their endings is recommended.

Further enhancements would also comprise the application of a thermocouple to measure the calibration temperature directly at the calibration loop, as well as the application of a tempered housing to accommodate the calibration (and sample) valve. Utilisation of thermocouples that are insensitive to voltage and power fluctuations would lead to more accurate temperature measurement at the solid adsorbent trap heating coil. A graphic user interface generating a remote control of the NMOC analyser would be desirable as well.

CONCLUSION

The experiments of the present study demonstrated that the total NMOC analyser provided good results for the performance of plant enclosure measurements, yielding an excellent agreement with other analytical techniques with respect to the qualitative and quantitative analysis of exchange rates. However, the quantitative analysis of NMOC measurements has still to be improved and recovery rates of other volatile organic molecules have to be investigated. Sample efficiencies of CO and CH_4 impurities were shown to be negligible. Sample efficiencies of CO_2 impurities were smaller than discovered for other total NMOC instruments, but still accounted up to 28% of the sampled NMOCs at low concentration ranges. Although the instrument needs further improvement and evaluation with regard to the recovery of several NMOC compounds, the results obtained by the present study are very promising. Applying the total NMOC analyser on a default setup for enclosure studies would enable a most comfortable and easy on-line monitoring of exchange processes between plants

and the atmosphere. Moreover, the simple data analysis enables a rapid evaluation of exchange processes.

SUMMARY

The present dissertation focused on the measurement of non methane organic carbon compounds and their exchange through biosphere-atmosphere interactions. To date, the analysis of biogenic volatiles is a complex task in terms of qualitative and quantitative aspects, and a great variety of analytical techniques has been developed in the past. To access the accuracy, precision, and reproducibility of conventional VOC analysis, a series of two intensive intercomparison experiments with 7 participating institutes was carried out during the present study. These experiments comprised the evaluation of two different analytical techniques:

(i) sampling of volatile organics on graphitised carbon blacks, followed by thermal desorption and analysis by gas chromatography coupled to flame ionisation detection, and

(ii) sampling of short chain carbonyls on two different solid phase extraction cartridges coated with 2,4-dinitrophenylhydrazine (DNPH) and analysis by high pressure liquid chromatography.

The application of syringe injections of liquid standard compounds for the calibration of the gas chromatographic analysis generated major problems for an accurate quantification of the respective volatile organics. Improved accuracy was obtained by utilisation of a gaseous calibration standard. Utilisation of the latter standard generated best results for the investigated monoterpene compounds α-pinene and 3-carene resulting in an underestimation of up to 12% for α-pinene and of 3 to 20% for 3-carene with respect to the specified reference. The accuracy of isoprene measurements exhibited a higher variability ranging between an underestimation of 35% and an overestimation of 32%. However, with exception of α-pinene, its reproducibility was better than for the monoterpene compounds. In general no dependency between the specified compound concentration and the measured accuracy was observed within the range of evaluated concentrations (i.e. 0.2 to 31 ppb). Tests, evaluating the performance of a particular ozone scrubber assembly demonstrated that neither adsorption nor desorption effects were detectable for isoprene and β-pinene.

For the measurement of short chain carbonyl compounds, two different solid phase extraction cartridges were evaluated. While the first system was based on an octadecyl carrier material, the other system was based on a pure silica carrier material. Both carrier materials were coated with DNPH either by the MPI laboratory (octadecyl carrier), or by the manufacturer (silica carrier). Best agreement with the reference concentrations was achieved by utilisation of the silica-DNPH cartridges. With the latter samples acetaldehyde was overestimated by 7% and acetone was underestimated by 3%.

The assessment of these quality assurance data is particular crucial for the evaluation of biosphere-atmosphere exchange processes. To date, conventional estimates that consider the emission of volatile organics on global scales, integrate emission factors only on an ecosystem level. Within this context, plant enclosure studies were performed on sunlit leaves of English oak as well as on sunlit and shaded leaves of European beech during two consecutive field experiments in the summers of 2002 and 2003. English oak was characterised being a strong emitter of isoprene, releasing the latter compound as a function of light and temperature. Basal emission rates, calculated by application of the G97 algorithm, reached 75 $\mu g\ g^{-1}\ h^{-1}$. In contrast, European beech was characterised as a monoterpene emitter, with sabinene being the predominant compound released. Moreover, monoterpene emission from European beech was demonstrated to be a function of light and temperature. Basal emission rates measured from sunlit leaves of European beech ranged up to values of 13 $\mu g\ g^{-1}\ h^{-1}$. Even though shaded leaves revealed low emission rates with respect to the instantaneous microclimatic conditions of their environment, the normalisation to standard light and temperature conditions resulted in a high emission potential of 20 $\mu g\ g^{-1}\ h^{-1}$. During high ambient temperature periods a midday depression of monoterpene emission was observed for one measurement day in June 2002. According to its broad geographical distribution and its substantial basal emission rate, specific consideration of European beech demonstrated a substantial impact on the European monoterpene budget, yielding increases of 16 to 54% relative to conventional inventories. On a local scale, increases of monoterpene emission exceeded 100%.

To date, all studies investigating the biosphere-atmosphere exchange of volatile organics, focussed only on the detection of a limited number of NMOC compounds. Measurements of the total NMOC exchange between vegetation and the atmosphere are not reported hitherto and only very few studies reported on total NMOC concentration measurements in ambient air. Although summation of reported single-VOC measurements resulted in carbon concentrations of up to hundreds of ppb, additional unidentified organics may represent a

major share of the total NMOC concentration. To investigate the biosphere-atmosphere exchange of total non methane organic carbon, a total NMOC analyser was developed in the present study. The instrument was tested under laboratory conditions and was evaluated versus an independent analytical technique performing branch enclosure measurements on European beech (*Fagus sylvatica* L.) under field conditions. The instrument is based on general methodologies of elementary analysis. The core elements of the analyser are:

(i) a solid adsorbent preconcentration unit, that enabled the adsorption of volatile organics as well as their separation from CO, CO_2, and CH_4,

(ii) an oxidation tube, that converted these volatile organics to CO_2, and

(iii) a CO_2 adsorption trap followed by an infrared gas analyser for the detection of the previously formed CO_2.

The detection limit of the instrument was 0.5 ng carbon and the reproducibility ± 0.5%. Oxidation efficiencies tested with CO and CH_4 ranged between 91 and 101%. Recovery rates of several NMOC compounds were as low as 48% and represent the strongest source of uncertainty. Intercomparison of diel courses of the NMOC exchange of European beech measured by means of enclosures showed a perfect agreement between the total NMOC analyser and a GC-FID approach as an independent method. According to these promising results, the improvement of the NMOC instrument may result in important contributions for the investigation of biosphere-atmosphere exchange processes of non methane organic carbon.

OUTLOOK

The evaluation of the quality assurance measurements clearly indicated the general need to improve the analysis of volatile organic compounds. Since errors introduced by utilisation of inappropriate calibrations were shown as a dominant factor leading to incorrect results, application of two independent reference systems is encouraged. Since biogenic volatiles are known to be very reactive, non storing techniques are recommended for the generation of reference concentrations (e.g. by utilisation of permeation devices). However, ad- and desorption effects of these techniques have to be identified by taking advantage of the linear carbon response of the FID and by use of a stable independent reference. Therefore, the additional application of gaseous standard compounds should be performed on a regular basis. Construction of an online gas chromatographic system would be desirable to obviate losses of volatile organics during the storage time of the solid sorbent cartridges.

Although the sampling of carbonyl compounds by silica-DNPH cartridges resulted in good results for their qualitative and quantitative determination, the latter method is very cost-intensive since these cartridges can be used only once. Therefore, further laboratory experiments are needed to regenerate these cartridges.

The plant enclosure studies that were performed during the present study, demonstrated the need for the intensive investigation of regulation processes controlling the emission of monoterpenes by deciduous plants. Until recently, it was well accepted that these volatiles were emitted only from storage pools of the respective organisms as a function of temperature. Consequently, model estimates calculating monoterpene budgets, integrated the release of these compounds only as a function of temperature. However, studies performed during the last decade revealed that a variety of deciduous plant species may emit monoterpenes as a function of light and temperature. Moreover, the investigation of other regulation processes (e.g. seasonality, drought and high ambient temperature effects) is strongly encouraged and the results of these experiments should be incorporated in future estimates of global VOC emissions.

To obtain estimates considering the biosphere-atmosphere exchange of total nonmethane organic carbon, techniques capable to perform these measurements are imperative. Within this context, the results obtained from the total NMOC analyser described by the present study are

very promising, but additional tests evaluating its performance are urgently needed. The most important improvement needed for the NMOC analyser, is the enhancement and quantification of the NMOC recovery rates for a wide variety of volatile organic compounds. Application of a second adsorption trap within the NMOC adsorption unit would double the instruments sample capacity, since desorption and analysis of an ambient air sample could be performed while collecting a subsequent sample on the second adsorbent trap. Furthermore, it would enable simultaneous sampling from two different sources, e.g. from a plant and a reference cuvette or from two different heights. This would significantly increase the reliability of different measurements. Finally, a graphic user interface generating a remote control of the NMOC analyser as well as the miniaturisation of the instrument would be desirable.

BIBLIOGRAPHY

Ackmann, R.G.: Fundamental groups in the response of flame ionisation detectors to oxygenated aliphatic hydrocarbons, Journal of Gas Chromatography, 2, 173-179, 1964.

Ammann, C., Spirig, C., Neftel, A., Steinbacher, M., Komenda, M., and Schaub, A.: Application of PTR-MS for measurements of biogenic VOC in a deciduous forest, International Journal of Mass Spectrometry, 239, 87-101, 2004.

Andreae, M.O. and Crutzen, P.J.: Atmospheric aerosols: Biogeochemical sources and role in atmospheric chemistry, Science, 276, 1052-1058, 1997.

Apel, E.C., Calvert, J.G., and Fehsenfeld, F.C.: The Nonmethane Hydrocarbon Intercomparison Experiment (Nomhice) - Task-1 and Task-2, Journal of Geophysical Research-Atmospheres, 99, 16651-16664, 1994.

Apel, E.C., Calvert, J.G., Gilpin, T.M., Fehsenfeld, F.C., Parrish, D.D., and Lonneman, W.A.: The Nonmethane Hydrocarbon Intercomparison Experiment (NOMHICE): Task 3, Journal of Geophysical Research-Atmospheres, 104, 26069-26086, 1999.

Apel, E.C., Calvert, J.G., Gilpin, T.M., Fehsenfeld, F., and Lonneman, W.A.: Nonmethane Hydrocarbon Intercomparison Experiment (NOMHICE): Task 4, ambient air (vol 108 art no 4359, 2003), Journal of Geophysical Research-Atmospheres, 108, 2003a.

Apel, E.C., Calvert, J.G., Gilpin, T.M., Fehsenfeld, F., and Lonneman, W.A.: Correction to: Nonmethane Hydrocarbon Intercomparison Experiment (NOMHICE): Task 4, ambient air, Journal of Geophysical Research-Atmospheres, 108, 2003b.

Arey, J., Winer, A.M., Atkinson, R., Aschmann, S.M., Long, W.D., and Morrison, C.L.: The Emission of (Z)-3-Hexen-1-Ol, (Z)-3-Hexenylacetate and Other Oxygenated Hydrocarbons from Agricultural Plant-Species, Atmospheric Environment Part A-General Topics, 25, 1063-1075, 1991.

Arimura, G., Kost, C., and Boland, W.: Herbivore-induced, indirect plant defences, Biochimica Et Biophysica Acta-Molecular and Cell Biology of Lipids, 1734, 91-111, 2005.

Arnts, R.R. and Tejada, S.B.: 2,4-Dinitrophenylhydrazine-Coated Silica-Gel Cartridge Method for Determination of Formaldehyde in Air - Identification of an Ozone Interference, Environmental Science & Technology, 23, 1428-1430, 1989.

Atkinson, R.: Atmospheric chemistry of VOCs and NO_x, Atmospheric Environment, 34, 2063-2101, 2000.

Atkinson, R. and Arey, J.: Gas-phase tropospheric chemistry of biogenic volatile organic compounds: a review, Atmospheric Environment, 37, S197-S219, 2003.

Bach, T.J., Boronat, A., Campos, N., Ferrer, A., and Vollack, K.U.: Mevalonate biosynthesis in plants, Critical Reviews in Biochemistry and Molecular Biology, 34, 107-122, 1999.

Backes, K. and Leuschner, C.: Leaf water relations of competitive *Fagus sylvatica* and *Quercus petraea* trees during 4 years differing in soil drought, Canadian Journal of Forest Research-Revue Canadienne De Recherche Forestiere, 30, 335-346, 2000.

Baldwin, I.T. and Preston, C.A.: The eco-physiological complexity of plant responses to insect herbivores, Planta, 208, 137-145, 1999.

Baldwin, I.T., Halitschke, R., Kessler, A., and Schittko, U.: Merging molecular and ecological approaches in plant-insect interactions, Current Opinion in Plant Biology, 4, 351-358, 2001.

Baldwin, I.T., Kessler, A., and Halitschke, R.: Volatile signaling in plant-plant-herbivore interactions: what is real?, Current Opinion in Plant Biology, 5, 351-354, 2002.

Bartram, S., Jux, A., Gleixner, G., Boland, W.: Dynamic pathway allocation in early terpenoid biosynthesis of stress-induced lima bean leaves, Phytochemistry, in press, 2006.

Bauer, J.E., Occelli, M.L., Williams, P.M., and McCaslin, P.C.: Heterogeneous Catalyst Structure and Function - Review and Implications for the Analysis of Dissolved Organic-Carbon and Nitrogen in Natural-Waters, Marine Chemistry, 41, 75-89, 1993.

BEMA-Project: Special Issue, Atmospheric Environment, 31 (SI), 1997.

Bertin, N. and Staudt, M.: Effect of water stress on monoterpene emissions from young potted holm oak (*Quercus ilex* L.) trees, Oecologia, 107, 456-462, 1996.

Bertin, N., Staudt, M., Hansen, U., Seufert, G., Ciccioli, P., Foster, P., Fugit, J.L., and Torres, L.: Diurnal and seasonal course of monoterpene emissions from *Quercus ilex* (L.) under natural conditions - Applications of light and temperature algorithms, Atmospheric Environment, 31, 135-144, 1997.

Birkett, M.A., Campbell, C.A.M., Chamberlain, K., Guerrieri, E., Hick, A.J., Martin, J.L., Matthes, M., Napier, J.A., Pettersson, J., Pickett, J.A., Poppy, G.M., Pow, E.M., Pye, B.J., Smart, L.E., Wadhams, G.H., Wadhams, L.J., and Woodcock, C.M.: New roles for cis-jasmone as an insect semiochemical and in plant defense, Proceedings of the National Academy of Sciences of the United States of America, 97, 9329-9334, 2000.

Blades, A.T.: Ion Formation in Hydrocarbon Flames, Canadian Journal of Chemistry-Revue Canadienne De Chimie, 54, 2919-2924, 1976.

Bleecker, A.B. and Kende, H.: Ethylene: A gaseous signal molecule in plants, Annual Review of Cell and Developmental Biology, 16, 2000.

Bohlmann, J., Meyer-Gauen, G., and Croteau, R.: Plant terpenoid synthases: Molecular biology and phylogenetic analysis, Proceedings of the National Academy of Sciences of the United States of America, 95, 4126-4133, 1998.

Brancaleoni, E., Scovaventi, M., Frattoni, M., Mabilia, R., and Ciccioli, P.: Novel family of multi-layer cartridges filled with a new carbon adsorbent for the quantitative determination of volatile organic compounds in the atmosphere, Journal of Chromatography A, 845, 317-328, 1999.

Bruner, F., Crescentini, G., and Mangani, F.: Graphitized Carbon-Black - a Unique Adsorbent for Gas-Chromatography and Related Techniques, Chromatographia, 30, 565-572, 1990.

Calogirou, A., Larsen, B.R., Brussol, C., Duane, M., and Kotzias, D.: Decomposition of terpenes by ozone during sampling on Tenax, Analytical Chemistry, 68, 1499-1506, 1996.

Cao, X.L. and Hewitt, C.N.: Study of the Degradation by Ozone of Adsorbents and of Hydrocarbons Adsorbed During the Passive Sampling of Air, Environmental Science & Technology, 28, 757-762, 1994.

Carter, W.P.L. and Atkinson, R.: Development and evaluation of a detailed mechanism for the atmospheric reactions of isoprene and NO_x, International Journal of Chemical Kinetics, 28, 497-530, 1996.

Chen, X.H., Hulbert, D., and Shepson, P.B.: Measurement of the organic nitrate yield from OH reaction with isoprene, Journal of Geophysical Research-Atmospheres, 103, 25563-25568, 1998.

Cheniclet, C.: Effects of Wounding and Fungus Inoculation on Terpene Producing Systems of Maritime Pine, Journal of Experimental Botany, 38, 1557-1572, 1987.

Chung, M.Y., Maris, C., Krischke, U., Meller, R., and Paulson, S.E.: An investigation of the relationship between total non-methane organic carbon and the sum of speciated hydrocarbons and carbonyls measured by standard GC/FID: measurements in the Los Angeles air basin, Atmospheric Environment, 37, 159-170, 2003.

Ciais, P., Denning, A.S., Tans, P.P., Berry, J.A., Randall, D.A., Collatz, G.J., Sellers, P.J., White, J.W.C., Trolier, M., Meijer, H.A.J., Francey, R.J., Monfray, P., and Heimann, M.: A three-dimensional synthesis study of delta O^{18} in atmospheric CO_2 .1. Surface fluxes, Journal of Geophysical Research-Atmospheres, 102, 5857-5872, 1997.

Ciccioli, P., Cecinato, A., Brancaleoni, E., Frattoni, M., and Liberti, A.: Use of Carbon Adsorption Traps Combined with High-Resolution Gas-Chromatography - Mass-Spectrometry for the Analysis of Polar and Nonpolar C_4-C_{14} Hydrocarbons Involved in Photochemical Smog Formation, Hrc-Journal of High Resolution Chromatography, 15, 75-84, 1992.

Ciccioli, P., Fabozzi, C., Brancaleoni, E., Cecinato, A., Frattoni, M., Loreto, F., Kesselmeier, J., Schäfer, L., Bode, K., Torres, L., and Fugit, J.L.: Use of the isoprene algorithm for predicting the monoterpene emission from the Mediterranean holm oak *Quercus ilex* L.: Performance and limits of this approach, Journal of Geophysical Research-Atmospheres, 102, 23319-23328, 1997.

Ciccioli, P., Brancaleoni, E., Frattoni, M., Di Palo, V., Valentini, R., Tirone, G., Seufert, G., Bertin, N., Hansen, U., Csiky, O., Lenz, R., and Sharma, M.: Emission of reactive terpene compounds from orange orchards and their removal by within-canopy processes, Journal of Geophysical Research-Atmospheres, 104, 8077-8094, 1999.

Ciccioli, P., Brancaleoni, E., Frattoni, M., and Maris, C.: Chapter 21: sampling of atmospheric volatile organic compounds (VOCs) with sorbent tubes and their analysis by GC-MS, *In* Environmental monitoring handbook, Ed. Burden F.R., Mc Graw-Hill, New York, 2002.

Claeys, M., Graham, B., Vas, G., Wang, W., Vermeylen, R., Pashynska, V., Cafmeyer, J., Guyon, P., Andreae, M.O., Artaxo, P., and Maenhaut, W.: Formation of secondary organic aerosols through photooxidation of isoprene, Science, 303, 1173-1176, 2004.

Croteau, R., Kutchan, T.M., and Lewis, N.: Natural Products (Secondary Metabolites), *In* Biochemistry & Molecular Biology of Plants, Ed. R. Jones, American Society of Plant Physiologists, 1250-1318, 2000.

De Saeger, E. and Tsani-Bazaca, E.: EC Intercomparison of VOC measurements. A contribution to subproject TOR., *In* EUROTRAC Symposium 1992, Ed. Borrell *et al.*, SPB Academic Publishing bv, 157-160, 1992

Delfine, S., Csiky, O., Seufert, G., and Loreto, F.: Fumigation with exogenous monoterpenes of a non-isoprenoid-emitting oak (*Quercus suber*): monoterpene acquisition, translocation, and effect on the photosynthetic properties at high temperatures, New Phytologist, 146, 27-36, 2000.

Dindorf, T.: Untersuchungen zum Austausch von Carbonylen zwischen Bäumen und der Atmosphäre, Johannes Gutenberg Universität, Mainz, Germany, 2000

Doerffel, K.: Statistik in der analytischen Chemie. Deutscher Verlag für Grundstoffindustrie GmbH, Leipzig, Germany, 1996.

Ehrenberger, F.: Quantitative organische Elementaranalyse: Analysenmethoden zur Bestimmung der Elemente im Makro-, Mikro- und Spurenbereich in organischer und anorganischer Matrix. VCH Verlagsgesellschaft mbH, Weinheim, New York, Basel, Cambridge, 1991.

Eisenreich, W., Bacher, A., Arigoni, D., and Rohdich, F.: Biosynthesis of isoprenoids via the non-mevalonate pathway, Cellular and Molecular Life Sciences, 61, 1401-1426, 2004.

Falkowski, P., Scholes, R.J., Boyle, E., Canadell, J., Canfield, D., Elser, J., Gruber, N., Hibbard, K., Hogberg, P., Linder, S., Mackenzie, F.T., Moore, B., Pedersen, T., Rosenthal, Y., Seitzinger, S., Smetacek, V., and Steffen, W.: The global carbon cycle: A test of our knowledge of earth as a system, Science, 290, 291-296, 2000.

Fall, R. and Benson, A.A.: Leaf methanol - The simplest natural product from plants, Trends in Plant Science, 1, 296-301, 1996.

Fall, R. and Wildermuth, M.C.: Isoprene synthase: From biochemical mechanism to emission algorithm, Journal of Geophysical Research-Atmospheres, 103, 25599-25609, 1998.

Fall, R., Karl, T., Hansel, A., Jordan, A., and Lindinger, W.: Volatile organic compounds emitted after leaf wounding: On-line analysis by proton-transfer-reaction mass spectrometry, Journal of Geophysical Research-Atmospheres, 104, 15963-15974, 1999.

Farmer, E.E.: Surface-to-air signals, Nature, 411, 854-856, 2001.

Fehsenfeld, F., Calvert, J., Fall, R., Goldan, P., Guenther, A., Hewitt, C.N., Lamb, B., Liu, S., Trainer, M., Westberg, H., and Zimmermann, P.: Emissions of volatile organic compounds from vegetation and the implications for atmospheric chemistry, Global Biogeochemical Cycles, 6, 389-430, 1992.

Ferrari, C.P., Durand-Jolibois, R., Carlier, P., Jacob, V., Roche, A., Foster, P., and Fresnet, P.: Comparison between two carbonyl measurement methods in the atmosphere, Analusis, 27, 45-53, 1999.

Fick, J., Pommer, L., Andersson, B., and Nilsson, C.: Ozone removal in the sampling of parts per billion levels of terpenoid compounds: An evaluation of different scrubber materials, Environmental Science & Technology, 35, 1458-1462, 2001.

Finlayson-Pitts, B. and Pitts, J.N.: Chemistry of the Upper and Lower Atmosphere, Theory, Experiments and Applications. Academic Press, San Diego, San Francisco, New York, Boston, London, Sydney, Tokyo, 2000.

Fischbach, R.J., Zimmer, I., Steinbrecher, R., Pfichner, A., and Schnitzler, J.P.: Monoterpene synthase activities in leaves of *Picea abies* (L.) Karst. and *Quercus ilex* L., Phytochemistry, 54, 257-265, 2000.

Fischbach, R.J., Staudt, M., Zimmer, I., Rambal, S., and Schnitzler, J.P.: Seasonal pattern of monoterpene synthase activities in leaves of the evergreen tree *Quercus ilex*, Physiologia Plantarum, 114, 354-360, 2002.

Fischer, N.H.: Plant terpenoids as allelopathic agents, *In* Ecological Chemistry and Biochemistry of Plant Terpenoids, Eds. J.B. Harborne and F.A. Tomas-Barberan, Clarendon Press, Oxford, 377-398, 1991.

Fuentes, J.D., Lerdau, M., Atkinson, R., Baldocchi, D., Bottenheim, J.W., Ciccioli, P., Lamb, B., Geron, C., Gu, L., Guenther, A., Sharkey, T.D., and Stockwell, W.: Biogenic hydrocarbons in the atmospheric boundary layer: A review, Bulletin of the American Meteorological Society, 81, 1537-1575, 2000.

Funk, C., Lewinsohn, E., Vogel, B.S., Steele, C.L., and Croteau, R.: Regulation of Oleoresinosis in Grand Fir (*Abies Grandis*) - Coordinate Induction of Monoterpen and Diterpene Cyclases and 2 Cytochrome-P450 Dependent Diterpenoid Hydroxylases by Stem Wounding, Plant Physiology, 106, 999-1005, 1994.

Gabriel, R., Schafer, L., Gerlach, C., Rausch, T., and Kesselmeier, J.: Factors controlling the emissions of volatile organic acids from leaves of *Quercus ilex* L. (Holm oak), Atmospheric Environment, 33, 1347-1355, 1999.

Galbally, I.E. and Kirstine, W.: The production of methanol by flowering plants and the global cycle of methanol, Journal of Atmospheric Chemistry, 43, 195-229, 2002.

Ganzeveld, L.N., Lelieveld, J., Dentener, F.J., Krol, M.C., Bouwman, A.J., and Roelofs, G.J.: Global soil-biogenic NO_x emissions and the role of canopy processes, Journal of Geophysical Research-Atmospheres, 107, doi: 10.1029/2001JD001289, 2002.

Gershenzon, J. and Croteau, R.: Terpenoids, *In* Herbivores: Their Interactions with Secondary Plant Metabolites, Eds. G. Rosenthal and M. Berenbaum, Academic press, 165-219, 1991.

Giese, M., Bauerdoranth, U., Langebartels, C., and Sandermann, H.: Detoxification of Formaldehyde by the Spider Plant (*Chlorophytum Comosum* L.) and by Soybean (*Glycine Max* L.) Cell-Suspension Cultures, Plant Physiology, 104, 1301-1309, 1994.

Gottwald, W.: GC für Anwender. *In* Praxis der instrumentellen Analytik Ed. W. Klein. Verlag Chemie, Weinheim, New York, Basel, Cambridge, Tokyo, 1995.

Griffith, H. and Parry, M.A.J.: Preface: Plant responses to water stress, Annals of Botany, 89, 801-802, 2002.

Guenther, A.B., Zimmerman, P.R., Harley, P.C., Monson, R.K., and Fall, R.: Isoprene and Monoterpene Emission Rate Variability - Model Evaluations and Sensitivity Analyses, Journal of Geophysical Research-Atmospheres, 98, 12609-12617, 1993.

Guenther, A., Zimmerman, P., and Wildermuth, M.: Natural Volatile Organic-Compound Emission Rate Estimates for United-States Woodland Landscapes, Atmospheric Environment, 28, 1197-1210, 1994.

Guenther, A., Hewitt, C.N., Erickson, D., Fall, R., Geron, C., Graedel, T., Harley, P., Klinger, L., Lerdau, M., Mckay, W.A., Pierce, T., Scholes, B., Steinbrecher, R., Tallamraju, R., Taylor, J., and Zimmerman, P.: A Global-Model of Natural Volatile Organic-Compound Emissions, Journal of Geophysical Research-Atmospheres, 100, 8873-8892, 1995.

Guenther, A.: Seasonal and spatial variations in natural volatile organic compound emissions, Ecological Applications, 7, 34-45, 1997.

Guenther, A.: Modeling Biogenic Volatile Organic Compound Emissions to the Atmosphere, *In* Reactive Hydrocarbons in the Atmosphere, Academic Press, San Diego, 1999.

Guenther, A.: The contribution of reactive carbon emissions from vegetation to the carbon balance of terrestrial ecosystems, Chemosphere, 49, 837-844, 2002.

Gut, A., Scheibe, M., Rottenberger, S., Rummel, U., Welling, M., Ammann, C., Kirkman, G.A., Kuhn, U., Meixner, F.X., Kesselmeier, J., Lehmann, B.E., Schmidt, W., Müller, E., and Piedade, M.T.F.: Exchange fluxes of NO_2 and O_3 at soil and leaf surfaces in an Amazonian rain forest, Journal of Geophysical Research-Atmospheres, 107, doi:10.1029/2001JD000654, 2002.

Gutman, G., Tarpley, D., Ignatov, A., and Olson, S.: The Enhanced Noaa Global Land Dataset from the Advanced Very High-Resolution Radiometer, Bulletin of the American Meteorological Society, 76, 1141-1156, 1995.

Hahn, J.: Results of the Hydrocarbon Interlaboratory Comparison Experiment in TOR. A contribution to subproject TOR, *In* EUROTRAC Symposium 1994, Ed. Borrell *et al.*, SPB Academic Publishing bv, 399-403, 1994.

Hakola, H., Rinne, J., and Laurila, T.: The hydrocarbon emission rates of tea-leafed willow (*Salix phylicifolia*), silver birch (*Betula pendula*) and European aspen (*Populus tremula*), Atmospheric Environment, 32, 1825-1833, 1998.

Hakola, H., Laurila, T., Lindfors, V., Hellen, H., Gaman, A., and Rinne, J.: Variation of the VOC emission rates of birch species during the growing season, Boreal Environment Research, 6, 237-249, 2001.

Halitschke, R., Schittko, U., Pohnert, G., Boland, W., and Baldwin, I.T.: Molecular interactions between the specialist herbivore Manduca sexta (Lepidoptera, Sphingidae) and its natural host Nicotiana attenuata. III. Fatty acid-amino acid conjugates in herbivore oral secretions are necessary and sufficient for herbivore-specific plant responses, Plant Physiology, 125, 711-717, 2001.

Hansel, A., Jordan, A., Holzinger, R., Prazeller, P., Vogel, W., and Lindinger, W.: Proton-Transfer Reaction Mass-Spectrometry - Online Trace Gas-Analysis at the Ppb Level, International Journal of Mass Spectrometry and Ion Processes, 150, 609-619, 1995.

Hatanaka, A. and Harada, T.: Leaf-Alcohol .22. Formation of Cis-3-Hexenal, Trans-2-Hexenal and Cis-3-Hexenol in Macerated *Thea Sinensis* Leaves, Phytochemistry, 12, 2341-2346, 1973.

Hatanaka, A., Kajiwara, T., and Sekiya, J.: Biosynthetic-Pathway for C_6-Aldehydes Formation from Linolenic Acid in Green Leaves, Chemistry and Physics of Lipids, 44, 341-361, 1987.

Hatanaka, A.: The fresh green odor emitted by plants, Food Reviews International, 12, 303-350, 1996.

Havaux, M.: Carotenoids as membrane stabilizers in chloroplasts, Trends in Plant Science, 3, 147-151, 1998.

Heiden, A.C., Hoffmann, T., Kahl, J., Kley, D., Klockow, D., Langebartels, C., Mehlhorn, H., Sandermann, H., Schraudner, M., Schuh, G., and Wildt, J.: Emission of volatile organic compounds from ozone-exposed plants, Ecological Applications, 9, 1160-1167, 1999.

Helas, G., Slanina, S., and Steinbrecher, R.: Biogenic volatile organic compounds in the Atmosphere. SPB, Academic Publishing, Amsterdam, 1997.

Helmig, D.: Ozone removal techniques in the sampling of atmospheric volatile organic trace gases, Atmospheric Environment, 31, 3635-3651, 1997.

Hewitt, C.N. and Street, R.A.: A Qualitative Assessment of the Emission of Nonmethane Hydrocarbon Compounds from the Biosphere to the Atmosphere in the Uk - Present Knowledge and Uncertainties, Atmospheric Environment Part a-General Topics, 26, 3069-3077, 1992.

Hoffmann, T., Jacob, P., Linscheid, M., and Klockow, D.: Measurements of Biogenic Hydrocarbons and Their Atmospheric Degradation in Forests, International Journal of Environmental Analytical Chemistry, 52, 29-37, 1993.

Hoffmann, T.: Adsorptive Preconcentration Technique Including Oxidant Scavenging for the Measurement of Reactive Natural Hydrocarbons in Ambient Air, Fresenius Journal of Analytical Chemistry, 351, 41-47, 1995.

Holm, T.: Aspects of the mechanism of the flame ionization detector, Journal of Chromatography A, 842, 221-227, 1999.

Holzinger, R., Sandoval-Soto, L., Rottenberger, S., Crutzen, P.J., and Kesselmeier, J.: Emissions of volatile organic compounds from *Quercus ilex* L. measured by Proton Transfer Reaction Mass Spectrometry under different environmental conditions, Journal of Geophysical Research-Atmospheres, 105, 20573-20579, 2000.

Holzke, C., Dindorf, T., Kuhn, U., Kesselmeier, J., and Koppmann, R.: Terpene emissions from European beech (*Fagus sylvatica* L.): pattern and emission behaviour within two vegetation periods, submitted to Journal of Atmospheric Chemistry, 2005.

IPCC, Intergovernmental Panel on Climate Change, Contribution of Working Group I to the Second Assessment Report (Houghton, J.T., Meira, L.G., Callander, B.A., Harris, N., Kattenberg, A., and Maskell, K.): Climate Change 1995: The Science of Climate Change, Cambridge University Press, Cambridge, UK, 1996.

IPCC, Intergovernmental Panel on Climate Change, Contribution of Working Group I to the Third Assessment Report (Houghton, J.T., Ding, Y., Griggs, D.J., Noguer, M.,van der Linden, P.J, Dai, X., Maskell, K., Johnson, C.A.): Climate Change 2001: The Scientific basis, Cambridge University Press, Cambridge, UK, 2001.

Isidorov, V.A., Zenkevich, I.G., and Ioffe, B.V.: Volatile Organic-Compounds in the Atmosphere of Forests, Atmospheric Environment, 19, 1-8, 1985.

Jork, E.M.: Laboruntersuchungen zum Austausch von organischen Säuren und Aldehyden zwischen landwirtschaftlichen Pflanzen und der Atmosphäre, Johannes Gutenberg Universität, Mainz, Germany, 1996

Jüttner, F.: A cryotrap technique for the quantitation of monoterpenes in humid and ozone-rich forest air, Journal of Chromatography, 442, 157-163, 1988.

Kahl, J., Hoffmann, T., and Klockow, D.: Differentiation between de novo synthesized and constitutively released terpenoids from *Fagus sylvatica*, Phytochemistry, 51, 383-388, 1999.

Karban, R., Baldwin, I.T., Baxter, K.J., Laue, G., and Felton, G.W.: Communication between plants: induced resistance in wild tobacco plants following clipping of neighboring sagebrush, Oecologia, 125, 66-71, 2000.

Karlik, J.F. and Winer, A.M.: Measured isoprene emission rates of plants in California landscapes: comparison to estimates from taxonomic relationships, Atmospheric Environment, 35, 1123-1131, 2001.

Keeling, C.D., Whorf, T.P., Wahlen, M., and Vanderplicht, J.: Interannual Extremes in the Rate of Rise of Atmospheric Carbon-Dioxide since 1980, Nature, 375, 666-670, 1995.

Kesselmeier, J., Schäfer, L., Ciccioli, P., Brancaleoni, E., Cecinato, A., Frattoni, M., Foster, P., Jacob, V., Denis, J., Fugit, J.L., Dutaur, L., and Torres, L.: Emission of monoterpenes and isoprene from a Mediterranean oak species *Quercus ilex* L. measured within the BEMA (Biogenic Emissions in the Mediterranean Area) project, Atmospheric Environment, 30, 1841-1850, 1996.

Kesselmeier, J., Bode, K., Hofmann, U., Müller, H., Schäfer, L., Wolf, A., Ciccioli, P., Brancaleoni, E., Cecinato, A., Frattoni, M., Foster, P., Ferrari, C., Jacob, V., Fugit, J.L., Dutaur, L., Simon, V., and Torres, L.: Emission of short chained organic acids, aldehydes and monoterpenes from *Quercus ilex* L. and *Pinus pinea* L. in relation to physiological activities, carbon budget and emission algorithms, Atmospheric Environment, 31, 119-133, 1997.

Kesselmeier, J., Bode, K., Schäfer, L., Schebeske, G., Wolf, A., Brancaleoni, E., Cecinato, A., Ciccioli, P., Frattoni, M., Dutaur, L., Fugit, J.L., Simon, V., and Torres, L.: Simultaneous field measurements of terpene and isoprene emissions from two dominant Mediterranean oak species in relation to a north American species, Atmospheric Environment, 32, 1947-1953, 1998a.

Kesselmeier, J., Bode, K., Gerlach, C., and Jork, E.M.: Exchange of atmospheric formic and acetic acids with trees and crop plants under controlled chamber and purified air conditions, Atmospheric Environment, 32, 1765-1775, 1998b.

Kesselmeier, J. and Staudt, M.: Biogenic volatile organic compounds (VOC): An overview on emission, physiology and ecology, Journal of Atmospheric Chemistry, 33, 23-88, 1999.

Kesselmeier, J.: Exchange of short-chain oxygenated volatile organic compounds (VOCs) between plants and the atmosphere: A compilation of field and laboratory studies, Journal of Atmospheric Chemistry, 39, 219-233, 2001.

Kesselmeier, J., Kuhn, U., Rottenberger, S., Biesenthal, T., Wolf, A., Schebeske, G., Andreae, M.O., Ciccioli, P., Brancaleoni, E., Frattoni, M., Oliva, S.T., Botelho, M.L., Silva, C.M.A., and Tavares, T.M.: Concentrations and species composition of atmospheric volatile organic compounds (VOCs) as observed during the wet and dry season in Rondonia (Amazonia), Journal of Geophysical Research-Atmospheres, 107, 2002a.

Kesselmeier, J., Ciccioli, P., Kuhn, U., Stefani, P., Biesenthal, T., Rottenberger, S., Wolf, A., Vitullo, M., Valentini, R., Nobre, A., Kabat, P., and Andreae, M.O.: Volatile organic compound emissions in relation to plant carbon fixation and the terrestrial carbon budget, Global Biogeochemical Cycles, 16, doi:10.1029/2001GB001813, 2002b.

Kesselmeier, J., Rottenberger, S., Kuhn, U., and Ciccioli, P.: Ecosystem seasonality affects biogenic emission of volatile organic compounds (VOC): Flooding and dry/wet season transition in tropical regions as an elicitor for emission changes at regular intervals?, *In* Integrated Land Ecosystem-Atmosphere Processes Study (ILEAPS). International Open Science Conference, Eds. A. Arneth, H Korhonene, M Kulmala, M Raivonen, T Ruuskanen and T Suni, Finnish Association for Aerosol Research, Helsinki, Finland, pp. 187-192, 2003.

Kesselmeier, J.: Interactive comment on "Seasonal cycles of isoprene concentrations in the Amazonian rainforest" by C.R. Trostdorf *et al.*, Atmospheric Chemistry and Physics, Discuss., 4, 528-530, 2004.

Kimmerer, T.W. and Kozlowski, T.T.: Ethylene, Ethane, Acetaldehyde, and Ethanol-Production by Plants under Stress, Plant Physiology, 69, 840-847, 1982.

Kirstine, W., Galbally, I., Ye, Y.R., and Hooper, M.: Emissions of volatile organic compounds (primarily oxygenated species) from pasture, Journal of Geophysical Research-Atmospheres, 103, 10605-10619, 1998.

Kleindienst, T.E., Corse, E.W., Blanchard, F.T., and Lonneman, W.A.: Evaluation of the performance of DNPH-coated silica gel and C-18 cartridges in the measurement of formaldehyde in the presence and absence of ozone, Environmental Science & Technology, 32, 124-130, 1998.

Kleiss, B.: Emissions of volatile organic compounds from tropical savannah vegetation and biomass burning, Johannes Gutenberg Universität, Mainz, 2004.

Köble, R. and Seufert, G.: Novel maps for forest tree species in Europe, *In* A changing atmosphere: 8th European symposium on the physico-chemical behaviour of atmospheric pollutants, Turin, 2001.

Kondo, T., Hasegawa, K., Uchida, R., Onishi, M., Mizukami, A., and Omasa, K.: Absorption of Formaldehyde by Oleander (*Nerium indicum*), Environmental Science & Technology, 29, 2901-2903, 1995.

Kondo, T., Hasegawa, K., Kitagawa, C., Uchida, R., and Onishi, M.: Absorption of atmospheric phenol by evergreen broad-leaved tree species, Chemistry Letters, 997-998, 1996a.

Kondo, T., Hasegawa, K., Uchida, R., Onishi, M., Mizukami, A., and Omasa, K.: Absorption of atmospheric formaldehyde by deciduous broad-leaved, evergreen broad-leaved, and coniferous tree species, Bulletin of the Chemical Society of Japan, 69, 3673-3679, 1996b.

Kondo, T., Hasegawa, K., Uchida, R., and Onishi, M.: Absorption of atmospheric C_2-C_5 aldehydes by various tree species and their tolerance to C_2-C_5 aldehydes, Science of the Total Environment, 224, 121-132, 1998.

Komenda, M., Parusel, E., Wedel, A., and Koppmann, R.: Measurements of biogenic VOC emissions: sampling, analysis and calibration, Atmospheric Environment, 35, 2069-2080, 2001.

Komenda, M.: Investigations of the emissions of monoterpenes from scots pine, *In* Institut für Chemie und Dynamik der Geosphäre, Institut II: Troposphäre, Universität Köln, Jülich, 2001.

Komenda, M., Kobel, K., Koppmann, R., and Wildt, J.: Comparability of biogenic VOC emission rate measurements under laboratory and ambient conditions at the example of monoterpene emissions from Scots pine (*Pinus sylvestris*), Journal of Atmospheric Chemistry, 45, 1-23, 2003.

König, G., Brunda, M., Puxbaum, H., Hewitt, C.N., Duckham, S.C., and Rudolph, J.: Relative Contribution of Oxygenated Hydrocarbons to the Total Biogenic VOC Emissions of Selected Mid-European Agricultural and Natural Plant-Species, Atmospheric Environment, 29, 861-874, 1995.

Kreuzwieser, J., Scheerer, U., and Rennenberg, H.: Metabolic origin of acetaldehyde emitted by poplar (*Populus tremula* x *P-alba*) trees, Journal of Experimental Botany, 50, 757-765, 1999.

Kuhn, U., Wolf, A., Gries, C., Nash, T.H., and Kesselmeier, J.: Field measurements on the exchange of carbonyl sulfide between lichens and the atmosphere, Atmospheric Environment, 34, 4867-4878, 2000.

Kuhn, U., Rottenberger, S., Biesenthal, T., Ammann, C., Wolf, A., Schebeske, G., Oliva, S.T., Tavares, T.M., and Kesselmeier, J.: Exchange of short-chain monocarboxylic acids by vegetation at a remote tropical forest site in Amazonia, Journal of Geophysical Research-Atmospheres, 107, doi: 10.1029/2000 JD000303, 2002a.

Kuhn, U., Rottenberger, S., Biesenthal, T., Wolf, A., Schebeske, G., Ciccioli, P., Brancaleoni, E., Frattoni, M., Tavares, T.M., and Kesselmeier, J.: Isoprene and monoterpene emissions of Amazonian tree species during the wet season: Direct and indirect investigations on controlling environmental functions, Journal of Geophysical Research-Atmospheres, 107, doi:10.1029/2001JD000978, 2002b.

Kuhn, U., Rottenberger, S., Biesenthal, T., Wolf, A., Schebeske, G., Ciccioli, P., Brancaleoni, E., Frattoni, M., Tavares, T.M., and Kesselmeier, J.: Seasonal differences in isoprene and light-dependent monoterpene emission by Amazonian tree species, Global Change Biology, 10, 663-682, 2004a.

Kuhn, U., Rottenberger, S., Biesenthal, T., Wolf, A., Schebeske, G., Ciccioli, P., and Kesselmeier, J.: Strong correlation between isoprene emission and gross photosynthetic capacity during leaf phenology of the tropical tree species *Hymenaea courbaril* with fundamental changes in volatile organic compounds emission composition during early leaf development, Plant Cell and Environment, 27, 1469-1485, 2004b.

Kuhn, U., Dindorf, T., Ammann, C., Rottenberger, S., Guyon, P., Holzinger, R., Ausma, S., Kenntner, T., Helleis, F., and Kesselmeier, J.: Design and field application of an automated cartridge sampler for VOC concentration and flux measurements, Journal of Environmental Monitoring, 7, 568-576, 2005.

Kuster, W.C., Jobson, B.T., Karl, T., Riemer, D., Apel, E., Goldan, P.D., and Fehsenfeld, F.C.: Intercomparison of volatile organic carbon measurement techniques and data at La Porte during the TexAQS2000 Air Quality Study, Environmental Science & Technology, 38, 221-228, 2004.

Larcher, W.: Ökophysiology der Pflanzen: Leben, Leistung und Stressbewältigung der Pflanzen in ihrer Umwelt. Ulmer, Stuttgart, Germany, 1994.

Larsen, B., Bomboi-Mingarro, T., Brancaleoni, E., Calogirou, A., Cecinato, A., Coeur, C., Chatzianestis, I., Duane, M., Frattoni, M., Fugit, J.L., Hansen, U., Jacob, V., Mimikos, N., Hoffmann, T., Owen, S., Perez-Pastor, R., Reichmann, A., Seufert, G., Staudt, M., and Steinbrecher, R.: Sampling and analysis of terpenes in air. An interlaboratory comparison, Atmospheric Environment, 31, 35-49, 1997.

Lenz, R., Köble, R., and Seufert, G.: Species-based mapping of biogenic emissions in Europe- case study Italy, *In* A changing atmosphere: 8th European symposium on the physico-chemical behaviour of atmospheric pollutants, Turin, 2001

Lerdau, M. and Gray, D.: Ecology and evolution of light-dependent and light-independent phytogenic volatile organic carbon, New Phytologist, 157, 199-211, 2003.

Lewinsohn, E., Gijzen, M., Savage, T.J., and Croteau, R.: Defense-Mechanisms of Conifers - Relationship of Monoterpene Cyclase Activity to Anatomical Specialization and Oleoresin Monoterpene Content, Plant Physiology, 96, 38-43, 1991a.

Lewinsohn, E., Gijzen, M., and Croteau, R.: Defense-Mechanisms of Conifers - Differences in Constitutive and Wound-Induced Monoterpene Biosynthesis among Species, Plant Physiology, 96, 44-49, 1991b.

Lichtenthaler, H.K.: The 1-deoxy-D-xylulose-5-phosphate pathway of isoprenoid biosynthesis in plants, Annual Review of Plant Physiology and Plant Molecular Biology, 50, 47-65, 1999.

Li-COR: Infrared gas analyser, model Li 6262, Instruction manual, 1996.

Lindinger, W., Hansel, A., and Jordan, A.: On-line monitoring of volatile organic compounds at pptv levels by means of proton-transfer-reaction mass spectrometry (PTR-MS) - Medical applications, food control and environmental research, International Journal of Mass Spectrometry, 173, 191-241, 1998.

Lloyd, J. and Farquhar, G.D.: The CO_2 dependence of photosynthesis, plant growth responses to elevated atmospheric CO_2 concentrations and their interaction with soil nutrient status. 1. General principles and forest ecosystems, Functional Ecology, 10, 4-32, 1996.

Llusia, J. and Peñuelas, J.: Seasonal patterns of terpene content and emission from seven Mediterranean woody species in field conditions, American Journal of Botany, 87, 133-140, 2000.

Loreto, F., Ciccioli, P., Cecinato, A., Brancaleoni, E., Frattoni, M., and Tricoli, D.: Influence of environmental factors and air composition on the emission of alpha-pinene from *Quercus ilex* leaves, Plant Physiology, 110, 267-275, 1996.

Loreto, F., Forster, A., Durr, M., Csiky, O., and Seufert, G.: On the monoterpene emission under heat stress and on the increased thermotolerance of leaves of *Quercus ilex* L. fumigated with selected monoterpenes, Plant Cell and Environment, 21, 101-107, 1998.

Loreto, F., Ciccioli, P., Brancaleoni, E., Frattoni, M., and Delfine, S.: Incomplete C-13 labelling of alpha-pinene content of *Quercus ilex* leaves and appearance of unlabelled C in alpha-pinene emission in the dark, Plant Cell and Environment, 23, 229-234, 2000.

Lozan, J.L. and Kausch, H.: Pareys Studientexte 74: Angewandte Statistik für Naturwissenschaftler. Parey Buchverlag im Blackwell Wissenschaftsverlag, Berlin, Wien, 1998.

Lucker, J., El Tamer, M.K., Schwab, W., Verstappen, F.W.A., van der Plas, L.H.W., Bouwmeester, H.J., and Verhoeven, H.A.: Monoterpene biosynthesis in lemon (*Citrus limon*) - cDNA isolation and functional analysis of four monoterpene synthases, European Journal of Biochemistry, 269, 3160-3171, 2002.

MacDonald, R.C. and Fall, R.: Detection of Substantial Emissions of Methanol from Plants to the Atmosphere, Atmospheric Environment Part a-General Topics, 27, 1709-1713, 1993.

Maris, C., Chung, M.Y., Lueb, R., Krischke, U., Meller, R., Fox, M.J., and Paulson, S.E.: Development of instrumentation for simultaneous analysis of total non-methane organic carbon and volatile organic compounds in ambient air, Atmospheric Environment, 37, 149-158, 2003.

Mastrogiacomo, A.R. and Pierini, E.: Discussion of thermodynamic data obtained by adsorption gas chromatography of hydrocarbons on a new graphitized carbon black with a high specific surface area, Chromatographia, 51, 455-460, 2000.

Mastrogiacomo, A.R., Ottaviani, M.F., Pierini, E., Cangiotti, M., Mauro, M., and Mangani, F.: Comparison of chemical and physical properties of carbon blacks for sampling and analysis of environmental pollutants, Chromatographia, 55, 345-348, 2002.

Matisova, E. and Skrabakova, S.: Carbon Sorbents and Their Utilization for the Preconcentration of Organic Pollutants in Environmental-Samples, Journal of Chromatography A, 707, 145-179, 1995.

Monson, R.K.: Volatile organic compound emissions from terrestrial ecosystems: A primary biological control over atmospheric chemistry, Israel Journal of Chemistry, 42, 29-42, 2002.

Moukhtar, S., Bessagnet, B., Rouil, L., and Simon, V.: Monoterpene emissions from Beech (*Fagus sylvatica*) in a French forest and impact on secondary pollutants formation at regional scale, Atmospheric Environment, 39, 3535-3547, 2005.

National Pollutant Inventory (NPI): Australian Government, Department of the Environment and Heritage, www.npi.gov.au, 2005.

Niinemets, U., Hauff, K., Bertin, N., Tenhunen, J.D., Steinbrecher, R., and Seufert, G.: Monoterpene emissions in relation to foliar photosynthetic and structural variables in Mediterranean evergreen *Quercus* species, New Phytologist, 153, 243-256, 2002a.

Niinemets, U., Seufert, G., Steinbrecher, R., and Tenhunen, J.D.: A model coupling foliar monoterpene emissions to leaf photosynthetic characteristics in Mediterranean evergreen *Quercus* species, New Phytologist, 153, 257-275, 2002b.

Niinemets, U. and Reichstein, M.: A model analysis of the effects of nonspecific monoterpenoid storage in leaf tissues on emission kinetics and composition in Mediterranean sclerophyllous *Quercus* species, Global Biogeochemical Cycles, 16, doi:10.1029/2002GB001927, 2002.

Niinemets, U. and Reichstein, M.: Controls on the emission of plant volatiles through stomata: A sensitivity analysis, Journal of Geophysical Research-Atmospheres, 108, doi:10.1029/2002JD002626, 2003.

Niinemets, U., Loreto, F., and Reichstein, M.: Physiological and physicochemical controls on foliar volatile organic compound emissions, Trends in Plant Science, 9, 180-186, 2004.

Olson, J.: World ecosystems (WE1.4): Digital raster data on a 10 minute geographic 1080` 2160 grid square. *In* Global Ecosystem Database, Version 1.0: Disc A Ed. NOAA National Geophysical Data Center, Boulder, USA, 1992.

O'Malley, A. and Hodnett, B.K.: The influence of volatile organic compound structure on conditions required for total oxidation, Catalysis Today, 54, 31-38, 1999.

Owen, S., Boissard, C., Street, R.A., Duckham, S.C., Csiky, O., and Hewitt, C.N.: Screening of 18 Mediterranean plant species for volatile organic compound emissions, Atmospheric Environment, 31, 101-117, 1997.

Owen, S.M., Harley, P., Guenther, A., and Hewitt, C.N.: Light dependency of VOC emissions from selected Mediterranean plant species, Atmospheric Environment, 36, 3147-3159, 2002.

Ozawa, R., Arimura, G., Takabayashi, J., Shimoda, T., and Nishioka, T.: Involvement of jasmonate- and salicylate-related signaling pathways for the production of specific herbivore-induced volatiles in plants, Plant and Cell Physiology, 41, 391-398, 2000.

Park, C.: The Environment. Routledge, Taylor and Francis Group, London, New York, 2001.

Parry, M.A.J., Andralojc, P.J., Khan, S., Lea, P.J., and Keys, A.J.: Rubisco activity: Effects of drought stress, Annals of Botany, 89, 833-839, 2002.

Pearcy, R.W., Schulze, E.D., and Zimmermann, R.: Measurement of transpiration and leaf conductance, *In* Plant Physiological Ecology, Chapman and Hall, New York, 141-142, 1989.

Pellizzari, E., Demian, B., and Krost, K.: Sampling of Organic-Compounds in the Presence of Reactive Inorganic Gases with Tenax-Gc, Analytical Chemistry, 56, 793-798, 1984.

Pellizzari, E.D. and Krost, K.J.: Chemical-Transformations During Ambient Air Sampling for Organic Vapors, Analytical Chemistry, 56, 1813-1819, 1984.

Peñuelas, J. and Llusia, J.: Seasonal emission of monoterpenes by the Mediterranean tree *Quercus ilex* in field conditions: Relations with photosynthetic rates, temperature and volatility, Physiologia Plantarum, 105, 641-647, 1999a.

Peñuelas, J. and Llusia, J.: Short-term responses of terpene emission rates to experimental changes of PFD in *Pinus halepensis* and *Quercus ilex* in summer field conditions, Environmental and Experimental Botany, 42, 61-68, 1999b.

Peñuelas, J. and Llusia, J.: The complexity of factors driving volatile organic compound emissions by plants, Biologia Plantarum, 44, 481-487, 2001.

Perkin Elmer: AutoSystem XL GC, User's Manual. *In* Gas Chromatography. Perkin Elmer Corporation, Germany, 1997.

Peters, R.J.B., Duivenbode, J.A.D.V.R.V., Duyzer, J.H., and Verhagen, H.L.M.: The Determination of Terpenes in Forest Air, Atmospheric Environment, 28, 2413-2419, 1994.

Pettersson, J., Pickett, J.A., Pye, B.J., Quiroz, A., Smart, L.E., Wadhams, L.J., and Woodcock, C.M.: Winter Host Component Reduces Colonization by Bird-Cherry Oat Aphid, *Rhopalosiphum-Padi* (L) (Homoptera, Aphididae), and Other Aphids in Cereal Fields, Journal of Chemical Ecology, 20, 2565-2574, 1994.

Peuke, A.D., Schraml, C., Hartung, W., and Rennenberg, H.: Identification of drought-sensitive beech ecotypes by physiological parameters, New Phytologist, 154, 373-387, 2002.

Phillips, M.A., Savage, T.J., and Croteau, R.: Monoterpene synthases of loblolly pine (*Pinus taeda*) produce pinene isomers and enantiomers, Archives of Biochemistry and Biophysics, 372, 197-204, 1999.

Pickett, J.A. and Poppy, G.M.: Switching on plant genes by external chemical signals, Trends in Plant Science, 6, 137-139, 2001.

Pio, C.A., Silva, P.A., Cerqueira, M.A., and Nunes, T.V.: Diurnal and seasonal emissions of volatile organic compounds from cork oak (*Quercus suber*) trees, Atmospheric Environment, 39, 1817-1827, 2005.

Preston, C.A., Laue, G., and Baldwin, I.T.: Methyl jasmonate is blowing in the wind, but can it act as a plant-plant airborne signal?, Biochemical Systematics and Ecology, 29, 1007-1023, 2001.

Richter, G.: Stoffwechselphysiologie der Pflanzen, Physiologie und Biochemie des Primär- und Sekundärstoffwechsels. Georg Thieme Verlag, Stuttgart, New York, 1988.

Rinne, H.J.I., Guenther, A.B., Greenberg, J.P., and Harley, P.C.: Isoprene and monoterpene fluxes measured above Amazonian rainforest and their dependence on light and temperature, Atmospheric Environment, 36, 2421-2426, 2002.

Roberts, J.M., Fehsenfeld, F.C., Albritton, D.L., and Sievers, R.E.: Sampling and analysis of monoterpene hydrocarbons in the atmosphere with Tenax gas chromatographic porous polymer, *In* Identification of and analysis of organic pollutants in air, Ed. L.H. Keith, Butterworth Publishers, London, Boston, 371-387, 1984.

Roberts, J.M., Bertman, S.B., Jobson, T., Niki, H., and Tanner, R.: Measurement of total nonmethane organic carbon (C_y): Development and application at Chebogue Point, Nova Scotia, during the 1993 North Atlantic Regional Experiment campaign, Journal of Geophysical Research-Atmospheres, 103, 13581-13592, 1998.

Rohmer, M., Knani, M., Simonin, P., Sutter, B., and Sahm, H.: Isoprenoid Biosynthesis in Bacteria - a Novel Pathway for the Early Steps Leading to Isopentenyl Diphosphate, Biochemical Journal, 295, 517-524, 1993.

Rohmer, M., Seemann, M., Horbach, S., BringerMeyer, S., and Sahm, H.: Glyceraldehyde 3-phosphate and pyruvate as precursors of isoprenic units in an alternative non-mevalonate pathway for terpenoid biosynthesis, Journal of the American Chemical Society, 118, 2564-2566, 1996.

Roth, H.: Quantitative organische Mikroanalyse, Springer Verlag, Wien, 1958.

Rottenberger, S.: Exchange of oxygenated volatile organic compounds between Amazonian and European vegetation and the atmosphere, Johannes Gutenberg Universität, Mainz, 2003.

Rottenberger, S., Kuhn, U., Wolf, A., Schebeske, G., Oliva, S.T., Tavares, T.M., and Kesselmeier, J.: Exchange of short-chain aldehydes between Amazonian vegetation and the atmosphere, Ecological Applications, 14, 247-262, 2004.

Rottenberger, S., Kuhn, U., Wolf, A., Schebeske, G., Oliva, S.T., Tavares, T.M., and Kesselmeier, J.: Formaldehyde and acetaldehyde exchange during leaf development of the Amazonian deciduous tree species *Hymenaea courbaril*, Atmospheric Environment, 39, 2275-2279, 2005.

Ruzicka, L.: Multimembered rings, higher terpene compounds and male sex hormones, Nobel Lecture, 1945

Sabillon, D. and Cremades, L.V.: Diurnal and seasonal variation of monoterpene emission rates for two typical Mediterranean species (*Pinus pinea* and *Quercus ilex*) from field measurements-relationship with temperature and PAR, Atmospheric Environment, 35, 4419-4431, 2001.

Sampaolo, L., Pierini, E., and Mastrogiacomo, A.R.: Evaluation of a new dualsorbent trap for organic pollutants of different volatility, Chromatographia, 50, 680-684, 1999.

Schäfer, L., Kesselmeier, J., and Helas, G.: Formic and Acetic acid emission from conifers measured with a "cuvette" technique, *In* CeC Air Pollution Research 39: Field Measurements and Interpretation of Species Related to Photooxidants and Acid Deposition, Ed. Beilke S. Angeletti G., and Slanina J., Brussels, 319-323, 1992.

Schäfer, L.: Untersuchungen zur Abgabe von Ameisen- und Essigsäure sowie Form- und Acetaldehyd durch mediterrane Pflanzen an die Atmosphäre, Johannes Gutenberg Universität, Mainz, Germany, 1997

Schimel, D.S., House, J.I., Hibbard, K.A., Bousquet, P., Ciais, P., Peylin, P., Braswell, B.H., Apps, M.J., Baker, D., Bondeau, A., Canadell, J., Churkina, G., Cramer, W., Denning, A.S., Field, C.B., Friedlingstein, P., Goodale, C., Heimann, M., Houghton, R.A., Melillo, J.M., Moore, B., Murdiyarso, D., Noble, I., Pacala, S.W., Prentice, I.C., Raupach, M.R., Rayner, P.J., Scholes, R.J., Steffen, W.L., and Wirth, C.: Recent patterns and mechanisms of carbon exchange by terrestrial ecosystems, Nature, 414, 169-172, 2001.

Schlesinger, W.H.: Biogeochemistry. *In* Treatise on Geochemistry Eds. H.D. Holland and K.K. Turekian. Elsevier BV, 2003.

Schmeil, O. and Fitschen, J.: Flora von Deutschland und angrenzenden Ländern Ed. Seybold Senghas K., S. Quelle & Meier Verlag, Heidelberg, Wiesbaden, Germany, 1993.

Schnitzler, J.P., Arenz, R., Steinbrecher, R., and Lehning, A.: Characterization of an isoprene synthase from leaves of *Quercus petraea* (Mattuschka) Liebl, Botanica Acta, 109, 216-221, 1996.

Schnitzler, J.P., Graus, M., Kreuzwieser, J., Heizmann, U., Rennenberg, H., Wisthaler, A., and Hansel, A.: Contribution of different carbon sources to isoprene biosynthesis in poplar leaves, Plant Physiology, 135, 152-160, 2004.

Schuh, G., Heiden, A.C., Hoffmann, T., Kahl, J., Rockel, P., Rudolph, J., and Wildt, J.: Emissions of volatile organic compounds from sunflower and beech: Dependence on temperature and light intensity, Journal of Atmospheric Chemistry, 27, 291-318, 1997.

Schulze, E.D.: Carbon-Dioxide and Water-Vapor Exchange in Response to Drought in the Atmosphere and in the Soil, Annual Review of Plant Physiology and Plant Molecular Biology, 37, 247-274, 1986.

Schwetlik, K.: Organikum. Wiley-VCH, Weinheim, Germany, 2004.

Seinfeld, J.H. and Pandis, S.N.: Atmospheric chemistry and physics: From air pollution to climate change. John Wiley & Sons, Inc., New York, 1997.

Seufert, G., Bartzis, J., Bomboi, T., Ciccioli, P., Cieslik, S., Dlugi, R., Foster, P., Hewitt, C.N., Kesselmeier, J., Kotzias, D., Lenz, R., Manes, F., Pastor, R.P., Steinbrecher, R., Torres, L., Valentini, R., and Versino, B.: An overview of the Castelporziano experiments, Atmospheric Environment, 31, 5-17, 1997.

Sharkey, T.D., Loreto, F., and Delwiche, C.F.: High-Carbon Dioxide and Sun Shade Effects on Isoprene Emission from Oak and Aspen Tree Leaves, Plant Cell and Environment, 14, 333-338, 1991.

Sharkey, T.D. and Loreto, F.: Water-Stress, Temperature, and Light Effects on Isoprene Emission and Photosynthesis of Kudzu Leaves, Plant Physiology, 102, 159-159, 1993.

Sharkey, T.D. and Singsaas, E.L.: Why Plants Emit Isoprene, Nature, 374, 769-769, 1995.

Sharkey, T.D. and Yeh, S.S.: Isoprene emission from plants, Annual Review of Plant Physiology and Plant Molecular Biology, 52, 407-436, 2001.

Silver, G.M. and Fall, R.: Enzymatic-Synthesis of Isoprene from Dimethylallyl Diphosphate in Aspen Leaf Extracts (Vol 97, Pg 1588, 1991), Plant Physiology, 106, 1233-1233, 1994.

Silver, G.M. and Fall, R.: Characterization of Aspen Isoprene Synthase, an Enzyme Responsible for Leaf Isoprene Emission to the Atmosphere, Journal of Biological Chemistry, 270, 13010-13016, 1995.

Simon, E., Kuhn, U., Rottenberger, S., Meixner, F.X., and Kesselmeier, J.: Coupling isoprene and monoterpene emissions from Amazonian tree species with physiological and environmental parameters using a neural network approach, Plant Cell and Environment, 28, 287-301, 2005.

Simpson, D., Winiwarter, W., Borjesson, G., Cinderby, S., Ferreiro, A., Guenther, A., Hewitt, C.N., Janson, R., Khalil, M.A.K., Owen, S., Pierce, T.E., Puxbaum, H., Shearer, M., Skiba, U., Steinbrecher, R., Tarrason, L., and Oquist, M.G.: Inventorying emissions from nature in Europe, Journal of Geophysical Research-Atmospheres, 104, 8113-8152, 1999.

Singh, H.B. and Zimmermann, P.B.: Atmospheric distribution and sources of nonmethane hydrocarbons, *In* Gaseous Pollutants: Characterisation and Cycling, Eds. J.O. Nriagu and J. Wiley, New York, pp. 177-235, 1992.

Singsaas, E.L., Lerdau, M., Winter, K., and Sharkey, T.D.: Isoprene increases thermotolerance of isoprene-emitting species, Plant Physiology, 115, 1413-1420, 1997.

Sirju, A.P. and Shepson, P.B.: Laboratory and Field Investigation of the DNPH Cartridge Technique for the Measurement of Atmospheric Carbonyl-Compounds, Environmental Science & Technology, 29, 384-392, 1995.

Slemr, J., Slemr, F., Partridge, R., D'Souza, H., and Schmidbauer, N.: Accurate Measurements of Hydrocarbons in the Atmosphere (AMOHA): Three European intercomparisons, Journal of Geophysical Research-Atmospheres, 107, 2002.

Solmon, F., Sarrat, C., Serca, D., Tulet, P., and Rosset, R.: Isoprene and monoterpenes biogenic emissions in France: modeling and impact during a regional pollution episode, Atmospheric Environment, 38, 3853-3865, 2004.

Spirig, C., Neftel, A., Ammann, C., Dommen, J., Grabmer, W., Thielmann, A., Schaub, A., Beauchamp, J., Wisthaler, A., and Hansel, A.: Eddy covariance flux measurements of biogenic VOCs during ECHO 2003 using proton transfer reaction mass spectrometry, Atmospheric Chemistry and Physics, 5, 465-481, 2005.

Staudinger, H., Kern, W., and Kämmerer, H.: Anleitung zur organischen qualitativen Analyse. Springer Verlag, Berlin, Heidelberg, New York, 1968.

Staudt, M. and Seufert, G.: Light-Dependent Emission of Monoterpenes by Holm Oak (*Quercus-Ilex* L.), Naturwissenschaften, 82, 89-92, 1995.

Staudt, M., Bertin, N., Hansen, U., Seufert, G., Ciccioli, P., Foster, P., Frenzel, B., and Fugit, J.L.: Seasonal and diurnal patterns of monoterpene emissions from *Pinus pinea* (L.) under field conditions, Atmospheric Environment, 31, 145-156, 1997.

Staudt, M. and Bertin, N.: Light and temperature dependence of the emission of cyclic and acyclic monoterpenes from holm oak (*Quercus ilex* L.) leaves, Plant Cell and Environment, 21, 385-395, 1998.

Staudt, M., Wolf, A., and Kesselmeier, J.: Influence of environmental factors on the emissions of gaseous formic and acetic acids from orange (*Citrus sinensis* L.) foliage, Biogeochemistry, 48, 199-216, 2000.

Staudt, M., Rambal, S., Joffre, R., and Kesselmeier, J.: Impact of drought on seasonal monoterpene emissions from *Quercus ilex* in southern France, Journal of Geophysical Research-Atmospheres, 107, doi:10.1029/2001JD002043, 2002.

Staudt, M., Joffre, R., and Rambal, S.: How growth conditions affect the capacity of *Quercus ilex* leaves to emit monoterpenes, New Phytologist, 158, 61-73, 2003.

Steinbrecher, R., Schürmann, W., Schreiner, A.M., and Ziegler, H.: Terpenoid emissions from common oak (*Quercus robur* L.) and Norway spruce (*Picea abies* L. Karst), *In* Proceedings of Joint Workshop of CEC/BIATEX of EUROTRAC, 251-257, 1993.

Sternberg, J.C., Gallaway, W.S., and Jones, D.T.L.: The mechanism of response of flame ionisation detectors, *In* Gas Chromatography, Eds. N. Brenner, J.E. Callin and M.D. Weiss, Academic press, New York, 1962.

Strasburger, E., Noll, F., Schenck, H., and Schimper, A.F.W.: Strasburger, Lehrbuch der Botanik. Gustav Fischer Verlag, Stuttgart, Jena, New York, 1993.

Street, R.A., Owen, S., Duckham, S.C., Boissard, C., and Hewitt, C.N.: Effect of habitat and age on variations in volatile organic compound (VOC) emissions from *Quercus ilex* and *Pinus pinea*, Atmospheric Environment, 31, 89-100, 1997.

Talbot, R.W., Andreae, M.O., Berresheim, H., Jacob, D.J., and Beecher, K.M.: Sources and Sinks of Formic, Acetic, and Pyruvic Acids over Central Amazonia .2. Wet Season, Journal of Geophysical Research-Atmospheres, 95, 16799-16811, 1990.

Tholl, D., Chen, F., Petri, J., Gershenzon, J., and Pichersky, E.: Two sesquiterpene synthases are responsible for the complex mixture of sesquiterpenes emitted from Arabidopsis flowers, Plant Journal, 42, 757-771, 2005.

Thomas, F.M.: Growth and water relations of four deciduous tree species (*Fagus sylvatica* L., *Quercus petraea* [MATT.] LIEBL., *Q. pubescens* WILLD., *Sorbus aria* [L.] CR.) occurring at Central-European tree-line sites on shallow calcareous soils: physiological reactions of seedlings to severe drought, Flora, 195, 104-115, 2000.

Tingey, D.: The effect of environmental factors on the emission of biogenic hydrocarbons from live oak and slash pine, *In* Atmospheric Biogenic Hydrocarbons, Eds. J. Bufalini and R. Arnts, Butterworth, Stoneham, USA, 53-72, 1981.

Tollsten, L. and Müller, P.M.: Volatile organic compounds emitted from beech leaves, Phytochemistry, 43, 759-762, 1996.

Vairavamurthy, A., Roberts, J.M., and Newman, L.: Methods for Determination of Low-Molecular-Weight Carbonyl-Compounds in the Atmosphere, Atmospheric Environment Part a-General Topics, 26, 1965-1993, 1992.

Volz-Thomas, A., Slemr, J., Konrad, S., Schmitz, T., Apel, E.C., and Mohnen, V.A.: Quality assurance of hydrocarbon measurements for the German Tropospheric Research Focus (TFS), Journal of Atmospheric Chemistry, 42, 255-279, 2002.

Wang, X.Q., Hanson, J.C., Frenkel, A.I., Kim, J.Y., and Rodriguez, J.A.: Time-resolved studies for the mechanism of reduction of copper oxides with carbon monoxide: Complex behavior of lattice oxygen and the formation of suboxides, Journal of Physical Chemistry B, 108, 13667-13673, 2004.

Waring, R.H., Landsberg, J.J., and Williams, M.: Net primary production of forests: a constant fraction of gross primary production?, Tree Physiology, 18, 129-134, 1998.

Weiss, A. and Norman, J.M.: Partitioning Solar-Radiation into Direct and Diffuse, Visible and near-Infrared Components, Agricultural and Forest Meteorology, 34, 205-213, 1985.

Went, F.W.: Blue Hazes in the Atmosphere, Nature, 187, 641-643, 1960.

Winer, A.M., Arey, J., Atkinson, R., Aschmann, S.M., Long, W.D., Morrison, C.L., and Olszyk, D.M.: Emission Rates of Organics from Vegetation in California Central Valley, Atmospheric Environment Part a-General Topics, 26, 2647-2659, 1992.

Wolfertz, M., Sharkey, T.D., Boland, W., Kuhnemann, F., Yeh, S., and Weise, S.E.: Biochemical regulation of isoprene emission, Plant Cell and Environment, 26, 1357-1364, 2003.

World Meteorological Organisation: Scientific assessment of ozone depletion; Global ozone research and Monitoring Project, Report No. 37, 1995.

Yang, S.F. and Hoffman, N.E.: Ethylene Biosynthesis and Its Regulation in Higher-Plants, Annual Review of Plant Physiology and Plant Molecular Biology, 35, 155-189, 1984.

Zhou, X.L. and Mopper, K.: Measurement of Sub-Parts-Per-Billion Levels of Carbonyl-Compounds in Marine Air by a Simple Cartridge Trapping Procedure Followed by Liquid-Chromatography, Environmental Science & Technology, 24, 1482-1485, 1990.

Zimmer, W., Steinbrecher, R., Korner, C., and Schnitzler, J.P.: The process-based SIM-BIM model: towards more realistic prediction of isoprene emissions from adult *Quercus petraea* forest trees, Atmospheric Environment, 37, 1665-1671, 2003.

Table A.1. Micrometeorological parameters measured on English oak in the year of 2002. Abbreviations: [a] Shading experiment.

Date	Photosynthetic active		Temperature						Relative humidity	
[dd.mm.yy]	radiation [µmol m^{-2} s^{-1}]		Ambient [°C]		Branch cuvette [°C]		Leaf [°C]		Branch cuvette [%]	
	Maximum	Average	Maximum	Average	Maximum	Average	Maximum	Average	Maximum	Average
25.06.2002	1722	444	26	17	28	18	30	18	58	40
26.06.2002	1564	473	28	20	29	20	32	20	62	42
27.06.2002 [a]	1837	265	29	21	27	21	29	21	68	38
28.06.2002	1720	340	20	14	22	14	24	15	66	50
29.06.2002	1510	247	22	15	23	15	25	15	50	48
30.06.2002	1656	408	23	16	24	17	26	17	49	43
01.07.2002	302	79	17	15	17	15	17	15	51	45

Table A.2. Physiological parameters measured on English oak in the year of 2002. Note that negative values indicate deposition of the respective compound (e.g. CO_2 deposition = photosynthesis). Due to technical problems no CO_2 and H_2O exchange rates were measured during the 29. and 30.06.2002. Abbreviations: [a] Shading experiment, [b] data till 22:55 h only.

Date	CO_2 exchange [mg g^{-1} h^{-1}]			H_2O exchange [mg g^{-1} h^{-1}]		Stomatal conductance [m h^{-1}]		Standard emission Factor (G97) [µg g^{-1} h^{-1}]	
[dd.mm.yy]	Minimum	Maximum	Average	Maximum	Average	Maximum	Average	Isoprene	Monoterpenes
25.06.2002	-13	1	-5	1201	370	13	4	75.9	----
26.06.2002	-13	1	-5	1179	404	12	5	74.7	----
27.06.2002 [a]	-14	1	-3	1033	404	21	5	no data	no data
28.06.2002 [b]	-13	1	-5	857	268	19	6	no data	no data
29.06.2002	no data	no data	no data	no data	no data	no data	no data	no data	no data
30.06.2002	no data	no data	no data	no data	no data	no data	no data	no data	no data
01.07.2002	-7	1	-2	277	77	7	3	no data	no data

Table A.3. Micrometeorological parameters measured on European beech (sunlit branch) in the year of 2002.

Date	Photosynthetic active		Temperature						Relative humidity	
[dd.mm.yy]	radiation [µmol m^{-2} s^{-1}]		Ambient [°C]		Branch cuvette [°C]		Leaf [°C]		Branch cuvette [%]	
	Maximum	Average	Maximum	Average	Maximum	Average	Maximum	Average	Maximum	Average
12.06.2002	1144	148	20	15	22	15	25	16	69	55
13.06.2002	502	73	17	15	18	15	20	15	65	54
14.06.2002	1736	283	28	21	32	21	37	22	64	47
15.06.2002	1564	274	22	19	27	20	34	21	69	52
16.06.2002	1625	275	26	20	31	21	37	21	75	51
17.06.2002	1568	378	36	26	38	26	43	27	63	48
18.06.2002	1525	386	36	27	40	28	44	28	53	40
19.06.2002	1589	237	25	19	28	20	35	20	66	51

Table A.4. Physiological parameters measured on European beech (sunlit branch) in the year of 2002. Note that negative values indicate deposition of the respective compound (e.g. CO_2 deposition = photosynthesis).

Date	CO_2 exchange [mg g^{-1} h^{-1}]			H_2O exchange [mg g^{-1} h^{-1}]		Stomatal conductance [m h^{-1}]		Standard emission Factor (G97) [µg g^{-1} h^{-1}]	
[dd.mm.yy]	Minimum	Maximum	Average	Maximum	Average	Maximum	Average	Isoprene	Monoterpenes
12.06.2002	-12	0	-3	397	72	29	4	----	13.2
13.06.2002	-8	0	-2	143	50	11	3	----	9.2
14.06.2002	-14	1	-4	1096	270	14	4	no data	no data
15.06.2002	-14	0	-4	898	219	13	3	no data	no data
16.06.2002	-13	0	-4	951	230	14	4	no data	no data
17.06.2002	-11	1	-3	1132	332	12	2	no data	no data
18.06.2002	-10	1	-3	1471	412	9	2	----	13.5
19.06.2002	-12	0	-4	1017	201	10	3	no data	no data

Table A.5.a. Micrometeorological parameters measured on European beech (sunlit branch) in the year of 2003. Abbreviations: [a] Shading experiment.

Date	Photosynthetic active		Temperature						Relative humidity	
[dd.mm.yy]	radiation [µmol m^{-2} s^{-1}]		Ambient [°C]		Branch cuvette [°C]		Leaf [°C]		Branch cuvette [%]	
	Maximum	Average	Maximum	Average	Maximum	Average	Maximum	Average	Maximum	Average
23.07.2003	1612	251	29	22	28	21	35	22	46	36
24.07.2003	1405	212	27	20	26	19	32	20	49	43
25.07.2003	1518	239	27	20	28	19	33	20	59	41
26.07.2003	1625	250	26	20	26	19	32	20	54	42
27.07.2003	1723	264	25	21	25	20	31	21	58	45
28.07.2003	1719	326	27	19	26	18	34	19	64	41
29.07.2003	1591	315	29	21	29	20	36	21	56	37
30.07.2003	1766	158	24	19	22	18	27	19	73	44
31.07.2003 [a]	1434	221	30	21	29	20	39	22	64	45
01.08.2003	1462	379	33	23	32	22	38	24	64	43
02.08.2003	1467	360	34	25	32	23	39	25	53	40

Table A.5.b. Micrometeorological parameters measured on European beech (sunlit branch*)* in the year of 2003.

Date	Photosynthetic active		Temperature						Relative humidity	
[dd.mm.yy]	radiation [µmol m^{-2} s^{-1}]		Ambient [°C]		Branch cuvette [°C]		Leaf [°C]		Branch cuvette [%]	
	Maximum	Average	Maximum	Average	Maximum	Average	Maximum	Average	Maximum	Average
03.08.2003	1393	378	35	25	34	24	40	26	60	41
04.08.2003	1378	380	37	26	34	25	41	26	57	37
05.08.2003	1130	332	35	26	34	24	38	25	66	38
06.08.2003	1352	377	38	27	37	26	44	28	52	32
07.08.2003	1345	352	42	29	38	28	44	29	49	30

Table A.6.a Physiological parameters measured on European beech (sunlit branch*)* in the year of 2003. Note that negative values indicate deposition of the respective compound (e.g. CO_2 deposition = photosynthesis). Abbreviations: [a] Shading experiment.

Date	CO_2 exchange [mg g^{-1} h^{-1}]			H_2O exchange [mg g^{-1} h^{-1}]		Stomatal conductance [m h^{-1}]		Standard emission Factor (G97) [µg g^{-1} h^{-1}]	
[dd.mm.yy]	Minimum	Maximum	Average	Maximum	Average	Maximum	Average	Isoprene	Monoterpenes
23.07.2003	-11	1	-3	1411	308	10	3	---	3.3
24.07.2003	-12	1	-3	1107	201	18	6	---	3.1
25.07.2003	-11	1	-3	1269	307	18	4	no data	no data
26.07.2003	-12	1	-3	1119	238	21	5	no data	no data
27.07.2003	-13	5	-4	1161	271	26	7	no data	no data
28.07.2003	-12	1	-4	1275	315	22	5	no data	no data
29.07.2003	-11	1	-3	1400	375	15	4	---	5.6
30.07.2003	-14	1	-3	821	115	28	5	no data	no data
31.07.2003 [a]	-13	2	-3	1479	273	22	5	---	3.1
01.08.2003	-13	1	-4	1390	396	17	4	no data	no data
02.08.2003	-11	1	-4	1466	405	10	4	no data	no data

Table A.6.b. Physiological parameters measured on European beech (sunlit branch) in the year of 2003. Note that negative values indicate deposition of the respective compound (e.g. CO_2 deposition = photosynthesis).

Date	CO_2 exchange [mg g^{-1} h^{-1}]			H_2O exchange [mg g^{-1} h^{-1}]		Stomatal conductance [m h^{-1}]		Standard emission Factor (G97) [µg g^{-1} h^{-1}]	
[dd.mm.yy]	Minimum	Maximum	Average	Maximum	Average	Maximum	Average	Isoprene	Monoterpenes
03.08.2003	-12	1	-3	1360	402	17	4	no data	no data
04.08.2003	-11	1	-3	1312	414	13	3	no data	no data
05.08.2003	-10	1	-3	1197	386	11	3	---	4.7
06.08.2003	-10	1	-2	1604	418	10	2	---	4.1
07.08.2003	-10	1	-2	1650	412	8	2	no data	no data

Table A.7. Micrometeorological parameters measured on European beech (shaded branch) in the year of 2003.

Date	Photosynthetic active		Temperature						Relative humidity	
[dd.mm.yy]	radiation [µmol m^{-2} s^{-1}]		Ambient [°C]		Branch cuvette [°C]		Leaf [°C]		Branch cuvette [%]	
	Maximum	Average	Maximum	Average	Maximum	Average	Maximum	Average	Maximum	Average
09.08.2003	63	13	30	24	30	25	30	25	52	40
10.08.2003	79	11	30	23	30	23	30	23	72	46
11.08.2003	57	14	32	24	32	24	32	24	75	54
12.08.2003	64	17	36	28	37	28	38	28	82	45

Table A.8. Physiological parameters measured on European beech (shaded branch*)* in the year of 2003. Note that negative values indicate deposition of the respective compound (e.g. CO_2 deposition = photosynthesis).

Date	CO_2 exchange [mg g^{-1} h^{-1}]			H_2O exchange [mg g^{-1} h^{-1}]		Stomatal conductance [m h^{-1}]		Standard emission Factor (G97) [µg g^{-1} h^{-1}]	
[dd.mm.yy]	Minimum	Maximum	Average	Maximum	Average	Maximum	Average	Isoprene	Monoterpenes
09.08.2003	-6	3	0	no data	no data	no data	no data	---	20.8
10.08.2003	-6	3	0	no data	no data	no data	no data	---	15.2
11.08.2003	-6	3	-1	no data	no data	no data	no data	no data	no data
12.08.2003	-5	4	0	no data	no data	no data	no data	no data	no data

APPENDIX 2 Software settings for NMOC analysis

SETTING FOR E-LAB™ CHROMATOGRAPHY SYSTEM, OMS TECH INC., USA

Method File:	15_01_02
Remarks:	Total carbon detection
Detector:	Li-cor 6262
Calibration File:	
Signal Input For Ch1:	Input 1
Data Points Per Second:	20
Full Scale (Volts):	1
Chart Speed:	1.00
PRN File Seconds Per Point:	1.00
Show Baseline:	Both
Peak Report Auto Print:	No
Peak Report Auto Save:	Yes
Chromatogram Auto Print:	No
Chromatogram Auto Save:	Yes
Auto Print Form Feed:	Yes
Wait For Printer Ready:	No
External Process Trigger:	+ Trig

Time:	0:00	14:00
Acquire:	Start	Stop
Integration:	VL to BL	
Auto Zero:	Z	
Zero Level:	10	
Attenuation:	5	
Peak Width:	20	
Threshold:	2000	
Area Reject:	0.0E+00	
Height Reject:	0.0E+00	
Board Relay:	OFF	
Output A, B, C, D:	A-B-C-D	
Output E, F, G, H:	E-F-G-H	
Output I, J, K:	I-J-K	

SETTING FOR EXTERNAL CONTROLLER DEVICE: CONFIGURATION FILE

```
program main;
uses system,pidreg,vsio;
type
offontype = (off,on);
advoffontype = (off,on,low,high);
switchtype = (error,ELabTrigger,logperiod,Pump,FlushValve,BypassValve,CalValve,SampleValve,VOCValve,
MFCCalHe,MFCCalCO2,MFCCarHe,MFCSample,HeaterVOC,HeaterCO2);
```

```
ReadStruct = object(AllInstanceRec)
RunTime : TimeInst; {show=timerel;wr=0}
ProcVar : SwitchType; {wr=0}
SetState : advoffontype; {wr=0}
SetValue : SingleInst; {wr=0;Dec=2}
end;

RFNStruct  = object(AllInstanceRec)
RunTime : TimeInst; {show=timerel;wr=0}
SetCtrlFile : StringInst; {wr=0}
end;

LicorStruct  = object(AllInstanceRec)
CO2_ppm : SingleInst; {Wr=0; Dec=3}
H2O_ppm : SingleInst; {Wr=0; Dec=3}
TLicor : SingleInst; {Wr=0; Dec=3}
end;

ControlStruct =  object(AllInstanceRec)
Process : BoolInst; {range=off,manual,standby,auto}
proctest : offontype;
Host : BoolInst; {range=off,on}
logger : BoolInst; {range=off,on}
ELabTrigg : BoolInst; {range=off,on}
BlowerCO2 : BoolInst; {range=off,on}
Pump : BoolInst; {range=off,on}
Valv14 : LongInst; {show=hex}
ParamSave : BoolInst; {range=_____,saving,loading}
ParamFile : FileInst;
CtrlFile : FileInst;
RFNFile : FileInst;
DataDir : FileInst; {wr=0}
DataFile : FileInst; {wr=0}
LogDir : FileInst; {wr=0}
LogFile : FileInst; {wr=0}
ReadRec : structinst;
RFNRec : structinst;
end;

DataStruct  = object(AllInstanceRec)
TimeDate : TimeInst; {show=timesys}
CO2Licor : SingleInst; {Wr=0; Dec=3}
H2OLicor : SingleInst; {Wr=0; Dec=3}
TLicor : SingleInst; {Wr=0; Dec=2}
TVOCTrap : SingleInst; {Wr=0; Dec=1}
TCO2Trap : SingleInst; {Wr=0; Dec=1}
FCalHe : SingleInst; {Wr=0; Dec=1}
FCalCO2 : SingleInst; {Wr=0; Dec=1}
FCarHe : SingleInst; {Wr=0; Dec=1}
FSmpl : SingleInst; {Wr=0; Dec=1}
TempRef : SingleInst; {Wr=0; Dec=2}
FlushValv : BoolInst; {range=off,on}
BypasValv : BoolInst; {range=off,on}
CalValv : OffOnType;
SmplValv : BoolInst; {range=off,on}
VOCValv : BoolInst; {range=off,on}
end;

CalibStruct = object(AllInstanceRec)
OffsFCalHe : SingleInst; {Dec=2}
SpanFCalHe : SingleInst; {Dec=4}
OffsFCalCO2 : SingleInst; {Dec=2}
```

```
SpanFCalCO2 : SingleInst; {Dec=4}
OffsFCarHe : SingleInst; {Dec=2}
SpanFCarHe : SingleInst; {Dec=4}
OffsFSmpl : SingleInst; {Dec=2}
SpanFSmpl : SingleInst; {Dec=4}
end;

ParamStruct =  object(AllInstanceRec)
AutoStart : BoolInst; {range=off,on}
SetVOCTrap : SingleInst; {Dec=1; Max=350}
SetCO2Trap : SingleInst; {Dec=1; Max=250}
SetTLicor : SingleInst; {Dec=1; Max=250}
SetFCalHe : SingleInst; {Dec=1}
SetFCalCO2 : SingleInst; {Dec=1}
SetFCarHe : SingleInst; {Dec=1}
SetFSmpl : SingleInst; {Dec=1}
LogPeriod : LongInst; {min=1}

RegVOCTrap : StructInst;
RegCO2Trap : StructInst;
RegTLicor : StructInst;
Calib : CalibStruct;
end;

UserStructP  =  ^UserStruct;
UserStruct = object(AllInstanceRec)
Data : StructInst;
Param : StructInst;
Control : StructInst;
 LicorData : LicorStruct;
 end;

Workstruct = object(AllInstanceRec)
WTempOven : LongInst;
WTempOvenI : LongInst;
WTVOCTrap : LongInst;
WTVOCTrapI : LongInst;
WTempRef : LongInst;
WTempRefI : LongInst;
DiodeTabl : ArrayInst; {Typ=Integer; NData=50}
ThermistTabl : ArrayInst; {Typ=Integer; NData=200}
ThermCoupTemp : ArrayInst; {Typ=Integer; NData=180}
end;

const
TamaraNum = 2150745;
TVOCTrapAddr = $A480;
TCO2TrapAddr = $A482;
TempRefAddr  = $A486;
FCalHeAddr = $A4A0;
FCalCO2Addr = $A4A2;
FCarHeAddr = $A4A4;
FSmplAddr = $A4A6;
DACTimBasAddr = $A404;
SetFCalHeAddr = $A440;
SetFCalCO2Addr = $A442;
SetFCarHeAddr  = $A444;
SetFSmplAddr = $A446;
HeatCO2Addr = $A410;
BlowLicAddr = $A46C;
PumpAddr = $A46E;
HeatVOCAddr = $A470;
```

```
Valv14PowAddr = $A478;
Valv14OutAddr = $A408;
FlushValvMask = $0001;
BypasValvMask = $0018;
VOCValvMask = $0006;
CalValvMask = $0080;
SmplValvMask = $0200;
BlowerCO2Mask = $0020;
ElabTriggMask = $2000;

Mux0 = $0;
Mux1 = $1;
Mux2 = $2;
Mux3 = $3;
Mux4 = $4;
Mux5 = $5;
Mux6 = $6;
Mux7 = $7;
BridgeEn = $8;
Gain1 = $0;
Gain10 = $10;
Gain100 = $20;
Gain1000 = $30;
Offs0 = $0;
Offs1 = $40;
Offs2 = $80;
Offs3 = $C0;

Wwork : workstruct = (ThermistTabl : (

11132       -5000       11119       -4800       11104       -4600
11087       -4400       11068       -4200       11047       -4000
11023       -3800       10996       -3600       10967       -3400
10933       -3200       10896       -3000       10856       -2800
10811       -2600       10762       -2400       10709       -2200
10651       -2000       10588       -1800       10521       -1600
10448       -1400       10371       -1200       10289       -1000
10202        -800       10111        -600       10016        -400
 9916        -200        9813           0        9707         200
 9598         400        9486         600        9373         800
 9259        1000        9144        1200        9028        1400
 8913        1600        8799        1800        8686        2000
 8575        2200        8466        2400        8359        2600
 8255        2800        8155        3000        8057        3200
 7963        3400        7873        3600        7786        3800
 7703        4000        7623        4200        7548        4400
 7476        4600        7407        4800        7343        5000
 7281        5200        7223        5400        7168        5600
 7116        5800        7068        6000        7022        6200
 6978        6400        6937        6600        6899        6800
 6863        7000        6829        7200        6797        7400
 6767        7600        6739        7800        6712        8000
 6687        8200        6664        8400        6642        8600
 6621        8800        6602        9000                    ); );

Com2 : SIO = (PortAddr : 0; Baud : 9600;
Bits : 8; StopBits : 1;
Parity : none;
Handshake : NoHandShake;
Protocol : MultiFile);

UserData : UserStruct = (Data : DataStruct;
```

```
Param : ParamStruct = (Calib : CalibStruct;
RegVOCTrap : PID = (PropBand : 200; IntTime : 5000; DiffTime : 1000; SamplePeriod : 500; OutMax : 2000;
OutMin : 0);
RegCO2Trap : PID = (PropBand : 200; IntTime : 15000; DiffTime : 5000; SamplePeriod : 500; OutMax : 255);
RegTLicor : PID = (PropBand : 200; IntTime : 120000; DiffTime : 5000; SamplePeriod : 500; OutMax : 3500));

Control : ControlStruct = (ParamFile : 'mc:\tamara.ini'; CtrlFile : 'mc:\dummy.txt'; RFNFile    : 'mc:\method.txt';
ReadRec : ReadStruct; RFNRec : RFNStruct); LicorData : LicorStruct;);

procedure Clock;
var Hour : Longinst;
begin with Userdata,Data,Control do begin
TimeDate := Now;
while 0 = 0 do begin
TimeDate := TimeDate + 1000;
waitfor(TimeDate);
end; end; end;

procedure ReceiveLicor;
var LicorFile : FileInst;
begin with UserData,LicorData do begin
LicorFile : = 'Com2';
Open(LicorFile,ReadMode or WriteMode);
SetDelimiter(LicorFile,$0D0A);
while 0 = 0 do begin
if ReadRecord(LicorFile,LicorData,500) = 0 then begin
Data.CO2Licor : = CO2_ppm;
Data.H2OLicor : = H2O_ppm;
Data.TLicor   : = TLicor;
end; end; end; end;

procedure HandleMulIO;
var LocTime : TimeInst; I : Longinst;
SampleCount : LongInst; IntCount1 : Longinst; IntCount2 : LongInst;
Begin with Userdata,Control,Param,Data,Calib,work do begin
WriteWord (TVOCTrapAddr + $10 ,Mux0 + Gain100);
WriteWord (TCO2TrapAddr + $10 ,Mux1 + Gain100);
WriteWord (TempRefAddr + $10 ,Mux3 + Gain1);
WriteWord (FCalHeAddr + $10 ,Mux0 shl 8);
WriteWord (FCalCO2Addr + $10 ,Mux1 shl 8);
WriteWord (FCarHeAddr + $10 ,Mux2 shl 8);
WriteWord (FSmplAddr + $10 ,Mux3 shl 8);

LocTime : = now;
while 0 = 0 do begin

TVOCTrap : = (Readword(TVOCTrapAddr) - 10055) * 0.200 + TempRef;
TCO2Trap : = (Readword(TCO2TrapAddr) - 10055) * 0.200 + TempRef;

InterPol(Readword(TempRefAddr),ThermistTabl,WTempRef,WTempRefI);
TempRef := WTempRef / 100;

LocTime : = LocTime + 200;
while now < LocTime do HandleEvents(0);

FCalHe   : = (Readword(FCalHeAddr) - 10000) * SpanFCalHe + OffsFCalHe;
FCalCO2  : = (Readword(FCalCO2Addr) - 10000) * SpanFCalCO2 + OffsFCalCO2;
FCarHe   : = (Readword(FCarHeAddr) - 10000) * SpanFCarHe + OffsFCarHe;
FSmpl    : = (Readword(FSmplAddr) - 10000) * SpanFSmpl + OffsFSmpl;

WriteWord(DACTimBasAddr,255);
```

```
If Process <> manual then begin
WriteWord(SetFCalHeAddr, round(SetFCalHe / 72.5 * 255));
WriteWord(SetFCalCO2Addr,round(SetFCalCO2 / 10 * 255));
WriteWord(SetFCarHeAddr, round(SetFCarHe / 725 * 255));
WriteWord(SetFSmplAddr,  round(SetFSmpl / 500 * 255));
end;

LocTime := LocTime + 200;
while now < LocTime do HandleEvents(0);
end; end; end;

procedure LogProc;
var LocTime : TimeInst; Day : LongInst;
begin with Userdata,Control,Param do begin
while 0 = 0 do begin
while (logger = off) do waitfor(logger);
LogDir : = 'mc:\' + JulianDate(BinDate(now),'_');
MkDir(LogDir);
LogFile : = LogDir + '\' + JulianTime(BinTime(now,0),'_',0) + '.log'; Open(LogFile,WriteMode);
LocTime : = now;
If logPeriod < 1 then logperiod := 1;
Writeln(LogFile,'.dataset');
Writeln(LogFile,'.data');
WriteHeader(LogFile,Data,9);
Day : = BinDate(LocTime);
while logger = on do begin
If BinDate(now) <> Day then break;
WriteRecord(LogFile,Data,9);
LocTime : = LocTime + (LogPeriod * 1000);
waitfor(LocTime);
end; Close(LogFile); end; end; end;

procedure ProcessProc;
var LocTime : TimeInst; StartTime : TimeInst; EndTime : TimeInst;
StartRFNTime : TimeInst; EndRFNTime : TimeInst;
Begin with UserData,Control,Data,Param,ReadRec do begin
while 0 = 0 do begin
logger : = off;
pump : = off,
SetFCalHe : = 0;
SetFCalCO2 : = 0;
SetFCarHe : = 25;
SetFSmpl : = 25;
FlushValv : = on;
CalValv : = off;
SmplValv : = off;
BypasValv : = off;
VOCValv : = off;
SetVocTrap : = 35;
SetCO2Trap : = 30;

while process <> auto do waitfor(process);
logger : = on;
pump : = on;

while process = auto do begin
LocTime : = now;
StartRFNTime : = LocTime;
Open(RFNFile,ReadMode);
while ReadRecord(RFNFile,RFNRec,200) = 0 do begin
SetFCalHe : = 0;
SetFCalCO2 : = 0;
```

```
SetFCarHe : = 100;
SetFSmpl : = 25;
FlushValv : = on;
CalValv : = off;
SmplValv : = off;
BypasValv : = off;
VOCValv : = off;
SetVocTrap : = 35;
SetCO2Trap : = 30;

EndRFNTime : = StartRFNTime + RFNRec.RunTime;
If EndRFNTIme < LocTime then EndRFNTime : = LocTime;

If proctest = on then begin
If EndRFNTime > LocTime + 5000 then EndRFNTime : = LocTime + 5000;
end;

while LocTime < EndRFNTime do begin
LocTime : = LocTime + 1000;
waitfor(LocTime);
RFNRec.RunTime := EndRFNTime - LocTime;

If process <> auto then break;
end;

If process <> auto then break;

CtrlFile : = 'mc:\' + RFNRec.SetCtrlfile + '.txt';
Open(CtrlFile,ReadMode);
ReadRecord(CtrlFile,ReadRec,100);
StartTime : = LocTime;
while ReadRecord(CtrlFile,ReadRec,200) = 0 do begin
EndTime := StartTime + RunTime;

If proctest = on then begin
If EndTime > LocTime + 5000 then EndTime : = LocTime + 5000;
end;

while LocTime < EndTime do begin
LocTime : = LocTime + 1000;
waitfor(LocTime);
RunTime : = EndTime - LocTime;

If process <> auto then break;
end;

If process <> auto then break;
if ProcVar = ELabTrigger then ELabTrigg : = SetState
else if ProcVar = logperiod then logperiod : = round(SetValue);
if ProcVar = FlushValve then FlushValv : = SetState
else if ProcVar = BypassValve then BypasValv : = SetState
else if ProcVar = CalValve then CalValv : = SetState
else if ProcVar = SampleValve then SmplValv : = SetState
else if ProcVar = VOCValve then VOCValv : = SetState;
if ProcVar = MFCCalHe then SetFCalHe : = SetValue
else if ProcVar = MFCCalCO2 then SetFCalCO2 : = SetValue
else if ProcVar = MFCCarHe then SetFCarHe : = SetValue
else if ProcVar = MFCSample then SetFSmpl : = SetValue;
if ProcVar = HeaterVOC then SetVOCTrap : = SetValue
else if ProcVar = HeaterCO2 then SetCO2Trap : = SetValue;
end; Close(CtrlFile); end; Close(RFNFile);
Process := standby;
```

```
end; end; end; end;

begin with UserData,Param,Control,Data do begin
with RegVOCTrap do begin
On TVOCTrap do Input : = round(TVOCTrap * 10);
On SetVOCTrap do SetPoint : = round(SetVOCTrap * 10);
On OutPut do If Process <> manual then begin
If (Process = off) or (TVOCTrap  < -200) then begin
WriteWord(HeatVOCAddr,0)
end

else begin
WriteWord(HeatVOCAddr,OutPut);
WriteWord(HeatVOCAddr+2,$2000);
WriteWord(HeatVOCAddr+4,$4000);
WriteWord(HeatVOCAddr+6,$6000);
end; end; end;

with RegCO2Trap do begin
On TCO2Trap do Input : = round(TCO2Trap * 10);
On SetCO2Trap do SetPoint : = round(SetCO2Trap * 10);
On OutPut do If Process <> manual then begin
If (Process = off) or (TCO2Trap  < -200) then begin
WriteWord(HeatCO2Addr,0);
SetBit(Valv14,BlowerCO2Mask,0);
end

else begin
WriteWord(HeatCO2Addr,OutPut);
SetBit(Valv14,BlowerCO2Mask,OutPut=0);
end; end; end;

with RegTLicor do begin
On TLicor do Input : = round(TLicor * 10);
On SetTLicor do SetPoint : = round(SetTLicor * 10);
On OutPut do If Process <> manual then begin
If (Process = off) then WriteWord(BlowLicAddr,0)
else WriteWord(BlowLicAddr,OutMax-OutPut);
end; end;

On CalValv do begin
If CalValv = on then
Valv14 := Valv14 and not CalValvMask or (CalValvMask shl 1);
else
Valv14 : = Valv14 and not (CalValvMask shl 1) or CalValvMask;
end;

On SmplValv do begin
If SmplValv = on then
Valv14 := Valv14 and not SmplValvMask or (SmplValvMask shl 1);
else
Valv14 := Valv14 and not (SmplValvMask shl 1) or SmplValvMask;
end;

On FlushValv do begin
SetBit (Valv14,FlushValvMask,FlushValv);
end;

On BypasValv do begin
SetBit (Valv14,BypasValvMask,BypasValv);
end;
```

```
On VOCValv do begin
SetBit (Valv14,VOCValvMask,VOCValv);
end;

On BlowerCO2 do begin
SetBit (Valv14,BlowerCO2Mask,BlowerCO2);
end;

On ElabTrigg do begin
SetBit (Valv14,ElabTriggMask,ElabTrigg);
end;

On Pump do begin
WriteWord(PumpAddr,12 * 140 * (Pump = on));
end;

On Valv14 do begin
WriteWord(Valv14PowAddr,20 * 140 * (Process > off));
WriteWord(Valv14OutAddr,Valv14);
end;

On ParamSave do begin
If ParamSave = saving then begin
ParamSave : = _____;
writetree(ParamFile,Param);
end;

If ParamSave = loading then begin
ParamSave : = _____;
readtree(ParamFile,Param);
end; end;

Logperiod : = 10;
readtree(ParamFile,Param);
CreateThread('Clock',2048,Clock);
CreateThread('Process',4096,ProcessProc);
CreateThread('Logger',3072,LogProc);
CreateThread('HandleMulIO',2048,HandleMulIO);
CreateThread('ReceiveLicor',4096,ReceiveLicor);
while 0 = 0 do HandleEvents(0);
end; end;
```

SETTING FOR EXTERNAL CONTROLLER DEVICE: PARAMETER FILE

```
AutoStart       off
SetVOCTrap      35.0
SetCO2Trap      30.0
SetTLicor       38.0
SetFCalHe       0.0
SetFCalCO2      0.0
SetFCarHe       0.0
SetFSmpl        0.0
LogPeriod       1

RegVOCTrap >
SetPoint        350
Input           Variable Value
Output          2999
OutOfs          28316
```

PropBand	500
IntTime	15000
DiffTime	1000
SamplePeriod	500
OutMax	3000
OutMin	0
IntBrake	0

RegCO2Trap >	
SetPoint	300
Input	Variable Value
Output	0
OutOfs	-30887
PropBand	100
IntTime	2000
DiffTime	0
SamplePeriod	400
OutMax	200
OutMin	0
IntBrake	1

RegTLicor >	
SetPoint	380
Input	Variable Value
Output	0
OutOfs	-27334
PropBand	200
IntTime	120000
DiffTime	5000
SamplePeriod	500
OutMax	3500
OutMin	0
IntBrake	0

Calib >	
OffsFCalHe	-0.85
SpanFCalHe	0.0534
OffsFCalCO2	0.4
SpanFCalCO2	0.0069
OffsFCarHe	0
SpanFCarHe	0.5350
OffsFSmpl	0.0
SpanFSmpl	0.3620

SETTING FOR EXTERNAL CONTROLLER DEVICE: PROGRAM FILE

CALIBRATION FILE

time	variable	state	value
00:00:00	ELabtrigger	on	
00:00:01	ELabtrigger	off	
00:00:02	MFCCalCO2	on	10
00:00:03	MFCCalHe	on	10
00:00:04	BypassValve	on	
00:03:00	CalValve	on	
00:06:58	CalValve	off	
00:07:00	HeaterCO2	on	200
00:07:01	MFCCalCO2	off	

00:07:02	MFCCalHe	off	
00:10:00	HeaterCO2	off	30

CO_2 BLANK FILE

time	variable	state	value
00:00:00	ELabtrigger	on	
00:00:01	ELabtrigger	off	
00:00:03	BypassValve	on	
00:07:00	HeaterCO2	on	200
00:10:00	HeaterCO2	off	30

CARBON BLANK FILE

time	variable	state	value
00:00:00	ELabtrigger	on	
00:00:01	ELabtrigger	off	
00:06:59	BypassValve	on	
00:07:00	HeaterCO2	on	200
00:10:00	HeaterCO2	off	30

CO_2 SAMPLE FILE

time	variable	state	value
00:00:00	ELabtrigger	on	
00:00:01	ELabtrigger	off	
00:00:02	HeaterVOC	on	35
00:00:04	FlushValve	off	
00:00:05	MFCSample	on	300
00:00:06	BypassValve	on	
00:01:00	VOCValve	on	
00:11:00	FlushValve	on	
00:11:01	MFCSample	on	500
00:12:30	SampleValve	on	
00:12:31	MFCSample	on	100
00:12:32	HeaterVOC	on	250
00:16:27	HeaterVOC	off	-100
00:16:28	SampleValve	off	
00:16:30	HeaterCO2	on	200
00:19:30	HeaterCO”	off	30

CARBON SAMPLE FILE

time	variable	state	value
00:00:00	ELabtrigger	on	
00:00:01	ELabtrigger	off	
00:00:02	HeaterVOC	on	35
00:00:04	FlushValve	off	
00:00:05	MFCSample	on	300
00:01:00	VOCValve	on	
00:11:00	FlushValve	on	
00:11:01	MFCSample	on	500
00:12:30	SampleValve	on	
00:12:31	MFCSample	on	100
00:12:32	HeaterVOC	on	250

00:16:27	HeaterVOC	off	-100
00:16:28	SampleValve	off	
00:16:29	BypassValve	on	
00:16:30	HeaterCO2	on	200
00:19:30	HeaterCO”	off	30

SETTING FOR EXTERNAL CONTROLLER DEVICE: METHOD FILE

CALIBRATION METHOD

00:00:00	BLANK FILE
00:15:00	BLANK FILE
00:30:00	BLANK FILE
00:45:00	CALIBRATION_1
01:00:00	CALIBRATION_2

etc.

APPENDIX 3 List of abbreviations

AcetylCoA
: Activated acetic acid, an acetic acid-residual that is bound to Coenzyme A

ACN
: Acetonitrile, C_2H_3N, an organic solvent that is used frequently in liquid chromatography

ADP
: Adenosine-diphosphate, energy-rich compound, consisting of adenosine that is linked to ribose which has a chain of two phosphate groups attached

ATP
: Adenosine-triphosphate, energy-rich compound, consisting of adenosine that is linked to ribose which has a chain of three phosphate groups attached

BOVOC
: Biogenic oxygenated volatile organic compound, an oxygenated volatile organic released from natural sources such as terrestrial vegetation

BVOC
: Biogenic volatile organic compound, a volatile organic released from natural sources such as terrestrial vegetation

CO
: Carbon monoxide

CO_2
: Carbon dioxide

CTP
: Cytidine-triphosphate, energy-rich compound, consisting of cytosine that is linked to ribose which has a chain of three phosphate groups attached

DMAPP
: Dimethylallyl-diphosphate, isomer of isopentenyldiphosphate

DNPH
: 2,4-Dinitrophenylhydrazine, $C_6H_6N_4O_4$, reagent used to collect carbonyl compounds from ambient air samples

DOXP
: 1-deoxy-D-xylulose-5-phosphate, intermediate compound of the plastidic synthesis of isopentenyldiphosphate

FID
: Flame ionisation detector

FPP
: Farnesyldiphosphate, intermediate compound of isoprenoid synthesis

GC
: Gas chromatograph(y)

Gg
Giga gram, 10^9

GGPP
Geranylgeranyldiphosphate, intermediate compound of isoprenoid synthesis

GPP
Geranyldiphosphate, intermediate compound of isoprenoid synthesis

GTP
guanosine-triphosphate, energy-rich compound, consisting of guanosine that is linked to ribose which has a chain of three phosphate groups attached

HC
Hydrocarbon, organic compounds that consist from carbon and hydrogen atoms

HMG-CoA
3-hydroxy-3-methyl-glutaryl-Coenzyme A, intermediate compound of the cytosolic formation of isopentenyldiphosphate

HPLC
High pressure liquid chromatograph(y)

IPP
Isopentenyldiphosphate, $C_5H_{12}O_7P_2$, basic component of all natural isoprenoid compounds

MA
Mevalonic acid, intermediate compound of the cytoplasmatic synthesis of isopentenyldiphosphate

MACR
Methacrolein, C_4H_6O, one of the major products of the atmospheric decomposition of isoprene

MEP
2-C-methyl-erythritol-4-phosphate, a key compound of the plastidic synthesis of isopentenyldiphosphate

MEP-pathway
Metabolic pathway localized in the plant's chloroplasts, synthesis of isopentenyldiphosphate

MS
Mass spectrometer

MVK
Methylvinylketone, C_4H_6O, one of the major products of the atmospheric decomposition of isoprene

$NADH_2$
Nicotinamide-adenine-dinucleotide, $NADH + H^+$, coenzyme that serves as a reductant in various metabolic processes

$NADPH_2$
Nicotinamide-adenine-dinucleotide phosphate, $NADPH + H^+$, coenzyme that serves as a reductant in various metabolic processes

NMHC
Non methane hydrocarbon, organic compounds that consist from carbon and hydrogen atoms with exception of methane

NMOC
Non methane organic carbon, organic compounds that consist from carbon, hydrogen, and other hetero-atoms with exception of methane

NMVOC
Non methane volatile organic compound, volatile organic compounds that consist from carbon, hydrogen, and other hetero- atoms with exception of methane

Pg
Peta gram, 10^{15}

ppb
Parts per billion, 10^{-9}, nmol mol^{-1}

ppm
Parts per million, 10^{-6}, µmol mol^{-1}

ppt
Parts per trillion, 10^{-12}, pmol mol^{-1}

PTR-MS
Proton transfer reaction mass spectrometry, analytical technique that enables the on-line monitoring of a variety of different volatile organic compounds

sccm
Standard cubic centimetre per minute, m^3 min^{-1}

SPE
Solid phase extraction, extraction method that uses a solid stationary phase to isolate an analyte from a solution

Tg
Tera gram, 10^{12}

VOC
Volatile organic compound

APPENDIX 4 List of figures

APPENDIX 5 List of tables